

**Conjugated Electroluminescent Polymers Synthesized by a
Ring-Opening Metathesis Polymerization Precursor Route**

Thesis by
Michael Wayne Wagaman

In Partial Fulfillment of the Requirements
for the Degree of
Doctor of Philosophy

California Institute of Technology
Pasadena, CA

1998
(Submitted December 5, 1997)

*To my family,
especially Megan*

Acknowledgments

I would first like to thank Bob Grubbs for the opportunity to be a member of his research group. His hands-off approach allowed me a lot of freedom to think for myself and pursue my own ideas. Of course, this led to considerable frustration at times since all of my ideas were not necessarily good, but from the perspective I have now, it is easy to see that this too is an important part of learning how to approach chemistry. In addition to the freedom Bob allowed me in the lab, I am also grateful to him for not discouraging me from seeing the outside of the lab. California is a beautiful place and I am glad I had the opportunity to see a lot of it both on the annual group camping trip and on my own excursions with my wife, Megan. Bob also provided me with the opportunity to collaborate with many accomplished research groups throughout the world. These collaborations added new dimensions to my project beyond synthetic chemistry by providing insight into a wide range of academic and practical considerations for the materials I was making.

I also want to thank the other members of my thesis committee — Professors Dennis Dougherty, John Bercaw and Erick Carreira. Trying to anticipate their questions always made me think about my research results and direction more thoroughly.

Throughout my time at Caltech an endless tide of intelligent and interesting people have passed through the Grubbs labs either as post-docs, undergraduates or fellow graduate students. All of these people have been important to the success of my research and/or provided diversions that helped me relax and forget chemistry for a little while. First on this list, I owe special thanks to Lin Pu who got me started on the conjugated, electroluminescent polymers project. Lin's knowledge and guidance not only helped me understand the project, but also assisted me in learning how to approach organic chemistry and polymer synthesis. Lin was also a great tour guide for trips to Monterey Park for Chinese food and ice cream.

I should also interject Vincent Conticello here. Although he was gone by the time I arrived at Caltech, his notebooks provided useful starting places for a few of the monomers I synthesized.

Other people whose work provided precedent for some of the important advancements in my research include Jérôme Claverie and Zhe Wu. Jérôme is responsible for the discovery of the notorious "alcohol effect" that makes certain group VI catalysts work better. I was lucky enough to get to use such a catalyst for the majority of my research, and had really hit a wall in trying to make decent polymers with this catalyst until I decided to see if the "alcohol effect" Jérôme discovered for the analogous tungsten catalysts could work for the molybdenum catalyst I was using. With his strange brand of French humor, Jérôme was also an interesting guy to talk to, and his cooking skills made dinner at his house a pleasure too. Zhe's work with Lewis bases was less mysterious than the "alcohol effect," but provided inspiration for attempting to further tweak the catalyst activity to get what I wanted from it.

I am also grateful to all of those people who developed and provided catalysts that made the polymerizations I have done possible — SonBinh Nguyen, Eric Dias, Osamu Fujimura, Peter Schwab, Mike "Psycho" Giardello, and Marcia France. I especially thank Eric and Osamu who provided most of the more useful catalysts for my particular monomers and even synthesized catalysts on demand when I wanted to test out a few ideas. Through the years there have also been a variety of people who provided organic synthesis ideas — Osamu Fujimura (OF seemed to know a lot about most chemistry related topics and more), Scott Miller, Bill Zeurcher, Bobby Maughon, Tom Kirkland and Marcus Weck come to mind. Alex Dunn was also a good person to talk to, as he was the only other member of the group testing the counterintuitive realm of synthesis known as fluorine chemistry.

Marcus Theman Weck deserves special thanks for being a great person to share lab space with and for being a good friend. Because he kept his glassware phenomenally

clean, people were usually too distracted by his shiny wares to bother borrowing mine. Being a die-hard opera/classical fan, Marcus also inspired me to get the most out of LA's cultural scene. We even survived five full hours of *Tristan und Isolde* together. Finally, I should thank Marcus for being a harsh critic who, through his honest appraisals, helped me improve my scientific writing style.

I also owe many thanks to the people in the Grubbs group who have worked on parts of the electroluminescent polymers project at some time — Tom Kirkland, Erika Bellmann, Shojiro Kaita, Delwin Elder and Michèle Cucullu — for their assistance, insights and challenges to think of new avenues to pursue.

Other groups I have collaborated with on different parts of this project have provided useful information as well and have expanded my knowledge of areas outside of synthetic chemistry. Günther Leising and his group provided the first electroluminescence studies of poly(naphthalenevinylene)s that I had prepared, thereby showing that the materials we were making could be useful and were worth pursuing. After this, Sean Shaheen in Nasser Peyghambarian's group at the University of Arizona picked up the torch and made LEDs with a few different polymers I prepared. By looking over Sean's shoulder for a week, I also learned a lot about fabricating and studying electroluminescent devices. Jérôme Cornil and Jean-Luc Brédas provided insight into the theory behind what we should expect from our polymers and thereby provided a better understanding of some of our experimental observations. Shintaro Yamada, who is a graduate student with C. Grant Willson at The University of Texas at Austin, recently provided me with a cool picture that he obtained by using one of my polymers as a photoresist. In addition, Eric Homlin and Sabine Coates deserve many thanks for their assistance with fluorescence measurements.

Many of the people mentioned previously have also been fun to hang out with, play softball with and/or go camping and hiking with. Others who belong on this list include Dave Lynn, Helen Blackwell, Tom Wilhelm (many thanks with the computer help too),

Amy Pangborn-Giardello, Geoff Coates, Bernhard Mohr, Volker Wege, Cassandra Fraser, Shokyoku Kanaoka (who also contributed to my training in the beginning), Andres Kim, Uwe Bünz, Jan-Karel Buijink, Takeharu Morita, Koshiro "Weakend Special" Yokota, Tomas Belderain, Stefan Friedrich, Leroy Jones II, Andrew Morehead, Todd Younkin, Heather Maynard and Melanie Sanford. Osamu Fujimura was especially diligent in his quest to climb the next mountain and often organized hiking trips that let us see some of the colder, snowy parts of Southern California. And of course I must mention Rob Li, who was definitely one of the more interesting people to have around. He also often led the dim-sum expeditions, but had a habit of looking at me for translations when the waitresses would try to speak Chinese to him.

How could I forget Dian Buchness, who always knew what paperwork needed to be filled out and who could answer a particular question, and Linda Clark who always knew when Bob could be found (well at least almost always) and whether that paper had been sent.

I also want to thank my professors at the University of Delaware for helping me make my way to Caltech. There were many great teachers there, but I especially thank Professors Klaus Theopold and Cynthia McClure who let me work in their laboratories when I didn't have the first clue about doing synthetic research. I also thank all of my teachers at Spring Grove who provided a great education and the inspiration to learn more. The always interesting Mr. Bierman deserves special mention here for laying the chemistry groundwork.

Of course, my family deserves many thanks as well for their support and encouragement all along.

My wife, Megan, deserves more than a simple "thank you" for all of her support throughout everything. Megan has not only been a wonderful wife and best friend, but always brightens my days with her seemingly ever-present smile and easy laugh. She has also contributed significantly to my research since, with her chemistry knowledge, she has

provided useful insight on many occasions. By being an eager listener she has also often helped me figure out a confusing result by letting me tell her all about it. Megan has also been a great help in putting this thesis together, as she proofread nearly all of it.

Financial support for the research presented in this thesis was provided by the United States Air Force, the Office of Naval Research and the Ballistic Missiles Defense Organization through an AASERT grant. I would also like to thank Dr. D. G. H. Ballard and ICI who provided a gift of *cis*-3,5-cyclohexadiene-1,2-diol, which is the biological oxidation product of benzene that made much of the research presented possible. I also thank Dr. Bruce Smart of DuPont who provided useful information concerning the synthesis of perfluoroalkylated acetylenes.

Abstract

A variety of substituted poly(*para*-phenylenevinylene) (PPVs) and poly(1,4-naphthalenevinylene) homopolymers, block copolymers and random copolymers have been synthesized by a ring-opening metathesis polymerization (ROMP) precursor route. In general the initiator $\text{Mo}=\text{CCH}(\text{CH}_3)_2\text{Ph}(\text{=NAr})(\text{OCCH}_3(\text{CF}_3)_2)_2$, **1**, was used to polymerize barrelene (bicyclo[2.2.2]octatriene) and benzobarrelene monomers. The precursor polymers obtained were then aromatized in solution using 2,3-dichloro-5,6-dicyanobenzoquinone (DDQ) to produce PPVs and PNVs, many of which are soluble in common organic solvents.

To prepare these polymers, new syntheses of the monomers were first developed as described in Chapters 1 and 2. The routes developed readily allow the preparation of a variety of substituted benzobarrelene and barrelene monomers in multigram quantities. As described in Chapter 3, several well-defined metathesis initiators were tested to determine the one best suited to the synthesis of homopolymers and copolymers of the monomers prepared. Tuning of the activity of **1** to achieve a living polymerization is also described.

In Chapter 4 the synthesis of PNV and PPV homopolymers, and studies of their absorbance and fluorescence properties, are described. These studies show that the different homopolymers exhibit luminescence from the blue (450 nm) to nearly the red (580 nm) depending on the substituents on the polymer, which were usually alkyl groups, electron withdrawing groups (halogens, esters, and perfluoroalkyl groups) or both. Polymers with electron withdrawing groups were found to be much more stable in air than unsubstituted PPV and PNV.

The synthesis of PNV and PPV random and block polymers and studies of their absorbance and fluorescence properties are described in Chapter 5. In general, polymers with a diblock or blocky distribution of monomer units showed migration of excitons (electron-hole pairs) into the smaller bandgap segments of the polymer. As a result, most

of the luminescence from these materials had a wavelength characteristic of the smaller bandgap homopolymer. More efficient transport was observed in films and in copolymers with shorter block segments.

In Chapter 6 the results of electroluminescence studies with three of the polymers are described. These measurements show that the polymers prepared exhibit electroluminescence. They also reveal that alkylated PNV is a better hole transporter than electron transporter but that diester substituted PPV is a better electron transporter and a poorer hole transporter.

Finally, use of a di-*t*-butylester substituted PPV in conjunction with a photo-acid generator as a photoresist is described in the Appendix.

Table of Contents

Introduction	1
Background and Introduction.....	2
Project Goals.....	6
References and Notes.....	9
Chapter 1 Synthesis of Benzobarrelene Monomers	13
Abstract.....	14
Introduction	15
Results and Discussion	16
Undecylbenzobarrelene Synthesis	16
Alkylated Trifluorobenzobarrelene Synthesis: First Attempts....	17
A Useful Route to Alkylated Benzobarrelenes	20
Conclusions.....	23
Experimental	23
References and Notes.....	31
Chapter 2 A New Efficient Synthesis of Substituted Bicyclo[2.2.2]octatrienes (Barrelenes).....	32
Abstract.....	33
Introduction	34
Results and Discussion	35
Conclusions.....	39
Experimental	39
References and Notes.....	58
Chapter 3 Catalyst Testing and Tuning.....	61
Abstract.....	62
Introduction	63
Results and Discussion	64
Catalyst Screening	64

Activation of 8 by 2?	67
Activation of 8 by Hexafluoro- <i>t</i> -butanol.....	68
Deactivation of 8 by Lewis Bases	69
"Livingness" Studies	72
Conclusions.....	76
Experimental	76
References and Notes.....	79
Chapter 4 Synthesis and Study of PNV and PPV Homopolymers....	82
Abstract.....	83
Introduction	84
Results and Discussion	85
Synthesis of Precursor Polymers	85
Polymer Purification and Aromatization	88
Deprotection of 23	90
Spectroscopic Study of PPVs and PNVs.....	91
Oxidation Stability	94
Conductivity of Doped 18	94
Conclusions.....	95
Experimental	96
References and Notes.....	106
Chapter 5 Synthesis and Luminescence Properties of Random and Block Copolymers.....	108
Abstract.....	109
Introduction	110
Results and Discussion	111
PNV Block Copolymer Synthesis	111
Aromatization of PNV Block Copolymer Precursors	112
Photoluminescence of 10 , 11 , and 13	113
PNV/PPV Copolymers.....	114
Photoluminescence of 3H-PNV/BC-PPV	117
Photoluminescence of 3Cl-PNV/BTF-PPV	120
Theoretical Considerations.....	125

Conclusions.....	126	
Experimental	127	
References and Notes.....	138	
Chapter 6	Electroluminescence Results	141
	Abstract.....	143
Part 1	Red-Orange Electroluminescence with New Soluble and Air Stable Poly(naphthalenevinylene)s.....	144
	Introduction	144
	Results and Discussion	144
	Conclusions.....	152
	Experimental	153
	References and Notes.....	154
Part 2	Electroluminescence of Alkylated PNV and Substituted PPVs	157
	Introduction	157
	Results and Discussion	157
	Study of Undeyl Substituted PNV, 1	157
	Study of Di- <i>t</i> -butylester Substituted PPV, 2	159
	Study of Trifluoromethylperfluoroctyl Substituted PPV, 3	160
	Conclusions.....	160
	Experimental	161
	References and Notes.....	168
Appendix	Use of Poly (di-<i>t</i>-butylester phenylenevinylene) as a Photoresist	169
	Abstract.....	170
	Introduction	171
	Results and Discussion	172
	References and Notes.....	176

List of Tables, Schemes, and Figures

Introduction

Schemes

Scheme 1	5
Scheme 2	6

Figures

Figure 1 Poly(<i>para</i> -phenylenevinylene) (PPV).....	2
Figure 2 A typical light emitting diode.....	2
Figure 3 Electroluminescence.....	3
Figure 4 Migration of polarons in a block copolymer.....	4

Chapter 1

Tables

Table 1 Alkylation of tetrafluoro benzenes	19
Table 2 Results of alkylation of 2 and 21	22

Schemes

Scheme 1	15
Scheme 2	16
Scheme 3	17
Scheme 4	18
Scheme 5	20
Scheme 6	21
Scheme 7	22

Chapter 2

Schemes

Scheme 1	35
Scheme 2	36
Scheme 3	37
Scheme 4	38
Scheme 5	39

Chapter 3

Tables

Table 1 Comparison of catalyst activity.....	66
--	----

Table 2	Effect of HFB on the activity of 8 and the properties of the resulting polymers.....	69
Table 3	Effect of Lewis bases on the activity of 8 and the properties of the resulting polymers.....	70
Schemes		
	Scheme 1	63
	Scheme 2	66
	Scheme 3	71
Figures		
Figure 1	Benzobarrelene monomers used for catalyst testing.....	64
Figure 2	Metathesis initiators tested for polymerizations of benzobarrelenes and barrelenes	65
Figure 3	Di- <i>t</i> -butylester barrelene, 10	72
Figure 4a	Monomer/initiator ratio vs. number average molecular weight for 1	73
Figure 4b	Monomer/initiator ratio vs. number average molecular weight for 2	73
Figure 4c	Monomer/initiator ratio vs. number average molecular weight for 10	74
Figure 5	Test for chain transfer, chain termination and backbiting	75
Chapter 4		
Tables		
Table 1	Results of polymerizations of benzobarrelenes and barrelenes	87
Table 2	Aromatization conditions for precursors polymers	89
Table 3	Absorbance and photoluminescence data for PPVs and PNVs.....	92
Schemes		
	Scheme 1	86
	Scheme 2	88
	Scheme 3	90
	Scheme 4	95
Figures		
Figure 1	Coordination of the growing polymer chain to the molybdenum initiator.....	87
Figure 2	Photoluminescence of polymer 23 containing 80% and 100% aromatized units	93

Chapter 5

Tables

Table 1	Energy of frontier orbitals and transition energy of lowest optical transition	126
---------	---	-----

Schemes

Scheme 1	112
Scheme 2	113
Scheme 3	115
Scheme 4	116
Scheme 5	116

Figures

Figure 1	Migration of polarons in a block copolymer.....	110
Figure 2	Emission spectra of PNV homopolymers and a block copolymer	114
Figure 3	Emission spectra of solutions of polymers 10 , 22 , 23 , and 24	117
Figure 4	Copolymers with quenching occurring in the smaller bandgap segments	118
Figure 5	Emission spectra of films of polymers 10 , 22 , 23 , and 24	119
Figure 6	Emission spectra of solutions of homopolymers and copolymers when irradiated at the excitation maximum for polymer 28 (345 nm).....	121
Figure 7	Migration of electrons and holes in copolymers.....	122
Figure 8	Emission spectra of solutions of homopolymers and copolymers when irradiated at the excitation maximum for polymer 14 (430 nm).....	123
Figure 9	Behavior of block copolymers irradiated at the excitation maximum of the smaller bandgap block.....	124
Figure 10	Emission spectra of films of homopolymers and copolymers when irradiated at the excitation maximum for polymer 28 (345 nm).....	125

Chapter 6

Part 1

Tables

Table 1	Molecular Weights.....	147
---------	------------------------	-----

Schemes

Scheme 1	145
Scheme 2	145

Figures	
Figure 1	Infrared absorbance spectra of MWA and PU2 146
Figure 2	EL, PL, excitation and absorption spectra of a PU2 film 147
Figure 3	Current - bias (I - V) characteristic of an ITO PU2 Al device 149
Figure 4	External EL quantum efficiency over the applied bias of an ITO PU2 Al device 150
Chapter 6	
Part 2	
Tables	
Table 1	Summary of electroluminescence results 159
Figures	
Figure 1	Conjugated polymers studied 157
Figure 2	Materials used to improve electron, 4 , and hole, 5 , injection and transport 158
Figure 3	Results for an ITO 1 40 nm Ca 100 nm device 163
Figure 4	Results for an ITO 1 40 nm 4 18 nm Mg 75 nm device .. 164
Figure 5	Results for an ITO 2 50 nm Mg 100 nm device 165
Figure 6	Results for an ITOx- 5 40 nm 2 40 nm 4 15 nm Mg 100 nm device 166
Figure 7	Results for an ITO 3 60 nm LiF 1.5 nm Mg 200 nm device 167
Appendix	
Schemes	
Scheme 1 171
Scheme 2 173
Figures	
Figure 1	Polymer 1 containing unaromatized units, and, photo-acid generator 4 172
Figure 2	Optical microscope picture of developed positive image 174

Introduction

Background and Introduction

In 1990, it was reported that poly(*para*-phenylenevinylene) (PPV), shown in Figure 1, can be used as the emissive layer in light emitting diodes, as shown in Figure 2.¹ Since this discovery, an enormous amount of work has been done to find other polymers that exhibit electroluminescence, which occurs by a process similar to photoluminescence as shown in Figure 3, and to optimize the performance of electroluminescent devices employing polymers as the emissive material. While electroluminescence of inorganic materials had been reported many years earlier,² using

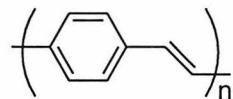


Figure 1. Poly(*para*-phenylenevinylene) (PPV).

organic materials and polymers for this application was desirable for several reasons. First, organic materials with a wide range of emission wavelengths, and hence colors, are known. This is important since making full color LED displays requires materials emitting the three primary colors of light — blue, green, and red. Although inorganic materials that exhibit green and red emission were known and had been used to make

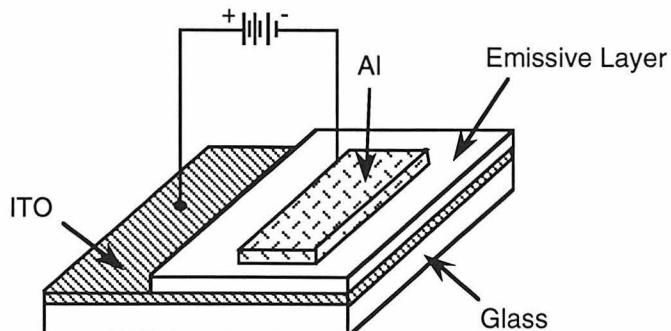


Figure 2. A typical light emitting diode. Shown with an aluminum anode (Al) and an indium tin oxide cathode (ITO).

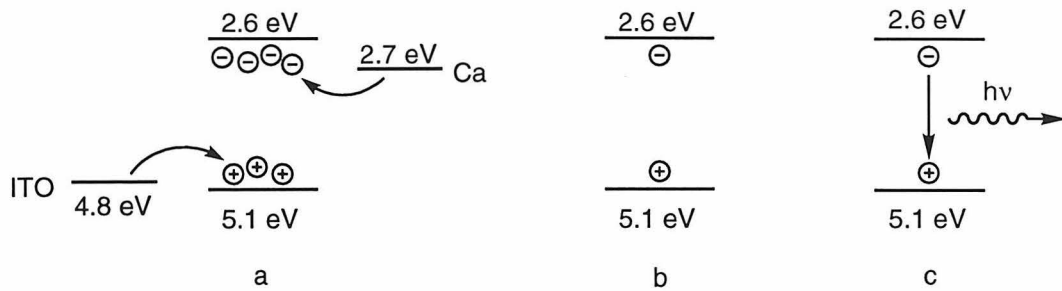


Figure 3. Electroluminescence a) Electrons and holes are injected. b) Two oppositely charged polarons pair to form an exciton. c) A singlet exciton relaxes and light is emitted. In photoluminescence, the singlet excitons are generated by absorption of light of the proper wavelength.

LEDs, obtaining efficient blue emission from inorganic materials has been difficult. Gallium nitride had been known to exhibit blue luminescence, but until recently efficient LEDs could not be made using this material.³⁻⁹ The main barrier to using gallium nitride was that defect free films of this material, which are required for efficient emission from crystalline inorganic materials, were difficult to grow.⁵ This problem is generally encountered when using crystalline inorganic materials and increases the cost of fabricating devices using these materials. In contrast, devices using polymers as the emissive layer do not require growth of crystalline films but can be made by simply spin casting the polymer onto the LED anode. This simpler process reduces the cost of LED fabrication and more readily allows electroluminescent devices with large surface areas to be made. Conjugated polymers also have the advantage that some of these materials, such as PPV, transport holes or electrons better than most unconjugated polymers.¹⁰ This improved transport can reduce the driving voltages required for LED operation.

Another potential advantage of polymers arises with conjugated block copolymers. These materials, which have been the subject of considerable theoretical attention,¹¹⁻¹⁷ are predicted to have improved luminescence efficiencies relative to homopolymers.^{12,13} The models developed indicate that when a conjugated block copolymer is made up of two polymers with different bandgaps, the electron-hole pairs (excitons) formed in the larger bandgap block will migrate to the smaller bandgap block

and become trapped, as shown in Figure 4. As a result, block copolymers exhibit luminescence characteristic only of the smaller bandgap material. Because excitons that originated in blocks of either type of polymer recombine in the smaller bandgap material, the luminescence intensity of this material is greater than that of a homopolymer of the same material. Emission efficiency is also improved in conjugated block copolymers because excitons trapped in the smaller bandgap blocks are not free to migrate throughout the entire length of the polymer.¹⁸⁻²¹ This reduced migration has been proposed to reduce the number of excitons that reach non-radiative quenching sites and thereby increases radiative recombination and device efficiency. Finally, conjugated block copolymers containing an electron transporting block and a hole transporting block should improve device performance by facilitating transport of both carriers into the emissive material.¹⁰

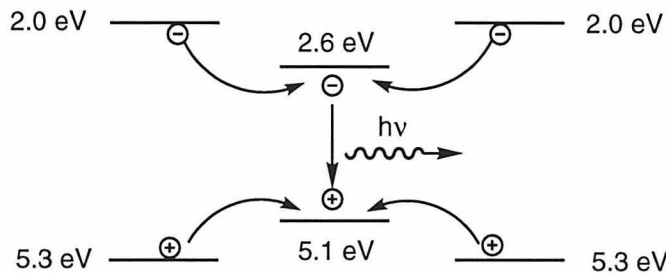


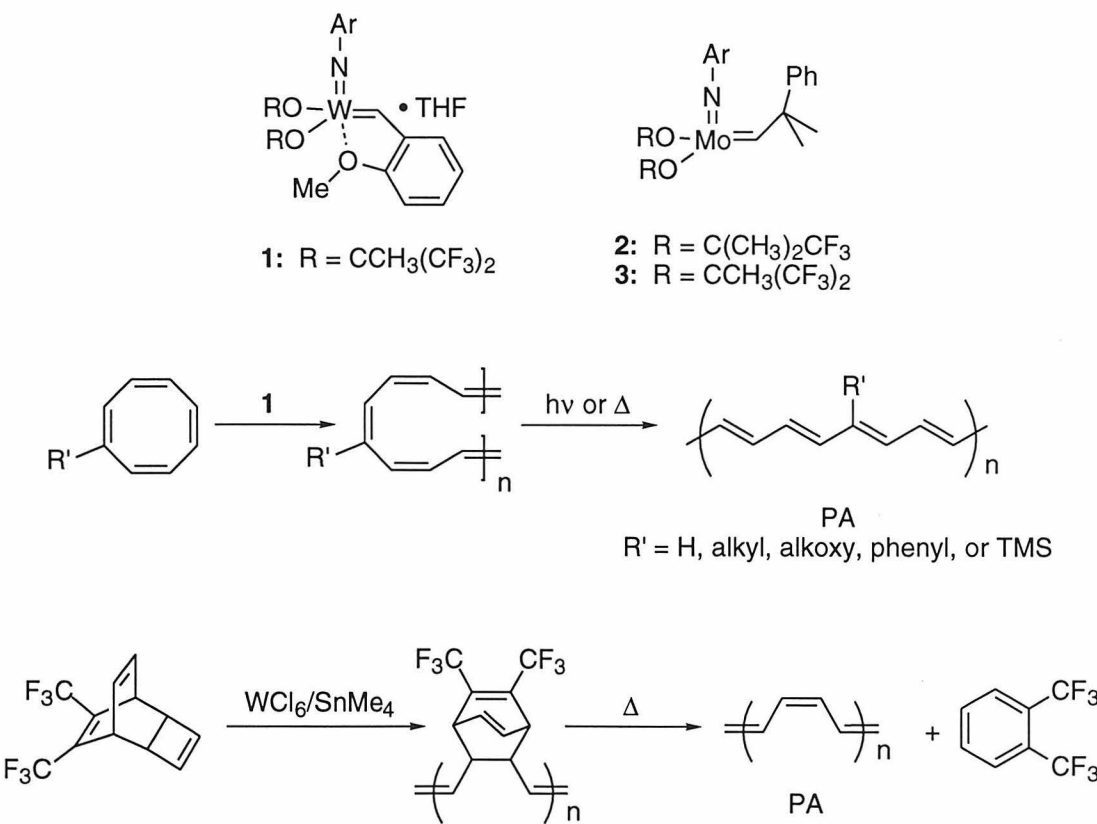
Figure 4. Migration of polarons in a block copolymer, followed by emission from the smaller bandgap block. Bandgaps shown were arbitrarily chosen.

Despite the theoretical interest in conjugated block copolymers and practical usefulness of the properties they are expected to possess, only a few of these materials have been reported.^{18,19,22-29} One likely reason that more block copolymers have not been synthesized is that most conjugated polymers are synthesized using methods that are not conducive to the synthesis of well-defined block copolymers. Many of the techniques employed for the synthesis of conjugated polymers are condensation polymerizations or other types of step-growth polymerizations and, therefore, yield polymers with relatively

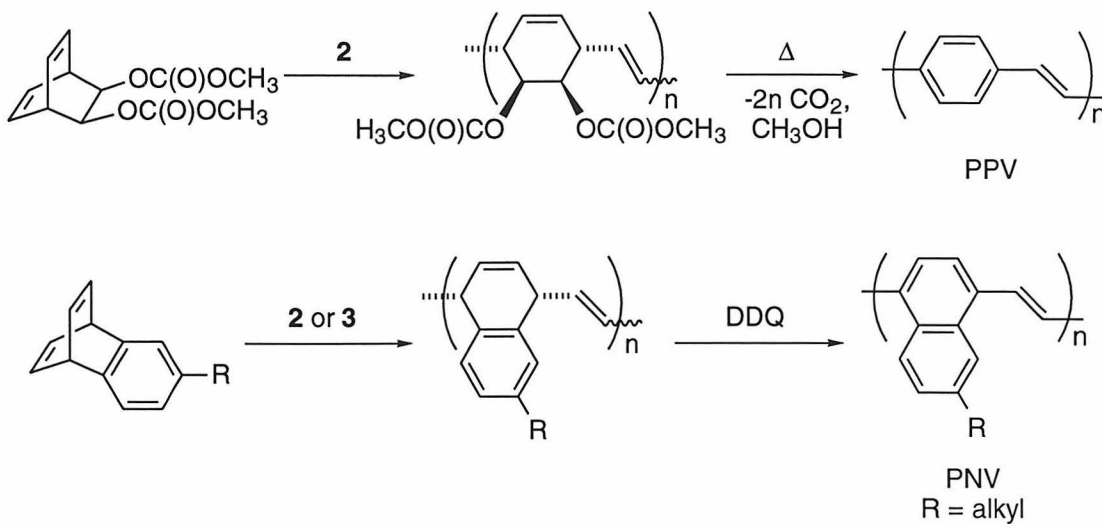
broad molecular weight distributions.^{10,18-20,30-39} In addition, these polymerizations are generally not living and therefore are not well suited to the synthesis of block copolymers.

In contrast, polymerizations carried out using ring-opening metathesis polymerization (ROMP) are often living and readily allow the synthesis of block copolymers.^{23,24,40-48} This polymerization technique is also conducive to the formation of conjugated polymers since, unlike radical, anionic, cationic and Ziegler-Natta polymerizations, olefin units present in the monomers used for ROMP are not consumed during the polymerization, but rather become part of the polymer backbone.^{35,39,49} As a result, ROMP can be used for the direct synthesis of fully conjugated materials including

Scheme 1



Scheme 2



polyacetylene (PA)⁵⁰ and soluble, substituted derivatives of PA.^{51,52} In addition, PA, PPV and PNV can be synthesized by using ROMP to prepare a precursor polymer that is subsequently converted into the desired conjugated material.⁵³⁻⁵⁸ Schemes 1 and 2 show direct and precursor routes that use ROMP to produce these conjugated polymers.

Project Goals

When I arrived at Caltech, the ROMP precursor routes to PPV⁵⁴ and PNV⁵⁵ shown in Scheme 2 had been worked out by Vincent Conticello and Lin Pu respectively. These syntheses were not ideally suited to the synthesis of conjugated block copolymers, however. To observe the properties of block copolymers predicted by theory, two polymers with different bandgaps are required. While PPV and PNV have different bandgaps, the synthesis of PNV did not allow block copolymers to be formed since, under the conditions employed, the polymerization was not living. We also wanted to make soluble polymers for facile device fabrication, but the unsubstituted PPV prepared was insoluble. Finally, the methods developed to synthesize these two materials by ROMP were not compatible since the temperatures required for the final elimination to

form PPV are near or above the temperature where the alkylated PNV prepared was observed to decompose.⁵⁷

Therefore several challenges remained to synthesizing theoretically interesting conjugated block copolymers by ROMP. First, at least two soluble polymers, which can be prepared by compatible routes and have different bandgaps, were required. Also, to obtain well-defined block copolymers, a polymerization system that allows living polymerizations had to be developed either by tuning the initiators used previously or by finding a different one. In addition, because there was a lack of blue chromophores, and a soluble, fully conjugated polymer that luminesces blue had not been reported,⁵⁹⁻⁶¹ finding such a material that could be synthesized by ROMP was desired. We also wanted to prepare conjugated, electroluminescent polymers bearing electron withdrawing groups. Such materials provide improved stability and performance, for reasons discussed in the introduction to Chapter 4, but only a few PPVs and PNVs bearing electron withdrawing groups have been reported.^{10,21,23,24,31-34} Of course, to prepare all of these new polymers, new monomers were also needed.

Achieving these goals was an interesting, exciting, and at times quite frustrating challenge. In the pages that follow, the route that was followed to develop a synthesis of the desired polymers is described.^{21,23,24,57,62-64} The information presented starts with synthesis of the monomers in Chapters 1 and 2. This is followed by synthesis and study of the homopolymers in Chapters 3 and 4, which include information on tuning the polymerization catalyst to achieve a living polymerization. After this, the synthesis and study of random and block copolymers is presented along with comparisons to the homopolymers in Chapter 5. Finally, Chapter 6 presents the results of electroluminescence studies on the polymers that have been found to be most compatible with the LED fabrication process.

Some of the goals were reached by applying knowledge gained here and at the University of Delaware, and others were achieved by trying everything that seemed to

hold some hope of working. As is most likely the case with all research, however, probably just as many of the important breakthroughs were made by sheer luck or by trying the things that everyone said could not possibly work.

References and Notes

- (1) Burroughs, J. H.; Bradley, D. D. C.; Brown, A. R.; Marks, R. N.; Mackay, K.; Friend, R. H.; Burns, P. L.; Holmes, A. B. *Nature* **1990**, *347*, 539.
- (2) Destriau, G. *J. Chem. Phys.* **1936**, *33*, 587.
- (3) Ziegler, J. P.; Howard, B. M. *Interface* **1994**, *Summer*, 27.
- (4) Dennis, N. *Science* **1997**, *275*, 1734.
- (5) Nakamura, S.; Harada, Y.; Seno, M. *Appl. Phys. Lett.* **1991**, *58*, 2021.
- (6) Nakamura, S.; Senoh, M.; Mukai, T. *Appl. Phys. Lett.* **1993**, *62*, 2390.
- (7) Nakamura, S.; Mukai, T.; Senoh, M. *Appl. Phys. Lett.* **1994**, *64*, 1687.
- (8) Nakamura, S.; Senoh, M.; Iwasa, N.; Nagahama, S. *Appl. Phys. Lett.* **1995**, *67*, 1868.
- (9) Nakamura, S.; Senoh, M.; Nagahama, S.; Iwasa, N.; Yamada, T.; Matsushita, T.; Kiyoku, H.; Sugimoto, Y. *Appl. Phys. Lett.* **1996**, *68*, 3269.
- (10) Greenham, N. C.; Moratti, S. C.; Bradley, D. D. C.; Friend, R. H.; Holmes, A. B. *Nature* **1993**, *365*, 628.
- (11) Bakhshi, A. K.; Liegener, C. M.; Ladik, J.; Seel, M. *Synth. Met.* **1989**, *30*, 79.
- (12) Meyers, F.; Heeger, A. J.; Brédas, J. L. *J. Chem. Phys.* **1992**, *97*, 2750.
- (13) Meyers, F.; Heeger, A. J.; Brédas, J. L. *Synthetic Metals* **1993**, *55-57*, 4308.
- (14) Musso, G. F.; Dellepiane, G.; Cuniberti, C.; Rui, M.; Borghesi, A. *Synth. Met.* **1995**, *72*, 209.
- (15) Santos, D. A. d.; Quattrocchi, C.; Friend, R. H.; Brédas, J. L. *J. Chem. Phys.* **1994**, *100*, 3301-3306.
- (16) Seel, M.; Liegener, C. M.; Förner, W.; Ladik, J. *Phys. Rev. B* **1988**, *37*, 956.
- (17) Ruckh, R.; Sigmund, E.; Kollmar, C.; Sixl, H. *J. Chem. Phys.* **1986**, *85*, 2797.
- (18) Burn, P. L.; Holmes, A. B.; Kraft, A.; Bradley, D. D. C.; Brown, A. R.; Friend, R. H. *J. Chem. Soc., Chem. Commun.* **1992**, 32.

(19) Burn, P. L.; Holmes, A. B.; Kraft, A.; Bradley, D. D. C.; Brown, A. R.; Friend, R. H.; Gymer, R. W. *Nature* **1992**, *356*, 47.

(20) Braun, D.; Staring, E. G. J.; Demandt, R. C. J. E.; Rikken, G. L. J.; Kessener, Y. A. R. R.; Venhuizen, A. H. J. *Synth. Met.* **1994**, *66*, 75.

(21) Wagaman, M. W.; Grubbs, R. H. *Macromolecules* **1997**, *30*, 3978.

(22) Wang, C.; Shieh, S.; LeGoff, E.; Kanatzidis, M. G. *Macromolecules* **1996**, *29*, 3147.

(23) Wagaman, M. W.; Bellmann, E.; Grubbs, R. H. *Phil. Trans. R. Soc. Lond. A* **1997**, *355*, 727.

(24) Wagaman, M. W.; Grubbs, R. H. *Synth. Met.* **1997**, *84*, 327.

(25) Jenekhe, S. A.; Chen, W. C. *Mat. Res. Symp. Proc.* **1990**, *173*, 589.

(26) Chen, X. L.; Jenekhe, S. A. *Synth. Met.* **1997**, *85*, 1431.

(27) Chen, X. L.; Jenekhe, S. A. *Appl. Phys. Lett.* **1997**, *70*, 487.

(28) Chen, X. L.; Jenekhe, S. A. *Macromolecules* **1996**, *29*, 6189.

(29) Brouwer, H. J.; Hilberer, A.; Krasnikov, V. V.; Werts, M.; Wildeman, J.; Hadzioannou, G. *Synth. Met.* **1997**, *84*, 881.

(30) Grob, M. C.; Feiring, A. E.; Auman, B. C.; Percec, V.; Zhao, M.; Hill, D. H. *Macromolecules* **1996**, *29*, 7284.

(31) Hanack, M.; Segura, J. L.; Spreitzer, H. *Adv. Mater.* **1996**, *8*, 663.

(32) Jin, J. I.; Lee, Y. H. *Macromolecules* **1993**, *26*, 1805.

(33) Kang, I. N.; Lee, G. J.; Kim, D. H.; Shim, H. K. *Polym. Bull.* **1994**, *33*, 89.

(34) McCoy, R. K.; Karasz, F. E. *Chem. Mater.* **1991**, *3*, 941.

(35) Odian, G. *Principles of Polymerization*; John Wiley & Sons, Inc.: New York, 1991.

(36) Skotheim, T. A., Eds. *Handbook of Conducting Polymers*. Marcel Dekker, New York, 1986.

(37) Gin, D. L.; Conticello, V. P.; Grubbs, R. H. *J. Am. Chem. Soc.* **1992**, *114*, 3167.

(38) Gin, D. L.; Conticello, V. P.; Grubbs, R. H. *J. Am. Chem. Soc.* **1994**, *116*, 10507.

(39) Allcock, H. R. *Contemporary Polymer Chemistry*; Prentice Hall: Englewood Cliffs, 1990.

(40) Maughon, B. R.; Weck, M.; Mohr, B.; Grubbs, R. H. *Macromolecules* **1997**, *30*, 257.

(41) Saunders, R. S.; Cohen, R. E.; Schrock, R. R. *Macromolecules* **1991**, *24*, 5599.

(42) Risse, W.; Grubbs, R. H. *J. Mol. Cat.* **1991**, *65*, 211.

(43) Nomura, K.; Schrock, R. R. *Macromolecules* **1996**, *29*, 540.

(44) Kanoaka, S.; Grubbs, R. H. *Macromolecules* **1995**, *28*, 4707.

(45) Komiya, Z.; Schrock, R. R. *Macromolecules* **1993**, *26*, 1387.

(46) Lynn, D. M.; Kanaoka, S.; Grubbs, R. H. *J. Am. Chem. Soc.* **1996**, *118*, 784.

(47) Watkins, D. M.; Fox, M. A. *Macromolecules* **1995**, *28*, 4939.

(48) Weck, M.; Schwab, P.; Grubbs, R. H. *Macromolecules* **1996**, *29*, 1789.

(49) Ivin, K. J. *Olefin Metathesis*; Academic Press: New York, 1983.

(50) Klavetter, F. L.; Grubbs, R. H. *J. Am. Chem. Soc.* **1988**, *110*, 7807.

(51) Gorman, C. B., Ph.D. Thesis, California Institute of Technology, 1991.

(52) Gorman, C. B.; Ginsburg, E. J.; Grubbs, R. H. *J. Am. Chem. Soc.* **1993**, *115*, 1397.

(53) Bott, D. C.; Brown, C. S.; Chai, C. K.; Walker, N. S.; Feast, W. J.; Foot, P. J. S.; Calvert, P. D.; Billingham, N. C.; Friend, R. H. *Synth. Met.* **1986**, *14*, 245.

(54) Conticello, V. P.; Gin, D. L.; Grubbs, R. H. *J. Am. Chem. Soc.* **1992**, *114*, 9708.

(55) Edwards, J. H.; Feast, W. J. *Polymer* **1980**, *21*, 595.

(56) Edwards, J. H.; Feast, W. J.; Bott, D. C. *Polymer* **1984**, *25*, 395.

(57) Pu, L.; Wagaman, M. W.; Grubbs, R. H. *Macromolecules* **1996**, *29*, 1138.

(58) Miao, Y. J.; Bazan, G. C. *J. Am. Chem. Soc.* **1994**, 9379.

(59) PPP was known to luminesce blue and LEDs were prepared using this insoluble material. see: Grem, G.; Leditzky, G.; Ullrich, B.; Leising, G. *Synth. Met.* **1992**, *51*, 383 and reference 60.

- (60) Grem, G.; Leditzky, G.; Ullrich, B.; Leising, G. *Adv. Mater.* **1992**, *4*, 36.
- (61) Recently, soluble forms of PPP that also luminesce blue have been reported.
Hamaguchi, M.; Yoshino, K. *Appl. Phys. Lett.* **1996**, *69*, 143.
- (62) Wagaman, M. W.; Bellmann, E.; Cucullu, M. E.; Grubbs, R. H. *J. Org. Chem.* , In Press.
- (63) Tasch, S.; Graupner, W.; Leising, G.; Pu, L.; Wagaman, M. W.; Grubbs, R. H. *Adv. Mater.* **1995**, *7*, 903.
- (64) Tasch, S.; Graupner, W.; Leising, G.; Pu, L.; Wagaman, M. W.; Grubbs, R. H. *Adv. Mater.* **1996**, *8*, 125.

Chapter 1

Synthesis of Benzobarrelene Monomers

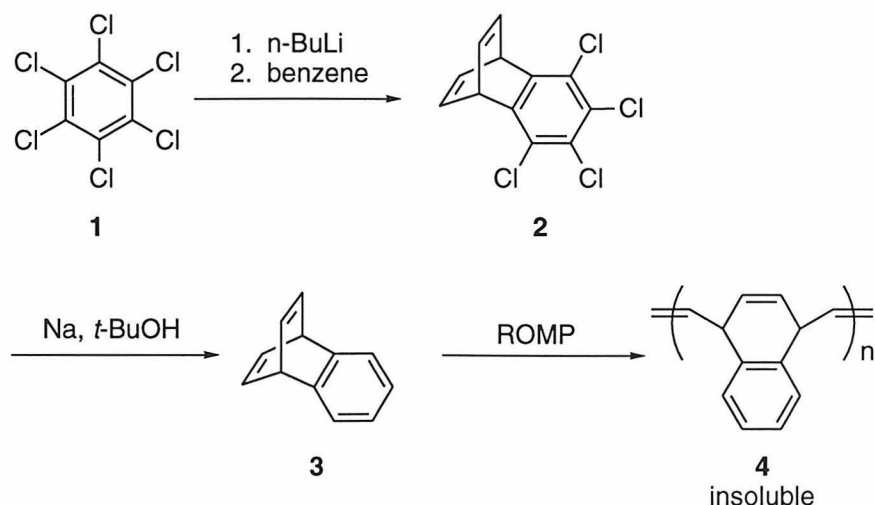
Abstract: In this chapter, two routes used for making alkylated benzobarrelene monomers are described. An undecyl substituted benzobarrelene was first prepared starting from *cis*-3,5-cyclohexadiene-1,2-diol, which serves as a benzene equivalent. Efforts to extend this route to an alkylated trifluorobenzobarrelene produced poor yields, so a new route was developed to synthesize these molecules. The procedure developed also allowed the synthesis of alkylated trichlorobenzobarrelene. It was found that the chlorines could be removed from this monomer to yield alkylated, unhalogenated benzobarrelenes in good yield.

Introduction

In general the monomers necessary for producing poly(1,4-naphthaleneylene)s (PNVs) and poly(*para*-phenyleneylene)s (PPVs) by ring-opening metathesis polymerization (ROMP) are derivatives of benzobarrelene and barrelene (bicyclo[2.2.2]octatriene) respectively. We first prepared benzobarrelene monomers, so their synthesis will be presented first.¹⁻⁴ Later, as the desire to make PPVs developed, a route to barrelenes was devised,^{5,6} which is described in Chapter 2.

Unsubstituted benzobarrelene, **3**, can be synthesized in two steps from the reaction of tetrachlorobenzyne with benzene,⁷ as shown in Scheme 1. The polymer obtained by ROMP of **3** is insoluble, however, and only low molecular weight material is obtained. Therefore, a synthesis of alkylated derivatives of benzobarrelene was desired, because the alkyl chains were expected to increase the ROMP polymers' solubility. Although the route shown in Scheme 1 is efficient for the preparation of **3**, original efforts to extend this method to the synthesis of benzobarrelene derivatives bearing alkyl substituents on the phenyl ring failed. The tetrachloro substituted benzobarrelene, **2**, was inert to alkyl Grignard reagents in the presence of either nickel or palladium catalysts,⁸ and all other procedures reported for the synthesis of benzobarrelene either involved

Scheme 1

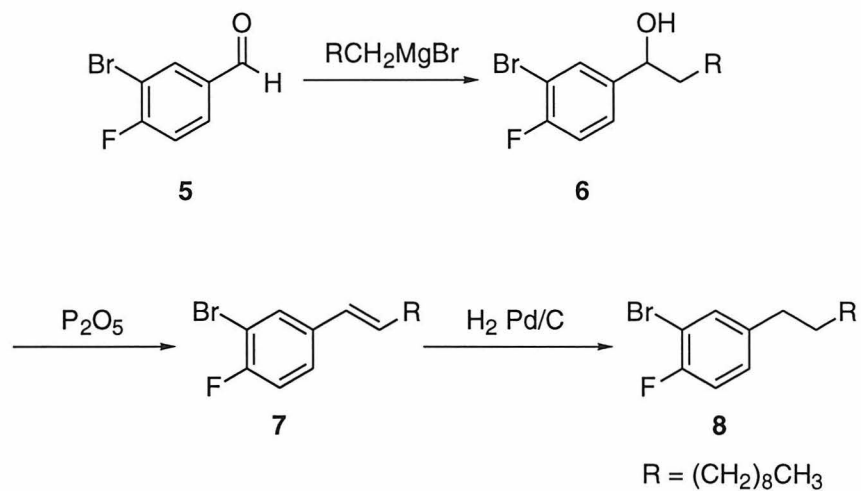


many synthetic steps or gave very low yields.⁹⁻¹³ Therefore, Lin Pu developed a new synthesis to obtain the desired alkyl substituted benzobarrelenes.¹ This method involved the addition of a substituted benzyne to a protected form of *cis*-3,5-cyclohexadiene-1,2-diol, followed by a base promoted thermal fragmentation.

Results and Discussion

Undecylbenzobarrelene Synthesis. The first benzobarrelene monomer I prepared, undecyl substituted benzobarrelene, **11**, was first synthesized using this method.² To make this monomer, an undecyl substituted benzyne precursor was first prepared as shown in Scheme 2. When commercially available 3-bromo-4-fluorobenzaldehyde was reacted with decyl Grignard, the alcohol, **6**, was obtained in high yield. Dehydration of **6** in hexane with P₂O₅ at 60 °C generated **7**, which was then hydrogenated to **8**.

Scheme 2

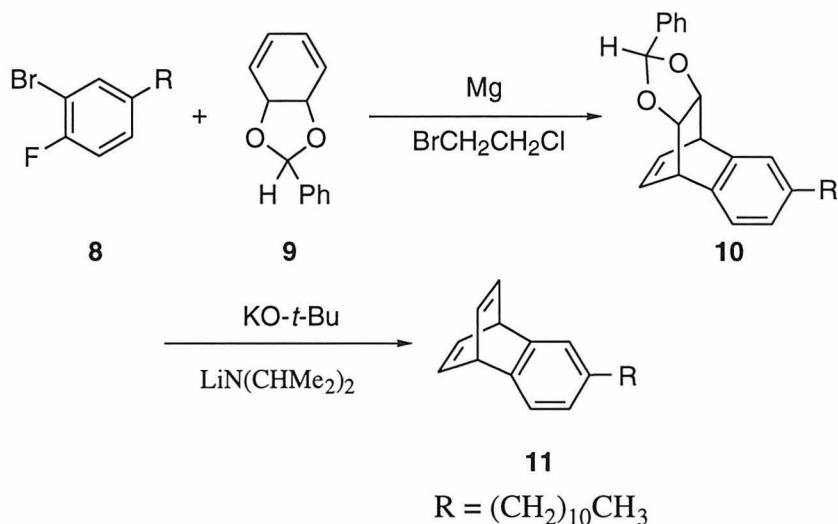


Reaction of **8** with Mg in the presence of the initiator 1-bromo-2-chloroethane generated the Grignard which then eliminated MgBrF to yield the alkylated benzyne. As shown in Scheme 3, this benzyne reacted with *cis*-1,2-benzylidenedioxy-3,5-

cyclohexadiene, **9**, to yield the Diels-Alder adduct **10**. Base promoted thermal elimination of benzoate from **10** then produced undecyl substituted benzobarrelene, **11**.

The previously reported acetal elimination procedure, which required 3 equivalents of potassium diisopropyl amide (KDA) to yield the unsubstituted and methyl substituted benzobarrelenes,¹ was found to be insufficient for elimination of benzoate from **10**. Because KDA decomposes quickly at the reaction temperature,¹⁴ the reaction of **10** was carried out by generating KDA slowly by adding LDA to a solution of the acetal

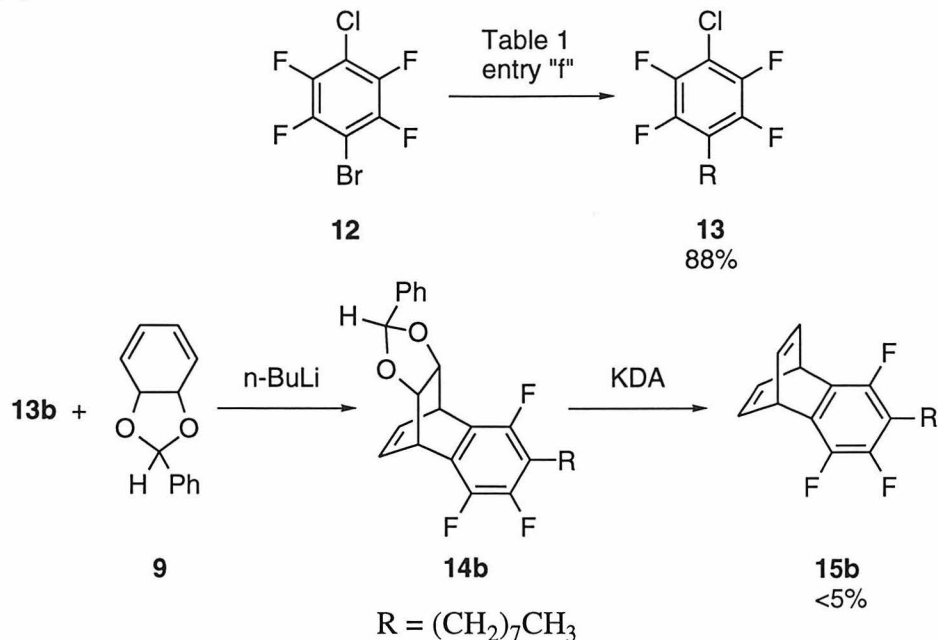
Scheme 3



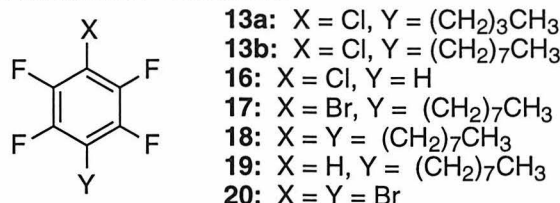
and potassium-*t*-butoxide in ether. Using this procedure, 15 equivalents of KDA were required to drive the reaction to completion, but the product, **11**, was obtained in good yields. The reaction also proceeds to completion with 7 equivalents of KDA in THF at 60 °C, but these conditions resulted in the production of side products, while the reaction in ether yielded only the desired benzobarrelene.

Alkylated Trifluorobenzobarrelene Synthesis: First Attempts. Alkylated trifluorobenzobarrelene, **15**, was desired so that the effect of the electron withdrawing fluorines on the band gap of PNV could be studied and compared to the unfluorinated polymer. However, attempts to synthesize this monomer using the method developed to

Scheme 4



prepare **11** produced only very low yields of **15**. As shown in Scheme 4 and Table 1, the necessary alkylated benzenes, **13** and **17**, were prepared by a modified procedure similar to that reported for the alkylation of bromonaphthalene.¹⁵ The main difference from the reported procedure was that a large excess of alkylbromide was added at low temperature to favor nucleophilic attack by the lithiated benzene over elimination of lithium fluoride to form the benzyne, which then forms a polymer. The yield is higher when **12** is the starting material, rather than **20**, since bromine can be selectively exchanged for lithium in the presence of chlorine, thereby minimizing the formation of dialkylated products. Reaction of 1-bromo-4-octyltetrafluorobenzene, **17**, using magnesium to generate the benzyne as for the synthesis of **10**, produced only decomposition of the starting materials. However, a similar reaction, which used n-BuLi to generate the lithiated benzene from **13b** and subsequently the benzyne, produced **14b** in 40% yield. All attempts to convert **14b** to **15b** by base catalyzed fragmentation of the acetal essentially failed, however, with the best yield of **15b** being less than 5%.

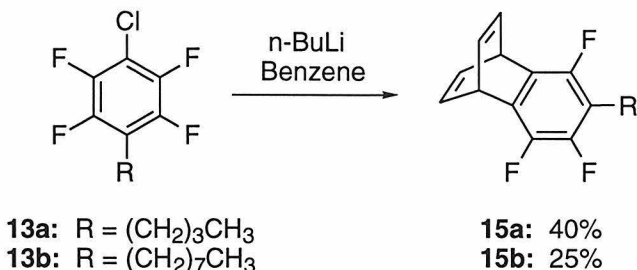
Table 1. Alkylation of tetrafluoro benzenes.

Entry	Reagents	Conditions*	Products
a [‡]	12 + 1 eq. n-BuLi	rt	polymer [†] <5% 13a
b	12 + 1 eq. n-BuLi	0 °C to rt	polymer <5% 13a
c	12 + 1 eq. n-BuLi	-78 °C to rt	polymer <5% 13a
d	12 + 1 eq. n-BuLi 5 eq. n-BuBr	-78 °C to -50 °C 7 hours	<5% 13a 16
e	12 + 1 eq. n-BuLi 10 eq. n-BuBr	-78 °C to rt overnight	88% 13a
f	12 + 1 eq. n-BuLi 10 eq. n-octylBr	-78 °C to rt overnight	88% 13b
g	20 + 1 eq. n-BuLi 10 eq. n-octylBr	-78 °C to rt overnight	63% 17

[‡]) Conditions reported for alkylation of bromonaphthalene¹⁵ *) The first temperature listed indicates the temperature at which the BuLi and alkylbromide were added. The second temperature indicates when water was added to quench the reaction. [†]) Product **13a** was observed by ¹H NMR for all reactions that formed mostly polymer.

To avoid the acetal elimination step and shorten the overall synthesis, Diels-Alder reaction of the benzyne of **13a** with benzene was carried out as reported for the synthesis of tetrachlorobenzobarrelene, **2**.⁷ As shown in Scheme 5, this method produced butyltrifluorobenzobarrelene, **15a**, in 40-45% yield, as determined by ¹H NMR. Because the products were not separable by column chromatography, purification was attempted by distillation. This resulted in isolation of some **15a**, but retro Diels-Alder decomposition of the benzobarrelene reduced the yield of isolated product to 10%. Sufficient monomer was obtained for use in polymerizations, but more importantly, **15a** made by this route was instrumental to the discovery of a better polymerization system as

Scheme 5



described in Chapter 3. When the analogous Diels-Alder reaction was carried out with the octyl substituted benzene, **13b**, the yield of benzobarrelene was only 25%, as determined by 1H NMR. As with **15a**, separation by column chromatography was difficult and distillation led to mostly decomposition, which was worse in the case of **15b** due to its higher distillation temperature.

A Useful Route to Alkylated Benzobarrelenes. Having tested the familiar and traditional routes to benzobarrelene with little success, I decided to revisit the problem of alkylating the readily available tetrachlorobenzobarrelene,⁷ **2**, and the related halotrifluorobenzobarrelene (halo = chlorine or bromine),¹⁶ **21**. As mentioned earlier, many previous attempts at alkylating **2** had been unsuccessful. However, it seemed that the procedure developed for the alkylation of dihalotetrafluorobenzene to produce **13** could be well suited to synthesizing the alkylated benzobarrelenes as well.

The major difference between alkylating **12** and alkylating **2** and **21** was the fact that the alkylated benzobarrelene products could not be purified by distillation since retro Diels-Alder decomposition occurs at high temperatures. The products are also difficult to purify by column chromatography and are generally not crystalline. With these limitations in mind, the best solution was to develop a reaction with very high yields. As shown in Table 1, alkylation of **12** was accomplished in good yields, but enough side products formed that distillation of the product mixture was still required. Therefore, alkyl iodides were used instead of the bromides since iodide is a better leaving group. Iodides had not been used to make **13** since their higher boiling points would have made

separation from the alkylated benzenes more difficult. This problem was expected to be reduced for the benzobarrelenes, however, since they contain six more carbons than the corresponding alkylated benzenes.

This approach, shown in Scheme 6, worked well for the alkylation of both **2** and **21**.^{3,4} As listed in Table 2, a variety of alkyl iodides can be used, with only the one branched on the carbon alpha to the iodine-substituted carbon producing low yields, presumably due to the competing elimination reaction. In the other cases, as long as all reagents were dried thoroughly, only the desired product was observed by ¹H NMR. The excess iodide present in these reactions was removed by distillation at reduced pressure, and the alkylated benzobarrelene products were separated from all remaining impurities, which were minimal, using a silica gel column. In all cases, only a single alkylated product was observed. This was not surprising for the trifluorobenzobarrelenes since alkylation should only occur by displacement of chlorine. For **2**, however, alkylation could conceivably occur by displacement of a chlorine in either the 3- or 4- position, or multiple alkylation could occur. In fact, only products of displacement of the chlorine in the 4-position were observed.

Scheme 6

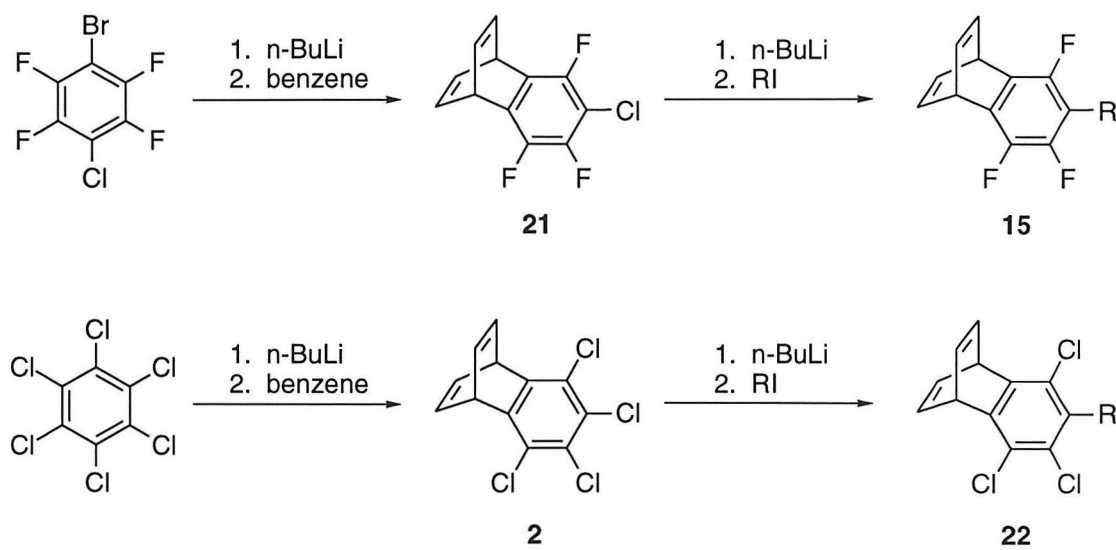
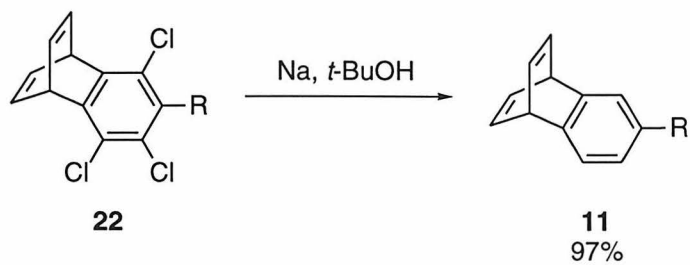


Table 2. Results of alkylation of **2** and **21**.

product	alkyl iodide	% yield
15a	I(CH ₂) ₃ CH ₃	88
15b	I(CH ₂) ₇ CH ₃	91
15c	I(CH ₂) ₂ CH(CH ₃) ₂	83
22a	I(CH ₂) ₇ CH ₃	78
22b	I(CH ₂) ₁₀ CH ₃	92
22c	I(CH ₂) ₂ CH(CH ₃) ₂	86
22d	I(CH ₂) ₂ CH(CH ₃)(CH ₂) ₃ CH(CH ₃) ₂	90
22e	ICH ₂ CH(CH ₂ CH ₃)(CH ₂) ₃ CH ₃	5

In addition to providing a short, high yielding synthesis of **15** and **22**, this route also allowed a shorter, more economical synthesis of **11**. As with tetrachlorobenzobarrelene, the chlorines can be removed from **22** in high yield as shown in Scheme 7. Conversion to the unhalogenated benzobarrelene also offered confirmation of the substitution pattern of **22**. Since the products obtained by dechlorination of **22** were found to have a ¹H NMR spectrum identical to that observed for **11** made by the previously described *cis*-3,5-cyclohexadiene-1,2-diol route,² **22** was substituted only in the position shown in Schemes 6 and 7.

Scheme 7

Conclusions

Several alkylated benzobarrelenes were prepared for the synthesis of poly(naphthalenevinylene)s (PNVs). While the route developed for the synthesis of alkylated benzobarrelenes from *cis*-3,5-cyclohexadiene-1,2-diol allowed preparation of an undecyl substituted benzobarrelene, this route produced very poor yields of alkylated trifluorobenzobarrelenes, **15**. These molecules were instead prepared by a new route that also allowed the synthesis of alkylated trichlorobenzobarrelenes, **22**. Removal of the chlorines from **22** produced alkylated, unhalogenated benzobarrelene in good yield, thus making the synthesis of **11** from *cis*-3,5-cyclohexadiene-1,2-diol obsolete.

Experimental

General Methods and Materials. NMR spectra were recorded on a QE Plus-300 MHz (300.1 MHz ¹H; 75.33 MHz ¹³C) spectrometer. Infrared spectra were recorded using a Perkin-Elmer 1600 series FT-IR spectrometer. Elemental analyses were performed by Oneida Research Corporation or Mid-West Microlab. High resolution mass spectra were obtained from UC Riverside Mass Spectrometry Facility. Ether was dried with sodium benzophenone. THF, hexane and benzene were dried by passing through activated alumina columns. Grignard reagents, lithium reagents, alkylhalides, 3-bromo-4-fluoro-benzaldehyde, 1,4-dihalotetrafluorobenzenes, lithium diisopropylamide, and potassium *t*-butoxide were purchased from Aldrich and used without further purification. Benzobarrelene **2** was prepared as previously reported⁷ and **21** was prepared by the synthesis described for bromotrifluorobenzobarrelene¹⁶ and purified by column chromatography (silica gel/hexane).

1-(3'-Bromo-4'-fluorophenyl)-undecanol (6). Under argon, decyl magnesium bromide (1.0 M ether solution, 100.8 mL) was added to a dry ether solution of 3-bromo-4-fluoro-benzaldehyde (20.1 g, 0.099 mol, 0.99 M) at 0 °C over 20 min. After the addition was complete, the reaction mixture was stirred at 0 °C for an additional 30 min

and then at room temperature for 2 hours. An aqueous solution of HCl (1.82 M, 100 mL) was then added to quench the reaction at 0 °C, and a white precipitate was formed. The mixture was extracted with ether (3 x 200 mL) and dried over Na₂SO₄. After filtration and removal of the solvent, the resulting product was dissolved in benzene and dried under vacuum. A yellow oil, **6**, was obtained in quantitative yield. ¹H NMR (CDCl₃,) δ 7.55 (dd, J = 9, 1 Hz, 1H), 7.23 (m, 1 H), 7.08 (t, J = 9 Hz, 1H), 4.64 (m, 1 H), 1.70 (m, 2H), 1.26 (br, 16H), 0.88 (t, J = 7 Hz, 3H). ¹³C NMR (CDCl₃) δ 158.1 (d, J_{C-F} = 981.6 Hz), 142.2 (d, J_{C-F} = 14.1 Hz), 130.8, 126.3 (d, J_{C-F} = 28.2 Hz), 116.1 (d, J_{C-F} = 88.2 Hz), 108.8 (d, J_{C-F} = 84 Hz), 73.24, 39.08, 31.85, 29.55, 29.49, 29.42, 28.28, 25.56, 22.63, 14.03. Exact mass (EI), m/e calcd for C₁₇H₂₆BrFO: 344.1151, obsd: 344.1159.

2-Bromo-1-fluoro-4-(1'-undecenyl)benzene (7). Under argon, a hexane (dry) solution of **6** (34.11 g, 0.099 mol, 0.40 M) was added, over 3.5 hours via an addition funnel, to a round bottom flask containing P₂O₅ (47 g, 0.33 mol) in refluxing hexane (dry, 250 mL). The resulting reaction mixture was refluxed for another 20 min. After filtration and removal of the solvent, ¹H NMR spectroscopy showed the formation of **7** with < 5% impurity. The crude product was used for the next reaction without further purification. ¹H NMR (CDCl₃,) δ 7.52 (dd, J = 9 Hz, 1 Hz, 1H), 7.20 (m, 1H), 7.02 (t, J = 9 Hz, 1H), 6.20 (m, 2H), 2.19 (q, J = 7 Hz, 2H), 1.45 (br m, 2H), 1.27 (br, 12H), 0.88 (t, J = 7 Hz, 3H). ¹³C NMR (CDCl₃,) δ 157.9 (d, J_{C-F} = 981 Hz), 135.6 (d, J_{C-F} = 16.2 Hz), 132.4 (d, J_{C-F} = 6.6 Hz), 130.5, 127.3, 126.2 (d, J_{C-F} = 27.3 Hz), 116.2 (d, J_{C-F} = 89.7 Hz), 109.0 (d, J_{C-F} = 86.7 Hz), 32.97, 31.93, 29.62, 29.56, 29.51, 29.38, 29.26, 22.72, 14.11. Exact mass, m/e calcd for C₁₇H₂₄BrF: 326.1045, obsd: 326.1049.

2-Bromo-1-fluoro-4-undecylbenzene (8). A mixture of **7** (0.094 mol) and 10% Pd/C (398 mg) in ethyl acetate (200 mL) was stirred under a hydrogen balloon for > 12 hours and filtered through celite. The solvent was then removed under vacuum. The resulting orange oil was distilled between 141 °C/140 mtorr and 148 °C/130 mtorr to yield a colorless oil, **8** (95%). The isolated yield of **8** based upon 3-bromo-4-fluoro-

benzaldehyde was 90%. ^1H NMR (CDCl_3 ,) δ 7.35 (dd, $J = 9, 1$ Hz, 1H), 7.05 (m, 1H), 7.00 (t, $J = 9$ Hz, 1H), 2.55 (t, $J = 9$ Hz, 2H), 1.58 (br m, 2H), 1.29 (br, 16H), 0.89 (t, $J = 7$ Hz, 3H). ^{13}C NMR (CDCl_3) δ 157.3 (d, $J_{\text{C}-\text{F}} = 972$ Hz), 140.2 (d, $J_{\text{C}-\text{F}} = 17.1$ Hz), 133.0, 128.6 (d, $J_{\text{C}-\text{F}} = 26.7$ Hz), 115.9 (d, $J_{\text{C}-\text{F}} = 87.9$ Hz), 108.5 (d, $J_{\text{C}-\text{F}} = 81.6$ Hz), 34.89, 31.97, 31.41, 29.69, 29.61, 29.48, 29.41, 29.18, 22.74, 14.12. Exact mass (EI), m/e calcd for $\text{C}_{17}\text{H}_{26}\text{BrF}$: 328.1202, obsd: 328.1211.

6-Undecyl-1,2,3,4-tetrahydro-2,3-(benzylidenedioxy)-1,4-ethenonaphthalene (10).

In a dry box, a THF (dry, 30 mL) solution of **8** (12.6 g, 0.038 mol) and 1-bromo-2-chloroethane (5.75 g, 0.040 mol) was loaded into a 50 mL syringe. Using a syringe pump, this solution was added over 3 hours to a THF (dry, 50 mL) solution of 1,2-benzylidenedioxy-3,5-cyclohexadiene (3.79 g, 0.019 mol) and magnesium (4.5 g, 0.185 mol) at 60 °C (oil bath temperature). During the addition, gas was evolved. After the addition was complete, the reaction mixture was continuously heated at 60 °C for 12 hours. The solvent was then removed under vacuum. The resulting residue was loaded onto a plug of silica gel (175 mL) and eluted with 1200 mL of ether. After removal of ether, a yellow solid was obtained. The product was recrystallized by partially dissolving in warm pentane and cooling at -50 °C for 12 hours. Filtration of the cold mixture afforded light yellow crystals of **10** (4.91 g, 60% yield based upon 1,2-benzylidenedioxy-3,5-cyclohexadiene). ^1H NMR (CDCl_3 ,) δ 7.54 (m, 2H), 7.39 (m, 3H), 7.16 (d, $J = 7.2$ Hz, 1H), 7.10 (s, 1H), 6.96 (d, $J = 7.2$ Hz, 1H), 6.62 (m, 2H), 5.80 (s, 1H), 4.34 (s, 2H), 4.26 (s, 2H), 2.57 (t, $J = 7.7$ Hz, 2H), 1.59 (br, 2H), 1.27 (br, 16H), 0.89 (t, $J = 6.6$ Hz, 3H). ^{13}C NMR (CDCl_3) δ 141.3, 140.4, 137.6, 136.5, 133.3, 133.0, 129.7, 128.3, 127.5, 126.2, 125.1, 124.6, 106.0, 79.80, 79.75, 45.34, 44.88, 35.77, 31.91, 31.65, 29.67, 29.63, 29.58, 29.51, 29.43, 29.35, 22.69, 14.13. Exact mass (EI), m/e calcd for $\text{C}_{30}\text{H}_{38}\text{O}_2+\text{H}^+$: 431.2950, obsd: 431.2964. Anal. Calcd for $\text{C}_{30}\text{H}_{38}\text{O}_2$: C, 83.68; H, 8.89. Found: C, 83.48; H, 8.84.

6-Undecyl-1,4-dihydro-1,4-ethenonaphthalene (11). Method A. Under argon,

a slurry of lithium diisopropyl amide (LDA, 7.70 g, 71.8 mmol) in diethyl ether (dry, 50 mL) was added to a mixture of **10** (2.03 g, 4.68 mmol) and potassium *t*-butoxide (7.91 g, 70.5 mmol) in diethyl ether (dry, 50 mL) at 60 °C (oil bath temperature) over 5 hours. After the addition was complete, the reaction mixture was kept at 60 °C for another hour. The resulting dark brown slurry was cooled with an ice bath, and water (4 mL) was added to quench the reaction. The mixture was then filtered through a plug of silica gel (100 mL) and eluted with 800 mL of ether. After removal of ether, the residue was loaded onto a silica gel column (7" x 2"), and eluted with hexane. The product was collected from 335 mL to 1300 mL. The solvent was removed to give a light yellow liquid, **11** (1.18 g, 81.6%). **Method B:** Compound **22b** was converted to **11** using the procedure previously reported for dechlorination of tetrachlorobenzobarrelene, **2**.⁷ A reaction starting with 0.5 g of **22b** produced 97% yield of **11** and a reaction starting with 15 g of **22b** produced 80% yield of **11** following purification by column chromatography (silica gel/hexane). Both reactions were heated overnight instead of the 4 hours reported for making **3**. ¹H NMR (, CDCl₃) δ 7.06 (d, J = 7.2 Hz, 1H), 7.02 (s, 1H), 6.88 (t, J = 3.6 Hz, 4H), 6.77 (d, J = 6.9 Hz, 1H), 4.89 (m, 2H), 2.51 (t, J = 7.8 Hz, 2H), 1.55 (p, J = 7.1 Hz, 2H), 1.27 (br, 16H), 0.89 (t, J = 6.6 Hz, 3H). ¹³C NMR (CDCl₃) δ 147.5, 144.8, 139.8, 139.5, 138.2, 122.9, 122.7, 121.7, 49.15, 48.74, 35.64, 31.91, 31.68, 29.67, 29.63, 29.59, 29.53, 29.48, 29.34, 22.69, 14.13. Exact mass (EI), m/e calcd for C₂₃H₃₂: 308.2504, obsd: 308.2505. Anal. calcd for C₂₃H₃₂: C, 89.54; H, 10.46. Found: C, 89.47; H, 10.43.

1-chloro-4-butyltetrafluorobenzene (13a). Under argon, 1-bromo-4-chloro-2,3,5,6-tetrafluorobenzene was dissolved in 83 mL of dry THF. This solution was cooled to -78 °C in a dry ice/acetone bath and then 12.1 mL of 1.57 M butyl lithium in hexane was added over 15 min. After stirring this solution for 45 min, 20.5 g (0.190 mol) of butyl bromide was added over 10 min while maintaining the bath temperature at -78 °C. The solution was then slowly warmed to rt over 18 hours (temperature = -10 °C after 5 h).

After removing the solvent and some of the excess butyl bromide by rotary evaporator, followed by distillation at 64 °C to 70 °C, the remaining residue was dissolved in methylene chloride and extracted with a mixture of 10 mL of water and 4 mL of 1 M HCl. The organic layer was removed, and the aqueous layer was extracted with 3x35 mL of ether. All organic fractions were then combined and dried over magnesium sulfate. The solvent was removed using a rotary evaporator, and the resulting residue was distilled under vacuum. Compound **13a** was collected as a colorless oil at 5 torr/56 °C. Yield = 4.023 g (88%). ¹H NMR (500 MHz, CDCl₃) δ 2.72 (tt, J_{H-H} = 7.5 Hz, J_{H-F} = 1.6 Hz, 2H), 1.57 (quintet, J = 7.5 Hz, 2H), 1.36 (sextet, J = 7.38 Hz, 2H), 0.93 (t, J = 7.2 Hz, 3H). ¹⁹F NMR (470.56 MHz, CDCl₃, referenced on CFCl₃ in benzene = 0.0 ppm) δ -142.52 (m, 2F), -143.82 (m, 2F). Mass Spec. calcd for C₁₀H₉F₄Cl: 240.032, found: 240.

1-chloro-4-octyltetrafluorobenzene (13b). Compound **13b** was prepared by the same procedure used for **13a**. Distillation yielded **13b** as a colorless liquid at 90 °C - 96 °C/200 mtorr with more product collected at the high temperature. 89% yield. ¹H NMR (500 MHz, CDCl₃) δ 2.7116 (t, J = 7.6 Hz, 2H), 1.58 (pentad, J = 7.4 Hz, 2H), 1.29 (m, 10H), 0.88 (t, J = 7.0 Hz, 3H). ¹⁹F NMR (470.56 MHz, CDCl₃, referenced on CFCl₃ in benzene = 0.0 ppm) δ -142.50 (m, 2F), -143.79 (m, 2F). Mass Spec. calcd for C₁₄H₁₇F₄Cl: 296.095, found: 296.

6-octyl-5,7,8-trifluoro-1,2,3,4-tetrahydro-2,3-(benzylidenedioxy)-1,4-ethenonaphthalene (14b). Compound **13b** (1.1187 g) and compound **9** (0.5045 g) were each dissolved in 5 mL of ether in separate flasks and then the two solutions were combined. After cooling this combined solution to 3 °C 2.53 mL of 1.57 M n-butyl lithium was added over 25 minutes. The reaction was stirred at 3 - 5 °C for an additional 20 minutes and then at room temperature for 1.5 hours. The flask was then cooled to 5 °C and 1.25 mL of 1.57M n-butyl lithium was added over 15 minutes. After stirring for 30 minutes at 5 °C the reaction was quenched by adding 2 mL of water. The total

mixture was added into 30 mL of water and this was extracted with (4 x 100 mL) of ether. After drying over magnesium sulfate, the ether was evaporated to yield a viscous oil. The product could not be recrystallized, so it was purified by column chromatography. The silica gel column was eluted first with 5% ethyl acetate/hexane then 10% ethyl acetate/hexane then 20% ethyl acetate/hexane. Product was obtained as 0.4483 g (40%) of a viscous yellow oil after removal of solvent. ¹H NMR (300 MHz, CDCl₃) δ 7.50 (m, 2H), 7.38 (m, 2H), 6.61 (m, 2H), 5.80 (s, 1H), 4.67 (m, 2H), 4.33 (br s, 2H), 2.64 (t, J = 7.7 Hz, 2H), 1.56 (m, 2H), 1.27 (m, 12H), 0.88 (t, J = 6.5 Hz, 3H). ¹⁹F NMR (470.56 MHz, CDCl₃, referenced on CFCl₃ in benzene = 0.0 ppm) δ -129.60 (d, J = 18.8 Hz, 1F), -141.67 (d, J = 22 Hz, 1F), -150.54 (t, J = 20.5 Hz, 1F).

5-butyl-1,8-dihydro-1,8-etheno3,4,6-trifluoronaphthalene (15a) by reaction of 13a with benzene. Under argon, 0.5071 g of **13a** was dissolved in 12.5 mL of ether. This solution was cooled to -78 °C in a dry ice/acetone bath and then 1.4 mL of 1.57 M n-BuLi in hexanes was added over 15 min. The solution was stirred for 40 min during which time the bath temperature rose to 60 °C. Next, 83 mL of dry benzene was added over 1 hour while warming the solution to 10 °C. The solution was then stirred overnight and then heated at 35 °C for 2.5 hours. After this, 200 mg of ammonium chloride was added. After evaporating the solvent, the remaining residue was added into 15 mL of water and 4 mL 1M HCl and then extracted with 5x30 mL of ether. The combined ether layers were dried with magnesium sulfate. Removing the ether yielded a yellow oil. ¹H NMR of this oil showed 43% **15a**. The oil was distilled under vacuum and a few drops of **15a** were collected as a colorless oil at 86 °C/10 mtorr. The remainder of the oil formed a dark tar that looked like polymer by ¹H NMR. ¹H NMR (500 MHz, CDCl₃) δ 6.89 (m, 4H), 5.26 (m, A-B splitting, 2H), 2.57 (t, J = 7.6 Hz, 2H), 1.50 (pentad, J = 7.6 Hz, 2H), 1.33 (sextet, J = 7.5 Hz, 2H), 0.91 (t, J = 7.3 Hz, 3H). ¹⁹F NMR (470.56 MHz, CDCl₃, referenced on CFCl₃ in benzene = 0.0 ppm) δ -153.69 (t, J = 20.5 Hz, 1F), -145.84 (d, J = 22.1 Hz, 1F), -133.46 (d, J = 17.9 Hz).

5-octyl-1,8-dihydro-1,8-etheno3,4,6-trifluoronaphthalene (15b) by alkylation of 21. The procedure was analogous to that described for the synthesis of **22**. Compounds **15a** and **15c** were also prepared by this method and had nearly identical NMR spectra except for the alkyl region of the spectrum. ^1H NMR (500 MHz, CDCl_3): δ 6.89 (m, 4H), 5.27 (m, 2H), 2.56 (t, J = 8 Hz, 2H), 1.52 (m, 2H), 1.27 (br m, 12H), 0.88 (t, J = 7 Hz, 3H). ^{19}F NMR (500 MHz, CDCl_3): δ -133.5 (d, J = 20 Hz, 1F), -145.8 (d, J = 24 Hz, 1F), -153.7 (d, J = 22 Hz, 1F). Anal. Calcd for $\text{C}_{20}\text{H}_{23}\text{F}_3$: C, 74.97; H, 7.24. Found: C, 74.85; H, 7.34.

1-bromo-4-octyltetrafluorobenzene (17). Compound **17** was prepared by the same procedure used for **13**. Distillation yielded **17** as a colorless liquid at 90 °C - 96 °C/200 mtorr. Total yield was 3.5 g of **17** (63%). ^1H NMR (500 MHz, CDCl_3) δ 2.7116 (t, J = 7.6 Hz, 2H), 1.58 (pentad, J = 7.4 Hz, 2H), 1.29 (m, 10H), 0.88 (t, J = 7.0 Hz, 3H). ^{19}F NMR (470.56 MHz, CDCl_3 , referenced on CFCl_3 in benzene = 0.0 ppm) δ -134.82 (m, 2F), -143.24 (m, 2F). Mass Spec. calcd for $\text{C}_{14}\text{H}_{17}\text{F}_4\text{Br}$: 340.044, found: 340 and 342.

5-alkyl-1,8-dihydro-1,8-etheno3,4,6-trichloronaphthalene (22). Under argon, 14 g of tetrachlorobenzobarrlene, **2**, were dissolved in 150 mL of dry THF and cooled to -78 °C. To this was added 31.5 mL of 1.6M n-BuLi over 20 minutes. The reaction, which turned dark purple, was stirred for 30 minutes. 10 equivalents of an alkyl iodide was added then to yield a cloudy mixture, or a solid with the higher melting iodides. The reaction was then removed from the dry ice acetone bath and allowed to warm to room temperature over several hours. After stirring overnight, THF was removed on by rotary evaporator and the remaining solution was diluted with 100 mL CHCl_3 . This solution was extracted with HCl (120 mL of 0.2M HCl) and brine (2x100 mL). After removing solvent by rotary evaporator the excess iodide was removed by distillation. To prevent retro Diels-Alder reaction of the benzobarrelene, the heating bath temperature was kept below 100 °C. The remaining oil was further purified by column chromatography

(silica/hexane) to yield a clear viscous liquid in 80 - 90% yield. Data presented is for undecyl substituted **22b**. Compounds **22a** and **22c-e** were also prepared by this method and had nearly identical NMR spectra except for the alkyl region of the spectrum. ¹H NMR (CDCl₃): δ 6.91 (m, 4H), 5.43 (m, 2H), 2.83 (t, J = 9 Hz, 2H), 1.25 (bs, 18H), 0.88 (t, J = 7.5 Hz, 3H). Anal. Calcd for C₂₃H₂₉Cl₃: C, 67.08; H, 7.10. Found: C, 67.17; H, 7.04.

References and Notes

- (1) Pu, L.; Grubbs, R. H. *J. Org. Chem.* **1994**, *59*, 1351.
- (2) Pu, L.; Wagaman, M. W.; Grubbs, R. H. *Macromolecules* **1996**, *29*, 1138.
- (3) Wagaman, M. W.; Bellmann, E.; Grubbs, R. H. *Phil. Trans. R. Soc. Lond. A* **1997**, *355*, 727.
- (4) Wagaman, M. W.; Grubbs, R. H. *Synth. Met.* **1997**, *84*, 327.
- (5) Wagaman, M. W.; Grubbs, R. H. *Macromolecules* **1997**, *30*, 3978.
- (6) Wagaman, M. W.; Bellmann, E.; Cucullu, M. E.; Grubbs, R. H. *J. Org. Chem.* , In Press.
- (7) Hales, N. J.; Heaney, H.; Hollinshead, J. H.; Singh, P. *Org. Synth.* **1979**, *59*, 71.
- (8) For a review on nickel and palladium complex catalyzed cross-coupling reactions of organometallic reagents with organic halides, see: Kumada, M. *Pure Appl. Chem.* **1980**, *52*, 669.
- (9) Balci, M.; Cakmak, O.; Harmandar, M. *Tetrahedron Lett.* **1985**, *26*, 5469.
- (10) Mazza, D. D.; Reinecke, M. G. *J. Org. Chem.* **1988**, *53*, 5799.
- (11) Kirahonoki, K.; Takano, Y. *Tetrahedron* **1969**, *25*, 2417.
- (12) Friedman, L.; Lindow, D. F. *J. Am. Chem. Soc.* **1968**, *90*, 2329.
- (13) Friedman, L. *J. Am. Chem. Soc.* **1967**, *89*, 3071.
- (14) Raucher, S.; Koolpe, G. A. *J. Org. Chem.* **1978**, *43*, 3794.
- (15) Merrill, R. E.; Negishi, E. *J. Org. Chem.* **1974**, *39*, 3452.
- (16) Brewer, J. P. N.; Eckhard, I. F.; Heaney, H.; Marples, B. A. *J. Chem. Soc. (C)* **1968**, 664.

Chapter 2

A New Efficient Synthesis of Substituted Bicyclo[2.2.2]octatrienes (Barrelenes)

Abstract: An efficient route to bicyclo[2.2.2]octatriene, barrelene, and substituted versions of this molecule has been developed starting from the benzene equivalent *cis*-3,5-cyclohexadiene-1,2-diol. Following the Diels-Alder reaction of this molecule with an activated acetylene, conversion of the diol to the final olefin was accomplished through formation of a thiocarbonate intermediate and subsequent reaction with 1,3-dimethyl-2-phenyl-1,3,2-diazaphospholidine (DPD). The synthesis developed allows a variety of barrelenes to be prepared in as few as three steps from commercially available starting materials.

Introduction

Since the synthesis of bicyclo[2.2.2]octatriene, barrelene, was first reported by Zimmerman,^{1,2} there has been considerable interest in the synthesis and study of this compound and its derivatives.³ Several syntheses of barrelene have been subsequently reported which allow this compound to be prepared by shorter routes than the original procedure.⁴⁻¹⁰ These routes have generally not been applied to the synthesis of substituted barrelenes, however. Conversely, methods employed for the synthesis of substituted barrelenes¹¹⁻²⁰ have generally not been applied to the synthesis of unsubstituted barrelene.²¹ One reason for this is that barrelenes such as dicyano- and bistrifluoromethylbarrelene are synthesized by the Diels-Alder reaction of highly activated acetylenes, dicyanoacetylene and hexafluoro-2-butyne, with benzene. This same procedure has not been used to prepare unsubstituted barrelene since acetylene is not sufficiently activated to undergo an efficient Diels-Alder reaction with benzene. In fact, while dicyanobarrelene¹⁵ is obtained in 63% yield by this procedure, bistrifluoromethylbarrelene¹¹⁻¹³ is produced in yields of only 8-10%.²² Following this trend further, Diels-Alder addition of the less activated, diester substituted acetylenes to benzene produces barrelene products only when the benzene derivative employed is also activated.^{20,23,24}



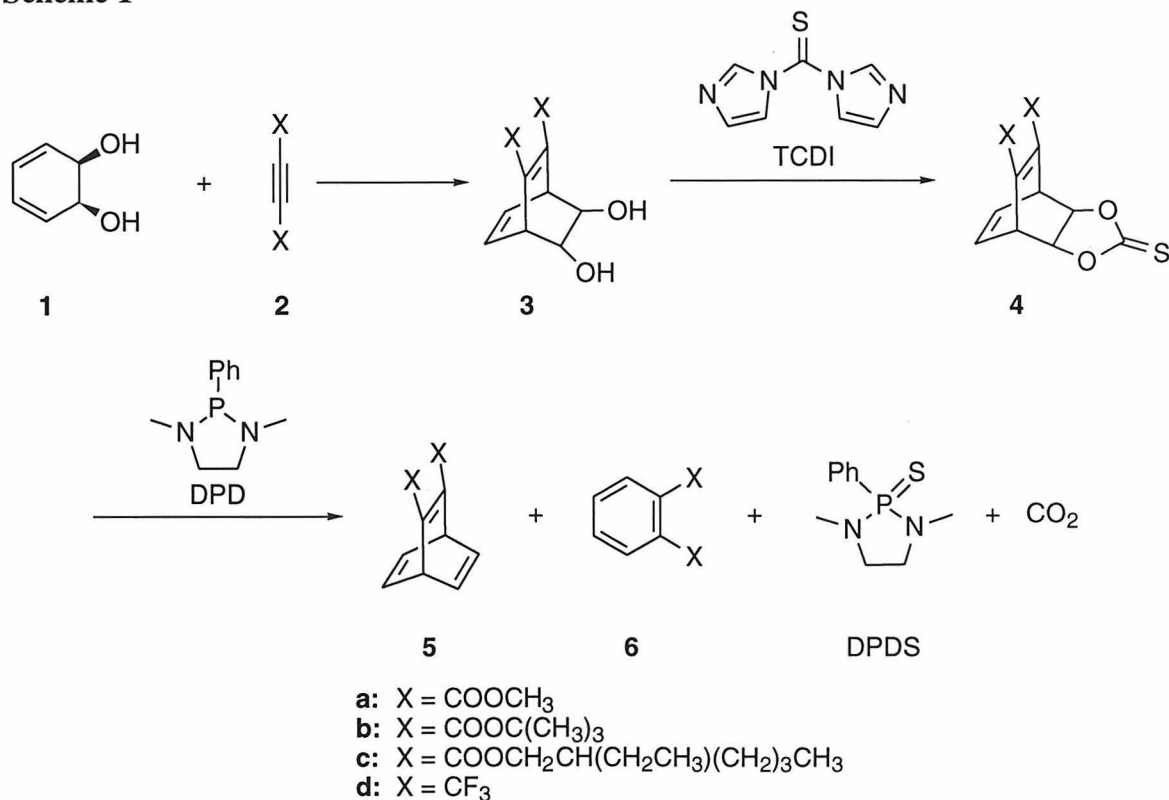
Barrelene

Since benzene is a poor diene for most dienophiles, we employed *cis*-3,5-cyclohexadiene-1,2-diol, or a protected form of this molecule, as a benzene equivalent. The route developed allows the preparation of a variety of barrelenes in as few as three steps from commercially available starting materials.

Results and Discussion

All syntheses were carried out in a similar manner with the Diels-Alder addition of an acetylene bearing electron withdrawing groups to the benzene equivalent *cis*-3,5-cyclohexadiene-1,2-diol, **1**, or the acetonide protected form of this molecule, **9**. The barrelenes were then obtained by conversion of the diol to the olefin. In cases where protection of the diol was not necessary, the Diels-Alder reaction was followed by conversion of the diol, **3**, to the thiocarbonate, **4**, using thiocarbonyldiimidazole (TCDI) as shown in Scheme 1. Conversion of **4** to barrelene was then accomplished using 1,3-dimethyl-2-phenyl-1,3,2-diazaphospholidine (DPD).^{25,26} In the case of **5d**, the product is volatile and can be obtained in pure form by vacuum transferring it out of the reaction mixture. Purification of **5a-c** can be accomplished by column chromatography or by a combination of column chromatography and recrystallization.^{26,27}

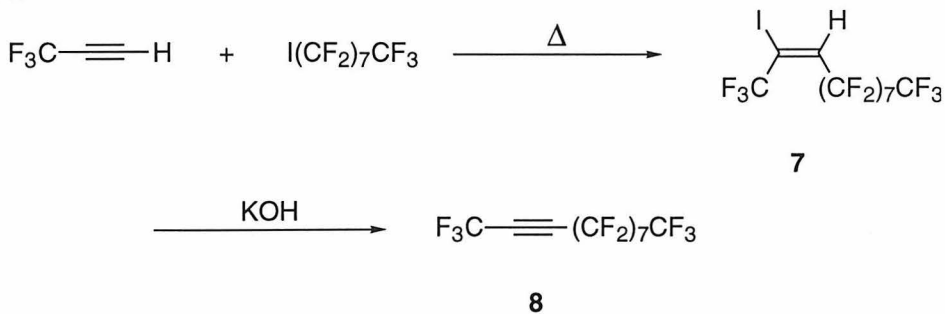
Scheme 1



Other methods to generate the final double bond either directly from the diol,^{28,29} or by base initiated thermal fragmentation of the benzaldehyde acetal as previously reported for benzobarrelene,^{30,31} failed. Fragmentation of the acetal using KDA led to complete decomposition of the starting material, and as previously observed for the synthesis of benzobarrelene, no reaction occurred when LDA was employed. In the case of direct reduction of the diol, only decomposition was observed when Ti⁰ reagents were employed²⁹ and the method reported by Barua et al.²⁸ produced only recovered starting material. An attempt to convert **4d** to **5d** using Ni(COD)₂³² resulted in complete consumption of the starting material, but yielded none of the desired product.

While the synthesis of **3a-d** was readily accomplished by direct reaction of an activated acetylene, **2**, with the unprotected diol, **1**, the synthesis of several other barrelenes was greatly improved by using a protected form of the diol, **9**. Using the acetonide has the dual advantage of protecting the diol from acid catalyzed decomposition to phenol and also activating the diene so that less reactive dieneophiles react more efficiently.³³⁻³⁵ Protection of the diol by thiocarbonate was also attempted, but rapid exothermic decomposition occurred when either TCDI or thiophosgene²⁶ was employed.

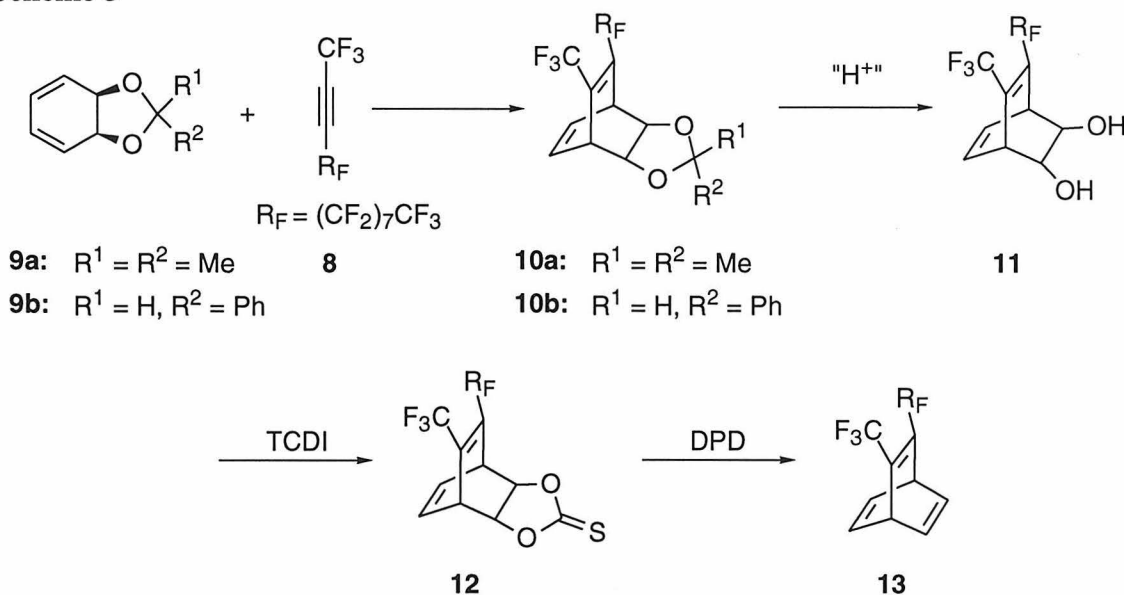
Scheme 2



To prepare a barrelene bearing a perfluorooctyl chain, the acetylene, **8**,³⁶⁻³⁸ was first synthesized as shown in Scheme 2, and this was then reacted with the acetal, **9**, as

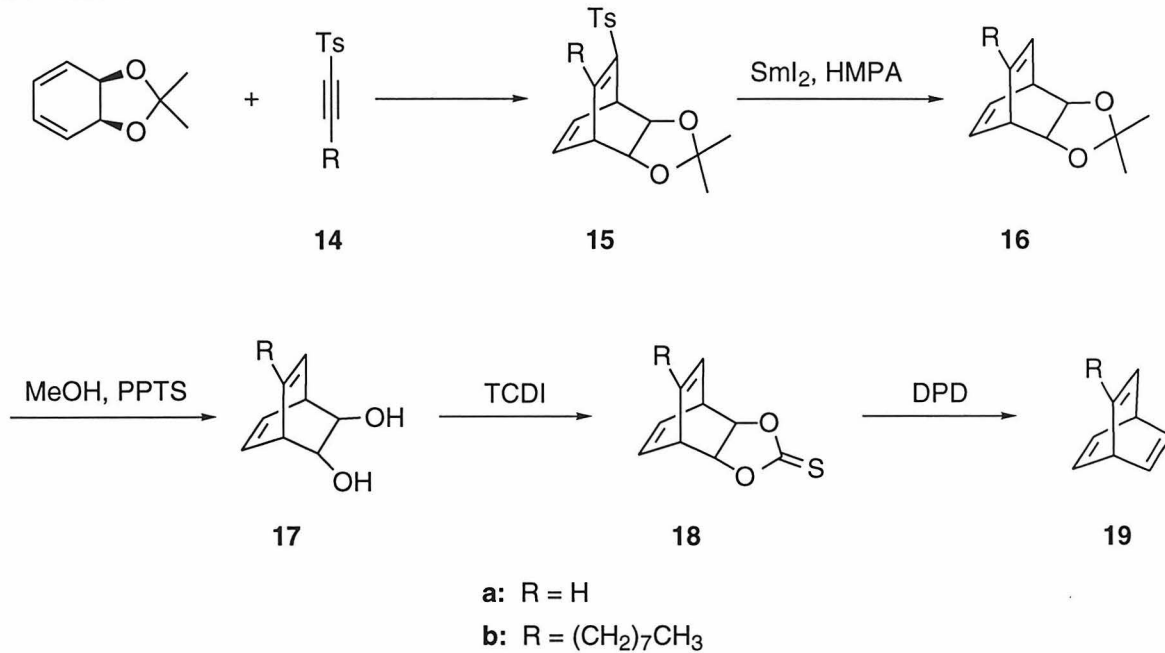
shown in Scheme 3. Use of **9** yielded the Diels-Alder adduct, **10**, in near quantitative yield in contrast to the reaction with **1** which resulted in decomposition to phenol, presumably due to the presence of residual hydrofluoric acid in **8**.³⁹ The acetonide protecting group was then removed under acidic conditions to yield the diol, **11**, in quantitative yield. To optimize the ease of performing and purifying this reaction and minimize the reaction time, several deprotection methods were tested. The fastest conversion was achieved using the dimethyl acetal, **10a**, and a 1:1 mixture of 6M HCl and dioxane. These conditions work well since the acetone generated boils off quickly, thus driving the reaction toward products. Methanol and pyridinium *p*-toluenesulfonate gave **11** in good yields, but these conditions required longer reaction times and periodic replenishment of methanol, which boiled off with the 2,2-dimethoxy propane produced. Deprotection of the benzaldehyde acetal, **10b**, required much longer reaction times since the benzaldehyde or benzaldehyde dimethyl acetal produced is much less volatile than the products of deprotection of **10a**. After the deprotection was complete, **11** was converted to barrelene **13** through the thiocarbonate, **12**.

Scheme 3



Synthesis of unsubstituted barrelene and octyl barrelene also required use of the protected diol, **9a**. The acetylenes, **14a,b**,^{40,41} activated by a *p*-toluenesulfone group, underwent the Diels-Alder reaction with **9a** as shown in Scheme 4. After the *p*-toluenesulfone group was removed by reductive desulfonylation,⁴² the diol was deprotected under acidic conditions as before, but in this case methanol and pyridinium *p*-toluenesulfonate were employed since the use of HCl resulted in decomposition. Using methanol was also an advantage since **17a** is rather soluble in water and is difficult to extract from the aqueous HCl. Formation of the final olefin bond was accomplished as previously described.

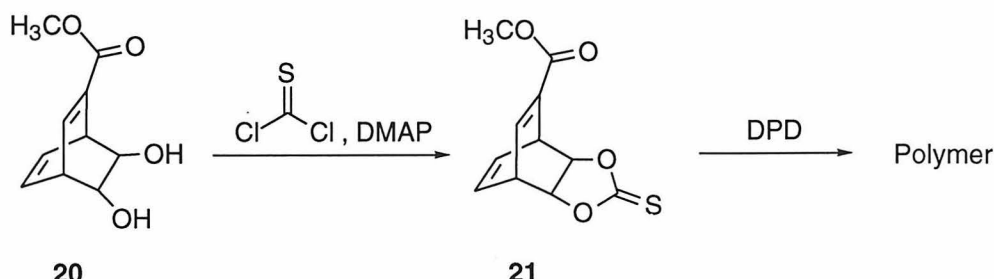
Scheme 4



Attempts to synthesize a monoester substituted barrelene by this route did not succeed. Starting from **9a** and methyl propiolate, the diol, **20**, was prepared by using the same procedure as for **17**. This intermediate, which was more heat sensitive than the other diols, was converted into the thiocarbonate, **21**, using thiophosgene and DMAP at 0 °C as shown in Scheme 5. Reaction of **21** with DPD under the same conditions employed

for the other thiocarbonates produced only polymeric products, presumably by reaction of the acrylate functionality.

Scheme 5



Conclusions

The synthesis presented here affords an efficient route to several substituted barrelenes in as few as three steps from commercially available starting materials, as well as a route to unsubstituted barrelenes. Reaction of activated acetylenes with *cis*-3,5-cyclohexadiene-1,2-diol or a protected form of this benzene equivalent generally afforded the Diels-Alder adduct in high yield. This intermediate was then converted to barrelenes by formation of the thiocarbonate followed by elimination of this moiety to yield the final olefin bond.

In addition to the barrelenes synthesized here, the route presented should allow the preparation of other related barrelenes and benzobarrelenes by using other dienophiles and/or any of the wide variety of substituted benzene equivalents similar to **1**.⁴³ We are currently exploring this possibility as well as the ring-opening metathesis polymerization of the compounds reported here.

Experimental

General Procedures. NMR spectra were recorded on a QE Plus-300 MHz (300.1 MHz ¹H; 75.49 MHz ¹³C) spectrometer or a Jeol JNM-GX400 (399.78 MHz ¹H,

100.53 MHz ^{13}C , 376.14 MHz ^{19}F) spectrometer as noted. Argon was purified by passage through columns of BASF R3-11 catalyst (Chemalog) and 4 Å molecular sieves (Linde). Elemental analyses were performed by Caltech Analytical Labs or Mid-West Microlab. High resolution mass spectra were obtained from UC Riverside Mass Spectrometry Facility.

Materials. THF and toluene were dried by passing through activated alumina columns. Acetylenes **2c**,⁴⁴ and **14a,b**^{40,41} and protected diols **9a,b**^{30,31,35} were prepared according to literature procedures. Hexamethylphosphoramide (HMPA) was purchased from Aldrich and dried over calcium hydride and then distilled under reduced pressure prior to use. 3,3,3-trifluoropropyne was purchased from PCR incorporated. *Cis*-3,5-cyclohexadiene-1,2-diol was obtained from ICI. Thiocarbonyldiimidazole (TCDI), 1,3-dimethyl-2-phenyl-1,3,2-diazaphospholidine (DPD), 2,2-dimethoxypropane, perfluorooctyliodide, pyridinium *p*-toluenesulfonate (PPTS), methyl propiolate, 2-ethyl hexanol, acetylenedicarboxylic acid, hexafluoro-2-butyne, and SmI₂ in THF were purchased from Aldrich and used without further purification except where noted otherwise.

Dimethyl-2,3-dihydroxy-5,7-bicyclooctadiene-5,6-dicarboxylate (3a). Under air, a 50 mL round bottom flask, RBF, was charged with 9 mL dimethylacetylenedicarboxylate (73.2 mmol) and 4.01 g (35.7 mmol) of *cis*-3,5-cyclohexadiene-1,2-diol. The solution was heated at 60 °C for 1 day. Excess acetylene was removed under vacuum to yield a viscous yellow oil. The oil was loaded onto a column containing 1000 mL of silica gel, and eluted with 1000 mL 50% ethyl acetate/hexane followed by 1000 mL 80% ethyl acetate/hexane and 1000 mL 90% ethyl acetate/hexane to yield two product isomers separately. Both isomers were light yellow oils initially, but the anti isomer became a waxy solid upon standing. Total yield of both isomers was 95% (8.61 g, 33.9 mmol). ^1H NMR (CDCl_3) anti isomer δ 6.47 (m, 2H), 4.21 (m, 2H), 3.89 (m, 2H), 3.78 (s, 6H), 2.64 (m, 2H, OH). syn isomer δ 6.28 (m, 2H),

4.20 (m, 2H), 3.81 (s, 6H), 3.78 (m, 2H), 3.25 (m, 2H). ^{13}C NMR (CDCl_3) anti δ 165.73, 140.01, 131.29, 66.46, 52.27, 46.14. syn δ 166.55, 139.45, 131.65, 65.87, 52.18, 45.86. FTIR anti 3430, 3001, 2955, 2848, 1716, 1646, 1604, 1437, 1401, 1356, 1280, 1223, 1168, 1147, 1093, 1061, 979, 881, 827, 803, 792, 775 cm^{-1} . HRMS Calcd for $\text{C}_{12}\text{H}_{15}\text{O}_6\text{H}$ (MH^+) 255.0865, found 255.0871. Anal. Calcd for $\text{C}_{12}\text{H}_{14}\text{O}_6$: C, 56.69; H, 5.55 Found: C, 56.14; H, 5.81.

Dimethyl-2,3-thiocarbonate-5,7-bicyclooctadiene-5,6-dicarboxylate (4a).

Compound **1a** (2.38 g, 9.35 mmol) and 1.94 g (90% pure, 9.80 mmol) of thiocarbonyldiimidazole, TCDI, were loaded into a 50 mL flask, and purged with argon. 30 mL of dry toluene was added to yield a yellow solution containing undissolved TCDI. The solution was heated in an oil bath that was preheated to 120 °C for 30 minutes. After cooling to room temperature, the solution was poured into 25 mL of 1 M HCl. The aqueous layer was extracted with 4 x 50 mL of ether. The combined organic layers were then extracted with 2 x 5 mL 1 M HCl and 10 mL brine and then dried over magnesium sulfate. Evaporation of the solvent yielded 1.9 g of the product as a yellow solid. Yield = 69%. ^1H NMR (CDCl_3) anti δ 6.54 (m, 2H), 5.00 (m, 2H), 4.57 (m, 2H), 3.82 (s, 6H). syn δ 6.43 (m, 2H), 4.95 (m, 2H), 4.60 (m, 2H), 3.83 (s, 6H). ^{13}C NMR (CDCl_3) anti δ 191.22, 164.25, 139.32, 131.14, 81.01, 52.70, 42.53. syn δ 191.08, 164.64, 138.88, 132.18, 80.65, 52.73, 42.40. MS: FTIR anti 3004, 2954, 2848, 1805, 1722, 1647, 1605, 1436, 1369, 1351, 1281, 1229, 1159, 1140, 1067, 996, 954, 914, 895, 820, 757, 737 cm^{-1} . HRMS Calcd for $\text{C}_{13}\text{H}_{12}\text{O}_6\text{S}$ 296.0352, found 296.0350. Anal. Calcd for $\text{C}_{13}\text{H}_{12}\text{O}_6\text{S}$: C, 52.70; H, 4.08 Found: C, 53.39; H, 4.20.

Dimethylbarrelene-2,3-dicarboxylate (5a). A 25 mL RBF was charged with 1.85 g (6.24 mmol) of **2a** and 3.6 mL (97% pure, 18.0 mmol) of **3** to yield a brown mixture with a lot of undissolved thiocarbonate. The mixture was heated under argon in an oil bath at 40 °C for 5 days. The brown solution was then loaded onto a silica gel column and eluted with methylene chloride. After evaporation of solvent, 0.814 g (3.70

mmol) of the product was obtained as a pale yellow oil. Yield = 61%. ^1H NMR (CDCl_3) δ 6.87 (m, 4H), 5.11 (m, 2H), 3.77 (s, 6H). ^{13}C NMR (CDCl_3) δ 165.79, 148.35, 139.39, 51.87, 49.00. FTIR 3075, 3003, 2954, 2845, 1714, 1648, 1602, 1580, 1435, 1331, 1313, 1270, 1236, 1192, 1118, 1056, 966, 939, 902, 885, 864, 844, 801, 751, 727. cm^{-1} HRMS Calcd for $\text{C}_{12}\text{H}_{13}\text{O}_4$ (MH^+) 221.0811, found 221.0806. Anal. Calcd for $\text{C}_{12}\text{H}_{12}\text{O}_4$: C, 65.45; H, 5.49. Found: C, 64.32; H, 5.72. (The sample contained \approx 5% dimethylbenzene-1,2-dicarboxylate.)

Di-*t*-butyl-2,3-dihydroxy-5,7-bicyclooctadiene-5,6-dicarboxylate (3b). Acid impurities were removed from the di-*t*-butyl acetylene dicarboxylate by loading it onto a plug of silica gel and eluting with 10% ethyl acetate/hexane. After removal of solvent, 3.8 g (16.8 mmol) of this purified material was put in a 50 mL RBF along with 0.924 g (8.24 mmol) of *cis*-3,5-cyclohexadiene-1,2-diol. The flask was purged with argon and then 2 mL of dry THF was added. The reaction was heated for 10 days at 60 °C after which time ^1H NMR showed no diol starting material. Upon heating, the acetylene melted, and the diol dissolved. As the reaction progressed, the solution became cloudy, and when the reaction was complete, a significant amount of product had precipitated as a yellow solid. Once complete, the reaction mixture was dissolved in ethyl acetate and 25 g of silica gel was added. Solvent was evaporated to yield a free flowing solid which was then loaded onto a plug of 100 mL of silica gel and eluted with 50% ethyl acetate/hexane. Following removal of solvent, 2.12 g (6.302 mmol) of the pale yellow solid product was obtained as a mixture of two isomers. Yield = 75%. *Note:* To obtain a good yield, it is important that the temperature is not allowed to rise much above 60 °C. This reaction can also be done on a larger scale using 15g of the diol starting material. Adding 3 equivalents of calcium carbonate relative to acetylene to this reaction was found to prevent the formation of phenol. ^1H NMR (CDCl_3) anti δ 6.44 (m, 2H), 4.11 (m, 2H), 3.87 (m, 2H), 2.64 (bs, 2H), 1.50 (s, 18H). syn 6.25 (m, 2H), 4.11 (m, 2H), 3.71 (m, 2H), 2.64 (bs, 2H), 1.52 (s, 18H). ^{13}C NMR (CDCl_3) anti δ 164.57, 139.89, 131.61,

82.49, 66.84, 46.60, 27.97. syn 165.86, 139.05, 131.68, 82.09, 66.27, 46.09, 27.90. FTIR anti 3401, 3072, 2890, 2934, 1708, 1645, 1605, 1478, 1458, 1437, 1368, 1283, 1256, 1165, 1142, 1083, 1058, 979, 845 cm ⁻¹. HRMS Calcd for C₁₈H₂₇O₆ (MH)⁺ 339.1801, found 339.1818. Anal. Calcd for C₁₈H₂₆O₆: C, 63.89; H, 7.74. Found: C, 63.79; H, 7.82.

Di-*t*-butyl-2,3-thiocarbonate-5,7-bicyclooctadiene-5,6-dicarboxylate (4b).

Compound **1b** (2.12 g, 6.30 mmol) and TCDI (1.31 g, 90% pure, 6.62 mmol) were loaded into a 100 mL flask, and the flask was purged with argon. 20 mL of dry toluene was added to yield a yellow solution containing undissolved TCDI. The solution was heated in an oil bath that was preheated to 120 °C for 15 minutes. After cooling to room temperature, the yellow solution, which also contained a black precipitate, was poured onto a plug of 100 mL of silica gel and eluted with 50% ethyl acetate/hexane. Evaporation of the solvent yielded 2.15 g (5.65 mmol) of the product as a light yellow solid. Yield = 90%. ¹H NMR (CDCl₃) anti δ 6.49 (m, 2H), 4.98 (m, 2H), 4.45 (m, 2H), 1.50 (s, 18H). syn δ 6.31 (m, 2H), 4.88 (m, 2H), 4.42 (m, 2H), 1.46 (s, 18H). ¹³C NMR (CDCl₃) anti δ 191.50, 163.08, 139.15, 131.27, 83.24, 81.36, 42.92, 27.97. syn δ 191.10, 163.37, 138.44, 131.94, 82.40, 80.63, 42.43, 27.82. FTIR: anti 2981, 2934, 1806, 1712, 1646, 1603, 1477, 1447, 1393, 1369, 1349, 1286, 1162, 1139, 1064, 1034, 995, 947, 893, 844, 821, 757, 710 cm ⁻¹. HRMS Calcd for C₁₉H₂₄O₆S 380.1288, found 380.1283. Anal. Calcd for C₁₉H₂₄O₆S: C, 59.98; H, 6.36. Found: C, 59.82; H, 6.53.

Di-*t*-butylbarrelene-2,3-dicarboxylate (5b). A 100 mL RBF was charged with 13.57 g (35.66 mmol) of **2b** and 21 mL of **3** to yield a brown mixture with a lot of undissolved **2b**. The mixture was heated under argon in an oil bath at 40 °C for 1 week. The brown solution was then loaded onto a silica gel column and eluted with 10% ethyl acetate/hexane. After evaporation of solvent, the product was obtained as 6.7 g of a white crystalline solid containing ≈10% of the retro Diels-Alder benzene product. This mixture was dissolved in 200 mL of hot hexane and then cooled to -50 °C overnight. Solvent was

decanted and the solid was washed with -50 °C pentane. Drying the solid under vacuum yielded the product as a colorless to white crystalline solid, and removal of solvent from the mother liquor yielded the benzene decomposition product as a clear colorless liquid. To remove any acid formed while heating, the solid was eluted through a plug of silica gel with 10% ethyl acetate hexane. Solvent was removed to yield 5.9 g (19.38 mmol) of the pure product as a white powder. Yield = 51%. ^1H NMR (CDCl_3) δ 6.84 (m, 4H), 5.02 (m, 2H), 1.49 (s, 18H) ^{13}C NMR (CDCl_3) δ 164.84, 148.33, 139.65, 81.55, 49.57, 28.02. FTIR 2974, 2936, 1728, 1695, 1647, 1601, 1581, 1472, 1452, 1392, 1365, 1337, 1315, 1273, 1158, 1123, 1108, 1051, 1021, 937, 901, 880, 845, 765, 742 cm^{-1} . HRMS Calcd for $\text{C}_{18}\text{H}_{24}\text{O}_4$ 304.1669, found 304.1675. Anal. Calcd for $\text{C}_{18}\text{H}_{24}\text{O}_4$: C, 71.03; H, 7.95. Found: C, 71.22; H, 7.95.

5,6-Bis(2-ethylhexyl)-2,3-dihydroxy-5,7-bicyclo[2.2.2]octa-5,7-diene-5,6-dicarboxylate (3c). A 100 mL round bottom flask was charged with 10.43 g (30.81 mmol) of 2-ethylhexyl acetylenedicarboxylate and 15.00 g (150 mmol) of CaCO_3 . After stirring for 30 minutes under a flow of argon, 1.73 g (15.43 mmol) of *cis* -3,5-cyclohexadiene-1,2-diol and 2.13 mL of dry THF was added to the flask. The reaction was heated at 60 °C for 3 days and then filtered to remove CaCO_3 . After rinsing the CaCO_3 with CHCl_3 , solvent was removed under vacuum to yield a yellow oil. The yellow oil was loaded onto a column of silica gel and eluted with 10% ethyl acetate/hexane. Following removal of solvent, 5.03 g (11.16 mmol, 71.20%) of a mixture of syn and anti product isomers was obtained as a yellow oil. *Note:* Calcium carbonate was added to this reaction to decrease formation of phenol. ^1H NMR (300 MHz, C_6D_6) anti δ 6.21 (m, 2H), syn δ 5.72 (dd, J = 4.2, 3.3 Hz, 2H), 4.21 (m, 2H) 4.19 - 4.02 (m, 6H), 3.73 (bs, 2H). 2.37 (bs, J = 2H), 1.53 (m, 2H), 1.40 - 1.02 (m, 16H) 0.89 - 0.79 (m, 12H); ^{13}C NMR (75 MHz, C_6D_6) anti δ 166.1, 141.0, 132.3, 68.5, 67.8, 47.9, 39.5, 31.1, 29.6, 24.5, 23.7, 14.6, 11.5; syn δ 167.35, 140.3, 132.4, 68.3, 67.2, 47.3, 39.5, 31.1, 29.6, 24.5, 23.7, 14.6, 11.5; HRMS calcd for $\text{C}_{26}\text{H}_{42}\text{O}_6$ ($\text{M}+\text{H}$) $^+$ 451.30594, found 451.3070.

Anal. Calcd for $C_{26}H_{42}O_6$: C, 69.30; H, 9.39. Found: C, 68.91; H, 9.34.

5,6-Bis(2-ethylhexyl)-2,3-thiocarbonate-5,7-bicyclo[2.2.2]octa-5,7-diene-5,6-dicarboxylate (4c). Compound **3c** (3.98 g, 8.84 mmol) and 1.93 g (90% pure, 9.72 mmol) of thiocarbonyldiimidazole (TCDI) were loaded into a 50 mL flask purged with argon. 30 mL of dry toluene was added to yield a solution containing undissolved TCDI. The solution was heated in an oil bath, which had been preheated to 135 °C, for 20 minutes. An additional 0.913g of TCDI was loaded into the flask and the reaction was heated for 15 minutes. After cooling to room temperature, the yellow solution was poured onto a plug of silica gel and eluted with 50% ethyl acetate/hexane. Removal of solvent under vacuum yielded 4.01 g (8.15 mmol, 92.12%) of **4c** as a yellow oil. 1H NMR (300 MHz, $CDCl_3$) anti δ 6.55 (dd, J = 4.2, 3.3 Hz, 2H), 5.00 (m, 2H), 4.55 (m, 2H), 4.12 (m, 4H), 1.60 (m, 2H), 1.4 - 1.29 (m, 16H), 0.90 (t, J = 7.2, 12H); syn δ 6.40 (dd, J = 4.5, 3.0 Hz, 2H), 4.91 (m, 2H), 4.55 (m, 2H), 4.14 (m, 4H), 1.64 (m, 2H), 1.46 - 1.23 (m, 16H), 0.90 (m, 12H); ^{13}C NMR (75 MHz, $CDCl_3$) anti δ 191.5, 164.3, 139.4, 131.3, 81.4, 69.1, 43.0, 38.9, 30.8, 29.1, 24.0, 23.9, 14.3, 11.1; syn δ 191.6, 165.5, 139.6, 132.4, 80.7, 68.5, 43.4, 39.6, 31.0, 29.7, 24.4, 23.8, 14.6, 11.6; HRMS Calcd. for $C_{27}H_{40}O_6S$ ($M+H$)⁺ 493.2624, found 493.2620. Anal. Calcd for $C_{27}H_{40}O_6S$: C, 65.82; H, 8.18. Found: C, 65.87; H, 8.21.

2,3-Bis(2-ethylhexyl)bicyclo[2.2.2]octa-2,5,7-triene-2,3-dicarboxylate (5c). A 50 mL round bottom flask was charged with 4.013g (8.15 mmol) of compound **4c** and 4.50 mL of 1,3-dimethyl-2-phenyl-1,3,2-diazaphospholidine (DPD) to yield a brown mixture. The mixture was heated under argon in an oil bath at 40 °C for 7 days. The brown solution was then loaded onto a silica gel column and eluted with 10% ethyl acetate/hexane. After evaporation of solvent, 1.78 g (4.27 mmol, 52.5%) of the product was obtained as a yellow oil. 1H NMR (300 MHz, $CDCl_3$) δ 6.87 (m, 4H), 5.08 (m, 2H), 4.06 (dd, J = 6.0, 3.0 Hz, 4H), 1.59 (m, 2H), 1.39 - 1.28 (m, 16H), 0.88 (m, 12H); ^{13}C NMR (75 MHz, C_6D_6) δ 167.5, 149.7, 140.9, 68.2, 50.7, 39.5, 31.1, 29.6, 24.5, 23.7,

14.6, 11.5; HRMS calcd for $C_{26}H_{40}O_4$ M^+ 416.2926, found 416.2920. Anal. Calcd for $C_{26}H_{40}O_4$: C, 74.95; H, 9.68. Found: C, 74.87; H, 9.86.

5,6-Bistrifluoromethylbicyclo[2.2.2]octa-5,7-diene-2,3-diol (3d). A Fischer-Porter bottle was charged with 9.16 g of *cis*-3,5-cyclohexadiene-1,2-diol (81.7 mmol) and purged with argon. 40 mL of dry THF was then added to yield a colorless solution. The flask was then closed and pressurized to 65 psi with hexafluoro-2-butyne. As the pressure slowly decreased, more gas was admitted to maintain the initial pressure. After 1 week, the pressure was released and solvent was removed by rotary evaporator to yield the product as 21 g (76.6 mmol, 94%) of a white solid. The crude product, which appeared clean by 1H NMR, was used in the next reaction without further purification. 1H NMR (300 MHz, $CDCl_3$) anti δ 6.50 (m, 2 H), 4.23 (br s, 2 H), 3.87 (br s, 2 H), 2.65 (br s 2 H); syn δ 6.32 (m, 2 H), 4.21 (m 2 H), 3.85 (br s, 2 H), 3.15 (br s, 2 H); ^{13}C NMR (75 MHz, $CDCl_3$) anti δ 139.95m, 131.46, 120.94 (q, $J = 275.47$ Hz), 66.45, 45.19; syn δ 137.14m, 131.91, 121.22(q, $J = 272.60$ Hz), 65.75, 45.03; ^{19}F NMR (376 MHz, $CDCl_3$) anti δ -61.49 s; syn δ -61.24 s; HRMS calcd for $C_{10}H_{12}F_6NO_2$ ($M+NH_4^+$) 292.0769, found 292.0775. Anal. Calcd for $C_9H_{12}F_6O_2$: C, 43.81; H, 2.94; F, 41.58. Found: C, 44.03; H, 3.07; F, 41.75.

5,6-Bistrifluoromethylbicyclo[2.2.2]octa-5,7-diene-2,3-thiocarbonate (4d). 3d (10.01 g, 36.5 mmol) and 7.53 g (90% pure, 38.0 mmol) of TCDI were put in a 500 mL round bottom flask and 150 mL of dry toluene was added. The flask was then put in an oil bath preheated to 130 °C. After 30 min, the reaction was cooled to rt and poured into a separatory funnel containing 10 mL of 1M HCl. The aqueous layer was extracted with 3x100 mL ether. All organic layers were combined and dried over magnesium sulfate. After removal of solvent under vacuum, the product was obtained as a brown solid. This was dissolved in 100 mL of ethyl acetate and 50 g of silica gel was added. Following evaporation of the solvent under vacuum, the free flowing solid was loaded onto a column containing 750 g of silica gel and eluted with 20% ethyl acetate/hexane and then

50% ethyl acetate/hexane. The product was obtained as two isomers (total = 9.91 g, 31.33 mmol, 86%). The major isomer, anti (identified by comparison to similar previously characterized compounds²⁷), was a white powder and the minor isomer, syn, was a slightly yellow crystalline solid. ¹H NMR (300 MHz, CDCl₃) anti δ 6.61 (m, 2H), 4.98 (m, 2H), 4.61 (m, 2H); syn δ 6.50 (m, 2H), 4.97 (br s, 2H), 4.64 (m, 2H); ¹³C (75 MHz, CDCl₃) anti δ 190.57, 137.28 m, 131.12, 120.17 (q, J = 272.1 Hz), 80.26, 41.631; syn δ 190.24, 137.01 m, 132.09, 120.36 (q, J = 273.95 Hz), 79.86, 41.54; ¹⁹F NMR (376 MHz, CDCl₃) anti δ -61.47 s; syn δ -61.22 s; HRMS calcd for C₁₁H₆F₆O₂S 315.99673, found 315.9985. Anal. Calcd for C₁₁H₆F₆O₂S: C, 41.78; H, 1.91, F, 36.05. Found: C, 41.82; H, 1.96; F, 36.13.

2,3-Bistrifluoromethylbicyclo[2.2.2]octa-2,5,7-triene (5d). A 450 mL Schlenk flask was loaded with 4.336 g (13.7 mmol) of **4d** and evacuated and then backfilled with argon three times. Next, 7.81 mL (97% pure, 41.1 mmol) of DPD, which was pumped down to 60 millitorr to remove volatile components, was added. This yielded a wet mixture, but most of the solid did not dissolve. The reaction was heated in an oil bath at 45 °C for 3 days. The flask was vented periodically to allow CO₂ formed by the reaction to escape. After cooling to rt, the product was vacuum transferred out of the reaction mixture into a Schlenk flask in liquid nitrogen. A second vacuum transfer yielded 2.078 g (8.65 mmol, 63%) of the desired product as a clear colorless liquid. ¹H NMR (300 MHz, CDCl₃) δ 6.90 (m, 4 H), 5.092 (m, 2 H); ¹³C NMR (75 MHz, CDCl₃) δ 145.18 m, 139.85, 122.07 (q, J = 272.07 Hz), 47.92; ¹⁹F NMR (376 MHz, CDCl₃) δ -61.73 s; HRMS calcd for C₁₀H₆F₆ 240.0372, found 240.0381. Anal. Calcd for C₁₀H₆F₆: C, 50.02; H, 2.52; F, 47.47. Found: C, 49.89; H, 2.48; F, 47.21.

1-Iodo-1-trifluoromethyl-2-perfluoroctylethylene (7). Under argon, 23.75g (43.5 mmol) of perfluoroctyliodide was loaded into a steel bomb and the bomb was then sealed and cooled to -78 °C. Approximately 4.8 g (51.0 mmol) of trifluoropropyne was condensed into the reaction vessel which was then sealed and warmed to rt; the pressure

increased to 100 psi. The reaction was then heated for 24 hours at 210 °C. The pressure initially increased to \approx 250 psi and then gradually decreased to <150 psi. After allowing the reaction to cool to room temperature, the pressure was released and the product mixture was seen to be a reddish-purple liquid with some white precipitate. Distillation of two combined reactions at 86 °C/14 torr yielded 43.79 g of product as a clear colorless liquid. ^{19}F NMR revealed this liquid to be 96% pure with some perfluoroctyl iodide impurity. Redistillation of this mixture at 94 °C/19 torr yielded 37.9 g (59.2 mmol, 65%) of pure **7**. ^1H NMR (300 MHz, CDCl_3) δ major 7.15 (t, J = 12.3 Hz); minor 6.893 (t, J = 14.6 Hz); ^{19}F (376 MHz, CDCl_3) δ -66.89 (s, 3F), -80.91 (t J = 9.2 Hz, 3F), -111.06 (d J = 11.4 Hz, 2F), -121.57 (s, 2F), -121.96 (br s, 4F), -122.89 (br s, 4F), -126.23 (s, 2F). HRMS calcd for $\text{C}_{11}\text{HF}_{20}\text{I}$ 639.8803, found 639.8787. Anal. Calcd for $\text{C}_{11}\text{HF}_{20}\text{I}$: C, 20.58; H, 0.16; F, 59.18. Found: C, 20.32; H, 0.15; F, 59.32.

Perfluoro-2-undecyne (8). Inside a nitrogen filled dry box, 17 g (88% pure, 267 mmol) of powdered KOH was loaded into a 250 mL round bottom flask. Outside the box, under argon, 38 g (59 mmol) of **7** was added to the KOH to produce a slightly yellow slurry. A 15 cm Vigoreux column and short path distillation condenser were placed on the flask and the pressure was reduced to 30 torr. The flask was put in an oil bath at 67 °C, and then the temperature of the bath was raised to 90 °C over 10 min. When the temperature reached 85 °C the reaction began to reflux and at 90 °C the reaction began refluxing vigorously and the distillation temperature was 76 °C. Redistillation of the mixture which collected in the receiver flask yielded 13.19 g (25.8 mmol, 44%) of the desired product and 8.3 g of recovered **7**. ^{13}C (100 MHz, neat w/ C_6D_6 tube to lock) 121.82 (t J = 36.0 Hz), 118.96 (t J = 32.9 Hz), 116.11 (t J = 32.9 Hz), 114.45 - 106.00 m, 104.35 (t J = 33.3 Hz), 76.88 (q J = 56.7 Hz), 71.29 (t J = 38.5 Hz); ^{19}F NMR (376 MHz neat w/ C_6D_6 tube to lock) -55.66 (s, 3F), -83.05 (t J = 10.3 Hz, 3F), -103.72 (s, 2F), -122.44 (s, 2F), -123.16 (br s, 4F), -123.83 (s, 2F), -124.08 (s, 2F), -127.80 (s, 2F); HRMS calcd for $\text{C}_{11}\text{F}_{20}$ 511.9680, found 511.9667. Anal. Calcd for

$C_{11}F_{20}$: C, 25.80; F, 74.20. Found: C, 24.95; F, 74.22. The high level of fluorine in this compound reportedly interfered with the carbon determination thus producing the low carbon value found. **Caution:** The reaction can become extremely rapid and explode. Best results were obtained with the pressure reported. Using higher pressures to try to improve the reaction yield usually resulted in an explosion. Use necessary precautions.

5-Perfluoroctyl-6-trifluoromethyl-5,7-bicyclo[2.2.2]octa-5,7-diene-2,3-dimethylacetal (10a). Under argon, 18.72 g (36.5 mmol) of compound **8** and 5.56 g (34.9 mmol) of **9a** were loaded into a 100 mL round bottom flask, and 13 mL of dry THF were added to yield two clear liquid phases. The reaction vessel was sealed with a Kontes valve and heated at 45 °C overnight. The reaction, which was now one clear colorless phase, was then cooled to room temperature, and solvent was removed to yield **10a** as a slightly cloudy liquid in quantitative yield. 1H NMR showed clean product with mainly one isomer. This crude material was used in the next reaction without further purification. 1H NMR (300 Hz, $CDCl_3$) δ 6.42 (m, 2H), 4.38-4.30 (m, 3H), 4.24 (br m, 2H) 1.33 (s, 3H), 1.27 (s, 3H); ^{19}F NMR (376 MHz, $CDCl_3$) δ -61.08 (m, 3F), -80.70 (s, 3F), -108.54 (dd J = 102.4 Hz, 2F), -120.13 (s, 2F), -121.74 (s, 6F), -122.67 (s, 2F), -126.07 (s, 2F); HRMS calcd for $C_{20}H_{13}F_{20}O_2$ 665.0596, found 665.0586. Anal. Calcd for $C_{20}H_{12}F_{20}O_2$: C, 36.16; H, 1.82; F, 57.20. Found: C, 36.28; H, 1.93; F, 57.23.

5-Perfluoroctyl-6-trifluoromethylbicyclo[2.2.2]octa-5,7-diene-2,3-diol (11).

Method A. **10a** (1.29g, 1.94 mmol) was dissolved in 30 mL of dioxane, and 30 mL of freshly prepared 6 M HCl was added to yield a slightly cloudy solution which separated into two clear phases when stirring was stopped. After heating the reaction at 65 °C for 1 day in an open flask, the solution turned brown and about half of the solvent evaporated. 1H NMR showed complete reaction and clean product. The reaction mixture was extracted with 4x100 mL of ether. Combined organic layers were extracted with 10 mL brine and 5 mL distilled water and then dried over sodium sulfate. Residual water was removed by dissolving the mixture in chloroform and evaporating this by rotary

evaporator. The crude material (1.1 g, 1.78 mmol, 92%) was used in the next reaction.

Method B. 10a (1.29g, 1.94 mmol) was dissolved in 9 mL of methanol and 97 mg of pyridinium *p*-toluenesulfonate was added to yield a clear colorless solution. The reaction was heated at 60 °C in an open flask. Methanol was added periodically to maintain the total volume around 9 mL. After 4 days, ¹H NMR showed complete reaction of the major isomer, but the minor isomer had not reacted much, so 11 mL of dioxane and 11 mL of 6M HCl was added. After heating 1 day at 60 °C, the reaction was complete. The reaction was purified as in method A to yield 1.1 g (1.78 mmol, 92%) of a brown oil. ¹H NMR (300 MHz, CDCl₃) δ 6.52 (m, 2H), 4.29 (br m, 1H), 4.22 (br m, 1H), 3.89 (s, 2H), 2.52 (br s, 2H); ¹⁹F NMR (376 MHz, CDCl₃) δ -61.12 (m, 3F), -80.83 (t, 3F, *J* = 9.2 Hz), -108.67 (m, 2F), -120.26 (br s, 2F), -121.83 (br s, 6F), -122.76 (br s, 2F), -126.19 (br s, 2F). HRMS calcd for C₁₇H₆F₂₀O₂S 665.9687, found 665.9766. Anal. Calcd for C₁₇H₈F₂₀O₂: C, 32.71; H, 1.29; F, 60.87. Found: C, 32.60; H, 1.27; F, 60.85.

5-Perfluorooctyl-6-trifluoromethylbicyclo[2.2.2]octa-5,7-diene-2,3-thiocarbonate (12). The procedure was essentially the same as for compound **4d**. Column chromatography was done on silica gel by eluting first with 10% ethyl acetate/hexane to obtain the major isomer and then 35% ethyl acetate/hexane to obtain the minor isomer. Both isomers were white solids (82%). ¹H NMR (300 MHz, CDCl₃) δ 6.62 (m, 2H), 4.99 (m, 2H), 4.66 (br m, 1H), 4.59 (br m, 1H); ¹⁹F NMR (376 MHz, CDCl₃) δ -60.99 (s, 3F), -80.68 (s, 3F), -108.59 (s, 2F), -119.99 (s, 2F), -121.68 (br s, 4F), -121.82 (br s, 2F), -127.67 (br s, 2F), -126.08 (br s, 2F); HRMS calcd for C₁₈H₁₀F₂₀NO₂S (M+NH₄⁺) 642.0545, found 642.0552. Anal. Calcd for C₁₈H₆F₂₀O₂S: C, 32.45; H, 0.91; F, 57.03. Found: C, 32.22; H, 1.03; F, 57.13.

2-Perfluorooctyl-3-trifluoromethylbicyclo[2.2.2]octa-2,5,7-triene (13). The major, anti isomer of compound **12** (3.3 g, 4.95 mmol) was put in a 25 mL round bottom flask and the flask was purged with argon. Addition of 3 mL (97% pure, 3.07 g, 15.8 mmol) of DPD only wetted the solid; none appeared to dissolve. The reaction was heated

in an oil bath at 45 °C and after 1 day the reaction was a brown liquid. After three days, the reaction mixture was loaded onto a plug of silica gel and eluted with 40% ethyl acetate/hexane. Removal of solvent yielded 1.9 g (3.22 mmol, 65%) of **13** as a slightly yellow oil. *Note:* This reaction has been done on larger scale to produce 11.5 g of **13**. The yield was reduced to 54% in this case. ^1H NMR (300 MHz, CDCl_3) δ 6.90 (m, 4H), 5.1415 (m, 1H), 5.1049 (m, 1H); ^{19}F NMR (376 MHz, CDCl_3) δ -61.50 (m, 3F), -80.70 (t, J = 9.2 Hz, 3F), -108.61 (br d, 2F), -193.04 (br s, 2F), -121.80 (br s, 6F), -122.67 (br s, 2F), -126.08 (br s, 2F); HRMS calcd for $\text{C}_{17}\text{H}_6\text{F}_{20}$ 590.0068, found 590.0170. Anal. Calcd for $\text{C}_{17}\text{H}_6\text{F}_{20}$: C, 34.60; H, 1.02; F, 64.38. Found: C, 34.40; H, 0.93; F, 64.24.

Bicyclo[2.2.2]octa-5,7-diene-2,3-dimethylacetal-5-sulfonate (15a). A 250 mL round bottom flask was charged with 8.22 g (45.6 mmol) of ethynyl *p*-toluenesulfonate, **14a**, and then purged with argon. Dry benzene (40 mL) was added to yield a colorless solution. In a separate flask, 6.94 g (45.6 mmol) of **9a** was dissolved in 10 mL of dry benzene and this solution was then added to the first solution. The flask was sealed with a Kontes valve and the reaction was heated to 80 °C and stirred for 14 hours. After this time, some white crystals had formed in the reaction mixture. The reaction was then cooled to rt and more crystals formed. Removal of solvent under vacuum yielded a white solid which was then recrystallized by dissolving it in hot acetone (250 mL) and then cooling the solution to -50 °C overnight. The white crystals obtained were rinsed with -78 °C acetone and dried under vacuum to yield 13.38 g (40.3 mmol, 88%) of **15a**. ^1H NMR (300 MHz, CDCl_3) δ 7.70 (d, J = 8.32 Hz, 2H), 7.32 (d, J = 8.12 Hz, 2H), 7.15 (dd, J = 1.89, 6.47, 1H), 6.27 (m, 1H), 6.20 (m, 1H), 4.25 (dd, J = 6.81, 3.36 Hz, 1 H), 4.12 (m, 1H), 4.07 (m, 1H), 4.00 (m, 1H), 2.43 (s, 3H), 1.28 (s, 3H), 1.21 (s, 3H); ^{13}C NMR (75 MHz, CDCl_3) δ 147.32, 144.53, 141.95, 135.39, 131.28, 130.95, 129.87, 127.83, 113.50, 78.35, 78.02, 43.45, 41.98, 25.60, 25.39, 21.54; HRMS calcd for $\text{C}_{18}\text{H}_{21}\text{O}_4\text{S}$ ($\text{M}+\text{H})^+$ 333.1161, found 333.1160. Anal. Calcd for $\text{C}_{18}\text{H}_{20}\text{O}_4\text{S}$: C, 65.04; H, 6.06. Found: C, 64.75; H, 6.07. **Caution:** **14a** can contain acidic impurities which cause rapid

exothermic decomposition of **9a**. This decomposition is especially violent if the two reactants are combined neat. Acid impurities were removed from **14a** by eluting it through a plug of silica gel (20% ethyl acetate/hexane).

Bicyclo[2.2.2]octa-5,7-diene-2,3-dimethylacetal (16a). Compound **15a** (10.68 g, 32.1 mmol) was put in a 2000 mL round bottom flask and the flask was evacuated and then backfilled with argon three times. The flask was then put in a bath at -20 °C and 1.6 L of SmI₂ solution (0.1 M in THF) was added while maintaining the bath temperature at or below -20 °C. 90 mL of HMPA, which had been dried over calcium hydride and then distilled, was then added to the solution and the color changed from blue-green to dark purple. The reaction was stirred under argon for 90 minutes at a temperature of -20 °C and then 150 mL of a saturated solution of aqueous NH₄Cl was added. After stirring for one hour, over which time the solution was allowed to warm to rt, THF was removed under vacuum. The remaining mixture was diluted with 50 mL of water and the aqueous layer was then extracted with (3x500) mL of ether. The combined organic layers were then extracted with (2x200) mL of brine and (2x200) mL 0.1 M NaOH. These aqueous layers were then extracted with (3x200) mL of ether. The combined organic layers were dried over MgSO₄ and solvent was then removed under vacuum to yield a pink liquid. This was loaded onto a plug of silica gel and eluted first with hexane until all HMPA was eluted and then with 10% ethyl acetate/hexane. Removal of solvent yielded **16a** as a light pink solid. Further purification was accomplished using a silica gel column eluted with 10% ethyl acetate/hexane to yield the product as 4.2 g (23.6 mmol, 73%) of a white waxy solid. ¹H NMR (300 MHz, CDCl₃) δ 6.32 (m, 2H), 6.26 (m, 2H), 4.21 (m, 2H), 3.83 (m, 2H), 1.33 (s, 3H), 1.26 (m, 3H); ¹³C NMR (75 MHz, CDCl₃) δ 133.65, 131.91, 112.51, 78.44, 41.91, 25.90, 25.45; HRMS calcd for C₁₁H₁₅O₂ (M+H)⁺ 179.1069, found 179.1077. Anal. Calcd for C₁₁H₁₄O₂: C, 74.13; H, 7.92. Found: C, 73.94; H, 8.02.

Bicyclo[2.2.2]octa-5,7-diene-2,3-diol (17a). In a 250 mL round bottom flask, **16a** (3.75 g, 21.04 mmol) was dissolved in 80 mL of methanol and 1.09 g of pyridinium

p-toluene sulfonate was added. The reaction, which was left open to the air, was heated at 70 °C and the methanol was replenished periodically as it boiled off. After 1 week, remaining methanol was removed under vacuum and the reaction was purified on a silica gel column eluted with 40% ethyl acetate/hexane. Removal of solvent under vacuum yielded 1.9 g (13.75 mmol, 66%) of **17a** as a white crystalline solid. ¹H NMR (300 MHz, CDCl₃) δ 6.42 (m, 2H), 6.24 (m, 2H), 3.82 (m, 2H), 3.70 (m, 2H), 2.30 (br s or m, 2H, -OH). ¹³C NMR (75 MHz, CDCl₃) δ 132.93, 132.40, 67.22, 44.33. HRMS calcd for C₈H₁₄NO₂ (M+NH₄⁺) 156.1021, found 156.1023.

Bicyclo[2.2.2]octa-5,7-diene-2,3-thiocarbonate (18a). Under argon, 1.64 g (11.87 mmol) of **17a** was dissolved in 40 mL of dry toluene in a 250 mL round bottom flask and 2.5 g (90% pure, 12.62 mmol) of TCDI was added. The flask was put in an oil bath that had been preheated to 130 °C and the reaction was stirred for 10 minutes. 0.12 g (0.61 mmol) of TCDI was then added and the reaction was stirred for an additional 5 minutes at 130 °C. After removing solvent under vacuum, the solid was redissolved in ethyl acetate and 18 g of silica gel was added. Solvent was removed to produce a free flowing powder which was then loaded onto a column of 600 g of silica gel, and eluted with 40% ethyl acetate/hexane. Removal of solvent under vacuum yielded 1.73 g (9.60 mmol, 81%) of **18a** as a white crystalline solid. ¹H (300 MHz, CDCl₃) δ 6.45 (m, 2H), 6.33 (m, 2H), 4.87 (m, 2H), 4.20 (m, 2H). ¹³C (75 MHz, CDCl₃) δ 192.42, 132.61, 131.58, 81.87, 40.42. HRMS calcd for C₉H₉O₂S (M+H)⁺ 181.0321, found 181.0323. Anal. Calcd for C₉H₈O₂S: C, 59.98; H, 4.47. Found: C, 59.64; H, 4.53.

Bicyclo[2.2.2]octa-2,5,7-triene, (19a). A 250 mL Schlenk flask was charged with 1.8 g (9.99 mmol) of **18a** and was then evacuated and filled with argon three times. Under argon, 6 mL (97% pure, 6.13 g, 31.6 mmol) of DPD which had been pumped down to remove all volatile components was added to yield a mixture containing a lot of undissolved **18a**. The flask was sealed and the reaction mixture was heated at 40 °C for 5 days. The flask was vented periodically to allow CO₂ formed by the reaction to escape.

19a (0.70 g, 6.72 mmol, 67.3%) was then vacuum transferred out of the reaction mixture as a colorless liquid. ^1H (300 MHz, CDCl_3) δ 6.78 (m, 6H), 4.842 (m, 2H). ^{13}C (75 MHz, CDCl_3) δ 140.60, 48.23. HRMS calcd for C_8H_8 104.0624, found 104.0627. Anal. Calcd for C_8H_8 : C, 92.26; H, 7.74. Found: C, 92.20; H, 7.74.

6-Octylbicyclo[2.2.2]octa-5,7-diene-2,3-dimethylacetal-5-sulfonate (15b). 100 mg (0.342 mmol) of **14b** and 52 mg (0.342 mmol) of **9a** were heated neat under argon for 3 days. Flash chromatography on silica gel (10% ethyl acetate/hexane) yielded **15b** (106 mg, 0.24 mmol, 70%) as a colorless oil. ^1H NMR (300 MHz, CDCl_3) δ 7.68 (d, J = 8.0 Hz, 2H), 7.30 (d, J = 8.0 Hz, 2H), 6.19 (m, 2H), 4.19 (m, 2H), 4.07 (m, 1H), 3.82 (m, 1H), 2.73 (t, J = 6.9 Hz, 2 H), 2.42 (s, 3H), 1.26 (br d, 17H), 1.20 (s, 3H), 0.88 (t, J = 6.3 Hz, 3H); ^{13}C NMR (75 MHz, CDCl_3) δ 158.4, 144.1, 138.0, 136.6, 131.9, 130.8, 129.8, 127.4, 113.1, 78.7, 78.0, 50.4, 44.0, 31.8, 31.4, 29.6, 29.4, 29.2, 27.4, 25.7, 25.6, 22.7, 21.6, 14.1; HRMS calcd for $\text{C}_{26}\text{H}_{36}\text{O}_4\text{S}$ ($\text{M}+\text{H}$) $^+$ 445.2413, found 445.2426. Anal. Calcd for $\text{C}_{26}\text{H}_{36}\text{O}_4\text{S}$: C, 70.24; H, 8.16. Found: C, 70.12; H, 8.16.

5-Octylbicyclo[2.2.2]octa-5,7-diene-2,3-dimethylacetal (16b). To 3.6 g (8.1 mmol) of **15b**, dissolved in 4 mL of dry THF, was added under argon 420 mL SmI_2 solution (0.1 M in THF). The mixture was cooled to -20 °C and 26.5 mL HMPA was added to yield a dark purple solution. The reaction was kept at - 20 °C for 1.5 h, treated with 42 mL saturated NH_4Cl solution and allowed to warm up to rt during which time the solution turned yellow and a white precipitate formed. The precipitate was filtered off and washed with diethyl ether several times, and then solvent was removed under vacuum. 20 mL brine was added to the remaining mixture and it was then extracted with diethyl ether. The ether was removed under reduced pressure and the product purified by passing through a plug of silica gel. HMPA was removed first by eluting with hexane and then **16b** was eluted using 10% ethyl acetate/hexane. Removal of solvent yielded 1.57 g (5.43 mmol, 67%) of **16b** as a colorless liquid. ^1H NMR (300 MHz, CDCl_3) δ 6.30 (m, 2H), 5.72 (dd, J = 6.3, 1.8 Hz, 1H), 4.19 (m, 2H), 3.69 (m, 1H), 3.54 (m, 1H),

2.06 (td, J = 7.5, 0.75 Hz, 2 H), 1.31 (s, 3H), 1.24 (br d, 15H), 0.86 (t, J = 7.2 Hz, 3H); ^{13}C NMR (75 MHz, CDCl_3) δ 147.8, 132.8, 131.7, 124.7, 112.5, 79.4, 78.7, 46.4, 42.0, 34.0, 31.9, 29.43, 29.32, 29.27, 27.2, 26.0, 25.6, 22.7, 21.6, 14.1; HRMS calcd for $\text{C}_{19}\text{H}_{30}\text{O}_2$ ($\text{M}+\text{H}$) $^+$ 291.2324, found 291.2317.

5-Octylbicyclo[2.2.2]octa-5,7-diene-2,3-diol (17b). **16b** (1.57 g, 5.43 mmol) and pyridinium *p*-toluene sulfonate (0.3 g, 1.1 mmol) were dissolved in 100 mL of methanol and heated to 60 °C in an open flask for 3 days. Methanol was removed under reduced pressure and the product purified by flash column chromatography on silica gel (50% ethyl acetate/hexane). Removal of solvent under vacuum yielded 1 g of 17b (4 mmol, 74%) as a colorless liquid. ^1H NMR (300 MHz, CDCl_3) δ 6.39 (m, 2H), 5.72 (m, 1H), 3.68 (m, 3H), 3.54 (m, 1H), 2.64 (s, 2H), 2.08 (t, J = 7.8 Hz, 2 H), 1.25 (br d, 12H), 0.87 (t, J = 7.5 Hz, 3H); ^{13}C NMR (75 MHz, CDCl_3) δ 147.2, 133.3, 132.6, 124.1, 68.4, 67.8, 48.9, 44.6, 33.9, 31.9, 29.47, 29.35, 29.30, 27.2, 22.7, 14.2; HRMS calcd for $\text{C}_{16}\text{H}_{26}\text{O}_2$ ($\text{M}+\text{H}$) $^+$ 249.1855, found 249.1859.

5-Octylbicyclo[2.2.2]octa-5,7-diene-2,3-thiocarbonate (18b). **17b** (1 g, 4 mmol) and TCDI (0.87 g, 4.4 mmol) were refluxed in 20 mL toluene for 30 min. The reaction mixture was eluted through a plug of silica with 30% ethyl acetate/hexane to afford 1.15 g (3.9 mmol, 98%) of **18b** as a white crystalline solid. ^1H NMR (300 MHz, CDCl_3) δ 6.42 (m, 2H), 5.79 (dd, J_1 = 6.3 Hz, J_2 = 1.5 Hz, 1H), 4.85 (m, 2H), 4.06 (m, 1H), 3.90 (m, 1H), 2.12 (t, J = 7.5 Hz, 2 H), 1.24 (br d, 12H), 0.86 (t, J = 6.9 Hz, 3H); ^{13}C NMR (75 MHz, CDCl_3) δ 192.64, 147.4, 132.6, 131.6, 128.2, 123.8, 82.6, 82.2, 45.0, 40.7, 33.9, 31.9, 29.3, 29.2, 27.0, 22.7, 14.1; HRMS calcd for $\text{C}_{17}\text{H}_{24}\text{O}_2\text{S}$ 292.1497, found 292.1504.

2-Octylbicyclo[2.2.2]octa-2,5,7-triene (19b). **18b** (1.15 g, 3.9 mmol) was suspended in DPD (0.76 g, 11.7 mmol) and heated at 40 °C under argon for 5 days. The reaction mixture was purified by flash column chromatography on silica gel (10% ethyl acetate/hexane) to yield 168 mg (0.78 mmol, 25%) of **19b** as a colorless liquid. ^1H NMR

(300 MHz, CDCl₃) δ 6.76 (m, 4H), 6.17 (dd, *J* = 6.1, 1.8 Hz, 1H), 4.68 (m, 1H), 4.49 (m, 1H), 2.06 (td, *J* = 7.1, 1.8 Hz, 2 H), 1.25 (br d, 12H), 0.88 (t, *J* = 7.3 Hz, 3H); ¹³C NMR (75 MHz, CDCl₃) δ 155.4, 141.0, 139.9, 131.5, 52.5, 47.8, 33.7, 31.9, 29.5, 29.3, 29.1, 27.2, 22.7, 14.1; HRMS calcd for C₁₉H₃₀O₂ (M+H)⁺ 216.1877, found 216.1878.

5-Methylbicyclo[2.2.2]octa-5,7-diene-2,3-dimethylacetal-5-carboxylate. 9a (6.7 g, 44 mmol) and 7.2 g (85.7 mmol) of methyl propiolate were refluxed in 70 mL of dry benzene overnight. Removal of solvent and excess methyl propiolate under vacuum yielded 10.4 g (44 mmol, 100%) of the desired product. ¹H NMR (300 MHz, C₆D₆) δ 6.93 (dd, *J* = 6.3, 1.8 Hz, 1H), 6.25 (t, *J* = 6.0 Hz, 1H), 6.09 (t, *J* = 6.0 Hz, 1H), 4.51 (m, 1H), 3.98 (m, 1H), 3.80 (m, 1H), 3.54 (m, 1H), 3.37 (s, 3H), 1.34 (s, 3H), 1.11 (s, 3H); ¹³C NMR (75 MHz, CDCl₃) δ 163.9, 143.9, 138.1, 131.9, 130.4, 112.6, 78.0, 77.8, 50.7, 42.9, 41.6, 25.5, 24.9; HRMS calcd for C₁₃H₁₆O₄ (M+H)⁺ 237.1127, found 237.1128. Anal. Calcd for C₁₃H₁₆O₄: C, 66.08; H, 6.83. Found: C, 66.07; H, 6.73.

5-Methylbicyclo[2.2.2]octa-5,7-diene-2,3-diol-5-carboxylate. The procedure was similar to that described for **17b** (60%). ¹H NMR (300 MHz, C₆D₆) δ 6.90 (dd, *J* = 6.3, 1.8 Hz, 1H), 6.27 (t, *J* = 6.0 Hz, 1H), 6.14 (t, *J* = 6.0 Hz, 1H), 4.46 (m, 1H), 3.50 (m, 2H), 3.30 (m, 1H), 3.22 (s, 3H), 2.85 (br d, 2H); ¹³C NMR (75 MHz, CDCl₃) δ 165.1, 143.9, 137.3, 132.6, 131.4, 66.9, 67.0, 52.0, 45.7, 43.9; HRMS calcd for C₁₀H₁₆NO₄ (M+NH₄⁺) 214.1075, found 214.1076. Anal. Calcd for C₁₀H₁₂O₄: C, 61.21; H, 6.17. Found: C, 60.95; H, 6.16.

5-Methylbicyclo[2.2.2]octa-5,7-diene-2,3-thiocarbonate-5-carboxylate (20). 3-methoxycarboxy-7,8-dihydroxy-[2,2,2]bicyclo-3,5-octadiene was reacted with thiophosgene and DMAP in analogy to the literature procedure¹⁰ to yield **20** as a light yellow solid following column chromatography (71%). ¹H NMR (300 MHz, C₆D₆) δ 6.36 (dd, *J*₁=6.3, 1.8 Hz, 1H), 5.85 (t, *J* = 6.0 Hz, 1H), 5.70 (t, *J* = 6.0 Hz, 1H), 4.31 (m, 1H), 3.82 (m, 1H), 3.59 (m, 1H), 3.24 (s, 3H), 3.14 (m, 1H); ¹³C NMR (75 MHz, CDCl₃) δ 192.0, 163.7, 142.2, 137.5, 132.3, 131.0, 81.7, 81.5, 52.4, 41.8, 40.4; HRMS calcd for

$C_{11}H_{14}NO_4S$ ($M+NH_4^+$) 239.0375, found 239.0373. Anal. Calcd for $C_{11}H_{10}O_4S$: C, 64.00; H, 4.85. Found: C, 63.94; H, 4.75.

2-Methylbicyclo[2.2.2]octa-2,5,7-triene-2-carboxylate (21). Using a procedure analogous to the one for preparation of **19b** yielded a very viscous brown mixture. The same result was obtained when THF was used to dilute the reaction and when radical inhibitors, 4-methoxyphenol and BHT, were added to the THF solution in concentrations of 10 mole percent and 100 mole percent versus **20**. Under all conditions decomposition occurred after 3 hours to 3 days.

References and Notes

- (1) Zimmerman, H. E.; Paufler, R. M. *J. Am. Chem. Soc.* **1960**, *82*, 1514. This reference also includes the rationale behind calling bicyclo[2.2.2]octatriene barrelene.
- (2) Zimmerman, H. E.; Grunewald, G. L.; Paufler, R. M.; Sherwin, M. A. *J. Am. Chem. Soc.* **1969**, *91*, 2330.
- (3) Zimmerman, H. E.; Armesto, D. *Chem. Rev.* **1996**, *96*, 3065.
- (4) Dauben, W. G.; Rivers, G. T.; Twieg, R. J.; Zimmerman, W. T. *J. Org. Chem.* **1976**, *41*, 887.
- (5) Taylor, G. N. *J. Org. Chem.* **1972**, *37*, 2904.
- (6) Weitemeyer, C.; Preuss, T.; deMeijere, A. *Chem. Ber.* **1985**, *118*, 3993.
- (7) Jefford, C. W.; Wallace, T. W.; Acar, M. *J. Org. Chem.* **1977**, *42*, 1654.
- (8) Weitemeyer, C.; deMeijere, A. *Angew. Chem. Int. Ed. Engl.* **1976**, *15*, 686.
- (9) Cossu, S.; Battaggia, S.; DeLucchi, O. *J. Org. Chem.* **1997**, *62*, 4162.
- (10) Lightner, D. A.; Paquette, L. A.; Chayangkoon, P.; Lin, H. S.; Peterson, J. R. *J. Org. Chem.* **1988**, *53*, 1969.
- (11) Liu, R. H.; Krespan, C. G. *J. Org. Chem.* **1969**, *34*, 1271.
- (12) Liu, R. S. H. *J. Am. Chem. Soc.* **1968**, *90*, 215.
- (13) Krespan, C. G.; McKusick, B. C.; Cairns, T. L. *J. Am. Chem. Soc.* **1961**, *83*, 3428.
- (14) Kopach, M. E.; Harman, W. D. *Abstr. Pap. Am. Chem. Soc.* **1994**, *208*, ORGN 289.
- (15) Ciganek, E. *Tetrahedron Lett.* **1967**, *34*, 3321.
- (16) Beerli, R.; Rebek, J. *Tetrahedron Lett.* **1995**, *36*, 1813.
- (17) Stapersma, J.; Rood, I. D. C.; Klumpp, G. W. *Tetrahedron* **1982**, *18*, 191.
- (18) Gompper, R.; Etzbach, K. H. *Angew. Chem. Int. Ed. Engl.* **1978**, *17*, 603.
- (19) LeGoff, E.; LaCount, R. B. *Tetrahedron Lett.* **1967**, *24*, 2333.

(20) Noble, K. L.; Hopf, H.; Jones, M.; Kammula, S. L. *Angew. Chem. Int. Ed. Engl.* **1978**, *17*, 602.

(21) The procedure described in reference 17 allows the synthesis of barrelene and substituted barrelenes in $\approx 5\%$ yield by the same route. Reference 18 describes the synthesis of a diether substituted barrelene by a route similar to that used for synthesizing unsubstituted barrelene from the diketone.^{6,7,8,10}

(22) Dicyano and bistrifluoromethyl acetylene both produce higher yields of barrelene products when reacted with more active, substituted benzenes.^{11,13,15}

(23) Magnussen, A.; Hansen, H. J. *Helv. Chim. Acta* **1997**, *80*, 545.

(24) Truesdale, E. A.; Cram, D. J. *J. Am. Chem. Soc.* **1973**, *95*, 5825.

(25) Corey, E. J.; Carey, F. A.; Winter, R. A. *E. J. Am. Chem. Soc.* **1965**, *87*, 934.

(26) Corey, E. J.; Hopkins, P. B. *Tetrahedron Lett.* **1982**, *23*, 1979.

(27) Wagaman, M. W.; Grubbs, R. H. *Macromolecules* **1997**, *30*, 3978.

(28) Barua, N. C.; Sharma, R. P. *Tetrahedron Lett.* **1982**, *23*, 1365.

(29) McMurry, J. E.; Fleming, M. P. *J. Org. Chem.* **1976**, *41*, 896.

(30) Pu, L.; Grubbs, R. H. *J. Org. Chem.* **1994**, *59*, 1351.

(31) Pu, L.; Wagaman, M. W.; Grubbs, R. H. *Macromolecules* **1996**, *29*, 1138.

(32) Semmelhack, M. F.; Stauffer, R. D. *Tetrahedron Lett.* **1973**, *29*, 2667.

(33) Pittol, C. A.; Pryce, R. J.; Roberts, S. M. *J. Chem. Soc., Perkins Trans. I* **1989**, 1160.

(34) Mahon, M. F.; Molloy, K.; Pittol, C. A.; Pryce, R. J.; Roberts, S. M.; Ryback, G.; Sik, V.; Williams, J. O.; Winders, J. A. *J. Chem. Soc., Perkins Trans. I* **1991**, 1255.

(35) Cotterill, I. C.; Roberts, S. M.; Williams, J. O. *J. Chem. Soc., Chem. Commun.* **1988**, 1628.

(36) Jeanneaux, F.; Santini, G.; LeBlanc, M.; Cambon, A.; Reiss, J. G. *Tetrahedron* **1974**, *30*, 4197.

- (37) Haszeldine, R. N. *J. Chem. Soc.* **1952**, 2504.
- (38) Hudlicky, M. *J. Fluorine Chem.* **1981**, *18*, 383.
- (39) Further evidence for the presence of hydrofluoric acid in compound **8**, which is a liquid, was the ability of the neat liquid to etch glass when left in contact for extended periods. Because the acetonide, **9a**, is deprotected by acid, the success of the reaction of **8** with **9a** probably also relies on the fact that this Diels-Alder reaction is much faster than the reaction of **8** with **1**.
- (40) Back, T. G.; Collins, S.; Kerr, R. G. *J. Org. Chem.* **1983**, *48*, 3077.
- (41) Waykole, L.; Paquette, L. A. *Org. Synth.* **1989**, *67*, 149.
- (42) Künzer, H.; Stahnke, M.; Sauer, G.; Weichert, R. *Tetrahedron Lett.* **1991**, *32* 1949.
- (43) Boyd, D. R.; Sharma, N. D.; Barr, S. A.; Dalton, H.; Chima, J.; Whited, G.; Seemayer, R. *J. Am. Chem. Soc.* **1994**, *116*, 1147.
- (44) Jeffery, G. H.; Vogel, A. I. *J. Chem. Soc.* **1948**, 674. Acetylene **2c** was purified on silica gel (10% ethyl acetate/hexane) rather than by distillation.

Chapter 3

Catalyst Testing and Tuning

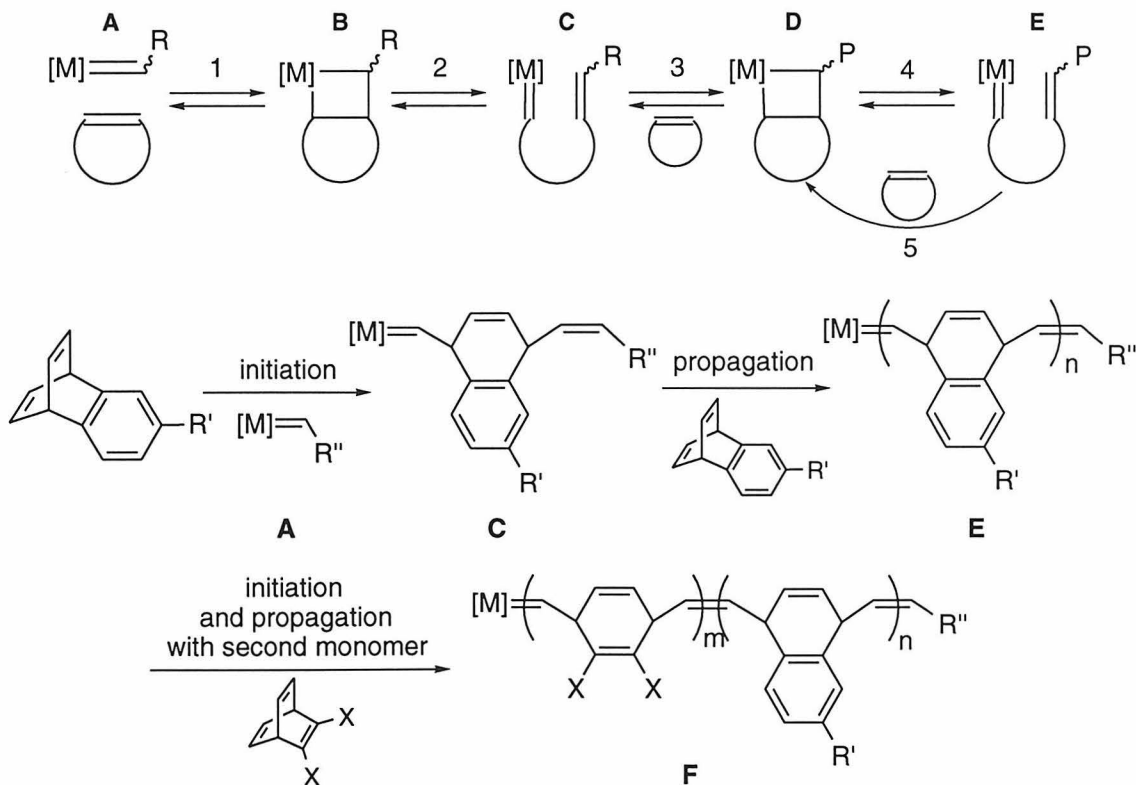
Abstract: In this chapter, testing of a variety of metathesis initiators to identify the best one for the synthesis of homopolymers and copolymers of the benzobarrelene and barrelene monomers is described. While many of the catalysts tested polymerized these monomers, the best results were obtained using a molybdenum initiator, **8**, bearing two hexafluoro-*t*-butoxy ligands. Polymerizations with **8** were originally not living, but tuning the activity of this catalyst using hexafluoro-*t*-butanol (HFB) and tetrahydrofuran (THF) yielded a living polymerization.

Introduction

Having prepared the benzobarrelene¹⁻³ and barrelene^{4,5} monomers necessary for synthesizing PNVs and PPVs, the only tasks remaining were to polymerize them and study the various homopolymers and copolymers. Ring-opening metathesis polymerization (ROMP) is generally a well behaved method of polymerization since reactions carried with the newer, well-defined metathesis initiators are often living,^{2,3,6-14} and because some of the initiators tolerate a wide range of functional groups.^{6,12,15-21}

A schematic representation of ROMP is shown in Scheme 1, along with the synthesis of a benzobarrelene/barrelene block copolymer. The polymerization is classified as living if chain termination and chain transfer reactions do not occur.²²⁻²⁴

Scheme 1



(a) Steps 1 and 2 show initiation (b) Steps 3-5 show propagation. (c) P represents the polymer chain, [M] represents the metal center and surrounding ligands of the metathesis initiator excluding the carbene carbon, which is shown, R and R'' are alkyl groups attached to the catalyst carbene carbon and R' is an alkyl group added to improve solubility of the polymer.

When this is the case, block copolymers can be prepared by adding a second monomer after polymerization of the first monomer is complete, as shown. For this reaction to work well for the synthesis of block copolymers, a few other conditions must also be met. First, all of the catalyst must become initiated when the first monomer is added (i.e., all of **A** must be converted to **C**). This criterion is important since any **A** remaining when the second monomer is added could react with this monomer and produce a homopolymer. Similarly, when the second monomer is added, all of **E** (and **C** if any catalyst molecules added only a single monomer unit) must be initiated by this monomer (i.e., all of **E** must be converted to **F**). When these conditions are met, all of the resulting polymer chains will contain a block made up of units of the first monomer and a block made up of units of the second monomer.

Results and Discussion

Catalyst Screening. Since a number of ROMP catalysts are available,^{15,25-30} the first necessary step was to find the catalyst best suited to polymerizing the different monomers. Because our ultimate goal was to make and study copolymers, and especially the block copolymers, a catalyst that could polymerize all the different monomers in a living fashion was required. Most testing of the different catalysts was done using the benzobarrelene monomers shown in Figure 1, since these were available first. The results obtained were generally applicable to the barrelene monomers as well, although modifications in the exact conditions were sometimes required. As shown in Table 1, the

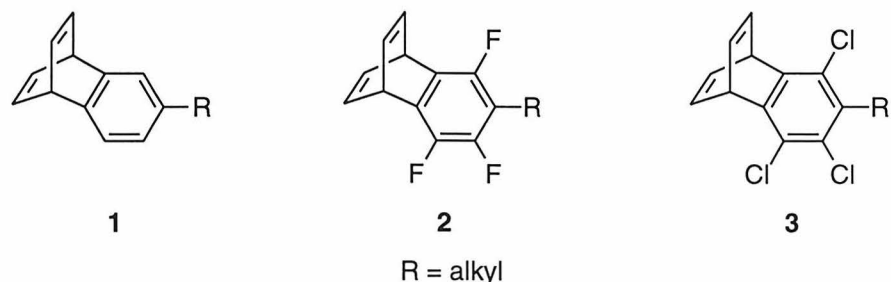


Figure 1. Benzobarrelene monomers used for catalyst testing.

benzobarrelenes could be polymerized with a number of catalysts, **4** - **9**, shown in Figure 2. The first ruthenium-based catalyst²⁷ tested, **4**, did not show much reaction with **1**, probably due lack of initiation. The tungsten-based catalyst,³⁰ **9**, had the opposite problem of activity that was too high, as an insoluble, crosslinked polymer formed almost instantly. The molybdenum-based catalysts,²⁹ **7** and **8**, both worked well for the polymerization of **1**, but only PNV prepared from precursor polymers made with **8** had

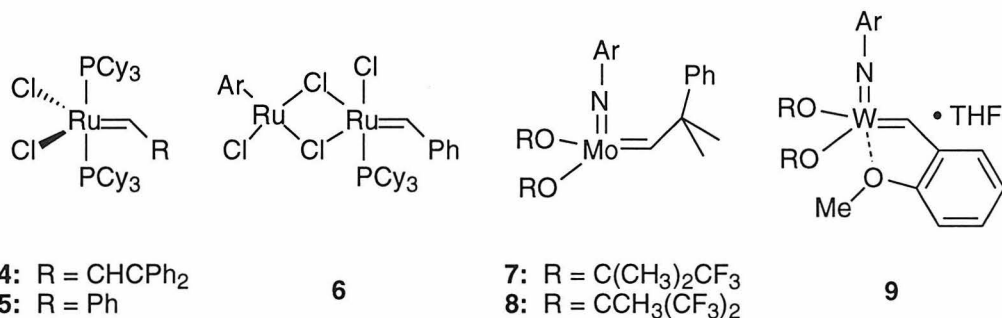


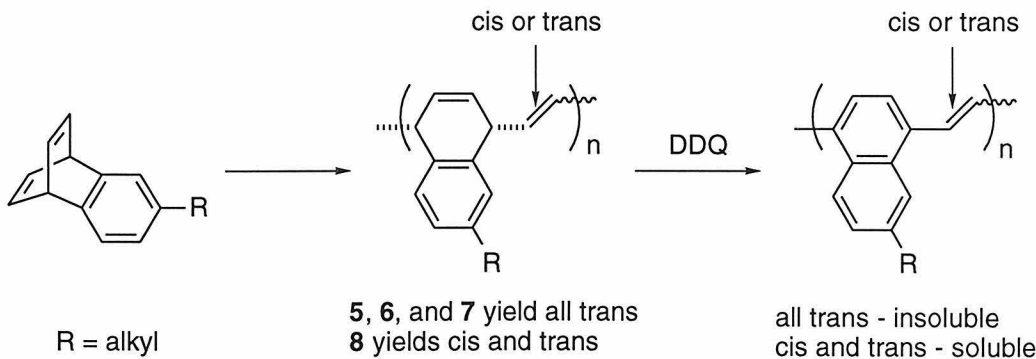
Figure 2. Metathesis initiators tested for polymerization of benzobarrelenes and barrelenes.

good solubility — the polymers are soluble in chloroform, dichloromethane, chlorobenzene, and *cis*-dichlorobenzene at room temperature. In contrast, PNV synthesized from precursor polymers prepared using **7** had only very low solubility and could be partially dissolved only when heated to 135 °C in *cis*-dichlorobenzene. A similar solubility problem was observed with polymers made using some of the newer, more active ruthenium-based catalysts,^{25,31} **5** and **6**, which were both capable of polymerizing the benzobarrelenes. The difference in solubility observed is explained by the fact that **8** produces polymers of **1** with some *cis* olefins in the polymer backbone while all of the olefins linking the cyclohexadiene units have a *trans* orientation when **1** is polymerized using **5**, **6**, or **7** as shown in Scheme 2.³²⁻³⁴ *Cis* units make the polymers more soluble because they produce a twist in the polymer backbone which disrupts the otherwise planar structure of PNV.

Table 1. Comparison of catalyst activity.

Initiator	Reaction Time	Initiation ^a	Block Copolymer Formed? ^b	Cis Olefins Observed? ^c
4	1: incomplete (10%)	not observed	no ^d	no
5	1: 27 hrs	100%	no ^e	no
	2: 27 hrs	(M/c = 25)		
	3: 1 week			
6	1: 15 hrs	100%	yes ^e	no
	3: 1 week	(M/c = 25)	bimodal distribution	
7	1: 5-10 min.	70% (M/c = 50)	yes	no
	2: 5-10 min.	100% (M/c = 100)	PDI \approx 1.7	
	3: 15-20 min.			
8	1: 12-18 hrs	<1%	no	yes
	2: 1 day			
	3: 1 day			
9	1: instantly gels	--	--	--

a) Percent initiation was calculated by the ratio of the initiated catalyst carbene to the total catalyst carbene as determined by integration of these peaks in the ^1H NMR spectrum. Carbene peaks for the catalysts are typically found at 21 - 17 ppm for **5** and **6** and 14 - 10 ppm for **7** and **8**. b) A second monomer was added when reaction of the first monomer was complete. c) See note 35. d) The first monomer was never completely consumed. e) Initiators **5** and **6** decomposed throughout the reaction. Initiator **5** decomposed almost completely by the time the first monomer was consumed. The second monomer either did not polymerize or a bimodal molecular weight distribution was observed.

Scheme 2

Despite the advantage of providing more soluble polymers, initiator **8** had some problems of its own. The main shortcomings of this catalyst were that polymerizations of **1** - **3** were found not to be living and most of the catalyst did not initiate during the polymerization.¹ As a result, this catalyst seemed incapable of allowing the synthesis of the desired well-defined block copolymers for several reasons. First, chains that terminate during the non-living polymerization of the first monomer would not continue to grow when the second monomer was added. Second, with uninitiated **8** remaining after the first monomer is polymerized, it is likely that the second monomer would react with uninitiated catalyst to produce a new homopolymer separate from the polymer produced by polymerization of the first monomer. Third, the poor initiation of **8** resulted in the synthesis of insoluble precursor polymers of **2** and **3**. This insolubility arose since the small amount of **8** that did initiate polymerized all of the monomer. Thus, much higher molecular weight polymers were generated than originally intended. Finally, as a result of both poor initiation and chain termination, the benzobarrelene polymers made with **8** typically had broad, and sometimes multimodal, molecular weight distributions. As all of these properties are undesirable for the synthesis of block copolymers, a solution needed to be found either in the form of a new catalyst or a way to tune the activity of **8**.

Activation of **8 by **2**?** A breakthrough that essentially solved all of these problems at once came nearly by accident. The first indication that **8** could be activated to achieve a living polymerization was observed with polymerizations of the first batches of butyl substituted **2**. When **2** that had been prepared by the Diels-Alder reaction of butyltrifluorobenzyne with benzene (see Scheme 5 in Chapter 1) was polymerized, nearly all of **8** was observed to initiate, and the polymerization was much faster than polymerizations of **1**. Furthermore, when **1** was added after polymerization of **2** was complete, a new initiated carbene was observed and the one present when the trifluorobenzobarrelene was polymerizing disappeared. In addition, this polymerization of **1** proceeded much more rapidly than usual. This reaction took about 1 hour versus the

usual reaction time of 12 - 18 hours. Therefore, by polymerizing **2** first, catalyst **8** seemed to be permanently activated and allowed the synthesis of block copolymers. The best initial explanation for these observations seemed to be that **2** effects more complete initiation of **8**, probably because the fluorinated benzobarrelene propagates more slowly, so initiation is favored. The initiated **8** then reacts more readily with other monomers than uninitiated catalyst does, thus allowing a more rapid, living polymerization of **1**.

These conclusions were quickly shown to be incorrect, however. When **2** was prepared by alkylating chlorotrifluorobenzobarrelene (see Scheme 6 in Chapter 1) rather than performing the Diels-Alder reaction with the alkylated benzene, the **2** obtained was not capable of activating the catalyst as it had before. The alkylated trichlorobenzobarrelenes, **3**, prepared also showed no ability to activate **8**. This result was also strange, given the explanation above, since **3** propagates even more slowly than **2**, so complete initiation should be favored even more strongly.

Activation of 8 by Hexafluoro-*t*-butanol. At this point, it seemed possible that some impurity in the first batches of **2** had caused the observed activation of **8**. Jérôme Claverie, who was working across the bench from me at that time, had shown that tungsten analogs of **8** could be activated with hexafluoro-*t*-butanol (HFB),³⁶ so this seemed to be worth a try, even though it was unclear how **2** could have gotten contaminated with HFB. The first trials using HFB in dichloromethane simply caused rapid decomposition of **8** before any polymer was made, but performing the reaction in benzene yielded better results. As shown in Table 2, reactions carried out in benzene in the presence of HFB all showed initiation and overall catalyst activity reminiscent of that observed for polymerizations of the first batches of **2**. The percentage of **8** that became initiated was observed to increase as the amount of HFB added was increased, but the catalyst began to decompose when about 50 equivalents were added. The best activity was observed when 14 - 20 equivalents of HFB were used,³⁷ so all subsequent polymerizations employing initiator **8** were carried out using an amount in this range. In

addition to achieving better initiation, the polymerizations were much more rapid. For example, polymerization of **1** takes 10 - 18 hours when HFB is not added, but is complete after 35 minutes when 14 equivalents of HFB are added. So overall, adding HFB increased both the rate of initiation and propagation. A higher percentage of **8** was initiated because the rate of initiation was increased more than the rate of propagation.

Table 2. Effect of HFB on the activity of **8** and the properties of the resulting polymers.

Monomer	Rxn. Time	Solvent	M/C	equiv. HFB	PDI	% Initiation*
1	12 - 18 hrs	CD ₂ Cl ₂	45	0	2.5 - 5	<1%
2	1 day	CD ₂ Cl ₂	45	0	≈ 5	<1%
3	1 day	CD ₂ Cl ₂	45	0	≈ 5	<1%
1	35 min	C ₆ D ₆	45	14	1.7	80%
1	35 min	C ₆ D ₆	99	14	1.86	100%
1	2 hrs	C ₆ D ₆	45	100	2.39	carbene not observed
2	1.5 hrs	C ₆ D ₆	45	14	1.26	75%
3	6 hrs	C ₆ D ₆	45	14	1.13	100%

* Percent initiation was calculated by the ratio of initiated **8** to total **8** as determined by integration of the carbene region of the ¹H NMR spectrum (≈ 14 - 10 ppm).

Deactivation of **8 by Lewis Bases.** Even when activated with HFB, complete initiation of **8** could be achieved with most benzobarrelene and barrelene monomers only when the monomer to initiator ratio was around 100 or above.³⁸ Because we wanted to have the capability to synthesize block copolymers with shorter block segments than this, additional studies were carried out to further tune **8**'s activity.

Since adding HFB seemed to have maximized the rate of initiation and propagation, we now sought to slow the rate of propagation relative to the rate of initiation so that complete initiation would be favored. Lewis bases such as phosphines,

phosphites and THF were known to reduce the activity of metathesis catalysts by reversibly coordinating to the catalyst's metal center.^{39,40} Coordinated Lewis bases cause deactivation because they occupy a coordination site and thereby prevent coordination of the monomers' olefin units, as shown for THF coordinated to **8** in Scheme 3. It had also been shown that, during polymerizations of cyclobutene with tungsten catalysts, Lewis bases coordinated more strongly to the initiated form of the catalysts, making initiated catalyst less able to coordinate to monomers than the uninitiated catalyst. As a result, initiation was favored over propagation and more catalyst became initiated.³⁹

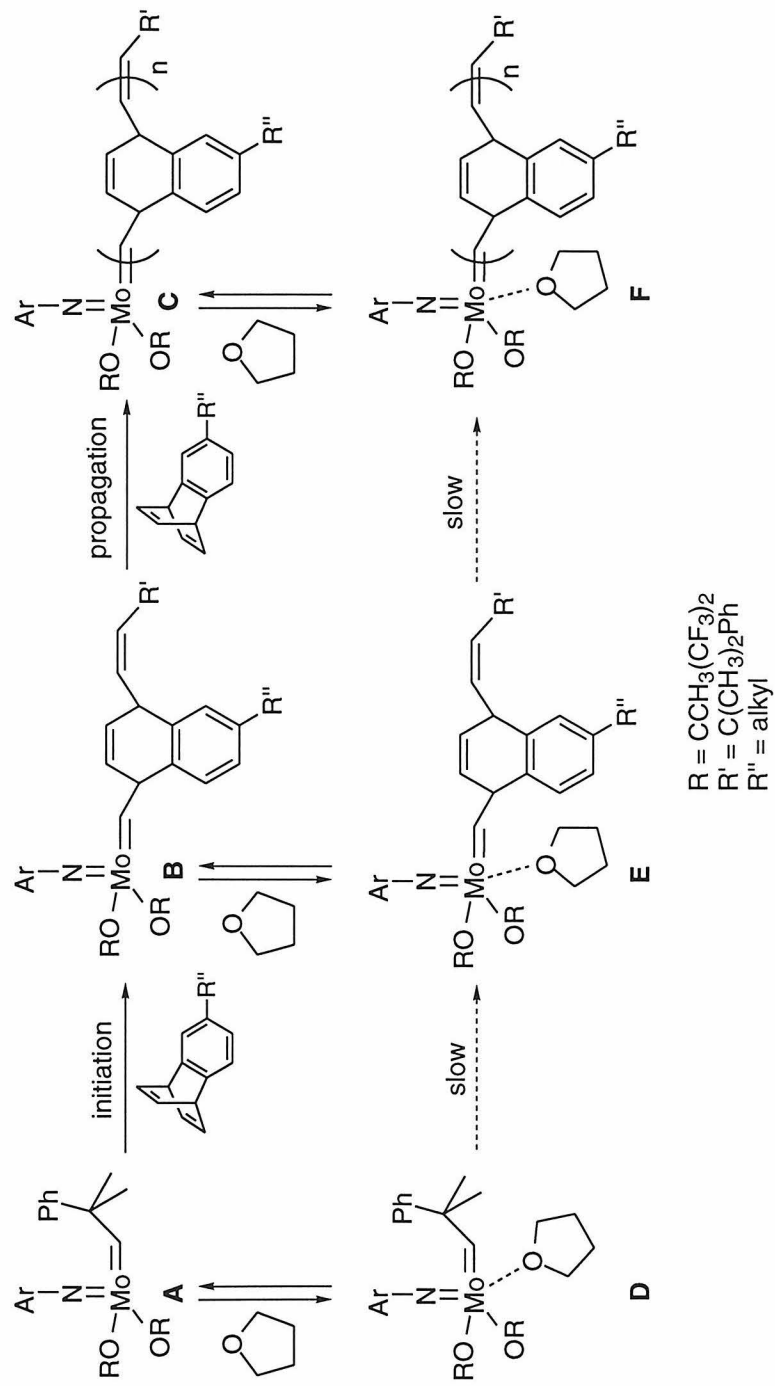
As shown in Table 3, using 50 equivalents of trimethyl phosphite with **8** for the polymerization of **1** did, in fact, produce complete initiation. However, peaks characteristic of *cis* olefin units were not observed in the ¹H NMR of the resulting polymers. These units were known to be necessary to obtain soluble PNVs, so other Lewis bases were tested to identify one that would not affect the polymer's configuration. Polymerizations carried out in the presence of triphenylphosphine were found to yield polymers with some *cis* units, but peaks characteristic of the proton on the carbene carbon

Table 3. Effect of Lewis bases on the activity of **8** and the properties of the resulting polymers.

monomer	Rxn. Time	LB ^a	Equiv. LB	M/C	PDI	Initiation ^b	trans:cis ^f
1	1 week	P(OMe) ₃	50	45	c	100%	no cis
1	2 days	PPh ₃	50	45	c	d	19
1	18 hrs	THF	50	45	1.35	100%	2 - 7
1	4 hrs	THF	10	45	1.42	100%	2 - 7
2	12 hrs	THF	10	45	1.14	100%	20
3^e	6 hrs	THF	0	45	1.14	100%	f

14 equivalents of HFB were used for all reactions. a) LB stands for Lewis base. b) See Table 2 note. c) Molecular weight data was not obtained for these polymers. d) Carbene protons were not observed. e) LB was not needed to achieve complete initiation of **8** when **3** was polymerized. Actually, 25 equivalents of **3** can effect complete initiation of **8** without LB added. f) See note 35.

Scheme 3



Species **A**, **B**, and **C** can more readily add monomer than species **D**, **E** and **F**, which are deactivated by the coordinated Lewis base (THF).

were not observed by ^1H NMR during the reaction, so the polymerizations may not have been living. Finally, THF was tested and found to yield complete initiation of **8**, when the ratio of **1** or **2** to **8** was 45. The polymers synthesized under these conditions had a *cis* content the same as that produced when no Lewis base was added, and the proton on the propagating carbene carbon was observed throughout the reaction. As shown in Table 3, essentially the same result was obtained when 10 equivalents of THF was used instead of 50 equivalents. The lesser amount of THF was used for most polymerizations since the reaction is more rapid with less THF present.

"Livingness" Studies. To determine whether polymerizations by **8** in the presence of HFB and THF were living, several tests were done to check for chain termination, chain transfer, chain coupling and backbiting reactions. For these experiments, THF was added only to those polymerizations that needed it to cause all of **8** to initiate. The first tests were done by polymerizing different amounts of monomers **1**, **2** and the di-*t*-butylester barrelenes monomer, **10** (see Figure 3), with the same amount of **8**. Results of these experiments, displayed in Figure 4, show that the molecular weight of the polymers obtained increased linearly with the monomer to initiator ratio, as is expected for a living polymerization.

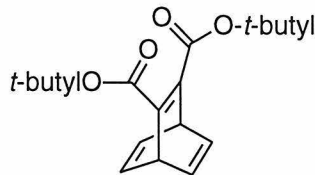


Figure 3. Di-*t*-butylester barrelenes, **10**.

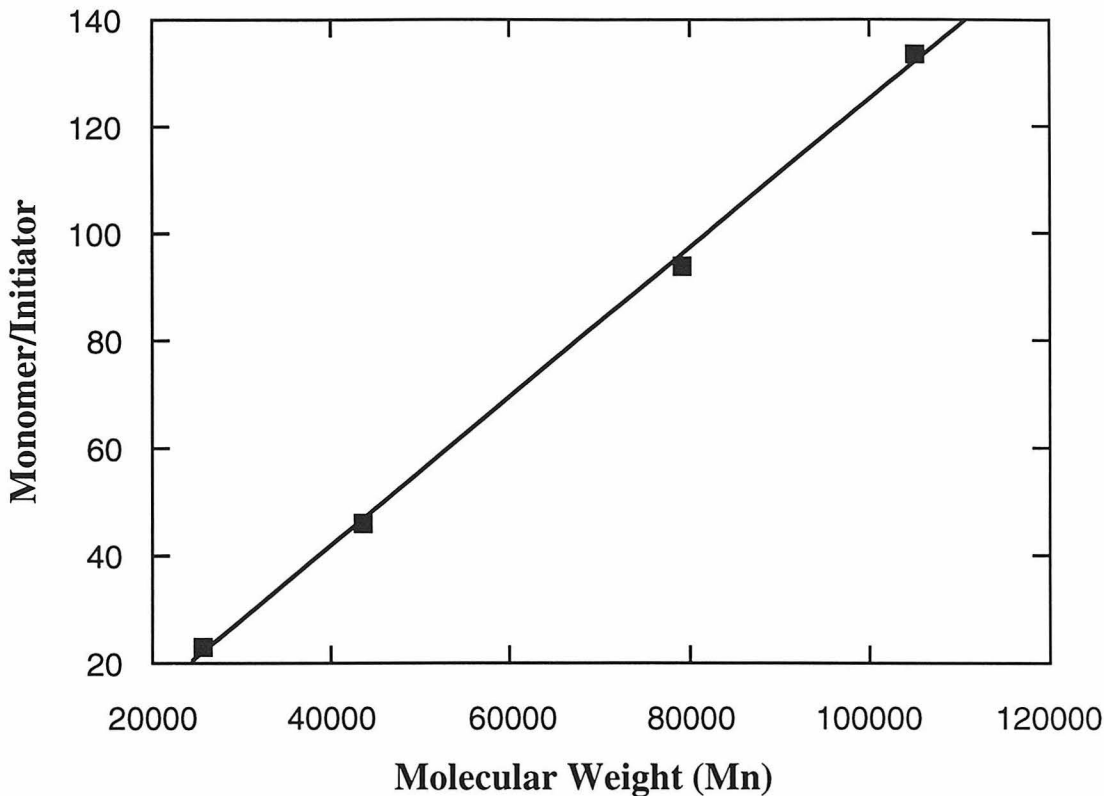


Figure 4a. Monomer/initiator ratio vs. number average molecular weight for **1**.

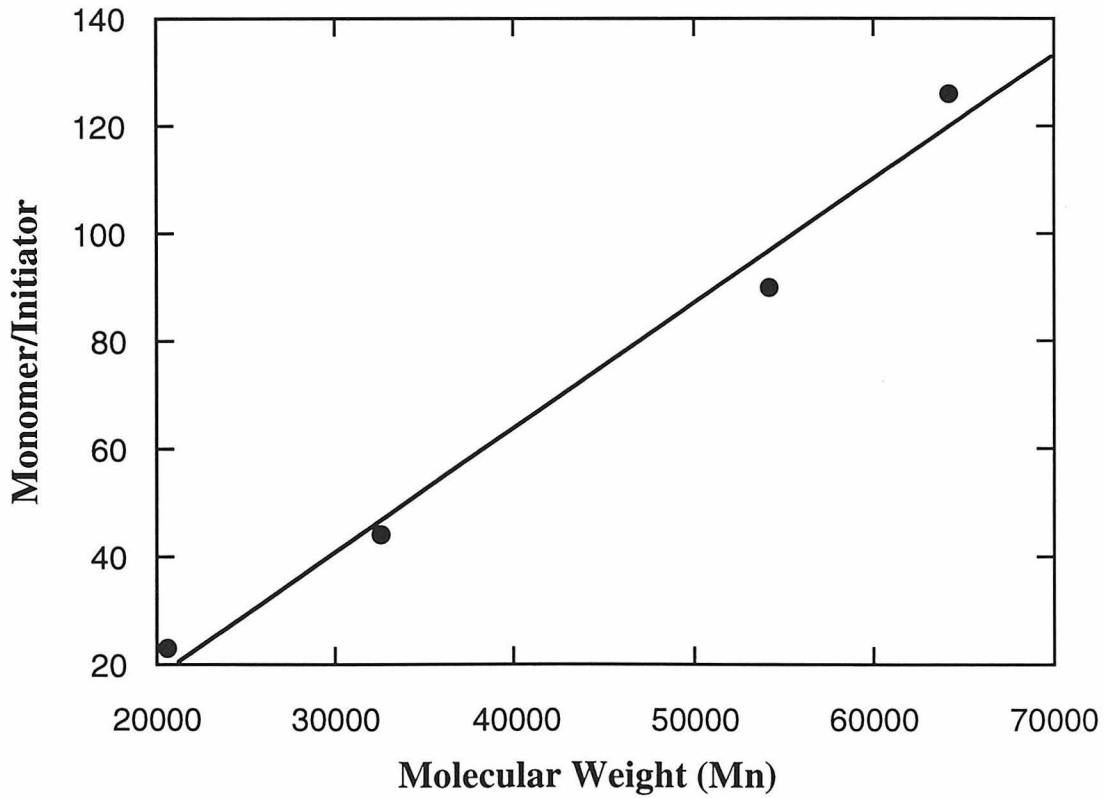


Figure 4b. Monomer/initiator ratio vs. number average molecular weight for **2**.

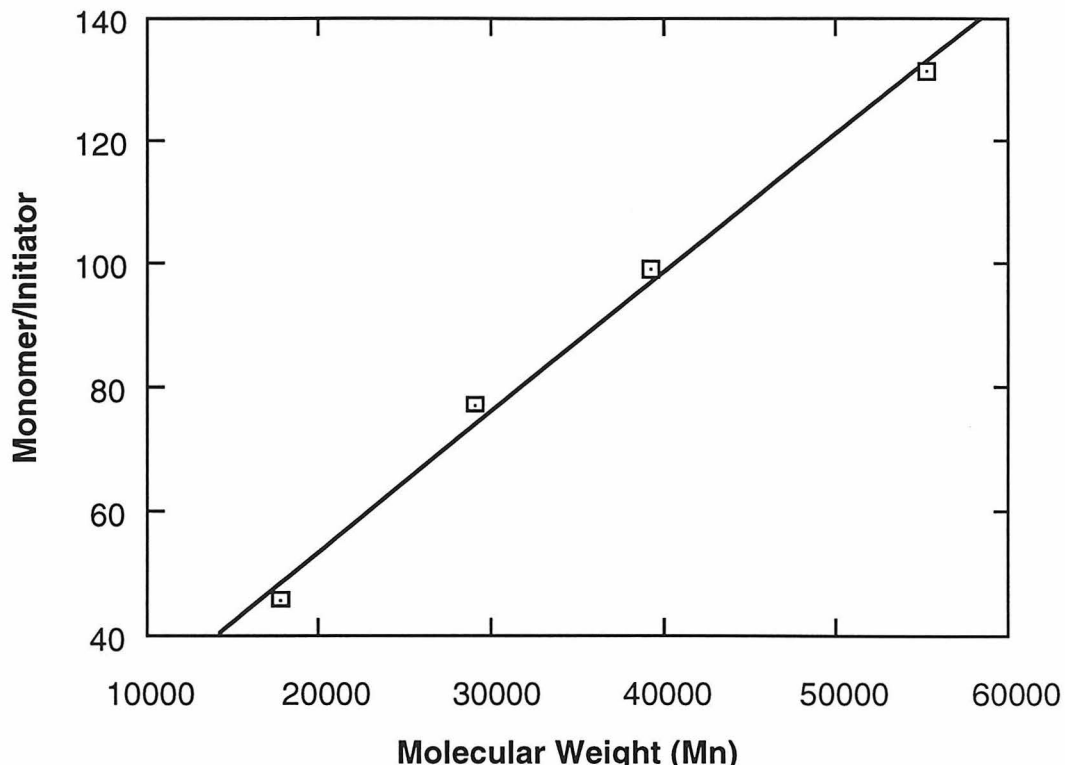


Figure 4c. Monomer/initiator ratio vs. number average molecular weight for **10**.

The second test was done by first polymerizing one batch of **10**, with a monomer to initiator ratio of 50, to completion. After the reaction was complete, the reaction mixture was divided into three equal amounts. One of the aliquots, **A**, was immediately quenched with benzaldehyde, which deactivates the initiator, to establish a reference point for molecular weight and polydispersity. The second aliquot, **B**, was saved to determine whether backbiting or chain coupling reactions, which would cause an increase in the polydispersity, occur over time. Additional monomer (250 equivalents) was added to the third aliquot, **C**, to continue the polymerization. This sample was used to determine if chain termination occurred before the second batch of monomer was added. Following completion of the polymerization in aliquot **C**, it and aliquot **B** were both quenched with benzaldehyde.⁴¹ As shown in Figure 5, aliquot **C** shows that little if any chain termination occurred before the second batch of monomer was added. While the

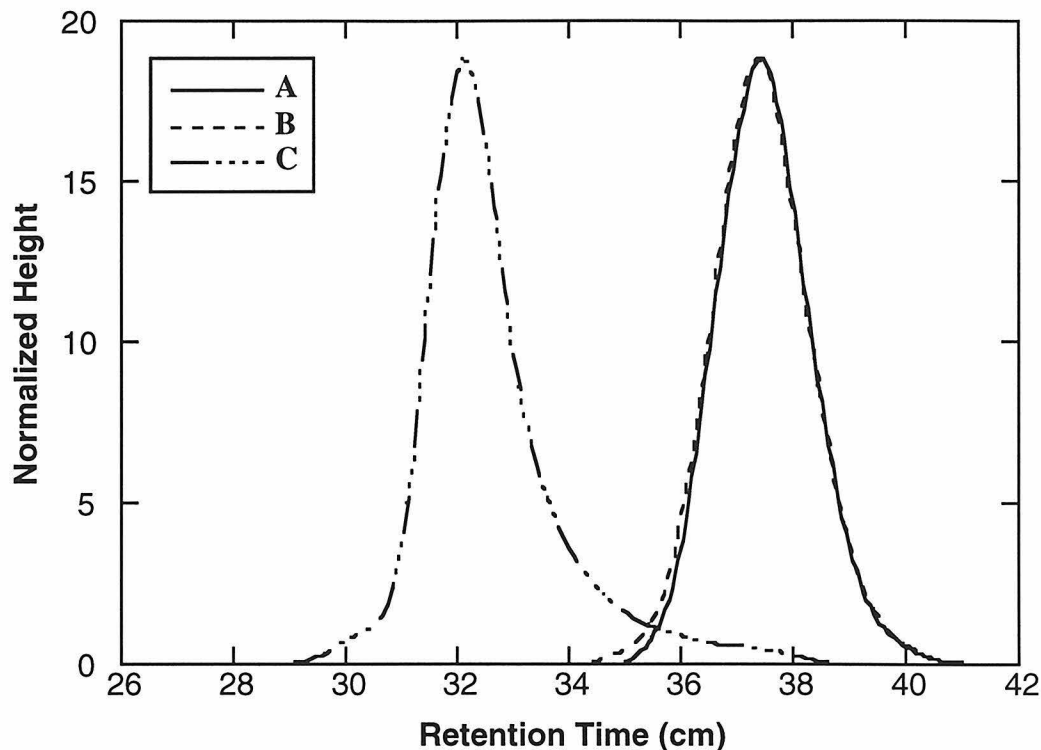


Figure 5. Test for chain transfer, chain termination and backbiting.

tailing of this peak indicates that some chain termination may be occurring as the polymer chains become longer, the fraction of terminated chains is quite small. In addition, the observed molecular weight increase is comparable to that expected using the data in Figure 4c as a calibration curve. Comparison of aliquots **A** and **B** shows that there was no broadening of the polymer's molecular weight distribution and no increase in molecular weight over time. This result indicates that the initiator at the end of the polymer chain is not backbiting into the chain that it is connected to, or into other polymer chains, and that coupling reactions or other polymer degradation reactions do not occur in the presence of unquenched initiator. Experiments similar to this one have been performed with the benzobarrelenes and similar results were obtained.

The results of these experiments present strong evidence that the reaction is living, and that this polymerization system is well suited to the synthesis of block copolymers. This possibility is explored more fully in Chapter 5.

Conclusions

From the tests conducted, metathesis initiator **8** was identified as the best choice for the synthesis of well defined, soluble homopolymers and copolymers of the barrelenes and benzobarrelenes. While several other initiators were found to polymerize the benzobarrelenes, these catalysts either crosslinked the precursor polymers or produced polymers that became insoluble when aromatized to yield PNVs. Initiator **8** produces precursor polymers with *cis* olefin linkages that make the PNVs obtained more soluble. Adding hexafluoro-*t*-butanol (HFB) to polymerizations using **8** was found to cause more of the catalyst to become initiated and also produced more rapid polymerizations. The percent of **8** that became initiated was observed to increase further with the addition of a Lewis base, usually THF, which reduced the rate of propagation more than the rate of initiation. Polymerizations of benzobarrelene and barrelene monomers were shown to be living when HFB activated **8** was employed.

Experimental

General Methods and Materials. NMR spectra were recorded on a QE Plus-300 MHz (300.1 MHz ¹H; 75.33 MHz ¹³C) spectrometer. Gel permeation chromatography (GPC) utilized an AM Gel Linear 10 column and a Knauer differential refractometer. Dichloromethane (Burdick and Jackson HPLC grade) was used as the eluent for all GPC measurements. Molecular weights are uncorrected and reported as compared to Shodex polystyrene standards with molecular weights ranging from 2.95 x 10³ to 2.40 x 10⁶. Benzene-d₆ was dried by passing through activated alumina columns. Dichloromethane-d₂, tetrahydrofuran-d₈, hexafluoro-*t*-butanol (HFB) were distilled from calcium hydride. Benzobarrelene and barrelene monomers were prepared as described in Chapters 1 and 2. Characterization data for the polymers studied is included in the Experimental section of Chapters 4 and 5. Initiators **4 - 9** were prepared as previously reported.²⁵⁻³⁰

Characterization data for the polymers prepared is included in the Experimental section of Chapter 4.

General Procedure for Polymerizations. Inside a nitrogen filled dry box the desired amount of monomer (\approx 50 - 150 mg depending on the monomer and the monomer to catalyst ratio desired) was dissolved in 0.5 - 0.6 g of dry degassed benzene and the required amount of dry hexafluoro-*t*-butanol (usually \approx 7.8 μ L) was added. Initiator **8** (3.5 - 3.9 mg) dissolved in 10 drops of dry C₆D₆ was then added to this solution. The reaction mixture changed color from yellow to light orange or orange-brown during the first few minutes after mixing. For following the reaction by ¹H NMR, the solution was transferred into an NMR tube equipped with a J-Young valve. After the polymerization was shown to be complete, if a block copolymer was being made, the NMR tube was returned to the dry box and the second monomer was added. After the polymerization was complete, degassed benzaldehyde was added to quench the initiator. The reaction mixture, which turned brown over 30 minutes, was then pipetted into degassed methanol and the resulting precipitate was recovered by centrifuging and then decanting the solvent. Further purification was accomplished by redissolving the polymer in dichloromethane or benzene and then reprecipitating the polymer in methanol. The polymer was then dried under vacuum. GPC studies were conducted by dissolving a sample of this polymer in dichloromethane.

Procedure for "Livingness" Studies. For the studies of monomer to catalyst ratio versus molecular weight, the procedure was essentially the same as that described above. The only difference was that a stock solution of **8** was prepared so that the same amount of catalyst could be added to each of the four polymerizations. This solution was prepared by dissolving 37.8 mg of **8** in 1 mL of C₆D₆. Using a syringe, 10 μ L of this solution was added to each of four vials which each contained a solution of the same monomer. The separate vials each contained different amounts of the monomer to be studied so that the resulting monomer to catalyst ratios were 25, 45, 95 and 125. For

polymerization of **1** with a monomer to catalyst ratio of 25, 50 equivalents (20 μ L) of THF-d₈ were added. For all of the other polymerizations 10 equivalents (4 μ L) of THF-d₈ were used. These polymerizations were terminated and purified as described in the "General Procedure for Polymerizations" section and then GPC was conducted on each sample. Synthesis of the diblock homopolymer of **10** was conducted as described for the synthesis of block copolymers.

References and Notes

- (1) Pu, L.; Wagaman, M. W.; Grubbs, R. H. *Macromolecules* **1996**, *29*, 1138.
- (2) Wagaman, M. W.; Bellmann, E.; Grubbs, R. H. *Phil. Trans. R. Soc. Lond. A* **1997**, *355*, 727.
- (3) Wagaman, M. W.; Grubbs, R. H. *Synth. Met.* **1997**, *84*, 327.
- (4) Wagaman, M. W.; Grubbs, R. H. *Macromolecules* **1997**, *30*, 3978.
- (5) Wagaman, M. W.; Bellmann, E.; Cucullu, M. E.; Grubbs, R. H. *J. Org. Chem.* , In Press.
- (6) Maughon, B. R.; Weck, M.; Mohr, B.; Grubbs, R. H. *Macromolecules* **1997**, *30*, 257.
- (7) Saunders, R. S.; Cohen, R. E.; Schrock, R. R. *Macromolecules* **1991**, *24*, 5599.
- (8) Rissee, W.; Grubbs, R. H. *J. Mol. Cat.* **1991**, *65*, 211.
- (9) Nomura, K.; Schrock, R. R. *Macromolecules* **1996**, *29*, 540.
- (10) Kanoaka, S.; Grubbs, R. H. *Macromolecules* **1995**, *28*, 4707.
- (11) Komiya, Z.; Schrock, R. R. *Macromolecules* **1993**, *26*, 1387.
- (12) Lynn, D. M.; Kanoaka, S.; Grubbs, R. H. *J. Am. Chem. Soc.* **1996**, *118*, 784.
- (13) Watkins, D. M.; Fox, M. A. *Macromolecules* **1995**, *28*, 4939.
- (14) Weck, M.; Schwab, P.; Grubbs, R. H. *Macromolecules* **1996**, *29*, 1789.
- (15) Ivin, K. J.; Mol, J. C. *Olefin Metathesis and Metathesis Polymerization*; Academic Press: San Diego, 1997.
- (16) Pugh, C.; Liu, H.; Arehart, S. V.; Narayanan, R. *Macromol. Symp.* **1995**, *98*, 293.
- (17) Schimetta, M.; Stelzer, F. *Macromolecules* **1994**, *27*, 3769.
- (18) Winkler, B.; Rehab, A.; Ungerank, M.; Stelzer, F. *Macromol. Chem. Phys.* **1997**, *198*, 1417.
- (19) Shon, Y. S.; Lee, T. R. *Tetrahedron Lett.* **1997**, *38*, 1283.
- (20) Komiya, Z.; Schrock, R. R. *Macromolecules* **1993**, *26*, 1393.

- (21) Komiya, Z.; Pugh, C.; Schrock, R. R. *Macromolecules* **1992**, *25*, 6586.
- (22) Webster, O. W. *Science* **1991**, *251*, 887.
- (23) Quirk, R. P.; Lee, B. *Polym. Int.* **1992**, *27*, 359.
- (24) Matyjaszewski, K. *Macromolecules* **1993**, *26*, 1787.
- (25) Dias, E. L. K., Ph.D. Thesis, California Institute of Technology, 1998.
- (26) Nguyen, S. T.; Johnson, L. K.; Grubbs, R. H.; Ziller, J. W. *J. Am. Chem. Soc.* **1992**, *114*, 3974.
- (27) Nguyen, S. T.; Grubbs, R. H.; Ziller, J. W. *J. Am. Chem. Soc.* **1993**, *115*, 9858.
- (28) Nguyen, S. T., Ph.D. Thesis, California Institute of Technology, 1995.
- (29) Fox, H. H.; Lee, J. K.; Park, L. Y.; Schrock, R. R. *Organometallics* **1993**, *12*, 759.
- (30) Johnson, L. K.; Virgil, S. C.; Grubbs, R. H. *J. Am. Chem. Soc.* **1990**, *112*, 5384.
- (31) Schwab, P. E.; France, M. B.; Grubbs, R. H.; Ziller, J. W. *Angew. Chem. Int. Ed. Engl.* **1995**, *34*, 2039.
- (32) Oskam, J. H.; Schrock, R. R. *J. Am. Chem. Soc.* **1993**, *115*, 11831.
- (33) Schrock, R. R.; Lee, J. K.; O'Dell, R.; Oskam, J. H. *Macromolecules* **1995**, *28*, 5933.
- (34) Ivin, K. J. *Olefin Metathesis*; Academic Press: New York, 1983.
- (35) *Cis* olefin content was determined from the presence of a peak downfield from the normal ex-bridgehead peak and the presence of extra olefin peaks on both sides of the major olefin peaks in the ^1H NMR spectrum (see Experimental section of Chapter 4). For polymers of **1**, *cis* olefin content was confirmed by ^{13}C NMR. The small amount of *cis* units present in polymers of **2** was not observed in the ^{13}C NMR spectrum. For **3** all ^1H NMR peaks are very broad and obscure the regions where *cis* peaks would be observed and peaks indicative of *cis* olefins were not observed by ^{13}C NMR.
- (36) Claverie, J., Ph.D. Thesis, California Institute of Technology, 1995.
- (37) Kaita, S.; Elder, D. L., personal communication.

- (38) A notable exception to this is the alkylated trichlorobenzobarrelene monomer, **3**, which causes all of **8** to initiate when the monomer to catalyst ratio is 25.
- (39) Wu, Z.; Wheeler, D. R.; Grubbs, R. H. *J. Am. Chem. Soc.* **1992**, *114*, 146.
- (40) Wu, Z.; Grubbs, R. H. *Macromolecules* **1994**, *27*, 6700.
- (41) Mitchell, J. P.; Gibson, V. C.; Schrock, R. R. *Macromolecules* **1991**, *24*, 1220.

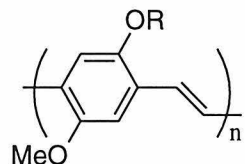
Chapter 4

Synthesis and Study of PNV and PPV Homopolymers

Abstract: Benzobarrelene and barrelene monomers were polymerized to make homopolymers using the hexafluoro-*t*-butanol activated molybdenum catalyst described in Chapter 3. These precursor polymers were then aromatized to yield poly(1,4-naphthalenevinylene)s (PNVs) and poly(*para*-phenylenevinylene)s (PPVs). The rate of the polymerization and ease of aromatization were both found to be dependent on the substituents present, with electron withdrawing groups generally inhibiting both processes. For the diester substituted barrelenes, the rate of polymerization was also found to depend on the alkyl group present on the ester. Photoluminescence measurements show that the different polymers prepared luminesce from the blue (450 nm) to near the red (580 nm). For the PNVs, polymers with electron withdrawing substituents were shown to be red shifted relative to PNV. The PPVs with electron withdrawing groups were blue shifted, however, as a result of twisting the polymer chain, which reduces the polymers' conjugation length. It was found that partially oxidizing the *t*-butyl ester substituted precursor polymer, **15**, so that only 80% of the polymer units are aromatized increases both the solubility and photoluminescence quantum yield of the resulting PPV, **23**. Deprotection of polymer **23** by acid catalyzed thermolysis of the *t*-butyl groups followed by treatment with aqueous base produced a dicarboxylate PPV, **27**, that is soluble in water. Conductivity studies of the alkyl-substituted PNV prepared here showed that this polymer has a conductivity of 15 S cm⁻¹ when doped using nitrosonium tetrafluoroborate.

Introduction

One feature common to the monomers and polymers described here is that they are substituted with electron withdrawing groups. This type of substitution contrasts with that of MEH-PPV and other dialkoxy-substituted poly(1,4-phenylenevinylene)s (PPVs), which are some of the most commonly used polymers for the study of light emitting diodes (LEDs).¹⁻⁸ The main advantage of these materials, however, is not the electron donating character of their alkoxy substituents, but their good solubility in common organic solvents, which allows easy fabrication of devices by spin casting the emissive layer onto the LED anode, usually indium tin oxide (ITO). Using MEH-PPV has yielded extensive progress in the study of device fabrication and optimization of both single layer and multilayer LEDs,^{5,6} and more recently this material has been used as the emissive layer in some of the first organic polymer lasers.^{4,7}



R = 2-ethylhexyl

MEH-PPV

One potential drawback of using MEH-PPV in electroluminescent (EL) devices, however, is that the electron-donating groups on the polymer destabilize its HOMO and LUMO.⁹ This destabilization renders the polymer more readily oxidized by oxygen than unsubstituted PPV. Because of this instability, devices made with MEH-PPV require rigorous encapsulation to prevent oxidation of the emissive layer.^{6,10,11} Oxidation of the polymer may remain a problem even with encapsulation, however, since recent studies show that ITO may be a source of oxygen.¹² In contrast to the effect of electron donating alkoxy groups, electron withdrawing groups stabilize the HOMO and LUMO of PPV and

PNV,⁹ making these polymers less susceptible to oxidation. Electron withdrawing groups also increase the polymers' electron affinity thus making it easier to inject electrons into the polymer. This increased electron affinity allows the use of electrodes with higher work functions than calcium, such as aluminum, which is more air stable than calcium. In addition, this heightened electron affinity can improve device efficiency by yielding a better balance between electrons and holes in the polymer. While PPV and PNV are good hole conductors and poor electron conductors, electron accepting substituents improve these materials' electron injection and electron transport properties and, therefore, improve device efficiency by increasing the number of holes that pair with electrons, thereby reducing the number of holes that are quenched at the negative electrode.¹¹

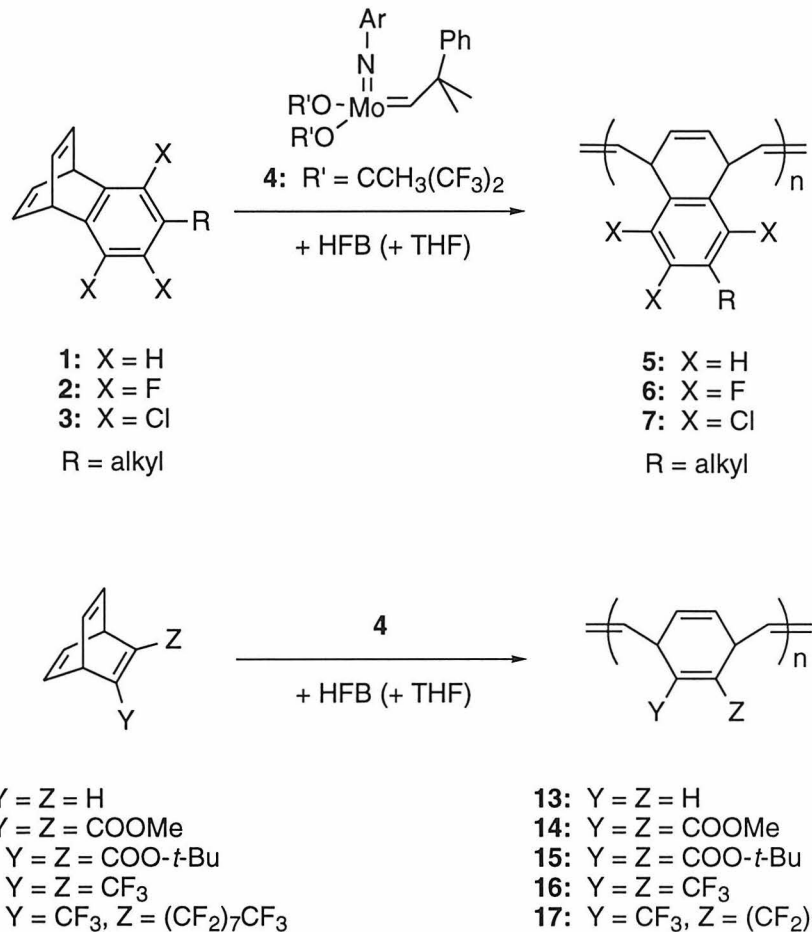
While electron withdrawing groups can improve the properties of conjugated polymers for EL applications for the variety of reasons mentioned above, only a few PPVs bearing electron withdrawing groups have been synthesized.^{11,13-17} The majority of these polymers have been soluble only in their unconjugated, precursor form, and therefore, are not ideal for LED applications since it is desirable to be able to spin cast the conjugated polymer. Of the polymers synthesized, several have shown a blue shift in their absorption and emission spectra, which contrasts with the red shift predicted for conjugated polymers bearing electron accepting groups.⁹ It is, therefore, desirable to synthesize new, soluble PPVs containing electron withdrawing groups not only for the advantages these polymers will have for LED applications, but also to examine how the emission wavelength of the polymers shifts with different electron withdrawing substituents.

Results and Discussion

Synthesis of Precursor Polymers. As shown in Scheme 1, both the benzobarrelene and barrelene monomers were polymerized using the HFB activated

molybdenum catalyst, **4**.¹⁸⁻²⁰ Benzobarrelene monomers substituted with electron withdrawing groups, **2** and **3**, polymerized more slowly than **1**, which did not have electron withdrawing substituents (see Table 1 and also see Tables 1 and 2 in Chapter 3).

Scheme 1



The cause of this trend is that the electron withdrawing groups make the olefins of **2** and **3** less electron rich. Therefore, these olefins have less electron density to donate to the electron poor metal center of the polymerization catalyst, so coordination of these monomers to the metal is less favorable than with **1**. As a result, the electron poor monomers polymerized more slowly.

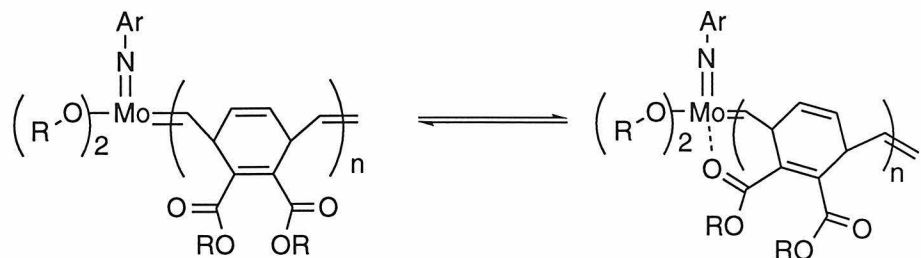
For the barrelenes, a similar trend was followed except in the case of the methyl ester substituted barrelene, **9**. Using HFB activated **4** it was observed that polymerization

Table 1. Results of polymerizations of benzobarrelenes and barrelenes.

Monomer	Rxn. Time	Solvent	PDI	% Initiation ^c
1	35 min	C ₆ D ₆	1.70	75 - 80%
2	1.5 hrs	C ₆ D ₆	1.26	75 - 80%
3	6 hrs	C ₆ D ₆	1.13	100%
8	5 min	C ₆ D ₆	a	a
9	1 week (90%)	C ₆ D ₆	1.44	carbene not observed
10	3 hrs	C ₆ D ₆	1.22	86%
11	overnight	C ₆ D ₆	1.07	100%
12	overnight	C ₆ F ₆	b	100%

a) The polymer was insoluble so GPC data could not be obtained and initiated catalyst did not remain in solution. b) This polymer is soluble only in fluorinated solvents, so GPC data could not be obtained. c) Percent initiation was calculated by the ratio of initiated **8** to total **8** as determined by integration of the carbene region (\approx 14 - 10 ppm) of the ¹H NMR spectrum.

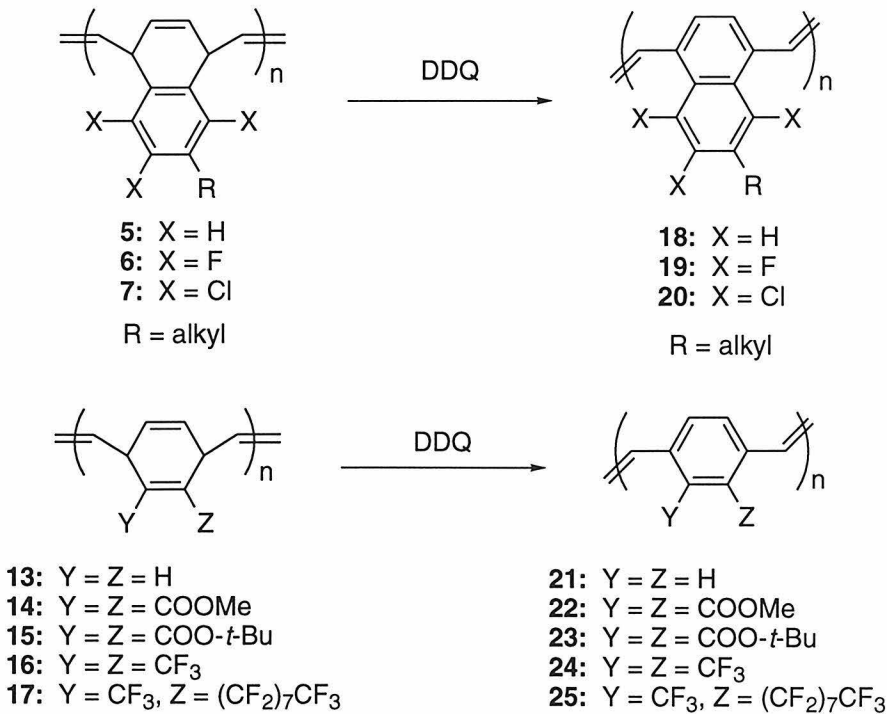
of **10** was much faster than **9**, with **10** being completely consumed after 3 hours, but with the polymerization of **9** reaching only 80 to 90% completion after 1 week. The slower reaction of **9** is most likely due to coordination of the polymer chain to the catalyst as shown in Figure 1. Such coordination is expected to deactivate the molybdenum carbene, and thereby reduce the rate of monomer consumption, by blocking a coordination site as described for THF in Chapter 3. Alternatively, the monomer could coordinate to the catalyst. Monomer coordination would not have the favorable chelate effect but would

**Figure 1.** Coordination of the growing polymer chain to the molybdenum initiator.

similarly deactivate the molybdenum initiator. For monomer **10** the polymerization reaction is much faster, and propagating carbene protons can be observed throughout the reaction. This indicates that coordination of the monomer or growing polymer to molybdenum is weaker than for **9**, due to the steric interaction between the *t*-butyl groups and the molybdenum and, therefore, deactivation of **4** is diminished.

Polymer Purification and Aromatization. Completed polymerizations were terminated by adding a few drops of benzaldehyde to the reaction mixture.²¹ Following this procedure, the polymers were purified by pipetting the reaction solution into degassed methanol (degassed solvents were used to prevent oxidation of the polymers by oxygen). The polymer precipitate was isolated by centrifuging this mixture and then decanting the solvent under argon. To further purify the polymers, they were redissolved in either degassed dichloromethane, benzene, or hexafluorobenzene (polymer **17**) and then reprecipitated using degassed methanol. The mixture was again centrifuged and the

Scheme 2



solvent decanted. This process was repeated until the decanted solvent mixture was colorless. The polymers were then dried under vacuum.

Aromatization of the precursor polymers was achieved using 2,3-dichloro-5,6-dicyano-1,4-benzoquinone, DDQ, as shown in Scheme 2.²² Overall, aromatization of the precursor polymers followed a trend similar to that observed for polymerization of the monomers. As shown in Table 2, precursor polymers without electron withdrawing groups were aromatized rapidly at room temperature while those bearing electron withdrawing groups required longer reaction times and/or elevated reaction temperatures. At the two extremes were polymer **5**, which turns the deep red color of PNV immediately when DDQ is added, and polymer **17** which required heating at 120 °C for 3 days using an excess of DDQ. While ¹H and ¹³C NMR of the precursor polymers showed peaks in

Table 2. Aromatization conditions for the precursor polymers.

Polymer	Rxn. Time	Temperature	Solvent
5	2 hrs	rt	CH ₂ Cl ₂
6	overnight	rt	CH ₂ Cl ₂
7	overnight	120	C ₆ H ₅ Br
13	3 hrs ^a	rt	CH ₂ Cl ₂
14	2 hrs	rt	CH ₂ Cl ₂
15	2 hrs	rt	CH ₂ Cl ₂
16	overnight	120	C ₆ H ₅ Br
17	3 days ^b	120	C ₆ F ₆

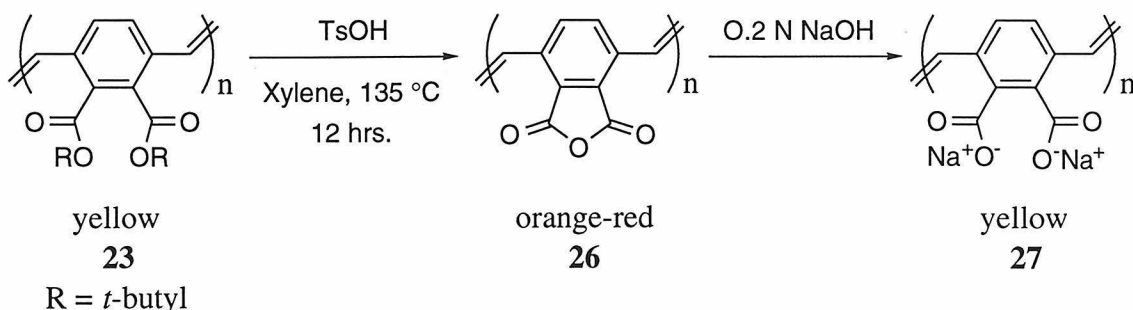
a) This reaction could not be followed by NMR since **13** is insoluble, so the reaction time was estimated from the color change of the reaction. The polymer's insolubility probably also increased its reaction time. b) This reaction took longer than that of **16** and required 2 equivalents of DDQ. One reason that these harsher conditions were required was that a polar solvent that would dissolve **17** and not cause decomposition of the DDQ could not be found. Polar solvents, such as the bromobenzene used for reaction of **16**, generally produce more facile aromatizations when DDQ is the oxidant.

the normal olefin region, upon complete aromatization all peaks not associated with the alkyl groups shifted to the aromatic region of the spectrum.

For polymers prepared for electroluminescence studies it was sometimes desirable to have the polymer be only partially aromatized since the partially converted polymers were much more soluble, and therefore better for spin casting films. Partial aromatization of the polymers was accomplished by adding less than one equivalent of the DDQ oxidant. In all cases, the polymers were purified by repeated precipitation as described above for the precursor polymers. Many of the polymers were soluble in dichloromethane and chloroform with **18**, **23** and **25** (dissolved in hexafluorobenzene) being the most soluble.

Deprotection of 23. An additional interesting property of the diester bearing polymer **23** was that it could be converted to a water soluble dicarboxylate PPV, **27**, as shown in Scheme 3. Conversion to the anhydride^{23,24} occurs rapidly in xylene at 135 °C in the presence of a small amount of acid catalyst. The bright orange-red anhydride formed, **26**, is insoluble in all organic solvents and water, but can be identified by its two strong carbonyl stretches in the infrared spectrum at 1839 and 1763 cm⁻¹. Upon conversion to **27**, which is readily accomplished by mixing **26** with aqueous base, the polymer dissolves and resumes the bright yellow color of **23**. Polymer **27** is soluble in aqueous base, and uniform, luminescent films of this polymer can be formed by spin casting the polymer from aqueous solution.

Scheme 3



Thermogravimetric analysis of **23** under argon reveals that the same conversion to the anhydride occurs at 237 °C in the absence of acid catalyst. Further decomposition begins around 512 °C and continues until all of the polymer is gone at 700 °C. The anhydride, **26**, loses very little mass until 506 °C and then undergoes the same course of decomposition observed for **23**. Because polymer **23** is converted to **26** at a lower temperature when acid is present, **23** can be used in conjunction with a photo-acid generator as a photoresist (see Appendix).

Spectroscopic Study of PPVs and PNVs. The aromatized polymers were usually brightly colored and luminesced strongly under a hand held UV lamp. As shown in Table 3, the different homopolymers obtained exhibit luminescence at a range of wavelengths that cover the visible spectrum from blue (polymers **24** and **25**; \approx 450 nm) to nearly red (polymer **19**; 579 nm). The emission spectra of the halogen substituted PNVs, **19** and **20**, exhibit a red shift relative to unhalogenated PNV, **18**, as predicted for conjugated polymers bearing electron withdrawing groups.⁹ In contrast, both the absorbance and emission maxima of solutions of polymers **22** - **25** and **27** are strongly blue shifted relative to films of unsubstituted PPV (emission spectra of most of the homopolymers are shown in Chapter 5). While electronic arguments have been invoked for blue shifts in other PPVs bearing electron withdrawing groups,^{13,15,16} the shifts observed for the polymers studied here are probably at least partially a result of a twist in the polymer backbone due to steric interactions of the carboxyl or perfluoroalkyl groups and also due to solution induced disorder. Recent model studies of short PPV segments bearing trifluoromethyl groups have shown the phenyl units of these model compounds to be nearly perpendicular to each other in the X-ray crystal structure.¹⁷

One important difference between the ester substituted PPVs and the perfluoroalkyl substituted PPVs is that even films of **24** and **25** exhibit a strong blue shift relative to films of unsubstituted PPV while films of **23** are much less blue shifted than solutions of this polymer. This difference indicates that the esters probably adopt a more

Table 3. Absorbance and photoluminescence data for the PNVs and PPVs.

Polymer ^a	Solvent	λ_{abs} soln.	λ_{em} soln. ^c	Φ soln. (%) ^h	λ_{em} film
18	CHCl ₃	444	551 ^d , 561 ^e	0.5	593
19	CHCl ₃	416	568 ^d , 579 ^e	0.05	f
20	CHCl ₃	437	569	14	570
21^b	insoluble	442 ^g	insoluble	15 ^g	558
22	CHCl ₃	400	479	33	f
23	CHCl ₃	410	479	72	527
23 (80%)	CHCl ₃	408	479	≈ 100	f
24	CHCl ₃	308	449	20	458
25	C ₆ F ₆	328	443	65 ⁱ	465
27	0.1 N NaOH (aq)	424	491	16	f

a) Samples were at least 95% aromatized except as noted in parentheses. b) See references 13, 15, and 25. c) Excitation wavelengths are as listed in the Experimental section. d) Value obtained by excitation at 403 nm, which is the excitation maximum of **19**. e) Value obtained by excitation at 485 nm, which is the excitation maximum of **18**. f) Data was not obtained for films of these materials. g) Since PPV is insoluble, the absorbance maximum and quantum yield for films of this material is listed. h) Quantum yield values were calculated by comparison to Ru(bpy)₃Cl₂.²⁶ i) This quantum yield is higher than that of **24** due to the different solvent used.²⁶

planar configuration in the solid state, which extends their conjugation length, while the perfluoroalkylated polymers either remain twisted or are blue shifted for a different reason.²⁷ The fact that **24** and **25** luminesce blue even in films means that these materials should be useful for the fabrication of blue LEDs.

As noted in Table 3, samples of **23** were studied at 80% and 100% aromatization. In addition to offering better solubility, the partially aromatized polymer shows a higher quantum yield than the fully conjugated version (see Figure 2). A similar quantum yield improvement has been observed for other conjugated polymers containing saturated units

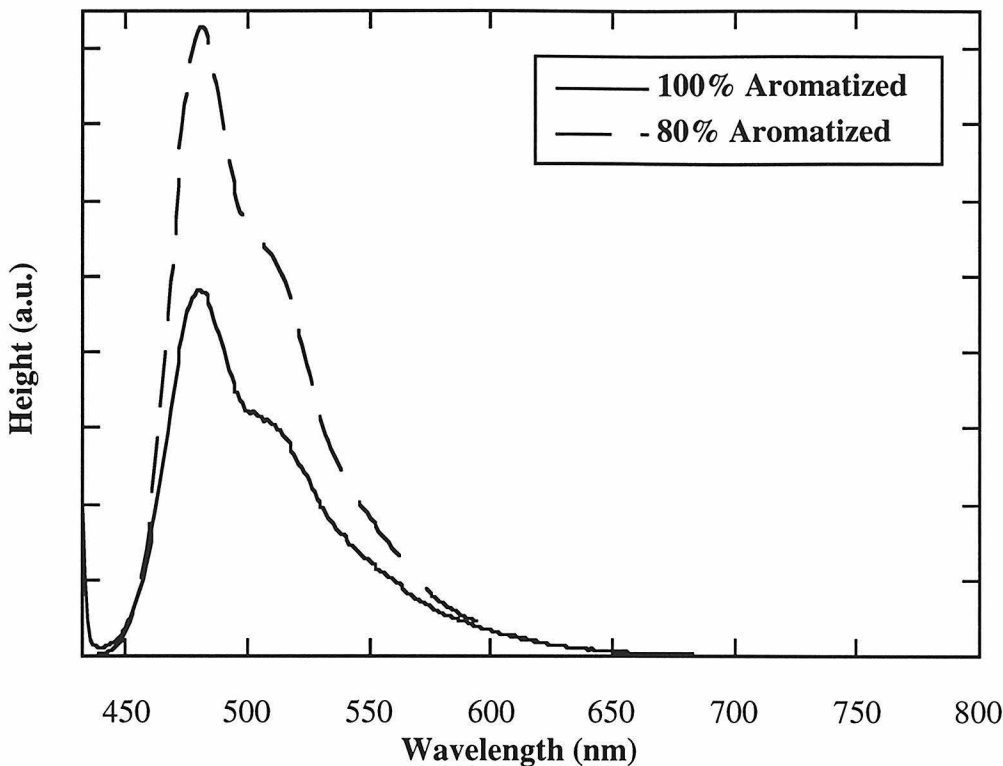


Figure 2. Photoluminescence of polymer **23** containing 80% and 100% aromatized units.

and was previously proposed to result from the unconjugated units acting as insulating segments which inhibit the movement of excitons and thereby reduce migration to quenching sites.¹

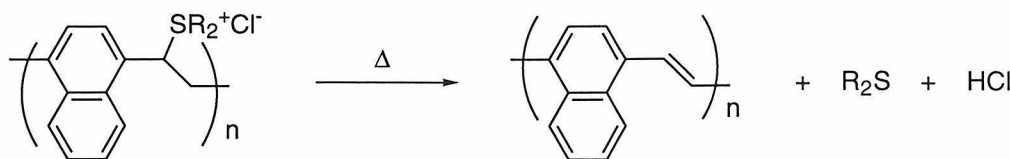
It is also important to note that polymers **22**, **23** and **27**, which each bear two carboxyl groups, are highly luminescent — in solution polymer **23** containing 80% aromatized units has a quantum yield of approximately unity while polymer **27** has a quantum yield of 10 - 20%. In contrast, the PPV anhydride, **26**, whose carbonyl groups are forced into the PPV plane and therefore are in conjugation with the rest of the polymer, appears to be much less luminescent than either **22**, **23** or **27**. So, while it has been proposed that carbonyl defects in the polymer backbone quench PPV's

luminescence,²⁸ the carbonyls present as pendant groups on **22**, **23** and **27** do not quench the luminescence of these polymers.

Oxidation Stability. Another potentially advantageous property of the polymers bearing electron withdrawing groups is that they are much more stable in air than PPV and PNV without electron withdrawing groups. By observing the luminescence intensity of films of these materials, it is apparent that polymers **18** and **21** decompose significantly after exposure to air and room lighting for one day, and they show almost no luminescence after being exposed to these conditions for one week. In contrast, polymers **19**, **20** and **22 - 25** show no appreciable change after one day in air and room lighting and polymers **20** and **23 - 25** have been observed to luminesce strongly after exposure to these conditions for one year. Quantitative measurements of polymer **23** have shown that this material retains 70 percent of its original luminescence output after being exposed to intense ultraviolet radiation in air for one hour.²⁹ Under similar conditions, MEH-PPV and aluminum trisquinolate, two commonly employed emissive materials, decompose almost entirely so that their luminescence is reduced to less than 5 percent of its original value. The oxidative stability of the polymers reported here is advantageous since devices made with more stable polymers may not require rigorous encapsulation to prevent degradation of the emissive layer.^{6,10,11}

Conductivity of Doped **18.** In addition to the luminescence measurements, polymer **18** was doped and its conductivity was measured using a four-point probe. Thin films of **18** were prepared by spin casting chloroform solutions of this polymer on glass slides. These films were then doped using a solution of nitrosonium tetrafluoroborate in acetonitrile. When immersed into the dopant solution, the color of the films immediately turned dark green from red-orange, suggesting that the polymers were oxidized. The doped conjugated polymer showed a conductivity of 15 Scm^{-1} . For comparison, previous reports describe the preparation of PNV via the precursor route shown in Scheme 4.^{30,31}

Scheme 4



This process, which requires a thermal elimination carried out at 300 °C, results in insoluble PNV. Doped polymers prepared by this route have been reported with conductivities of 0.032 Scm^{-1} by doping with AsF_5^{31} and 3 Scm^{-1} by electrochemical doping.³⁰ One possible explanation for the increased conductivity of the soluble polymers presented here is that the route used avoids the high temperature thermal elimination, which may cause cross-linking or degradation of the polymer which could decrease the polymer's conductivity.

Conclusions

The results presented show that PPVs and PNVs with and without electron withdrawing groups are readily accessible through a ROMP precursor route starting from barrelene and benzobarrelene monomers. Polymerizations were carried out using the molybdenum-based ROMP initiator **4**, which was tuned using HFB and THF to yield a living polymerization system as described in Chapter 3. Use of this system allowed the synthesis of homopolymers with low PDIs. Examining different diester substituted monomers has shown that the alkyl groups on these monomers, **9** and **10**, strongly affect the rate of polymerization by determining how strongly the monomer or polymer chain can coordinate to the molybdenum initiator.

Chemical aromatization of the ROMP precursor polymers to yield soluble PPVs and PNVs was carried out in solution using DDQ. Incomplete aromatization of the precursor polymers increased the solubility of the resulting PPVs and PNVs. For polymer **23**, the luminescence quantum yield was also shown to increase as a result of

incomplete aromatization. In addition to the organic soluble polymers, a dicarboxylate PPV, **27**, which is soluble in aqueous base, was prepared by removing the *t*-butyl groups from polymer **23** through acid catalyzed thermal elimination.

Polymers **22**, **23** and **27** were all highly luminescent, showing that their pendant carbonyl groups do not act as efficient quenching sites. The absorbance and emission maxima of solutions of these polymers and polymers **24** and **25** showed a strong blue shift relative to films of unsubstituted PPV. This shift is most likely due to a reduction in the polymers' conjugation length resulting from a twist in the polymer backbone caused by steric interaction of the pendant groups and by solution induced disorder. Films of the carboxyl substituted polymers were shown to exhibit much less of a blue shift than solutions of these materials while the emission spectra of films of the perfluoroalkylated materials were still strongly blue shifted relative to films of unsubstituted PPV.

Conductivity studies of polymer **18** show higher conductivities than PNV prepared by other routes, thereby indicating that the route developed here causes less decomposition than methods requiring high temperature elimination steps.

Experimental

General Methods and Materials. Monomers were prepared as described in Chapters 2 and 3. NMR spectra were recorded on a QE Plus-300 MHz (300.1 MHz ¹H; 75.33 MHz ¹³C) spectrometer. Infrared spectra were recorded using a Perkin-Elmer 1600 series FTIR spectrometer. Elemental analyses were performed by Caltech Analytical Labs or Mid-West Microlab. UV/Vis spectra were recorded on a HP Vectra ES/12 spectrometer. Thermogravimetric analyses were carried out using a TGA 7 Thermogravimetric Analyzer. Gel permeation chromatography (GPC) utilized an AM Gel Linear 10 column and a Knauer differential refractometer. Methylene chloride (Burdick and Jackson HPLC grade) was used as the eluent for all GPC measurements. Molecular weights are uncorrected and reported as compared to Shodex polystyrene

standards with molecular weights ranging from 2.95×10^3 to 2.40×10^6 . Emission spectra were recorded on an SLM 8000 C Spectrofluorometer. Benzene and benzene-d₆ were dried by passing through activated alumina columns. Xylene was purchased from Aldrich in a Sure Seal container. Methanol, dichloromethane and chloroform were degassed by purging with dry argon for a minimum of 30 minutes. Hexafluoro-*t*-butanol (HFB) and THF-d₈ were distilled from calcium hydride. Initiator **4** was prepared as previously reported.³²

General Procedure for Polymer Synthesis. Inside a nitrogen filled dry box the desired amount of monomer was dissolved in dry benzene (C₆D₆ was used in most cases, hexafluorobenzene was used for monomer **12**) and the required amount of hexafluoro-*t*-butanol was added. Initiator **4** dissolved in dry C₆D₆ was then added to this solution. The reaction mixture changed color from yellow to light orange or orange-brown during the first few minutes after mixing. For following the reaction by ¹H NMR, the solution was transferred into an NMR tube equipped with a J-Young valve. After the polymerization was observed to be complete by ¹H NMR, degassed benzaldehyde was added to quench the initiator. The reaction mixture, which turned brown over 30 minutes, was then pipetted into degassed methanol and the resulting precipitate was recovered by centrifuging and then decanting the solvent. Further purification was accomplished by redissolving the polymer in methylene chloride or benzene (hexafluorobenzene was used for polymer **17**) and then reprecipitating the polymer in methanol. The polymer was then dried under vacuum.

General Procedure for Polymer Aromatization. The desired amount of polymer was dissolved in methylene chloride, C₆D₅Br or hexafluorobenzene (polymer **17** only) and DDQ, was added. For fast reactions done in dichloromethane the DDQ was dissolved in dichloromethane before adding it to the polymer solution. In most cases slightly less (≈ 0.95 equiv.) than equivalent of DDQ was added since polymers containing some unaromatized units were found to be significantly more soluble than the fully

aromatized polymers. Aromatization of **16** required 1.5 - 2 equivalents of DDQ to reach the desired levels of aromatization. Reactions done in dichloromethane generally proceeded at room temperature. For reactions done in C₆D₅Br or hexafluorobenzene the reaction flask was sealed and heated in an oil bath at 120 °C for 1 - 3 days. After this time, ¹H NMR of the crude mixture showed <5% of the unaromatized polymer remaining. The reaction mixture was then added to methanol to yield a precipitate which was isolated by centrifuge and further purified by repeated precipitation as for the precursor polymers. To ensure that all of the polymer precipitated each time, the solvent layer above the precipitated polymer was spotted several times on a non-luminescent TLC plate. This plate was then irradiated with a hand-held UV lamp to see if any polymer, which is luminescent, had remained in solution. In some cases, adding a minimal amount (0.5 - 1 mL was added to the 40 - 50 mL of solvent mixture generated by the precipitation procedure) of methanol saturated with sodium chloride was found to facilitate precipitation.

General Procedure for Preparation of Polymer Solutions for Photoluminescence Measurements. Approximately 2 mg of each polymer was dissolved in 50 mL of chloroform to yield solutions of each polymer so that each solution (A) contained the same concentration of total monomer units. 1 mL of each of these solutions was then diluted to 25 mL using chloroform to yield solutions B. 1 mL of each of these solutions was then diluted to 25 mL using chloroform to yield solutions C. Solutions B and C were used for most luminescence measurements, but for polymers **18** and **19**, solution A was sometimes used since these materials luminesce weakly.

Photoluminescence Measurements. All measurements were performed on solutions that were diluted so that the emission maximum was on scale with a Ru(bpy)₃Cl₂ standard that was approximately 1 x 10⁻⁵M. The exact concentration used in calculating quantum yields (7.6 x 10⁻⁶ M) was calculated from the absorbance of this solution at 453 nm and the reported extinction coefficient.²⁶ All polymer solutions were

prepared using degassed solvent. Quantum yields for the polymers were calculated by comparison to a Ru(bpy)₃Cl₂ standard using the equation:

$$\Phi_{poly} = \frac{I_{poly} \cdot \epsilon_{Ru} c_{Ru}}{I_{Ru} \cdot \epsilon_{poly} c_{poly}} \cdot \Phi_{Ru}$$

Integration values, I , were measured on spectra that had been corrected for detector response using the software provided with the SLM 8000 C Spectrofluorometer. A value of 0.028±0.002 was used for Φ_{Ru} .³³ The Ru(bpy)₃Cl₂ solution was equilibrated with air.

Precursor Polymer 5. Reacted 68.5 mg **1**, 3.8 mg **4**, 7.8 μ L HFB, in 0.6 g C₆D₆ for 40 minutes. Yield = quantitative ¹H NMR (CDCl₃, all peaks were broad) δ 7.09, 6.03 (cis), 5.93 (cis), 5.86, 5.54, 5.36 (cis), 4.62 (cis), 3.93, 2.57, 1.60, 1.28, 0.89; carbene proton in C₆D₆ δ 12.28 (br m). ¹³C NMR (CDCl₃) δ 140.9 (m), 135.8 (m), 133.7 (m), 132.3 (m), 128.7 (m), 127.9 (m), 126.6 (m), 43.44, 43.22, 37.86 (cis, m), 31.93, 31.73, 31.56, 29.68, 29.39, 22.70, 14.14. UV/Vis (chloroform): λ_{max} /nm = 236. IR (KBr, pellet): 3032 (s), 2924 (s), 2852 (s), 1665 (w), 1614 (m), 1573 (m), 1499 (s), 1464 (s), 1378 (s), 1154 (w), 1080 (m), 1025 (m), 964 (s), 890 (m), 819 (s), 789 (s), 722 (s), 647 (w), 495 (m) cm⁻¹. Anal. Calcd for C₂₃H₃₂: C, 89.54; H, 10.46. Found: C, 89.29; H, 10.46. GPC data (CH₂Cl₂): Mn = 47700, Mw = 81000, PDI = 1.70.

Undecyl Substituted PNV (18). Reacted 199.5 mg **5** with 12.3 mg DDQ in 20 mL methylene chloride for 3 hours at rt. 1 mL of NaCl-methanol solution was found to facilitate the precipitation of the polymer in methanol. After being dried under vacuum, **18** was obtained in 90% yield. ¹H NMR (CDCl₃, all peaks were broad) δ 8.29, 8.02, 7.47, 2.82, 1.73, 1.23, 0.88; ¹³C NMR (CDCl₃) δ 141.0 (m), 134.9 (m), 131.9 (m), 130.1 (m), 129 - 128.6 (m), 127.7 (m), 124.0 (m), 123.1 (m), 36.45 (br), 31.91, 31.70, 29.67, 29.36, 27.69, 14.13. UV/Vis (chloroform): λ_{max} = 253, 444 nm. Emission spectrum (chloroform, excited at 485 nm): λ_{max} = 561 nm; Φ (solution, λ_{ex} = 485 nm) = 0.5%. IR (KBr, pellet): 3038 (m), 2954 (s), 2926 (s), 2854 (s), 1622 (m), 1574 (m), 1510 (m),

1457 (s), 1377 (s), 956 (s), 821 (s) cm^{-1} .

Precursor Polymer 6. Reacted 70.1 mg **2**, 3.7 mg **4**, 7.8 μL HFB, in 0.6 g C_6D_6 for 1.5 hours at rt. Yield = 99%. (alkyl = $(\text{CH}_2)_7\text{CH}_3$) ^1H NMR (C_6D_6 , all peaks were broad): δ 6.22(cis), 5.87, 5.68, 5.24 (cis) (4H), 4.82 (cis), 4.17 (2H), 2.64 (2H), 1.55 (2H), 1.26 (10H), 0.94 (3H); carbene proton in C_6D_6 δ 12.07 (br m). ^{13}C NMR (CDCl_3) δ 155.0, 152.6, 148.7, 146.3, 145.9, 143.5, 131.4, 127.4, 126.8, 124.0, 120.1, 117.7 (phenyl region with fluorine coupling), 37.2 (br s), 31.9, 29.5, 29.3, 29.2, 22.7, 14.1. FTIR (film on NaCl): 3035, 2956, 2926, 2856, 1644, 1476, 1464, 1366, 1334, 1322, 1247, 1126, 1077, 990, 960, 866, 828, 752, 720 cm^{-1} . GPC (CH_2Cl_2): Mn = 28800, Mw = 36100, PDI = 1.26.

Octyl Trifluoro-PNV (19). Reacted 64 mg **6** with 41 mg DDQ in 10 mL methylene chloride overnight at rt. Yield = 96%. During the course of reaction, ^1H NMR (CDCl_3) showed broad peaks at δ 7.6-6.8, 1.54, 1.26, 0.85. FTIR (KBr, pellet): 2956, 2925, 2854, 1648, 1570, 1458, 1387, 1276, 1203, 1123, 1049, 1035, 972, 891, 842, 594 cm^{-1} . UV/Vis (chloroform): $\lambda_{\text{max}} = 416$ nm. Emission spectrum (chloroform, $\lambda_{\text{ex}} = 403$ nm): $\lambda_{\text{max}} = 568$ nm; (chloroform, $\lambda_{\text{ex}} = 485$ nm): $\lambda_{\text{max}} = 579$ nm; Φ (solution, $\lambda_{\text{ex}} = 403$ nm) = 0.05%.

Precursor Polymer 7. Reacted 84.4 mg **3**, 3.7 mg **4**, 7.8 μL HFB, in 0.6 g C_6D_6 overnight. Yield = quantitative (alkyl = $(\text{CH}_2)_7\text{CH}_3$) ^1H NMR (C_6D_6 , all peaks were broad): δ 6.02 (2H), 5.65 (2H), 4.37 (2H), 3.03 (2H), 1.62, 1.29 (12H), 0.93 (3H); carbene proton in C_6D_6 δ 11.97 (br s). ^{13}C NMR (CDCl_3) δ 139.0, 135.2, 133.3, 132.1, 131.6 (m), 128.3 (m), 43.0 (m), 33.3 (br s), 31.9, 29.7 (br s), 29.4, 27.9 (br s), 22.7, 14.1. FTIR (film on NaCl): 3035, 2952, 2925, 2854, 1463, 1392, 1379, 1288, 1270, 1170, 1105, 1066, 963, 918, 876, 759 cm^{-1} . GPC data (CH_2Cl_2): Mn = 15000, Mw = 16700, PDI = 1.11.

Octyl Trichloro-PNV (20). Reacted 21.2 mg **7** with 12.3 mg DDQ in 1.2 mL $\text{C}_6\text{D}_6\text{Br}$ or toluene-d₈ overnight at 120 °C. Yield = 96%. ^1H NMR (toluene-d₈): broad

peaks were observed at δ 7.8-6.6, 1.8-0.8 with peaks at δ 1.3, 0.93. FTIR (KBr pellet): 3041, 2934, 2852, 1553, 1458, 1376, 1354, 1322, 1261, 1236, 1104, 980, 838, 788, 759, 721, 683, 667, 559 cm^{-1} . UV/Vis (chloroform): $\lambda_{\text{max}} = 437$ nm. Emission spectrum (chloroform, $\lambda_{\text{ex}} = 430$ nm): $\lambda_{\text{max}} = 569$ nm; (Film, $\lambda_{\text{ex}} = 430$ nm): $\lambda_{\text{max}} = 570$ nm; Φ (solution, $\lambda_{\text{ex}} = 430$ nm) = 14%.

Precursor Polymer 14. Reacted 0.423 g **9**, 32.7 mg **4** (was added as a solution in 40 drops of C_6D_6), 66 μL HFB, in 4.37 g C_6D_6 . The reaction mixture gradually became orange and then dark reddish-brown over the course of 30 minutes. After 1 week, ^1H NMR of the reaction showed that it was 89% complete and that reaction had stopped. Yield = 85.5%. ^1H NMR (CDCl_3 , all peaks were broad) δ 5.55, 5.53, 5.23, 4.95, 3.65, 3.63; carbene proton in C_6D_6 not observed. ^{13}C NMR (CDCl_3) 167.52 m, 137-125 (m, backbone olefins), 52.27, 52.06, 41.23 m. FTIR 3032, 2951, 2843, 1719 s, 1636, 1436, 1382, 1352, 1252, 1151, 1061, 979, 789, 754, 670 cm^{-1} . Anal. Calcd for $\text{C}_{12}\text{H}_{12}\text{O}_4$: C, 65.45; H, 5.49. Found: C, 67.06; H, 5.91. GPC data (CH_2Cl_2): Mn = 16700, Mw = 24000, PDI = 1.44.

Dimethylester-PPV (22). Reacted 100 mg **14** with 105.2 mg DDQ in 16 mL dichloromethane at rt. During the course of the reaction, the mixture became cloudy yellow green and eventually cloudy orange. After purification, drying the polymer yielded a dark orange to red solid. Yield = 92%. UV/Vis (chloroform): $\lambda_{\text{max}} = 400$ nm. Emission spectrum (chloroform, $\lambda_{\text{ex}} = 415$ nm): $\lambda_{\text{max}} = 479$ nm; Φ (solution, $\lambda_{\text{ex}} = 415$ nm) = 33%. FTIR 3024, 2950, 1725, 1636, 1478, 1438, 1263, 1220, 1152, 1111, 1063, 1008, 959, 834, 795, 752, 702 cm^{-1} . *Note:* Following a smaller scale reaction by NMR showed that all of **14** is aromatized after 2 hours. Adding 0.5 mL of a saturated sodium chloride solution in methanol was found to facilitate much more rapid and complete precipitation of the polymer.

Precursor Polymer 15. Reacted 0.501 g **10**, 28.2 mg **4** (was added as a solution in 40 drops of benzene), 56 μL HFB, in 3.8 g dry benzene. Over the course of 10 minutes,

the reaction mixture changed color from yellow to light orange-brown. The mixture was stirred overnight and then quenched by adding 5 drops of degassed benzaldehyde. After purification and drying under vacuum, 0.385 g of **15** was obtained as a brittle light yellow solid. Yield = 77%. *Note:* Following a smaller scale reaction by NMR shows that all monomer is consumed after 2.5 hours. If any of the monomer has decomposed to form the acid, however, reaction times will be considerably longer. ^1H NMR (C_6D_6 , all peaks are broad) δ 5.67, 5.65, 5.54, 5.40 (4H), 4.30 (small), 3.76 (2H), 1.52 (18H). (CDCl_3) δ 5.52, 5.50 (2H), 5.21, 5.17 (2H), 3.95, 3.56 (2H), 1.37 (18H); carbene proton in C_6D_6 δ 12.50 (br m) and 12.41 (br m) during polymerization, 11.92 (br m) after polymerization was complete. ^{13}C NMR (CDCl_3) δ 166.19 (m, C=O), 135.33 - 126.22 (m, C=C), 81.33 (C of *t*-butyl), 81.26 (C of *t*-butyl), 41.70, 28.05 (CH_3 of *t*-butyl). FTIR 3006, 2979, 2933, 1716, 1674, 1636, 1477, 1456, 1393, 1368, 1351, 1273, 1256, 1155, 1087, 1060, 1034, 967, 848, 755, 667 cm^{-1} . Anal. Calcd for $\text{C}_{18}\text{H}_{24}\text{O}_4$: C, 71.03; H, 7.95. Found: C, 71.48; H, 7.69. GPC data (CH_2Cl_2): Mn = 19600, Mw = 23900, PDI = 1.22.

Di-*t*-butylester-PPV (23). Reacted 0.369 g **15** with 0.281 g DDQ in 28 mL dichloromethane overnight at rt. During the course of the reaction, the mixture gradually became cloudy yellow and somewhat luminescent under the room lighting. Following purification, the polymer was dried under vacuum to yield 0.34 g of a yellow-orange solid. Yield = 93%. For preparing polymer that was 80% aromatized, the procedure was identical except that 0.8 equivalents of DDQ were used. In this case, the polymer always dissolved completely in methylene chloride to yield a transparent yellow solution during purification. ^1H NMR (CDCl_3) δ 7.66 (bs, 2H), 7.32 (bs, 2H), 1.62 (bs, 18H) ^{13}C NMR (CDCl_3) δ 167.05, 134.66, 133.13, 127.99, 126.74, 83.15, 28.21. UV/Vis (chloroform): $\lambda_{\text{max}} = 410$ nm. Emission spectrum (chloroform, $\lambda_{\text{ex}} = 422$ nm): $\lambda_{\text{max}} = 479$ nm; (film, $\lambda_{\text{ex}} = 480$ nm): $\lambda_{\text{max}} = 527$ nm; Φ (solution, $\lambda_{\text{ex}} = 422$ nm) = 72%. FTIR 2878, 2933, 1720, 1560, 1477, 1458, 1420, 1394, 1369, 1290, 1155, 1148, 1118, 957, 844, 824, 752, 696, 668 cm^{-1} . Anal. Calcd for $\text{C}_{18}\text{H}_{22}\text{O}_4$: C, 71.50; H, 7.33. Found: C, 69.49; H,

7.20. *Note:* Following a smaller scale reaction by NMR showed that all of **15** is aromatized after 2 hours. Adding 0.5 mL of a saturated sodium chloride solution in methanol was found to facilitate much more rapid and complete precipitation of the polymer.

Polyphenylenevinylene anhydride (26). This reaction was best performed by using 100% aromatized **23** that had not been dried. (i.e., it was still wet with the methanol/methylene chloride mixture). For a typical reaction, 0.35 g (1.15 mmol) of wet **23** was transferred into a 250 mL round bottom flask with 80 mL of xylene (dry Aldrich Sure Seal). To this was added \approx 40 - 50 mg of tosyl acid, and the yellow mixture was stirred under argon and heated to 125 °C. After the low boiling solvent boiled off, the reaction mixture quickly changed color from yellow to bright red. Heating was continued for 12 hours to ensure complete reaction and the reaction mixture was then transferred to two 40 mL centrifuge tubes. After centrifuging, the light brown solvent was decanted from the bright red precipitate. The precipitate was then rinsed by shaking it with acetone and recentrifuging the mixture. After decanting the solvent, this process was repeated 2-3 more times using acetone as the solvent. The dark red solid was then dried under vacuum to yield 0.197 g of a dark red brittle solid. Yield = 99%. This solid is only soluble in aqueous base, which opens the anhydride to yield the diacid, so it was identified by its infrared spectrum, which clearly shows the two carbonyl stretches expected of an anhydride. FTIR 3067, 3025, 2921, 1839, 1764, 1702, 1562, 1498, 1363, 1288, 1213, 1152, 974, 923, 893, 847, 798, 753, 696, 635, 603, 574 cm⁻¹. Anal. Calcd for C₁₀H₄O₃: C, 69.78; H, 2.34. Found: C, 66.42; H, 2.74.

Polyphenylenevinylene sodium dicarboxylate (27). The sodium salt was prepared by dissolving **26** in 0.2 N aqueous NaOH. Depending on the size of pieces of **26** used, this reaction occurred nearly immediately, or it took a few hours of stirring, with the fastest reaction occurring when **26** was a fine powder. Upon reaction, the solution became the bright yellow luminescent color of **23**. Upon acidifying the solution with 1 M

HCl, the polymer reprecipitated as an orange solid that was recollected by centrifuging the solution. FTIR of this solid showed it to be a mixture of the starting anhydride and the diacid. Precipitating the basic polymer solution by adding it into acetone, however, yielded a bright yellow solid. After drying under vacuum, FTIR of this material showed it to be the sodium salt, **27**, with some water coordinated. NMR of **27** was obtained by dissolving **26** in 0.2 N NaOH in D₂O. ¹H NMR (D₂O) δ 7.50 (bs, 2H), 7.05 (bs, 2H) ¹³C NMR (D₂O, CD₃OD was set at 49.00) δ 178.02, 138.39, 132.93, 128.20, 125.41. FTIR 3416 br (coordinated H₂O), 3031, 2922, 2850, 1578, 1451, 1384, 1229, 1030, 964, 881, 831, 804, 754, 697 cm⁻¹. Anal. Calcd for C₁₀H₄O₄Na₂•3H₂O: C, 41.68; H, 3.50. Found: C, 42.67; H, 3.54.

Precursor Polymer 16. Reacted 487.8 mg **11**, 63.8 mg **4**, 129 μL HFB, in 0.6 g C₆H₆ for 3 hours. The polymer did not completely precipitate in methanol, so it was purified by eluting it through a plug of silica gel using methylene chloride. The dried product recovered was a white solid. Yield = 50%. ¹H NMR (CDCl₃, all peaks were broad): δ 5.71 (2H), 5.30 (2H), 3.75 (2H); carbene proton in C₆D₆ δ 11.87 (br m). FTIR (KBr pellet): 3049, 2965, 2929, 1646, 1300-1100, 1077, 1019, 965, 918, 776, 738, 700, 660, 605, 535, 479 cm⁻¹. GPC data (CH₂Cl₂): Mn = 29600, Mw = 31700, PDI = 1.07.

Bistrifluoromethyl-PPV (24). Reacted 20.7 mg **16** with 19.8 mg DDQ in 1.2 mL C₆D₆Br overnight at 120 °C. Yield = 95%. ¹H NMR (C₆D₅Br): broad peaks were observed at δ 7.6-6.6. FTIR (KBr pellet): 3049, 2968, 1475, 1421, 1383, 1300-1100, 1073, 1022, 971, 932, 872, 842, 764, 741, 695, 670, 659, 603, 563, 527, 480 cm⁻¹. UV/Vis (chloroform): λ_{max} = 308 nm. Emission spectrum (chloroform, λ_{ex} = 345 nm): λ_{max} = 449 nm; (Film, λ_{ex} = 345 nm): λ_{max} = 458 nm; Φ (solution, λ_{ex} = 345 nm) = 20%.

Precursor Polymer 17. Reacted 106.9 mg **12**, 3.5 mg **4**, 7.8 μL HFB, in 0.9 g C₆F₆/10 drops C₆D₆ overnight. Yield = 90%. ¹H NMR (C₆F₆/C₆D₆, all peaks were broad): δ 5.98 (2H), 5.59 (2H), 4.04 (2H), 3.88 (2H); carbene proton δ 11.92 (br m) and

11.73 (br m). Anal. Calcd for C₁₇H₆F₂₀: C, 34.60; H, 1.02; F, 64.38. Found: C, 34.44; H, 1.15; F, 64.15.

Trifluoromethylperfluoroctyl-PPV (25). Reacted 18 mg **17** with 16 mg DDQ in 1.2 mL C₆F₆ for 3 days at 120 °C. This produced a polymer that contained <5% unaromatized units. Polymers containing more unaromatized units were obtained by using less DDQ or employing shorter reaction times. Yield = 89%. ¹H NMR (C₆F₆/C₆D₆, all peaks were broad): δ 8.02, 7.80, 7.48, 7.39. FTIR (KBr pellet): 1531, 1465, 1409, 1369, 1288, 1241, 1211, 1146, 1055, 978, 913, 851, 804, 746, 735, 725, 708, 668, 638, 562, 531 cm⁻¹. UV/Vis (C₆F₆): λ_{max} = 328 nm. Emission spectrum (C₆F₆, λ_{ex} = 356nm): λ_{max} = 443 nm; (Film, λ_{ex} = 352nm): λ_{max} = 465 nm; Φ (solution, λ_{ex} = 356 nm) = 65%.

Doping Conjugated Polymer 18. The red-orange thin films of polymer **18** were obtained by spin-coating their saturated chloroform solution on glass slides. In a dry box, when the thin films were immersed into a glass dish containing a solution of nitrosonium tetrafluoroborate (≈ 300 - 400 mg) in acetonitrile (30 mL), the red-orange films immediately turned dark green. After 10 seconds the films were removed from the dopant solution and rinsed with acetonitrile. The doped films were dried under vacuum. The thickness of the films was ca. 500 - 2000 nm. Conductivity was measured with a standard four-point probe using a Princeton Applied Research (PAR) model 173 potentiostat, and a PAR model 175 universal programmer. Thickness of thin films was measured with a Sloan Dektak 3030 Profilingmeter. Conductivities were calculated using the equation:

$$\sigma = \frac{\ln 2}{\pi d} \cdot \frac{i}{V}$$

where σ is the conductivity, d is the film thickness, i is current, and V is potential.

References and Notes

- (1) Braun, D.; Staring, E. G. J.; Demandt, R. C. J. E.; Rikken, G. L. J.; Kessener, Y. A. R. R.; Venhuizen, A. H. J. *Synth. Met.* **1994**, *66*, 75.
- (2) Burn, P. L.; Holmes, A. B.; Kraft, A.; Bradley, D. D. C.; Brown, A. R.; Friend, R. H.; Gymer, R. W. *Nature* **1992**, *356*, 47.
- (3) Burn, P. L.; Kraft, A.; Baigent, D. R.; Bradley, D. D. C.; Brown, A. R.; Friend, R. H.; Gymer, R. W.; Holmes, A. B.; Jackson, R. W. *J. Am. Chem. Soc.* **1993**, *115*, 10117.
- (4) Hide, F.; Schwartz, B. J.; Díaz-García, M. A.; Heeger, A. J. *Chem. Phys. Lett.* **1996**, *256*, 424.
- (5) Parker, I. D. *J. Appl. Phys.* **1993**, *75*, 1656.
- (6) Sheats, J. R.; Antoniadis, H.; Hueschen, M.; Leonard, W.; Miller, J.; Moon, R.; Roitman, D.; Stocking, A. *Science* **1996**, *273*, 884.
- (7) Wittmann, H. F.; Grüner, J.; Friend, R. H.; Spencer, G. W. C.; Moratti, S. C.; Holmes, A. B. *Adv. Mater.* **1995**, *7*, 541.
- (8) Woo, H. S.; Graham, S. C.; Halliday, D. A.; Bradley, D. D. C.; Friend, R. H. *Phys. Rev. B: Solid State* **1992**, *12*, 7379.
- (9) Brédas, J. L.; Heeger, A. J. *Chem. Phys. Lett.* **1994**, *217* 507.
- (10) Heeger, A. J.; Long, J. *Optics and Photonics News* **1996**, *August*, 24.
- (11) Greenham, N. C.; Moratti, S. C.; Bradley, D. D. C.; Friend, R. H.; Holmes, A. B. *Nature* **1993**, *365*, 628.
- (12) Scott, J. C. *J. Appl. Phys.* **1996**, *79*, 2745.
- (13) Jin, J. I.; Lee, Y. H. *Macromolecules* **1993**, *26*, 1805.
- (14) Hanack, M.; Segura, J. L.; Spreitzer, H. *Adv. Mater.* **1996**, *8*, 663.
- (15) Kang, I. N.; Lee, G. J.; Kim, D. H.; Shim, H. K. *Polym. Bull.* **1994**, *33*, 89.
- (16) McCoy, R. K.; Karasz, F. E. *Chem. Mater.* **1991**, *3*, 941.

(17) Lux, A.; Holmes, A. B.; Cervini, R.; Davies, J. E.; Moratti, S. C.; Grüner, J.; Cacialli, F.; Friend, R. H. *Synth. Met.* **1997**, *84*, 293.

(18) Wagaman, M. W.; Grubbs, R. H. *Macromolecules* **1997**, *30*, 3978.

(19) Wagaman, M. W.; Bellmann, E.; Grubbs, R. H. *Phil. Trans. R. Soc. Lond. A* **1997**, *355*, 727.

(20) Wagaman, M. W.; Grubbs, R. H. *Synth. Met.* **1997**, *84*, 327.

(21) Mitchell, J. P.; Gibson, V. C.; Schrock, R. R. *Macromolecules* **1991**, *24*, 1220.

(22) Walker, D.; Hiebert, J. D. *Chem. Rev.* **1967**, *67*, 153.

(23) Weber, G.; Menke, K.; Hopf, H. *Chem. Ber.* **1980**, *113*, 531.

(24) Böhm, I.; Herrmann, H.; Menke, K.; Hopf, H. *Chem. Ber.* **1978**, *111*, 523.

(25) Stenger-Smith, J. D.; Lenz, R. W.; Wegner, G. *Polymer* **1992**, *30*, 1048.

(26) Juris, A.; Balzani, V.; Barigelli, F.; Campagna, S.; Belser, P.; Zelewsky, A. V. *Coord. Chem. Rev.* **1988**, *84*, 85.

(27) Calculations predict that polymer **24** may have a larger bandgap than unsubstituted PPV even when both polymers are in a planar geometry. Cornil, J.; Brédas, J. L., personal communication.

(28) Papadimitrakopoulos, F.; Konstadinidis, K.; Miller, T. M.; Opila, R.; Chandross, E. A.; Galvin, M. E. *Chem. Mater.* **1994**, *6*, 1563.

(29) Shaheen, S.; Peyghambarian, N., personal communication.

(30) Onada, M.; Morita, S.; Iwasa, T.; Nakayama, H.; Yoshino, K. *J. Phys. D: Appl. Phys.* **1991**, *24*, 1658-1664.

(31) Antoun, S.; Gagnon, D. K.; Karasz, F. E.; Lenz, R. W. *J. Polym. Sci., Part C: Polym. Lett.* **1986**, *24*, 503.

(32) Fox, H. H.; Lee, J. K.; Park, L. Y.; Schrock, R. R. *Organometallics* **1993**, *12*, 759.

(33) Nakamaru, K. *Bull. Chem. Soc. Jpn.* **1982**, *55*, 2697.

Chapter 5

Synthesis and Luminescence Properties of Random and Block Copolymers

Abstract: In this chapter, the synthesis and study of copolymers of substituted poly(*para*-phenylenevinylene)s (PPVs) and substituted poly(1,4-naphthalenevinylene)s (PNVs) is described. Three block copolymers and two random copolymers were prepared and compared to the corresponding homopolymers. The first copolymer studied consisted of a diblock of an alkylated PNV substituted with three fluorines (3F-PNV) and a PNV bearing an alkyl chain (3H-PNV). In solution, this block copolymer showed exciton transfer into the smaller bandgap block, 3F-PNV, as all luminescence from the block copolymer had a wavelength characteristic of the 3F-PNV homopolymer. Similarly, a block copolymer of bistrifluoromethyl substituted PPV (BTF-PPV) and PNV substituted with three chlorines and an alkyl group (3Cl-PNV) was found to show transport of excitons into the smaller bandgap 3Cl-PNV block, in solution. More complete transport was observed for films of this block copolymer and for solutions and films of a random/blocky copolymer of 3Cl-PNV and BTF-PPV. For the other copolymers studied, which were comprised of units of di-*t*-butylester substituted PPV (BC-PPV) and 3H-PNV, transport properties similar to those found for the 3Cl-PNV/BTF-PPV copolymers were observed. In this case, however, emission from the smaller bandgap block, 3H-PNV, was weak in solution due to incomplete transport of excitons into the 3H-PNV block and due to quenching occurring in this material.

Introduction

Since the discovery that poly(*para*-phenylenevinylene) (PPV) can be used as the emissive layer in light emitting diodes (LEDs),¹ there has been considerable interest in the synthesis and study of PPV and other luminescent, conjugated polymers. One class of materials that has been the subject of extensive theoretical study is the conjugated block copolymers.²⁻⁸ When a conjugated block copolymer is made up of two polymers with different bandgaps, the electron-hole pairs (excitons) formed in the larger bandgap block are predicted to migrate to the smaller bandgap block and become trapped, as shown in Figure 1. As a result, these polymers exhibit luminescence characteristic only of the smaller bandgap material, where all recombination of excitons occurs, and may also show increased emission efficiency relative to the corresponding homopolymer.^{3,4} Despite the interest in these properties, only a few conjugated block copolymers have been reported.⁹⁻¹⁸

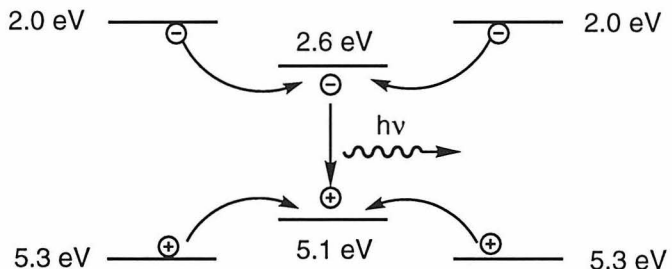


Figure 1. Migration of polarons in a block copolymer, followed by emission from the smaller bandgap block. Bandgaps shown were chosen arbitrarily.

One technique that is particularly well suited to the synthesis of conjugated block copolymers is ring-opening metathesis polymerization (ROMP). First, polymerizations using this method are often living, so block copolymers can be readily prepared by sequential addition of the different monomers.^{10,11,19-28} Second, ROMP is conducive to the synthesis of conjugated polymers since olefin units present in the monomer are not consumed during the polymerization, but rather become part of the polymer backbone. It

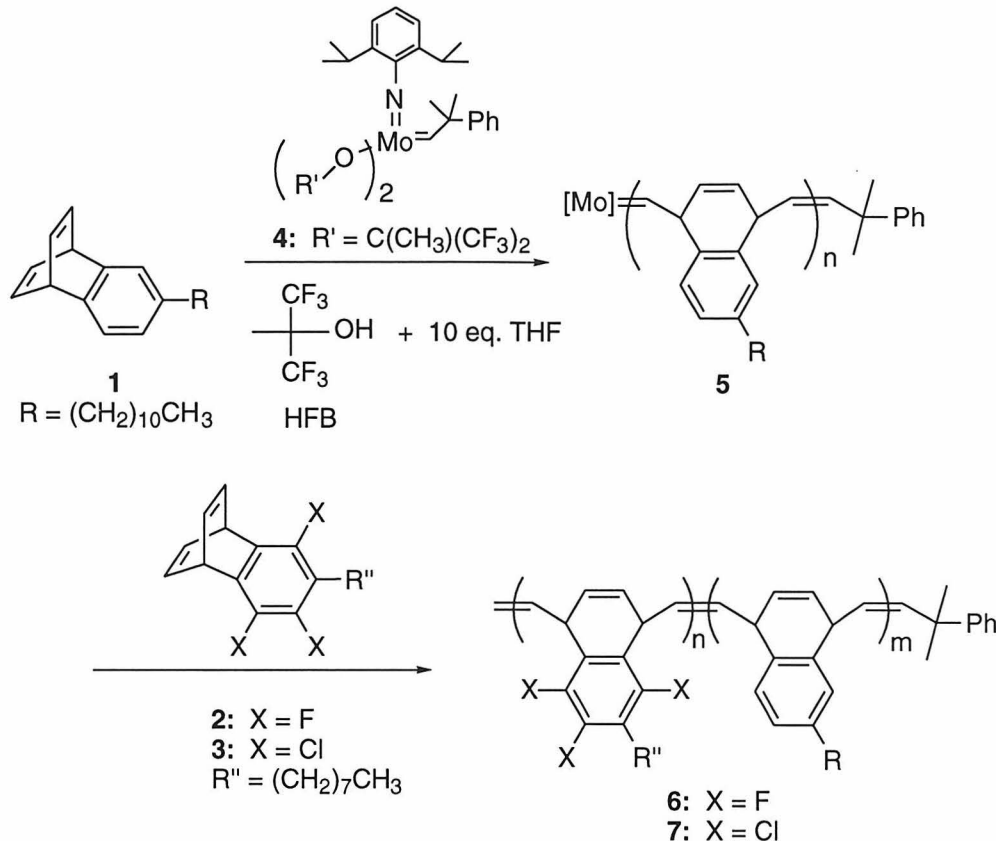
has been previously shown that ROMP can directly yield fully conjugated polymers^{29,30} and can also produce precursor polymers that are easily converted to fully conjugated materials.^{10,11,31-36} In Chapter 4 the latter technique was applied to the synthesis of PPV and soluble, substituted derivatives of PPV and poly(1,4-naphthalenevinylene) (PNV).

This chapter describes the synthesis and study of PNV and PPV block and random copolymers using the same monomers and polymerization system employed for the synthesis of the homopolymers. All of the copolymers prepared were comprised of two polymers with different bandgaps. The bandgap difference was made as large as possible to minimize overlap in the emission spectra of the two polymers that comprised the blocks. Where this condition was achieved, and the two polymers had similar emission intensities, any electron-hole pairs that recombined in the larger bandgap block were observed as a separate luminescence peak that is distinct from that of the smaller bandgap material. The two homopolymers that made up each block copolymer, and in some cases the corresponding random copolymer, were also prepared and studied for comparison to the block copolymer.

Results and Discussion

PNV Block Copolymer Synthesis. Because the benzobarrelene monomers were prepared first, the homopolymers and block copolymers of these materials were studied first as well. Block copolymers were prepared by sequential polymerization of the two monomers, with the second monomer being added after ¹H NMR showed that the first monomer was fully consumed. As shown in Scheme 1, copolymers of benzobarrelene **1** with **2**, and **1** with **3** were both prepared using this method. For these syntheses, the best results were obtained when **1** was polymerized first since this monomer is less capable of causing all of **4** to initiate. This strategy seemed counterintuitive at first since it is important to initiate all of **4** at the beginning of the reaction to prevent formation of homopolymers of the second monomer, which could grow from catalyst that was not

Scheme 1

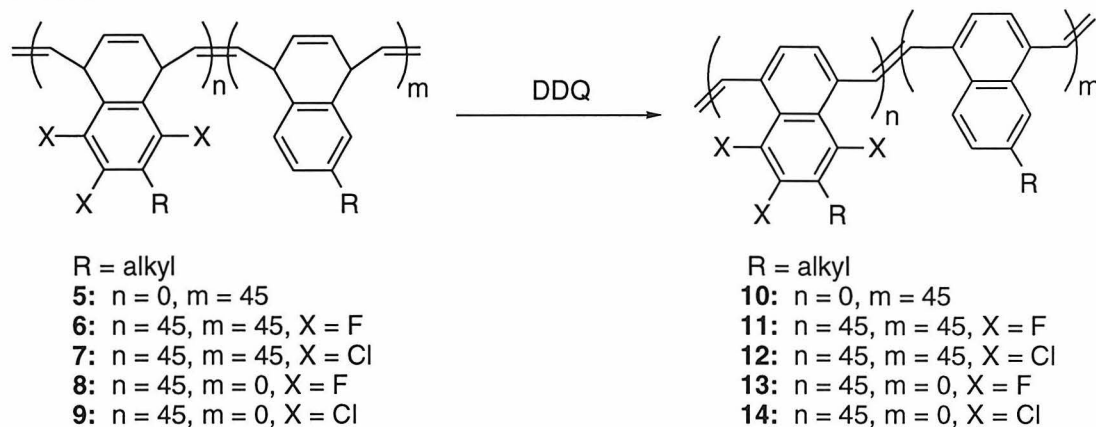


initiated by the first monomer. While this is true, the important point to be made is that conditions are adjusted so that the monomer less capable of initiating **4** *does* cause all of the catalyst to become initiated. Under these conditions, any monomer added later which produces better initiation than the first monomer will be added to all of the polymer chains. When the monomer less capable of initiating **4** is added second, this monomer does not necessarily add to all of the polymer chains. As a result, some homopolymers made from the first monomer remain, and irregular molecular weight distributions are observed. For the polymerizations in Scheme 1, complete initiation of **4** was achieved by adding 10 equivalents of THF to the polymerization when the monomer to catalyst ratio was around 45, or by using a monomer to catalyst ratio near or above 100.

Aromatization of PNV Block Copolymer Precursors. Aromatization of the precursor polymers was achieved using DDQ as for the homopolymers. This method

worked well for copolymer **6**, but caused decomposition of **7**. The problem with copolymer **7** was that the trichlorinated PNV (3Cl-PNV) precursor requires high temperatures for aromatization and these conditions caused decomposition or crosslinking of the unhalogenated PNV block (3H-PNV), as the polymer became a dark brown insoluble gel.

Scheme 2



Photoluminescence of **10, **11**, and **13**.** As shown in Figure 2, photoluminescence measurements of **11** revealed that this diblock copolymer luminesces with an emission maximum at 577 nm when excited at 485 nm. This emission wavelength is nearly the same as that observed for the luminescence maximum of the trifluorinated PNV (3F-PNV) homopolymer, **13**. One important difference between **13** and **11**, however, is that the copolymer's emission intensity more closely matches that of the 3H-PNV homopolymer, **10**, which has an emission intensity approximately ten times stronger than that of **13**. These results indicate that excitons formed in the 3H-PNV block migrate to the smaller bandgap, 3F-PNV block, and recombine with emission of light that has a wavelength characteristic of 3F-PNV. The emission intensity is increased at this wavelength relative to the homopolymer since excitons that originated in both blocks recombine in the 3F-PNV block.

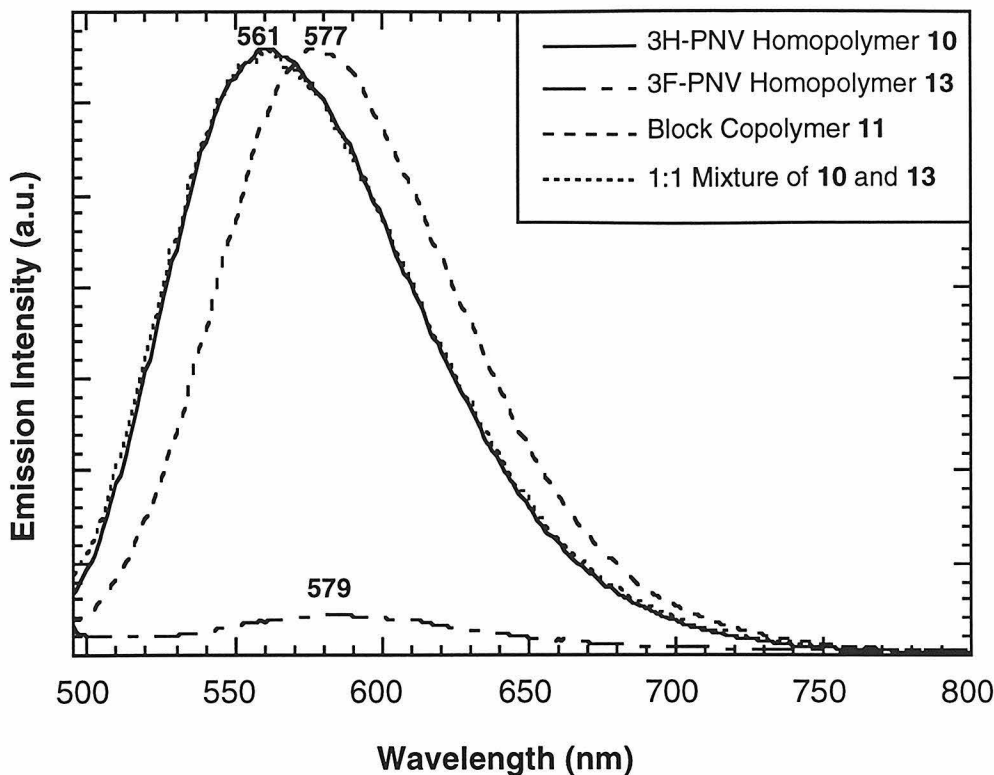


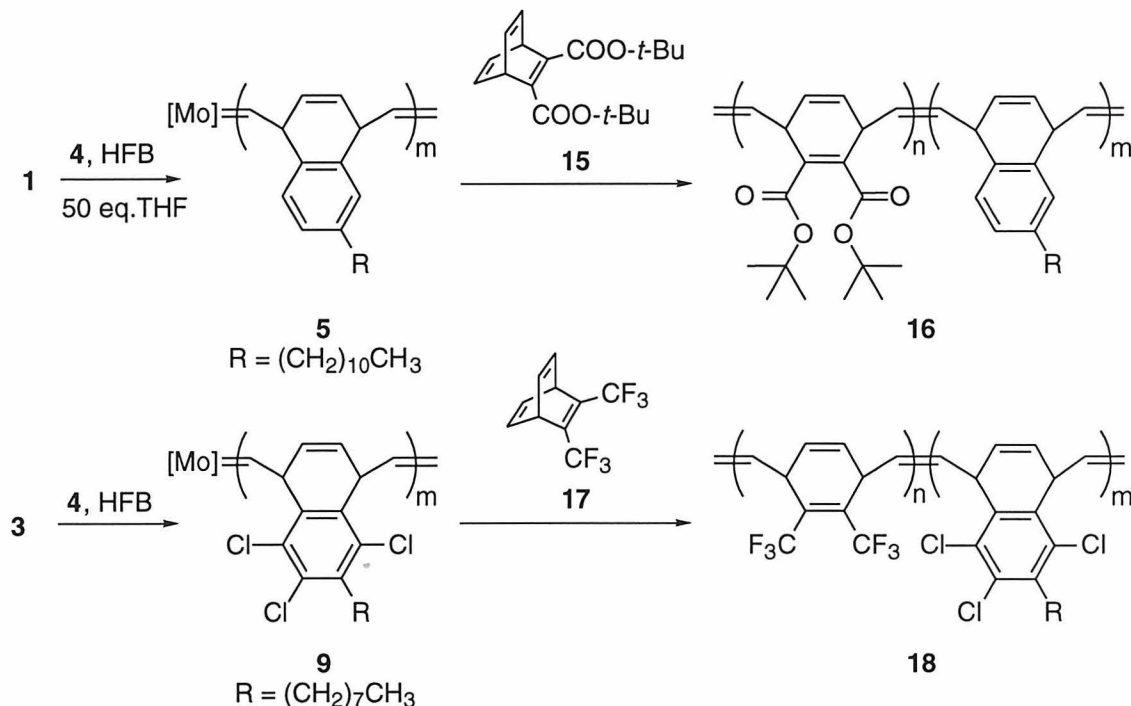
Figure 2. Emission spectra of PNV homopolymers and a block copolymer. Excitation wavelength = 485 nm.

PNV/PPV Copolymers. Despite the differences in the emission spectra of the PNV homopolymers and copolymers, it was unclear whether all electrons and holes created by excitation of the larger bandgap polymer were transported into the smaller bandgap block since, due to the overlap of these spectra, luminescence from the larger bandgap block may have been obscured. To more clearly observe whether complete transport of electrons and holes occurs, copolymers comprised of two polymers with larger bandgap differences were prepared.

As shown in Schemes 3 through 5, copolymers of 3H-PNV with di-*t*-butylester substituted PPV (BC-PPV) and 3Cl-PNV with bistrifluoromethyl substituted PPV (BTF-PPV) were synthesized for these studies. These polymer combinations were chosen both for the large difference in the homopolymers' emission wavelengths and for the similar conditions under which the precursor polymers included in the same copolymer can be

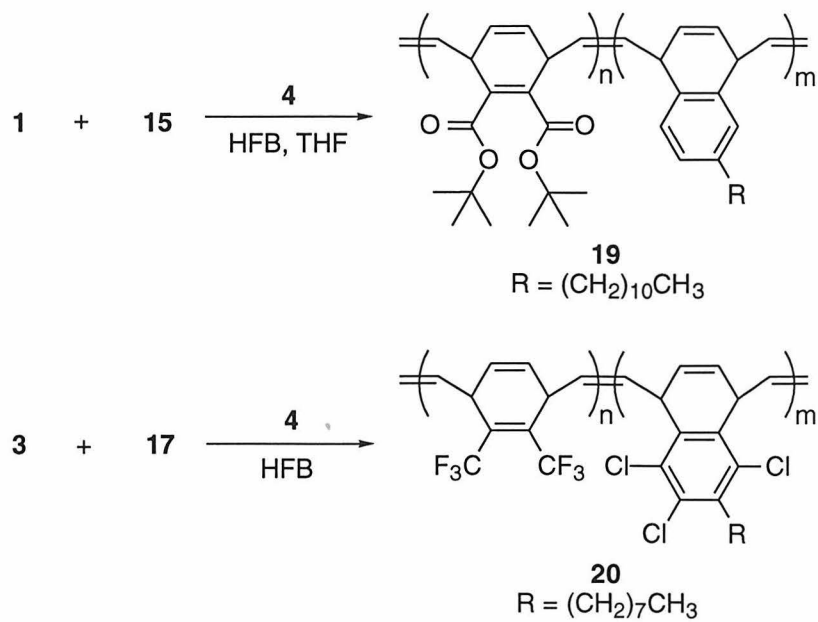
aromatized. This second criterion was important to avoid the decomposition observed for polymer **7**. The 3Cl-PNV/BTF-PNV combination also has the advantage that the emission intensities of the two homopolymers are similar and, therefore, emission from either polymer is readily observed in the presence of the other polymer.

Scheme 3

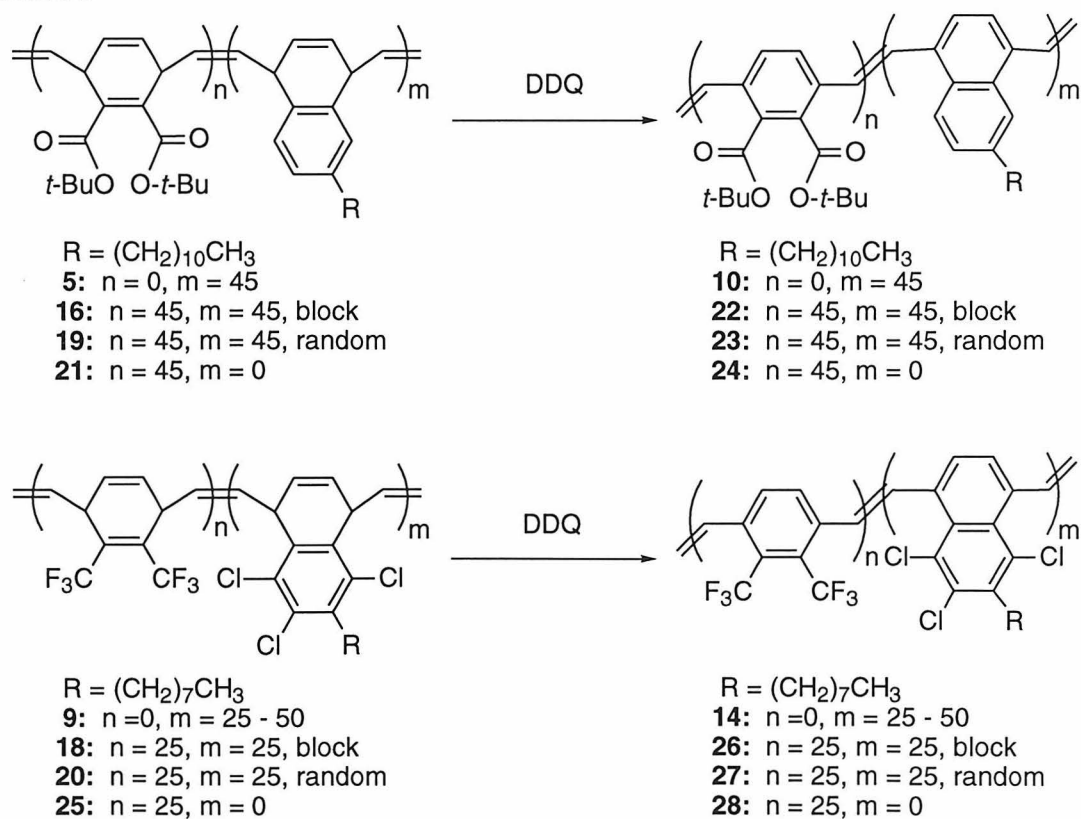


Random copolymers of monomer **1** with **15**, and monomer **3** with **17** were synthesized as well by adding **4** to a 1:1 mixture of the required monomers as shown in Scheme 4. For the polymerization of **1** and **15**, 50 equivalents of THF were added to the reaction. From previous observations, these conditions seemed likely to cause both monomers to polymerize at similar rates. Following this polymerization by ^1H NMR revealed this to nearly be the case, but showed slightly faster consumption of **1** near the beginning of the reaction. The polymerization of **3** and **17** followed a similar path with ^1H NMR revealing that, near the beginning of this reaction, **3** was consumed more quickly than **17**. Polymerization of **3** became slower as its concentration was reduced,

Scheme 4



Scheme 5



however, so that unreacted **3** was observed until the reaction was nearly complete. As before, aromatization of the precursor polymers was accomplished by oxidizing them in solution with DDQ as shown in Scheme 5.^{10,11,35,36}

Photoluminescence of 3H-PNV/BC-PPV. Photoluminescence measurements of polymers **10** and **22** to **24** were performed on both solutions and films of these materials. As shown in Figure 3, the block copolymer, **22**, mainly exhibited luminescence at a wavelength characteristic of the larger bandgap homopolymer, **24**. This result seems to indicate that excitons are not transported into the smaller bandgap material, 3H-PNV. However, one point that draws this possibility into question is that the luminescence intensity of **22** is significantly reduced relative to the BC-PPV homopolymer, **24**. In Figure 3 the emission peak heights were normalized so that all of the spectra could be displayed on the same graph, but as shown by the intensity data listed, **24** luminesces four

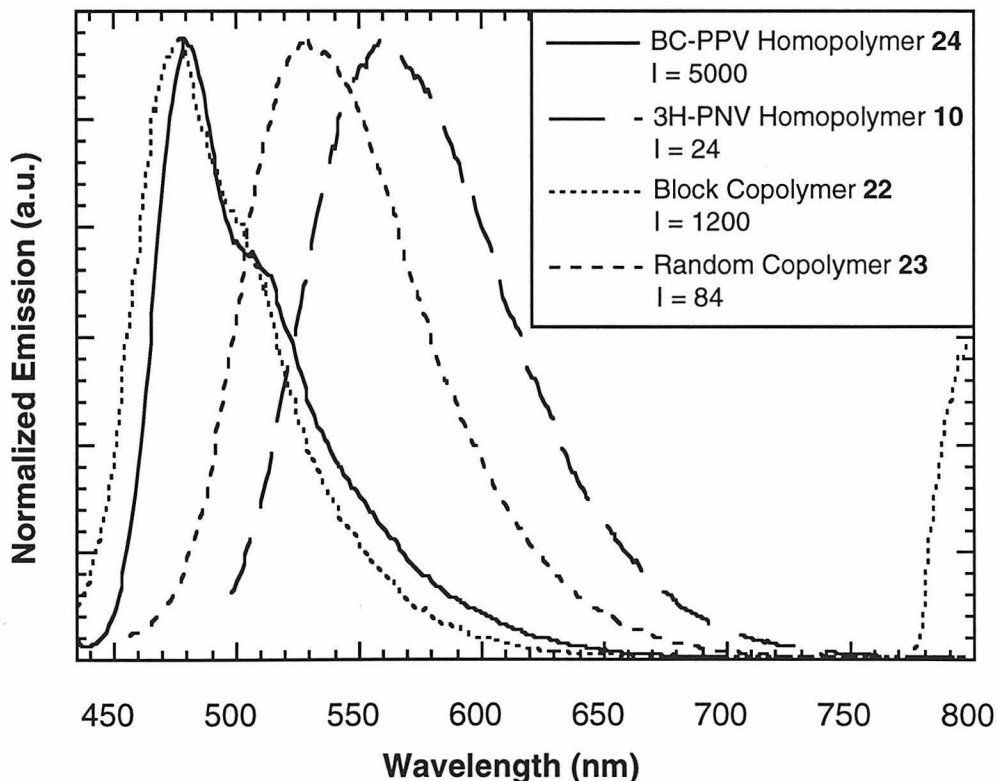


Figure 3. Emission spectra of solutions of polymers **10**, **22**, **23**, and **24**. "I" is the peak intensity given by the spectrofluorometer (units for this number are arbitrary, but all peaks were measured on the same scale). Quantum yields are included in the Experimental section.

times more strongly than **22** and 200 times more strongly than **10**. These discrepancies in the polymers' luminescence intensities, and the low quantum yield of the 3H-PNV homopolymer ($\approx 0.5\%$), raise the possibility that the 3H-PNV homopolymer and block contain non-radiative quenching sites.³⁷ With this being the case, excitons that migrate to the PNV block would mostly be quenched while the luminescence from those not quenched would be overpowered by luminescence from the BC-PPV block, as observed. As shown in Figure 4, luminescence from the BC-PPV block results from excitons that did not reach the 3H-PNV block before recombining. Measurements of solutions of the random copolymer, which has units of 3H-PNV throughout most of its length, similarly reveal an emission intensity more closely resembling that of 3H-PNV, thus providing additional support to the possibility that 3H-PNV is quenching the photoluminescence of the block copolymer.

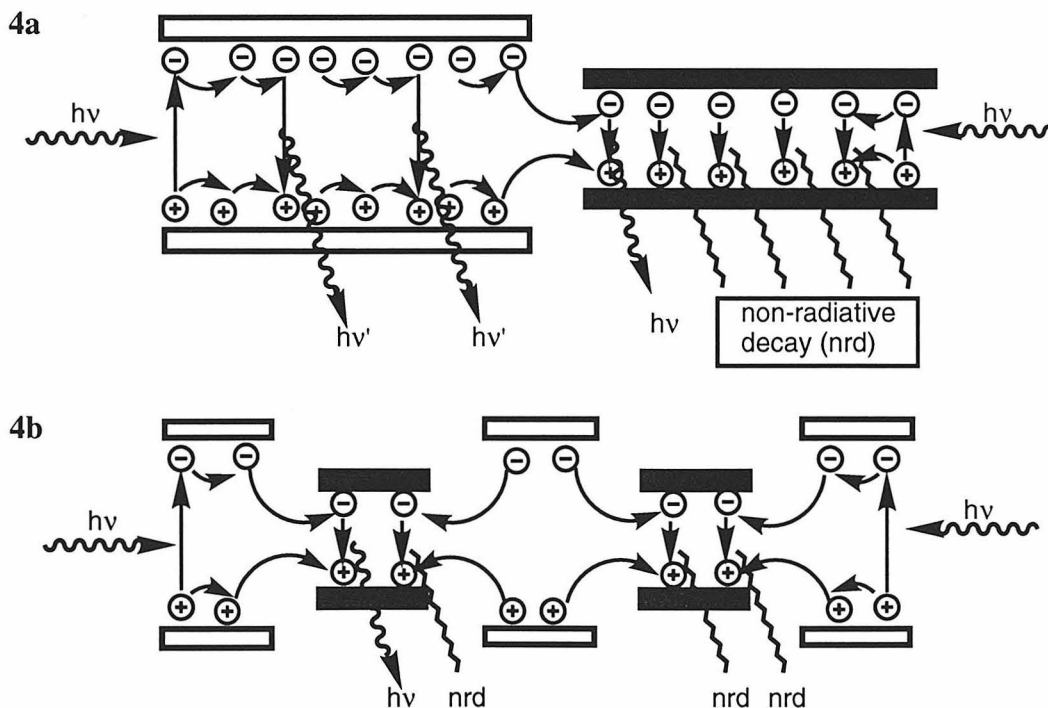


Figure 4. a) A diblock copolymer with quenching occurring in the smaller bandgap block. b) A multiblock (or random/blocky) copolymer with quenching occurring in the smaller bandgap segments.

Further evidence for this scenario is provided by spectra of films of these materials. As shown in Figure 5, in contrast to the solutions, films of block copolymer **22** exhibit luminescence at wavelengths characteristic of the smaller bandgap material, 3H-PNV. More complete transfer occurs in films since excitons are transported into the smaller bandgap block by both intramolecular (travel along a chain) and intermolecular (hopping between chains) processes — only intramolecular transport occurs in solution. Quantitative measurements of these films³⁹ reveal that the quantum yield of **22** ($\Phi < 0.5\%$) is much less than that of **24** ($\Phi \approx 43\%$) and similar to that of **10** ($\Phi < 0.5\%$). Thus, in films most of the excitons are transported into the 3H-PNV block and, as in solution, most of them relax by non-radiative pathways. As in solution, films of the random copolymer, **23** ($\Phi \approx 1.1\%$) also possess an emission intensity more closely resembling that of homopolymer **10**.

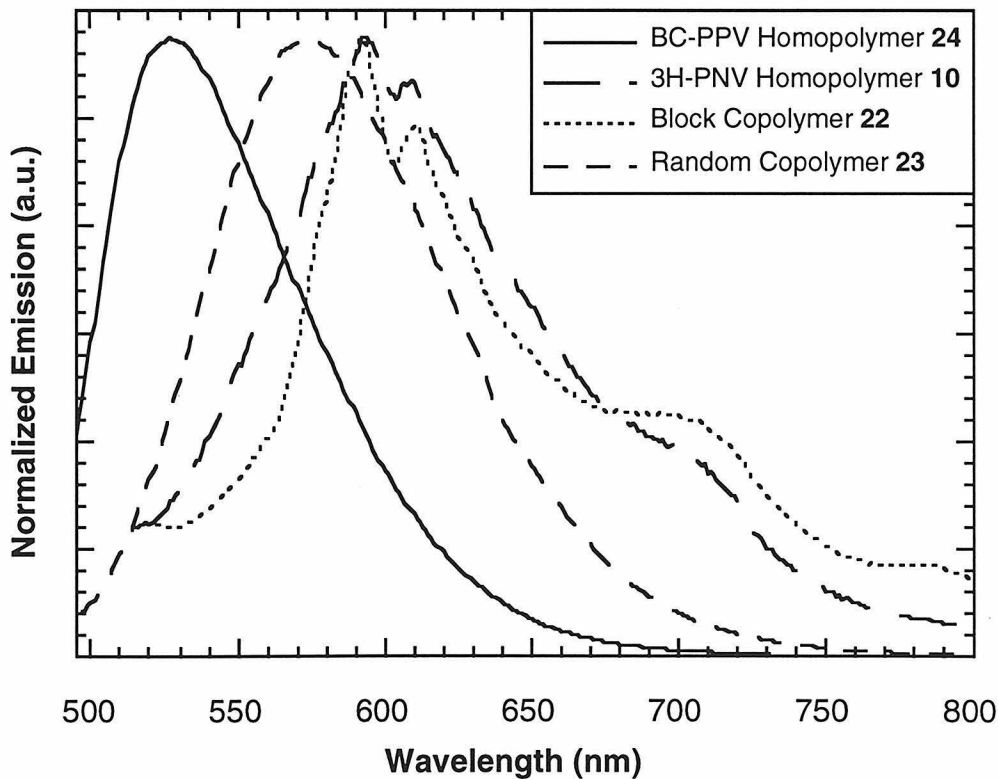


Figure 5. Emission spectra of films of polymers **10**, **22**, **23**, and **24**.³⁸

One additional point to be made concerning the random copolymer, **23**, is that its emission wavelength is between the emission wavelengths of the two homopolymers, in agreement with theory. This shift relative to the homopolymers is expected since a perfectly random copolymer is predicted to luminesce at a wavelength halfway between that of the two homopolymers that comprise it.^{3,4,6} The emission maximum of **23** is actually closer to that of the smaller bandgap material, however, indicating that polymer **23** is not perfectly alternating but probably contains clusters of 3H-PNV and BC-PPV units. Similar behavior has been reported for copolymers of PPV and dimethoxy substituted PPV(DMeOPPV) when the DMeOPPV units were in clusters instead of being evenly distributed.⁶ These clusters are predicted to have a bandgap closer to the homopolymer that is present in a higher concentration in that particular section of the polymer. As in polymers containing distinct blocks, excitons are predicted to migrate to the smaller bandgap segments and, therefore, most of the luminescence emitted has a wavelength characteristic of the those segments, which have a bandgap more similar to the smaller bandgap homopolymer.

Photoluminescence of 3Cl-PNV/BTF-PPV. Because of the problems associated with the large difference in the emission intensities of BC-PPV and 3H-PNV, we next wanted to study a block polymer that was comprised of two polymers with similar emission intensities but which still had well separated emission wavelengths. These requirements led to the examination of copolymers of 3Cl-PNV and BTF-PPV. In addition to having well separated emission maxima, at 450 nm for homopolymer **28** and 569 nm for homopolymer **14**, the emission intensities of these polymers are similar when each of these polymers is irradiated at its excitation maximum. As with the 3H-PNV/BC-PPV copolymers, photoluminescence measurements were performed on both solutions and films of the homopolymers and copolymers.

Solutions of polymers containing units of 3Cl-PNV were all prepared to contain the same concentration of 3Cl-PNV units. The solution of homopolymer **28** contained

the same concentration of monomer units as the solution of homopolymer **14**. As shown in Figure 6, when the block copolymer, **26**, was irradiated at the excitation maximum of homopolymer **28**, the emission peak characteristic of 3Cl-PNV was more intense than that measured for homopolymer **14**, indicating that some excitons migrated to the block of 3Cl-PNV before recombining. This spectrum also shows emission at wavelengths characteristic of BTF-PPV, indicating that some electrons and holes recombined before they reached the smaller bandgap block, as shown in Figure 7a.

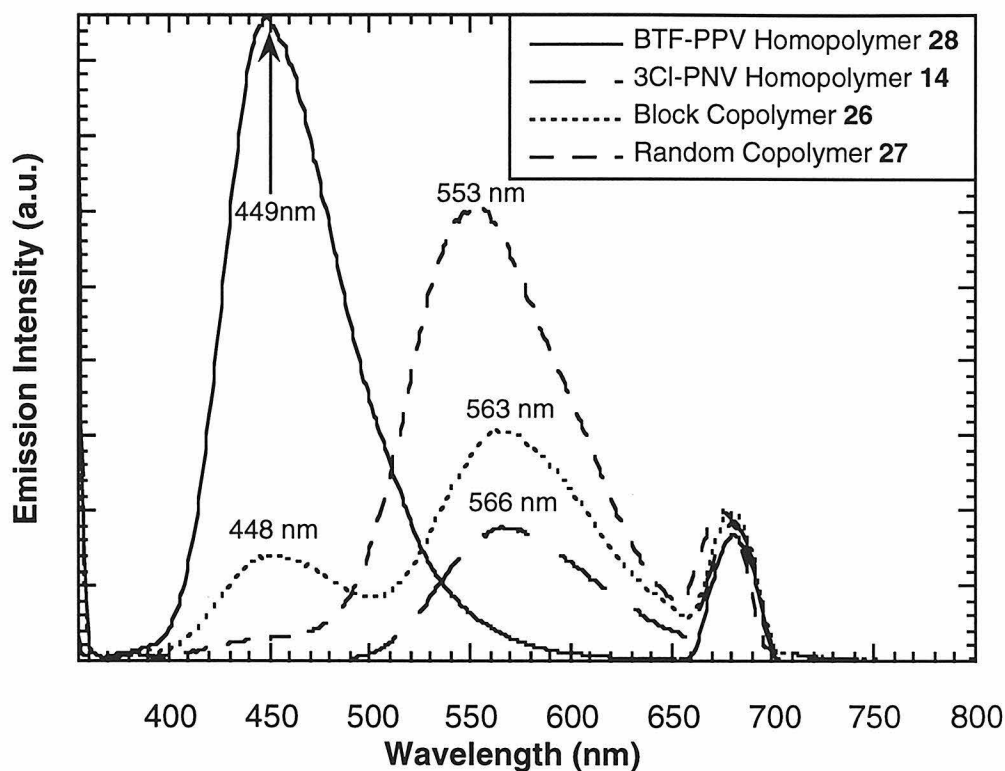


Figure 6. Emission spectra of solutions of homopolymers and copolymers when irradiated at the excitation maximum for polymer **28** (345 nm).

The spectrum of the random copolymer, **27**, shows that its luminescence intensity is increased and that its luminescence maximum is blue shifted relative to that of **14**. Polymer **27** is blue shifted only slightly relative to **14** since, as for the 3H-PNV/BC-PPV random copolymer, a tapered block or blocky copolymer was formed rather than a perfectly alternating copolymer.^{3,4,6} The luminescence wavelength maximum of **27** more

closely matches that of **14** since electrons and holes formed in larger bandgap segments, where the concentration of BTF-PPV is higher, migrate to smaller bandgap segments, where there is a higher concentration of 3Cl-PNV. As with the block copolymer, the luminescence intensity of the smaller bandgap region is increased since excitons formed in large and small bandgap regions all recombine in the smaller bandgap regions. Emission measured at the wavelength characteristic of BTF-PPV is much less intense for

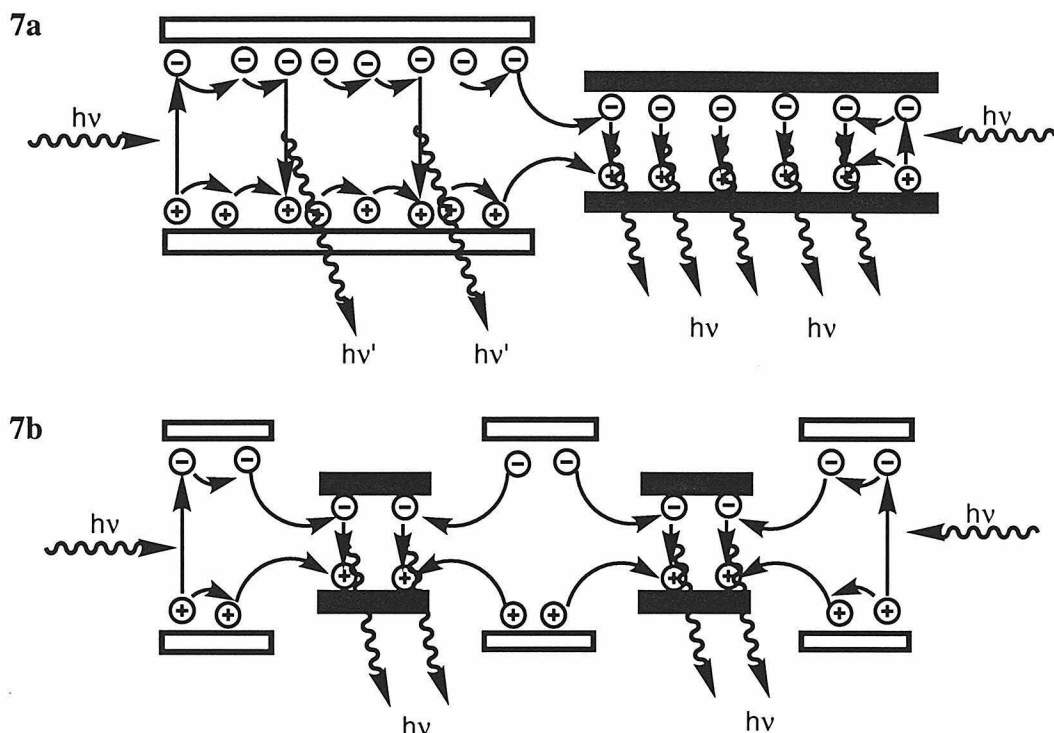


Figure 7. a) Migration of electrons and holes in a diblock copolymer. b) Migration of electrons and holes in a multiblock (or random/blocky) copolymer.

polymer **27** than for polymer **26**, showing that migration of electrons and holes into smaller bandgap segments of **27** is more complete in this material than in the diblock copolymer. This more complete migration most likely results from the fact that polymer **27** contains units of both BTF-PPV and 3Cl-PNV along the entire polymer chain, so short blocks of large bandgap material and short blocks of smaller bandgap material are interspersed throughout the length of the polymer. As a result, electrons and holes reach

a smaller bandgap segment after traveling a shorter distance than they need to travel in the diblock copolymer, as shown in Figure 7b.

Further evidence supporting a blocky structure for polymer **27** is provided by the emission spectrum of this polymer when irradiated at the excitation maximum of **14**, the smaller bandgap homopolymer. As shown in Figure 8, under these conditions the emission intensity of polymer **27** is still greater than that of **14** or **26**. As with polymers containing conjugated and unconjugated segments, the increased emission intensity of **27** is due to a reduction of non-radiative quenching of excitons.^{16,17,36,40} Quenching, which occurs at defects in the polymer backbone, is reduced in **27** due to the presence of both large and small bandgap regions throughout the polymer backbone. Excitons become trapped in the smaller bandgap segments of **27** and recombine with emission of light in these segments, as shown in Figure 9b. The larger bandgap segments have been proposed to prevent migration out of the smaller bandgap regions and thereby diminish

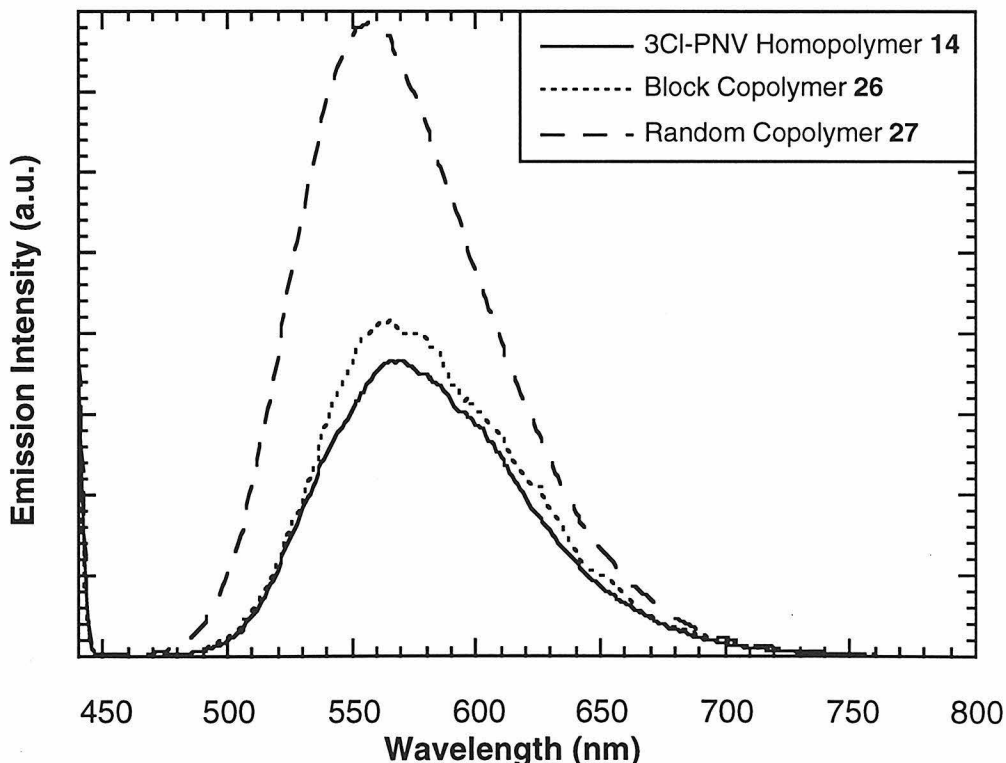


Figure 8. Emission spectra of solutions of homopolymers and copolymers when irradiated at the excitation maximum for polymer **14** (430 nm).

the number of electrons and holes that migrate to quenching sites. As shown in Figure 9a, the emission intensity of polymer **26** is essentially the same as that of the polymer **14** since only the 3Cl-PNV block of **26** is excited by 430 nm radiation. As in the homopolymer, excitons in the diblock copolymer are free to move throughout the entire length of 3Cl-PNV. Therefore, excitons in the 3Cl-PNV block of **26** are as likely to reach quenching sites as they are in the homopolymer, **14**.

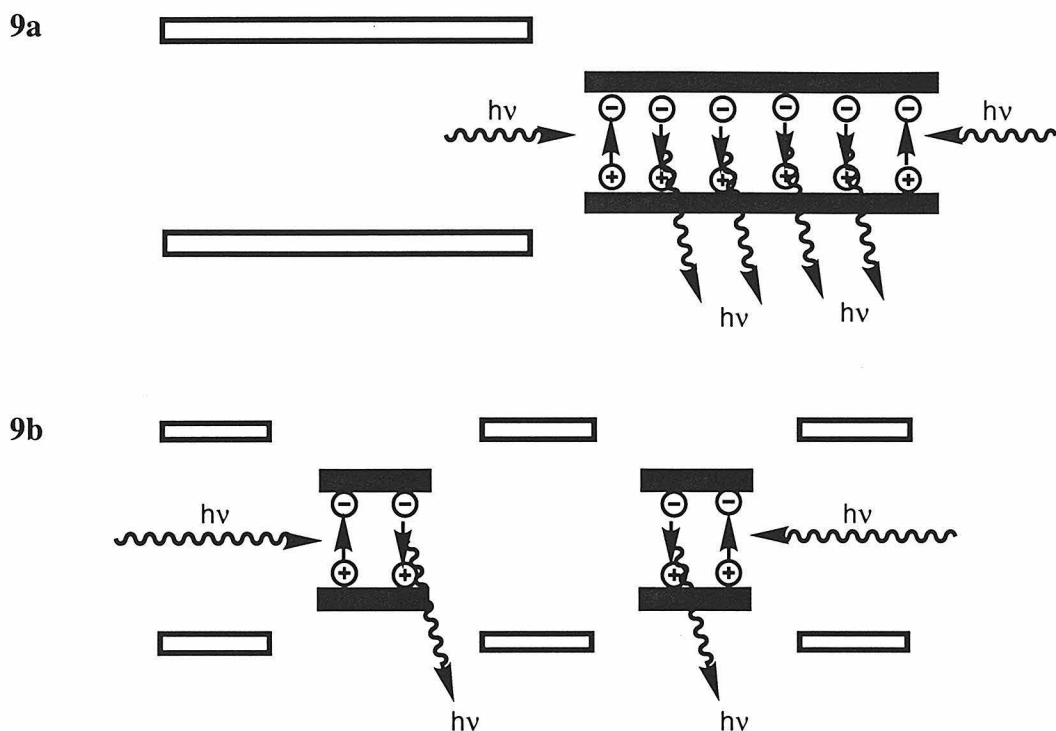


Figure 9. a) Behavior of a diblock copolymer irradiated at the excitation maximum of the smaller bandgap block. b) Behavior of a multiblock copolymer irradiated at the excitation maximum of the smaller bandgap block.

In films, the diblock copolymer **26** shows luminescence characteristic only of the smaller bandgap homopolymer, **14**, as shown in Figure 10. This more complete migration results from the increased interaction among the polymer chains in the solid state, which allows electrons and holes to be transferred between chains as well as along the polymer chain. The spectrum of a 1:1 mixture of **14** and **28**, shown for comparison, does not show complete transport to the smaller bandgap polymer. The difference in these results is due to the fact that the 1:1 mixture can more readily phase separate into

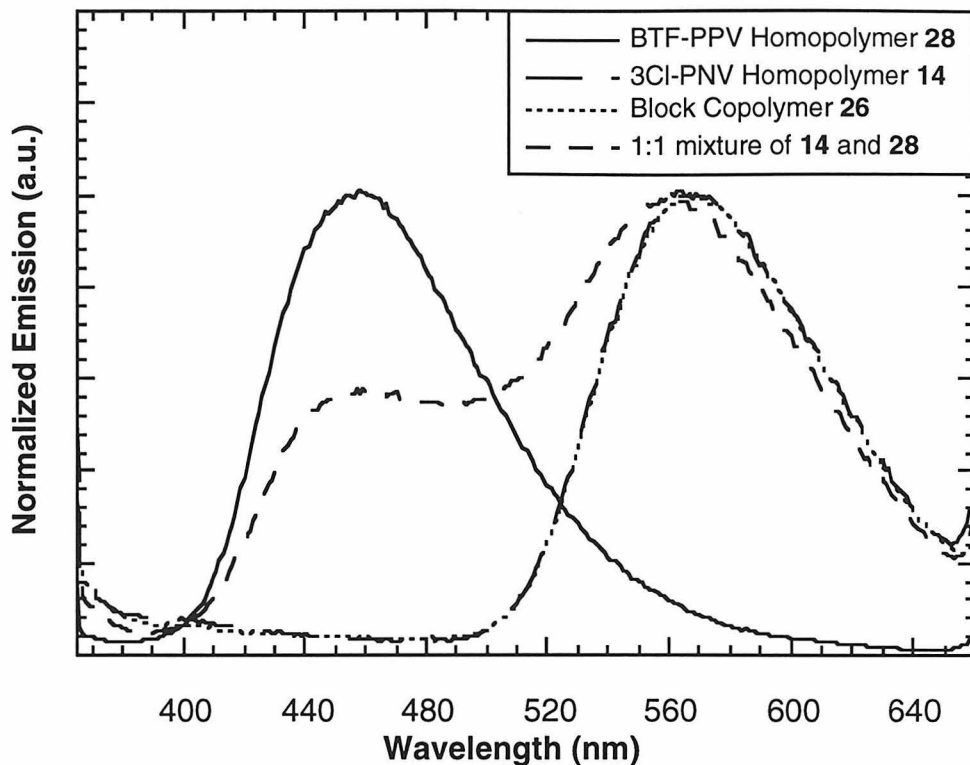


Figure 10. Emission spectra of films of homopolymers and the block copolymer when irradiated at the excitation maximum for polymer **28** (345 nm).

macroscopic regions containing only one type of homopolymer. Migration of electrons and holes from **28** into **14** may, therefore, require transport to occur over larger distances than in films of the block copolymer.

Theoretical Considerations. Calculations have been performed⁴¹ to determine the geometry, bandgap, and HOMO/LUMO positions of the homopolymers and copolymers prepared. Geometry determinations, which predicted that all of the polymers are twisted in their ground-state geometry, were carried out using a semiempirical Hartree-Fock Austin Model 1 method. The other parameters were calculated using a Hartree-Fock intermediate neglect of differential overlap Hamiltonian coupled to a single configuration interaction technique (INDO/SCI). The results of these calculations essentially agree with the experimental observations made here in that the calculated

Table 1. Energies of frontier orbitals (HOMO, HOMO-1, LUMO and LUMO+1) calculated at the INDO level, and transition energy of lowest optical transition (E_{tr}) calculated using the INDO/SCI method.

Polymer	HOMO-1	HOMO	LUMO	LUMO+1	E_{tr} in eV (nm)
3Cl-PNV ^t	-7.66	-7.50	-1.03	-0.96	3.49 (355)
BTF-PPV ^t	-8.46	-8.25	-1.03	-0.89	3.98 (312)
3Cl/BTF ^{t,b}	-7.98	-7.66	-1.01	-0.93	3.61 (343)
3H-PNVP	-6.78	-6.47	-1.12	-0.85	2.68 (463)
BC-PPVP	-7.79	-7.50	-1.55	-1.50	3.07 (403)
3H/BCP ^b	-7.25	-6.62	-1.46	-1.43	2.76 (449)
3F-PNVP	-7.12	-6.80	-1.53	-1.30	2.62 (473)
3H/3Fp, ^b	-6.99	-6.62	-1.43	-1.08	2.63 (471)

All HOMO and LUMO values have units of eV relative to vacuum which is 0 eV. All calculations were performed for oligomers containing six monomer units.⁴¹ t) Results shown are for a polymer in a twisted geometry. p) Results shown are for a polymer in a planar geometry. Except for 3Cl-PNV, these results more accurately reflected the actual bandgap of the polymers. b) These results are for block copolymers.

bandgaps of the polymers decrease in the order BTF-PPV > 3Cl-PNV > BC-PNV > 3H-PNV > 3F-PNV (see Table 1 for exact numbers). From these bandgaps, the results observed for the block copolymers are expected since excitons should migrate to the smaller bandgap materials (3F-PNV, 3H-PNV and 3Cl-PNV in the copolymers studied). The calculated bandgap for 3Cl-PNV is larger than that of BC-PPV and 3H-PNV, in contrast with experimental measurements, due to using a twisted geometry for the 3Cl-PNV backbone and using a planar geometry for BC-PPV and 3H-PNV in the calculations performed.

Conclusions

Overall the results obtained for the copolymers agree with the expectations predicted by theory.^{3,4,6,41} The block copolymers all showed transfer of excitons from

the larger bandgap material to the smaller bandgap material. In 3H-PNV/3F-PNV and 3Cl-PNV/BTF-PPV this transfer was manifested as an increase in the luminescence intensity of the smaller bandgap material. In the 3H-PNV/BC-PPV block copolymer a much smaller increase was observed due to quenching by the smaller bandgap material. In general, more complete transport was observed in films of the block copolymers where both intrachain and interchain transport to the smaller bandgap material can occur and in random/blocky copolymers which provide more small-bandgap sections over shorter distances. The intensity was further increased in the 3Cl-PNV/BTF-PPV random copolymer since larger bandgap segments of this material prevent migration of electrons and holes and thereby diminish the number that reach nonradiative relaxation sites. A similar increase was not observed for the 3H-PNV/BC-PPV random copolymer since the smaller bandgap segments, where excitons should get trapped, are rich in 3H-PNV which seems to be responsible for non-radiative decay.

Experimental

General Methods and Materials. Monomers were prepared as described in Chapters 2 and 3. Initiator **4** was prepared as previously reported.⁴² NMR spectra were recorded on a QE Plus-300 MHz (300.1 MHz ¹H; 75.33 MHz ¹³C) spectrometer. Infrared spectra were recorded using a Perkin-Elmer 1600 series FTIR spectrometer. Elemental analyses were performed by Caltech Analytical Labs or Mid-West Microlab. UV/Vis spectra were recorded on a HP Vectra ES/12 spectrometer. Gel permeation chromatography (GPC) utilized an AM Gel Linear 10 column and a Knauer differential refractometer. Dichloromethane (Burdick and Jackson HPLC grade) was used as the eluent for all GPC measurements. Molecular weights are uncorrected and reported as compared to Shodex polystyrene standards with molecular weights ranging from 2.95 x 10³ to 2.40 x 10⁶. Emission spectra were recorded on an SLM 8000 C spectrofluorometer. Benzene and benzene-d₆ were dried by passing through activated

alumina columns. Methanol, dichloromethane and chloroform were degassed by purging with dry argon for a minimum of 30 minutes. Hexafluoro-*t*-butanol (HFB) and THF-d₈ were distilled from calcium hydride.

General Procedure for Polymer Synthesis. Inside a nitrogen filled dry box the desired amount of monomer was dissolved in dry benzene (C₆D₆ was used in most cases) and the required amounts of HFB and THF were added. Initiator **4** dissolved in dry C₆D₆ was then added to this solution. The reaction mixture changed color from yellow to light orange or orange-brown during the first few minutes after mixing. For following the reaction by ¹H NMR, the solution was transferred into an NMR tube equipped with a J-Young valve. If a block copolymer was being made, after the polymerization was shown to be complete the NMR tube was returned to the dry box and the second monomer, which was dissolved in a minimum amount of C₆D₆, was added. After the polymerization was complete, degassed benzaldehyde was added to quench the initiator. The reaction mixture, which turned brown over 30 minutes, was then pipetted into degassed methanol and the resulting precipitate was recovered by centrifuging and then decanting the solvent. Typically reactions using up to 0.5 g of monomer were precipitated using 30 mL of degassed methanol. Further purification was accomplished by redissolving the polymer in dichloromethane or benzene and then reprecipitating the polymer in methanol. The polymer was then dried under vacuum. All operations were carried out under argon when possible, to avoid oxidation of the polymer. In some cases, adding a 0.5 - 1.0 mL of methanol saturated with sodium chloride was found to facilitate more complete precipitation.

General Procedure for Polymer Aromatization. The desired amount of polymer was dissolved in dichloromethane or C₆D₅Br and DDQ was added. For fast reactions done in dichloromethane, the DDQ was dissolved in dichloromethane before adding it to the polymer solution. In most cases slightly less (\approx 0.95 equiv.) than equivalent of DDQ was added since polymers containing some unaromatized units were

found to be significantly more soluble than the fully aromatized polymers. Reactions done in dichloromethane generally proceeded at room temperature. For reactions done in C₆D₅Br the reaction flask was sealed and heated in an oil bath at 120 °C for 1 - 3 days. The reaction mixture was then added to methanol to yield a precipitate which was isolated by centrifuge and further purified by repeated precipitation as for the precursor polymers. To ensure that all of the polymer precipitated each time, the solvent layer above the precipitated polymer was spotted several times on a non-luminescent TLC plate. This plate was then irradiated with a hand-held UV lamp to see if any polymer, which is luminescent, had remained in solution. In some cases, adding a 0.5 - 1.0 mL of methanol saturated with sodium chloride was found to facilitate more complete precipitation.

General Procedure for Preparation of Polymer Solutions for Polymers 10 - 14, 22, 23, 24. Approximately 2 mg of each polymer was dissolved in 50 mL of chloroform to yield solutions of each polymer so that each solution (A) contained the same concentration of total monomer units. 1 mL of each of these solutions was then diluted to 25 mL using chloroform to yield solutions B. 1 mL of each of these solutions was then diluted to 25 mL using chloroform to yield solutions C. Solutions B and C were used for most luminescence measurements, but for polymers **10, 11** and **13**, solution A was often used since these materials luminesce weakly. For polymer **23** the best results were obtained using solution B.

General Procedure for Preparation of Polymer Solutions for Polymers 14, 26, 27, and 28. The total amount of each purified, aromatized polymer (usually ≈20 mg) was dissolved in 20 mL of chloroform. An appropriate amount of this solution was then diluted to 50 mL to yield solutions of each polymer so that each 50 mL solution contained 2 mg of 3Cl-PNV. The solution of homopolymer **28** was prepared to contain the same concentration of monomer units as the solution of homopolymer **14**. 1 mL of each of these solutions was then diluted to 25 mL to produce the solutions used for

fluorescence measurements.

Photoluminescence Measurements. All solution measurements were performed on solutions that were diluted so that the emission maximum was on scale with a Ru(bpy)₃Cl₂ standard that was approximately 1 x 10⁻⁵M. The exact concentration used in calculating quantum yields (7.6 x 10⁻⁶ M) was calculated from the absorbance of this solution at 453 nm and the reported extinction coefficient.⁴³ All polymer solutions were prepared using degassed solvent. Quantum yields for the polymers were calculated by comparison to a Ru(bpy)₃Cl₂ standard using the equation:

$$\Phi_{poly} = \frac{I_{poly} \cdot \epsilon_{Ru} c_{Ru}}{I_{Ru} \cdot \epsilon_{poly} c_{poly}} \cdot \Phi_{Ru}$$

Integration values, *I*, were measured on spectra that had been corrected for detector response using the software provided with the SLM 8000 C Spectrofluorometer. A value of 0.028±0.002 was used for Φ_{Ru} .⁴⁴ The Ru(bpy)₃Cl₂ solution was equilibrated with air.

Most measurements on films were also performed using the SLM 8000 C Spectrofluorometer. In this case a film of the polymer was formed by putting a few drops of a concentrated solution of the polymer on a glass slide and allowing the solvent to evaporate. The slide was then cut to fit into the cuvette holder in the spectrofluorometer. This technique allowed collection of the emission spectrum, but did not provide quantitative data. Quantum yields for films of the polymers were measured as previously reported.^{39,45}

3H-PNV Precursor Polymer (5). Reacted 68.5 mg **1**, 3.8 mg **4**, 7.8 μ L HFB, in 0.6 g C₆D₆ for 40 minutes. Yield = quantitative ¹H NMR (CDCl₃, all peaks were broad) δ 7.09, 6.03 (cis), 5.93 (cis), 5.86, 5.54, 5.36 (cis), 4.62 (cis), 3.93, 2.57, 1.60, 1.28, 0.89; carbene proton in C₆D₆ δ 12.28 (br m). ¹³C NMR (CDCl₃) δ 140.9 (m), 135.8 (m), 133.7 (m), 132.3 (m), 128.7 (m), 127.9 (m), 126.6 (m), 43.44, 43.22, 37.86 (cis, m), 31.93, 31.73, 31.56, 29.68, 29.39, 22.70, 14.14. UV/Vis (chloroform): λ_{max} /nm = 236.

FTIR (KBr, pellet): 3032 (s), 2924 (s), 2852 (s), 1665 (w), 1614 (m), 1573 (m), 1499 (s), 1464 (s), 1378 (s), 1154 (w), 1080 (m), 1025 (m), 964 (s), 890 (m), 819 (s), 789 (s), 722 (s), 647 (w), 495 (m) cm^{-1} . Anal. Calcd for $\text{C}_{23}\text{H}_{32}$: C, 89.54; H, 10.46. Found: C, 89.29; H, 10.46. GPC data (CH_2Cl_2): Mn = 47700, Mw = 81000, PDI = 1.70.

3H-PNV (10). Reacted 199.5 mg **5** with 12.3 mg DDQ in 20 mL dichloromethane for 3 hours at rt. Adding 1 mL of sodium chloride saturated methanol solution was found to facilitate the precipitation of the polymer in methanol. After being dried under vacuum, **10** was obtained in 90% yield. ^1H NMR (CDCl_3 , all of the peaks were broad) δ 8.29, 8.02, 7.47, 2.82, 1.73, 1.23, 0.88; ^{13}C NMR (CDCl_3) δ 141.0 (m), 134.9 (m), 131.9 (m), 130.1 (m), 129 - 128.6 (m), 127.7 (m), 124.0 (m), 123.1 (m), 36.45 (br), 31.91, 31.70, 29.67, 29.36, 27.69, 14.13. UV/Vis (chloroform): $\lambda_{\text{max}} = 253, 444$ nm. Emission spectrum (chloroform, $\lambda_{\text{ex}} = 485$ nm): $\lambda_{\text{max}} = 561$ nm; Φ (solution, $\lambda_{\text{ex}} = 485$ nm) = 0.5%. FTIR (KBr, pellet): 3038 (m), 2954 (s), 2926 (s), 2854 (s), 1622 (m), 1574 (m), 1510 (m), 1457 (s), 1377 (s), 956 (s), 821 (s) cm^{-1} .

3F-PNV Precursor Polymer (8). Reacted 70.1 mg **2**, 3.7 mg **4**, 7.8 μL HFB, in 0.6 g C_6D_6 for 1.5 hours at rt. Yield = 99%. (alkyl = $(\text{CH}_2)_7\text{CH}_3$) ^1H NMR (C_6D_6 , all peaks were broad): δ 6.22(cis), 5.87, 5.68, 5.24 (cis) (4H), 4.82 (cis), 4.17 (2H), 2.64 (2H), 1.55 (2H), 1.26 (10H), 0.94 (3H); carbene proton in C_6D_6 δ 12.07 (br m). ^{13}C NMR (CDCl_3) δ 155.0, 152.6, 148.7, 146.3, 145.9, 143.5, 131.4, 127.4, 126.8, 124.0, 120.1, 117.7 (phenyl region with fluorine coupling), 37.2 (br s), 31.9, 29.5, 29.3, 29.2, 22.7, 14.1. FTIR (film on NaCl): 3035, 2956, 2926, 2856, 1644, 1476, 1464, 1366, 1334, 1322, 1247, 1126, 1077, 990, 960, 866, 828, 752, 720 cm^{-1} . GPC (CH_2Cl_2): Mn = 28800, Mw = 36100, PDI = 1.26.

3F-PNV (13). Reacted 64 mg **8** with 41 mg DDQ in 10 mL dichloromethane overnight at rt. Yield = 96%. During the course of reaction, ^1H NMR (CDCl_3) showed broad peaks at δ 7.6-6.8, 1.54, 1.26, 0.85. FTIR (KBr, pellet): 2956, 2925, 2854, 1648, 1570, 1458, 1387, 1276, 1203, 1123, 1049, 1035, 972, 891, 842, 594 cm^{-1} . UV/Vis

(chloroform): $\lambda_{\text{max}} = 416$ nm. Emission spectrum (chloroform, $\lambda_{\text{ex}} = 403$ nm): $\lambda_{\text{max}} = 568$ nm; (chloroform, $\lambda_{\text{ex}} = 485$ nm): $\lambda_{\text{max}} = 579$ nm; Φ (solution, $\lambda_{\text{ex}} = 403$ nm) = 0.05%.

3H-PNV/3F-PNV Block Copolymer Precursor (6). Reacted 68.5 mg **1**, 3.9 mg **4**, 7.8 μL HFB, 4 μL THF in 0.6 g C_6D_6 for 4.5 hours. Then added 73.1 mg **2** dissolved in 10 drops C_6D_6 and reacted for 3 days. Yield = 91%. ^1H NMR (C_6D_6 , all peaks were broad): δ 7.18 (3H), 6.11, 5.85, 5.59, 5.46 (8H), 4.63, 4.15, 3.94 (4H), 2.61 (4H), 1.65, 1.53, 1.30, 1.22 (30H), 0.93, 0.92 (6H). GPC (CH_2Cl_2): Mn = 46400, Mw = 66000, PDI = 1.42.

3H-PNV/3F-PNV Block Copolymer (11). Reacted 51.6 mg **6** with 33.5 mg DDQ in 10 mL dichloromethane overnight at rt. Yield = 95%. ^1H NMR (CDCl_3) shows broad peaks as for the two homopolymers. UV/Vis (chloroform): $\lambda_{\text{max}} = 439$ nm. Emission spectrum (chloroform, $\lambda_{\text{ex}} = 403$ nm): $\lambda_{\text{max}} = 568$ nm; (chloroform, $\lambda_{\text{ex}} = 485$ nm): $\lambda_{\text{max}} = 577$ nm; Φ (solution, $\lambda_{\text{ex}} = 485$ nm) = 0.5%.

3H-PNV/3Cl-PNV Block Copolymer Precursor (7). Reacted 66.2 mg **1**, 3.5 mg **4**, 6.9 μL HFB, 3.6 μL THF in 0.6 g C_6D_6 for 3.5 hours. Then added 81.4 mg **3** dissolved in 10 drops C_6D_6 and reacted for 3 days. Yield = 88%. ^1H NMR (C_6D_6 , all peaks were broad): δ 7.16 (3H), 6.23, 5.89, 5.61, 5.46 (8H), 4.66, 4.37, 3.94 (4H), 3.03 (2H), 2.62 (2H), 1.66, 1.31 (30H), 0.94 (6H). GPC (CH_2Cl_2): 1st block Mn = 35400, Mw = 61400, PDI = 1.73; 2nd block Mn = 47900, Mw = 67600, PDI = 1.41.

3H-PNV/3Cl-PNV Block Copolymer (12). Decomposed upon oxidation with DDQ.

BC-PPV Precursor Polymer (21). Reacted 0.501 g **15**, 28.2 mg **4** (was added as a solution in 40 drops of benzene), 56 μL HFB, in 3.8 g dry benzene. After purification and drying under vacuum, 0.385 g of **21** was obtained as a brittle light yellow solid. Yield = 77%. *Note:* Following a smaller scale reaction by NMR showed that all monomer was consumed after 2.5 hours. If any of the monomer has decomposed to form

the acid, however, reaction times will be considerably longer. ^1H NMR (C_6D_6 , all peaks are broad) δ 5.67, 5.65, 5.54, 5.40 (4H), 4.30 (small), 3.76 (2H), 1.52 (18H). (CDCl_3) δ 5.52, 5.50 (2H), 5.21, 5.17 (2H), 3.95, 3.56 (2H), 1.37 (18H); carbene proton in C_6D_6 δ 12.50 (br m) and 12.41 (br m) during polymerization, 11.92 (br m) after polymerization was complete. ^{13}C NMR (CDCl_3) δ 166.19 (m, C=O), 135.33 - 126.22 (m, C=C), 81.33 (C of *t*-butyl), 81.26 (C of *t*-butyl), 41.70, 28.05 (CH_3 of *t*-butyl). FTIR 3006, 2979, 2933, 1716, 1674, 1636, 1477, 1456, 1393, 1368, 1351, 1273, 1256, 1155, 1087, 1060, 1034, 967, 848, 755, 667 cm^{-1} . Anal. Calcd for $\text{C}_{18}\text{H}_{24}\text{O}_4$: C, 71.03; H, 7.95. Found: C, 71.48; H, 7.69. GPC data (CH_2Cl_2): Mn = 19600, Mw = 23900, PDI = 1.22.

BC-PPV (24). Reacted 0.369 g **21** with 0.281 g DDQ in 28 mL dichloromethane overnight at rt. Adding 0.5 mL of a saturated sodium chloride solution in methanol was found to facilitate much more rapid and complete precipitation of the polymer. Following purification, the polymer was dried under vacuum to yield 0.34 g of a yellow-orange solid. Yield = 93%. For preparing polymer that was 80% aromatized, the procedure was identical except that 0.8 equivalents of DDQ were used. ^1H NMR (CDCl_3) δ 7.66 (br s, 2H), 7.32(br s, 2H), 1.62 (br s, 18H) ^{13}C NMR (CDCl_3) δ 167.05, 134.66, 133.13, 127.99, 126.74, 83.15, 28.21. FTIR: 2878, 2933, 1720, 1560, 1477, 1458, 1420, 1394, 1369, 1290, 1155, 1148, 1118, 957, 844, 824, 752, 696, 668 cm^{-1} . Anal. Calcd for $\text{C}_{18}\text{H}_{22}\text{O}_4$: C, 71.50; H, 7.33. Found: C, 69.49; H, 7.20. UV/Vis (chloroform): $\lambda_{\text{max}} = 410$ nm. Emission spectrum (chloroform, $\lambda_{\text{ex}} = 422$ nm): $\lambda_{\text{max}} = 479$ nm; (film, $\lambda_{\text{ex}} = 480$ nm): $\lambda_{\text{max}} = 527$ nm; Φ (solution, $\lambda_{\text{ex}} = 422$ nm) = 72%. *Note:* Following a smaller scale reaction by NMR showed that all of **21** is aromatized after 2 hours.

3H-PNV/BC-PPV Block Copolymer Precursor (16). Reacted 67.7 mg **1**, 3.7 mg **4**, 7.8 μL HFB, 20 μL THF in 0.5 g C_6D_6 for 21 hours. Then added 67.2 mg **15** dissolved in 10 drops C_6D_6 and reacted for 36 hours. Yield = 95%. ^1H NMR (C_6D_6 , all peaks were broad): δ 7.14 (3H), 6.09, 5.89, 5.66, 5.58, 5.41 (8H), 4.65, 4.31, 3.93, 3.75

(4H), 2.57 (2H), 1.37, 1.29 (36H), 0.93 (3H). FTIR (film on NaCl): 3005, 2925, 2853, 1721, 1715, 1673, 1635, 1499, 1456, 1392, 1368, 1351, 1273, 1256, 1155, 1085, 1060, 1033, 966, 848, 820, 757, 667 cm^{-1} . GPC (CH_2Cl_2): 1st block Mn = 76900, Mw = 155800, PDI = 2.03; 2nd block Mn = 165800, Mw = 252100, PDI = 1.52.

3H-PNV/BC-PPV Block Copolymer (22). Reacted 39.5 mg **16** with 30.3 mg DDQ in 8 mL dichloromethane for 5 hours at rt. ^1H NMR shows broad peaks characteristic of both homopolymers. Yield = 96% UV/Vis (chloroform): $\lambda_{\text{max}} = 248$, 398, 434 nm. Emission spectrum (chloroform, $\lambda_{\text{ex}} = 420$ nm): $\lambda_{\text{max}} = 476$ (peak), 504 (shoulder) nm; (Film, $\lambda_{\text{ex}} = 449$ nm): $\lambda_{\text{max}} = 597$ nm; (Film, $\lambda_{\text{ex}} = 480$ nm): $\lambda_{\text{max}} = 592$ nm; Φ (solution, $\lambda_{\text{ex}} = 406$ nm) = 25%. FTIR (film on NaCl, 90% aromatized): 2975, 2925, 2853, 1721, 1715, 1634, 1455, 1414, 1392, 1368, 1276, 1255, 1151, 1119, 959, 845, 824, 748 cm^{-1} .

3H-PNV/BC-PPV Random Copolymer Precursor (19). Reacted 67.1 mg **1**, 66.2 mg **15**, 3.6 mg **4**, 7.8 μL HFB and 20 μL THF in 0.5 g C_6D_6 for 18 hours. Yield = 90%. ^1H NMR (C_6D_6 , all peaks were broad): δ 7.09 (3H), 6.12, 5.85, 5.53 (8H), 4.61, 4.38, 3.91, 3.74 (4H), 2.57 (2H), 1.64, 1.56, 1.29 (36H), 0.90 (3H). FTIR (film on NaCl): 3412, 3006, 2978, 2925, 2853, 1722, 1714, 1673, 1636, 1499, 1456, 1393, 1369, 1351, 1285, 1256, 1216, 1154, 1086, 1061, 1033, 966, 846, 757, 667 cm^{-1} . GPC (CH_2Cl_2): Mn = 208800, Mw = 388900, PDI = 1.86.

3H-PNV/BC-PPV Random Copolymer (23). Reacted 41.5 mg **19** with 28.6 mg DDQ in 8 mL dichloromethane for 5 hours at rt. ^1H NMR shows broad peaks characteristic of both homopolymers. Yield = 95% UV/Vis (chloroform): $\lambda_{\text{max}} = 248$, 428 nm. Emission spectrum (chloroform, $\lambda_{\text{ex}} = 420$ nm): $\lambda_{\text{max}} = 528$ nm; (Film, $\lambda_{\text{ex}} = 406$ nm): $\lambda_{\text{max}} = 562$ nm; (chloroform, $\lambda_{\text{ex}} = 440$ nm): $\lambda_{\text{max}} = 529$ nm; (Film, $\lambda_{\text{ex}} = 480$ nm): $\lambda_{\text{max}} = 573$ nm; Φ (solution, $\lambda_{\text{ex}} = 426$ nm) = 4.3%. FTIR (film on NaCl, 90% aromatized): 2977, 2925, 2854, 1722, 1715, 1634, 1621, 1470, 1455, 1416, 1392, 1368, 1286, 1256, 1150, 1118, 955, 846, 825, 757, 722, 668 cm^{-1} .

BTF-PPV Precursor Polymer (25). Reacted 487.8 mg **17**, 63.8 mg **4**, 129 μ L HFB, in 0.6 g C₆H₆ for 3 hours. The polymer did not completely precipitate in methanol, so it was purified by eluting it through a plug of silica gel using dichloromethane. The dried product recovered was a white solid. Yield = 50%. ¹H NMR (CDCl₃, all peaks were broad): δ 5.71 (2H), 5.30 (2H), 3.75 (2H). FTIR (KBr pellet): 3049, 2965, 2929, 1646, 1300-1100, 1077, 1019, 965, 918, 776, 738, 700, 660, 605, 535, 479 cm⁻¹. GPC data (CH₂Cl₂): Mn = 29600, Mw = 31700, PDI = 1.07.

BTF-PPV (28). Reacted 20.7 mg **25** with 19.8 mg DDQ in 1.2 mL C₆D₆Br overnight at 120 °C. Yield = 95%. ¹H NMR (C₆D₅Br): broad peaks were observed at δ 7.6-6.6. FTIR (KBr pellet): 3049, 2968, 1475, 1421, 1383, 1300-1100, 1073, 1022, 971, 932, 872, 842, 764, 741, 695, 670, 659, 603, 563, 527, 480 cm⁻¹. UV/Vis (chloroform): $\lambda_{\text{max}} = 308$ nm. Emission spectrum (chloroform, $\lambda_{\text{ex}} = 345$ nm): $\lambda_{\text{max}} = 449$ nm; (Film, $\lambda_{\text{ex}} = 345$ nm): $\lambda_{\text{max}} = 458$ nm; Φ (solution, $\lambda_{\text{ex}} = 345$ nm) = 20%.

3Cl-PNV Precursor Polymer (9). Reacted 84.4 mg **3**, 3.7 mg **4**, 7.8 μ L HFB, in 0.6 g C₆D₆ overnight. Yield = quantitative ¹H NMR (C₆D₆, all peaks were broad): δ 6.02 (2H), 5.65 (2H), 4.37 (2H), 3.03 (2H), 1.62, 1.29 (12H), 0.93 (3H). ¹³C NMR (CDCl₃) δ 139.0, 135.2, 133.3, 132.1, 131.6 (m), 128.3 (m), 43.0 (m), 33.3 (br s), 31.9, 29.7 (br s), 29.4, 27.9 (br s), 22.7, 14.1. FTIR (film on NaCl): 3035, 2952, 2925, 2854, 1463, 1392, 1379, 1288, 1270, 1170, 1105, 1066, 963, 918, 876, 759 cm⁻¹. GPC data (CH₂Cl₂): Mn = 15000, Mw = 16700, PDI = 1.11.

3Cl-PNV (14). Reacted 21.2 mg **9** with 12.3 mg DDQ in 1.2 mL C₆D₆Br overnight. Yield = 96%. ¹H NMR (toluene-d₈): broad peaks were observed at δ 7.8-6.6, 1.8-0.8 with peaks at δ 1.3, 0.93. FTIR (KBr pellet): 3041, 2934, 2852, 1553, 1458, 1376, 1354, 1322, 1261, 1236, 1104, 980, 838, 788, 759, 721, 683, 667, 559 cm⁻¹. UV/Vis (chloroform): $\lambda_{\text{max}} = 437$ nm. Emission spectrum (chloroform, $\lambda_{\text{ex}} = 430$ nm): $\lambda_{\text{max}} = 569$ nm; (Film, $\lambda_{\text{ex}} = 430$ nm): $\lambda_{\text{max}} = 570$ nm; Φ (solution, $\lambda_{\text{ex}} = 430$ nm) = 14%.

3Cl-PNV/BTF-PPV Block Copolymer Precursor (18). Reacted 83.9 mg **3**, 6.8 mg **4**, 15.6 μ L HFB, in 0.6 g C₆D₆ for 5 hours. Then added 58.6 mg **17** dissolved in 10 drops C₆D₆ and reacted for 8 hours. Yield = quantitative. ¹H NMR (C₆D₆, all peaks were broad): δ 6.00, 5.44, 5.29 (8H), 4.36 (2H), 3.54 (2H), 3.03 (2H), 1.60, 1.30 (12H), 0.94 (3H). FTIR (film on NaCl): 3035, 2952, 2926, 2855, 1645, 1464, 1392, 1277, 1197, 1154, 1076, 1018, 965, 917, 760, 677, 660 cm⁻¹. GPC data (CH₂Cl₂): 1st block Mn = 8300, Mw = 9400, PDI = 1.14; 2nd block Mn = 15000, Mw = 17800, PDI = 1.18.

3Cl-PNV/BTF-PPV Block Copolymer (26). Reacted 21 mg **18** with 15.3 mg DDQ in 1.2 mL C₆D₆Br overnight. Yield = 93%. ¹H NMR (toluene-d₈): broad peaks were observed at δ 7.8-6.6, 1.8-0.8 with peaks at δ 1.3, 0.93. FTIR (KBr pellet): 3047, 2926, 2854, 1554, 1466, 1459, 1420, 1356, 1279, 1195, 1157, 1105, 981, 966, 931, 870, 839, 787, 759, 740, 696, 684, 668, 560 cm⁻¹. UV/Vis (chloroform): $\lambda_{\text{max}} = 435$ nm. Emission spectrum (chloroform, $\lambda_{\text{ex}} = 430$ nm): $\lambda_{\text{max}} = 565$ nm; (Film, $\lambda_{\text{ex}} = 430$ nm): $\lambda_{\text{max}} = 570$ nm; (chloroform, $\lambda_{\text{ex}} = 345$ nm): $\lambda_{\text{max}} = 563$ nm; (Film, $\lambda_{\text{ex}} = 345$ nm): $\lambda_{\text{max}} = 567$ nm; Φ (solution, $\lambda_{\text{ex}} = 430$ nm) = 15%.

3Cl-PNV/BTF-PPV Random Copolymer Precursor (20). Reacted 51 mg **3**, 33.5 mg **17**, 4.6 mg **4**, 9.3 μ L HFB, in 0.6 g C₆D₆ for 10 hours. Yield = quantitative. ¹H NMR (C₆D₆, all peaks were broad): δ 5.87, 5.43, 5.29 (8H), 4.32 (2H), 3.56 (2H), 3.00 (2H), 1.60, 1.29 (12H), 0.94 (3H). FTIR (film on NaCl): 3039, 2956, 2927, 2856, 1644, 1463, 1392, 1278, 1195, 1155, 1129, 1073, 1017, 965, 921, 878, 760, 671, 660 cm⁻¹. GPC data (CH₂Cl₂): Mn = 17000, Mw = 21900, PDI = 1.26.

3Cl-PNV/BTF-PPV Random Copolymer (27). Reacted 21 mg **20** with 15.2 mg DDQ in 1.2 mL C₆D₆Br overnight. Yield = 94%. ¹H NMR (toluene-d₈): broad peaks were observed at δ 7.8-6.6, 1.8-0.8 with peaks at δ 1.3, 0.95. FTIR (KBr pellet): 3044, 2926, 2855, 1625, 1554, 1467, 1415, 1378, 1355, 1278, 1196, 1159, 1104, 981, 930, 840, 760, 742, 696, 669, 559 cm⁻¹. UV/Vis (chloroform): $\lambda_{\text{max}} = 424$ nm. Emission spectrum (chloroform, $\lambda_{\text{ex}} = 430$ nm): $\lambda_{\text{max}} = 556$ nm; (Film, $\lambda_{\text{ex}} = 430$ nm): $\lambda_{\text{max}} =$

562 nm; (chloroform, $\lambda_{\text{ex}} = 345$ nm): $\lambda_{\text{max}} = 553$ nm; (Film, $\lambda_{\text{ex}} = 345$ nm): $\lambda_{\text{max}} = 561$ nm; Φ (solution, $\lambda_{\text{ex}} = 430$ nm) = 26%.

References and Notes

- (1) Burroughs, J. H.; Bradley, D. D. C.; Brown, A. R.; Marks, R. N.; Mackay, K.; Friend, R. H.; Burns, P. L.; Holmes, A. B. *Nature* **1990**, *347*, 539.
- (2) Bakhshi, A. K.; Liegener, C. M.; Ladik, J.; Seel, M. *Synth. Met.* **1989**, *30*, 79.
- (3) Meyers, F.; Heeger, A. J.; Brédas, J. L. *J. Chem. Phys.* **1992**, *97*, 2750.
- (4) Meyers, F.; Heeger, A. J.; Brédas, J. L. *Synth. Met.* **1993**, *55-57*, 4308.
- (5) Musso, G. F.; Dellepiane, G.; Cuniberti, C.; Rui, M.; Borghesi, A. *Synth. Met.* **1995**, *72*, 209.
- (6) Santos, D. A. d.; Quattrochi, C.; Friend, R. H.; Brédas, J. L. *J. Chem. Phys.* **1994**, *100*, 3301.
- (7) Seel, M.; Liegener, C. M.; Förner, W.; Ladik, J. *Phys. Rev. B* **1988**, *37*, 956.
- (8) Ruckh, R.; Sigmund, E.; Kollmar, C.; Sixl, H. *J. Chem. Phys.* **1986**, *85*, 2797.
- (9) Wang, C.; Shieh, S.; LeGoff, E.; Kanatzidis, M. G. *Macromolecules* **1996**, *29*, 3147.
- (10) Wagaman, M. W.; Grubbs, R. H. *Synth. Met.* **1997**, *84*, 327.
- (11) Wagaman, M. W.; Bellmann, E.; Grubbs, R. H. *Phil. Trans. R. Soc. Lond. A* **1997**, *355*, 727.
- (12) Jenekhe, S. A.; Chen, W. C. *Mat. Res. Symp. Proc.* **1990**, *173*, 589.
- (13) Chen, X. L.; Jenekhe, S. A. *Appl. Phys. Lett.* **1997**, *70*, 487.
- (14) Chen, X. L.; Jenekhe, S. A. *Synth. Met.* **1997**, *85*, 1431.
- (15) Chen, X. L.; Jenekhe, S. A. *Macromolecules* **1996**, *29*, 6189.
- (16) Burn, P. L.; Holmes, A. B.; Kraft, A.; Bradley, D. D. C.; Brown, A. R.; Friend, R. H. *J. Chem. Soc., Chem. Commun.* **1992**, 32.
- (17) Burn, P. L.; Holmes, A. B.; Kraft, A.; Bradley, D. D. C.; Brown, A. R.; Friend, R. H.; Gymer, R. W. *Nature* **1992**, *356*, 47.
- (18) Brouwer, H. J.; Hilberer, A.; Krasnikov, V. V.; Werts, M.; Wildeman, J.;

Hadzioannou, G. *Synth. Met.* **1997**, *84*, 881.

(19) Kanoaka, S.; Grubbs, R. H. *Macromolecules* **1995**, *28*, 4707.

(20) Komiya, Z.; Schrock, R. R. *Macromolecules* **1993**, *26*, 1387.

(21) Lynn, D. M.; Kanaoka, S.; Grubbs, R. H. *J. Am. Chem. Soc.* **1996**, *118*, 784.

(22) Maughon, B. R.; Weck, M.; Mohr, B.; Grubbs, R. H. *Macromolecules* **1997**, *30*, 257.

(23) Nomura, K.; Schrock, R. R. *Macromolecules* **1996**, *29*, 540.

(24) Risse, W.; Grubbs, R. H. *J. Mol. Cat.* **1991**, *65*, 211.

(25) Watkins, D. M.; Fox, M. A. *Macromolecules* **1995**, *28*, 4939.

(26) Weck, M.; Schwab, P.; Grubbs, R. H. *Macromolecules* **1996**, *29*, 1789.

(27) Wu, Z.; Grubbs, R. H. *Macromolecules* **1994**, *27*, 6700.

(28) Saunders, R. S.; Cohen, R. E.; Schrock, R. R. *Macromolecules* **1991**, *24*, 5599.

(29) Gorman, C. B.; Ginsburg, E. J.; Grubbs, R. H. *J. Am. Chem. Soc.* **1993**, *115*, 1397.

(30) Klavetter, F. L.; Grubbs, R. H. *J. Am. Chem. Soc.* **1988**, *110*, 7807.

(31) Bott, D. C.; Brown, C. S.; Chai, C. K.; Walker, N. S.; Feast, W. J.; Foot, P. J. S.; Calvert, P. D.; Billingham, N. C.; Friend, R. H. *Synth. Met.* **1986**, *14*, 245.

(32) Conticello, V. P.; Gin, D. L.; Grubbs, R. H. *J. Am. Chem. Soc.* **1992**, *114*, 9708.

(33) Edwards, J. H.; Feast, W. J. *Polymer* **1980**, *21*, 595.

(34) Edwards, J. H.; Feast, W. J.; Bott, D. C. *Polymer* **1984**, *25*, 395.

(35) Pu, L.; Wagaman, M. W.; Grubbs, R. H. *Macromolecules* **1996**, *29*, 1138.

(36) Wagaman, M. W.; Grubbs, R. H. *Macromolecules* **1997**, *30*, 3978.

(37) Also see: Krasovitskii, B. M.; Bolotin, B. M. *Organic Luminescent Materials*; VCH: Weinheim, 1988; Ch 3.

(38) When measured by other methods, the emission wavelengths for polymers **10** and **22** are similar to those shown, but the spectra are smooth and unstructured.^{39,45} (Also see: Tasch, S.; Grapner, W.; Leising, G.; Pu, L.; Wagaman, M. W.; Grubbs, R. H. *Adv. Mater.* **1995**, *11*, 903. and Chapter 6) The spectra shown were

measured using a spectrofluorometer intended for solutions, and non-uniform reflection may have caused the structure shown.

- (39) Shaheen, S.; Peyghambarian, N., personal communication.
- (40) Braun, D.; Staring, E. G. J.; Demandt, R. C. J. E.; Rikken, G. L. J.; Kessener, Y. A. R. R.; Venhuizen, A. H. J. *Synth. Met.* **1994**, *66*, 75.
- (41) Cornil, J.; Brédas, J. L., personal communication.
- (42) Fox, H. H.; Lee, J. K.; Park, L. Y.; Schrock, R. R. *Organometallics* **1993**, *12*, 759.
- (43) Juris, A.; Balzani, V.; Barigelletti, F.; Campagna, S.; Belser, P.; Zelewsky, A. V. *Coord. Chem. Rev.* **1988**, *84*, 85.
- (44) Nakamaru, K. *Bull. Chem. Soc. Jpn.* **1982**, *55*, 2697.
- (45) deMello, J. C.; Wittmann, H. F.; Friend, R. H. *Adv. Mater.* **1997**, *9*, 230.

Chapter 6

Electroluminescence Results

Electroluminescence measurements were carried out by Günther Leising's group at the Technische Universität Graz in Austria (Part 1) and by Nasser Peyghambarian's group at the University of Arizona (Part 2). For the studies in Part 1, which were published in Advanced Materials (Vol. 7, p. 903; Vol. 8, p. 125), I supplied the undecyl substituted PNV. I got to have more involvement in the second set of studies, which are presented in Part 2, since traveling to Arizona was more convenient. While my major contribution to this work was devising syntheses of the polymers and supplying these materials to Sean Shaheen, who carried out device fabrication and characterization, I also had the opportunity to spend a week in the lab with Sean. Through this experience, I learned a lot about the fabrication and characterization of LEDs, got to have a more active role in deciding what devices would be interesting to study, and hopefully made some helpful suggestions for handling the polymers I had prepared.

Abstract: In Part 1, the results of studies of the absorbance (IR, UV/vis) and emission (photoluminescence and electroluminescence) properties of hexyl and undecyl substituted poly(1,4-naphthalenevinylene)s are presented. Using aluminum as the air stable, medium work function electrode, internal electroluminescence quantum efficiencies, η_F , up to 0.05% and external electroluminescence quantum efficiencies, η_{ext} , up to 0.008% were measured.

In Part 2, electroluminescence studies using undecyl substituted PNV, and two soluble, substituted derivatives of PPV are described. Devices employing alkylated PNV as the emissive layer were found to exhibit higher external electroluminescence quantum efficiencies ($\eta_{ext} = 0.12\%$) when an electron transporting layer was added between the layer of PNV and the electron injection electrode, which was magnesium. Conversely, devices using diester substituted PPV were found to operate more efficiently when a hole transporting layer was added between the layer of PPV and the ITO anode, which serves as the hole injection electrode ($\eta_{ext} = 0.2\%$). Studies of a bisperfluoroalkyl substituted PPV showed that this material, which is soluble in fluorinated solvents, exhibits blue electroluminescence ($\eta_{ext} = 0.005\%$).

Part 1: Red-Orange Electroluminescence with New Soluble and Air Stable Poly(naphthalenevinylene)s

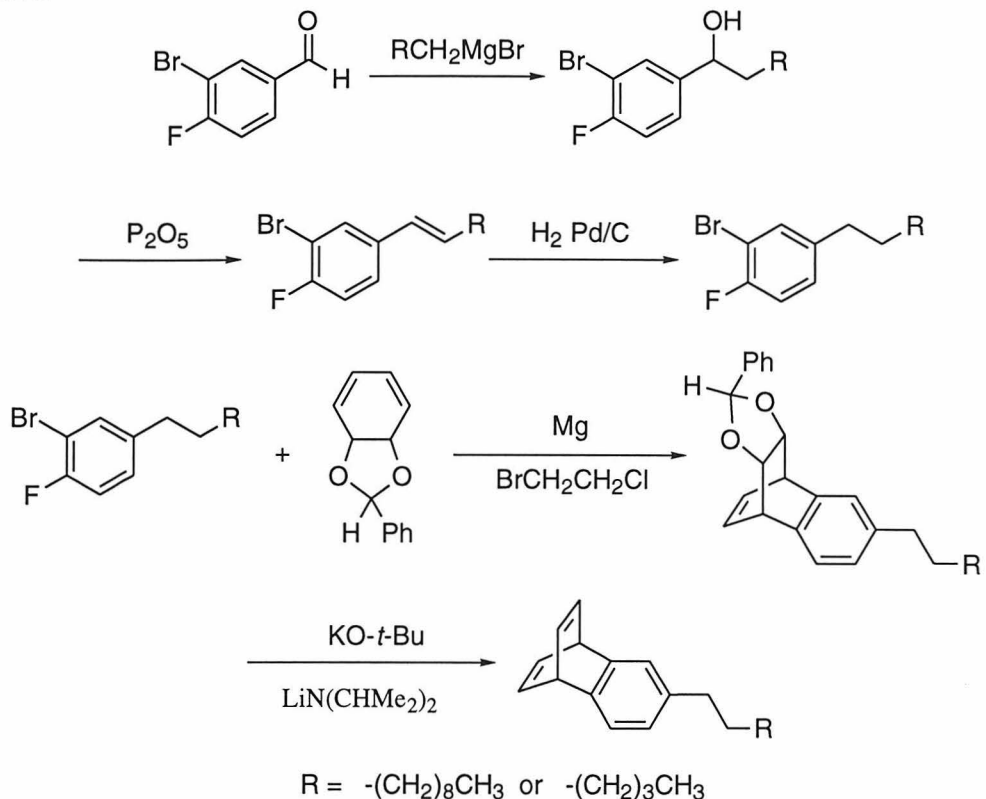
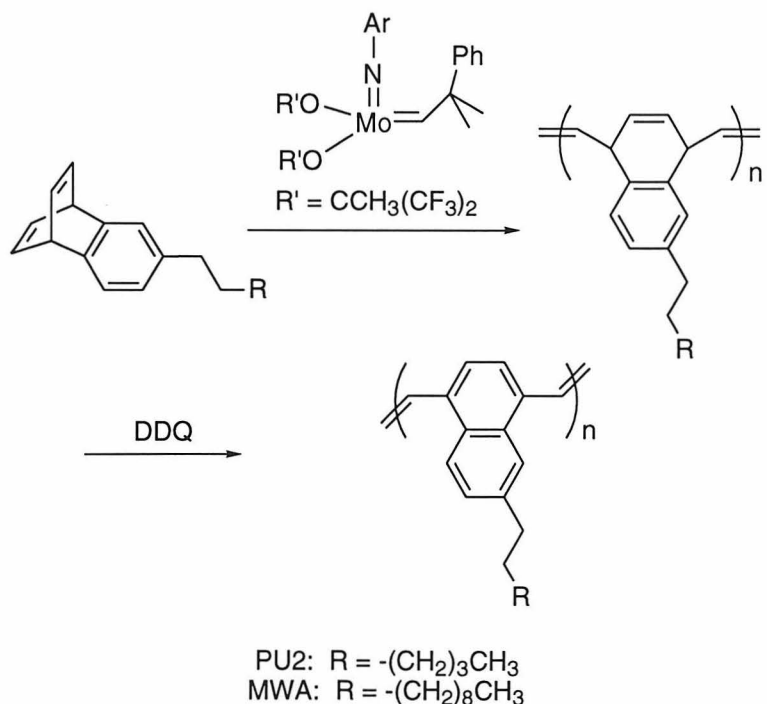
Introduction

The application of conjugated polymers as processable active layers in electroluminescence (EL) devices¹ stimulated many groups worldwide to work on synthesizing suitable polymers and on fabricating and characterizing light-emitting diodes (LEDs) based on these polymers.^{2,3} Conjugated polymers are especially attractive for use as active layers in LEDs because the polymer properties, including solubility and emission spectra, can be altered to improve processing or to achieve the desired emission wavelength. The most common polymers used as active layers are poly(*para*-phenylenevinylene), PPV,¹ poly(*para*-phenylene), PPP,⁴ poly(alkylfluorene)⁵ and poly(alkylthiophene).^{6,7}

In this paper we report the optical properties of new soluble derivatives of poly(1,4-naphthalenevinylene) (PNV) with different alkyl substituents, studied using UV/vis absorption and steady state photoluminescence (PL). We also comment on the application of this polymer in EL-devices. The EL-devices prepared with these polymers showed a high external quantum efficiency compared to other devices with similar configurations.⁸⁻¹⁰

Results and Discussion

The synthesis of the fully conjugated polymers was accomplished through a precursor route, as described in the literature.¹¹ The monomers were synthesized by the route shown in Scheme 1. As shown in Scheme 2, the benzobarrelene monomers were then polymerized by ring-opening metathesis polymerization (ROMP) to yield the well-defined, soluble precursor polymers, which were then chemically oxidized to yield the polymers used in these studies.

Scheme 1**Scheme 2**

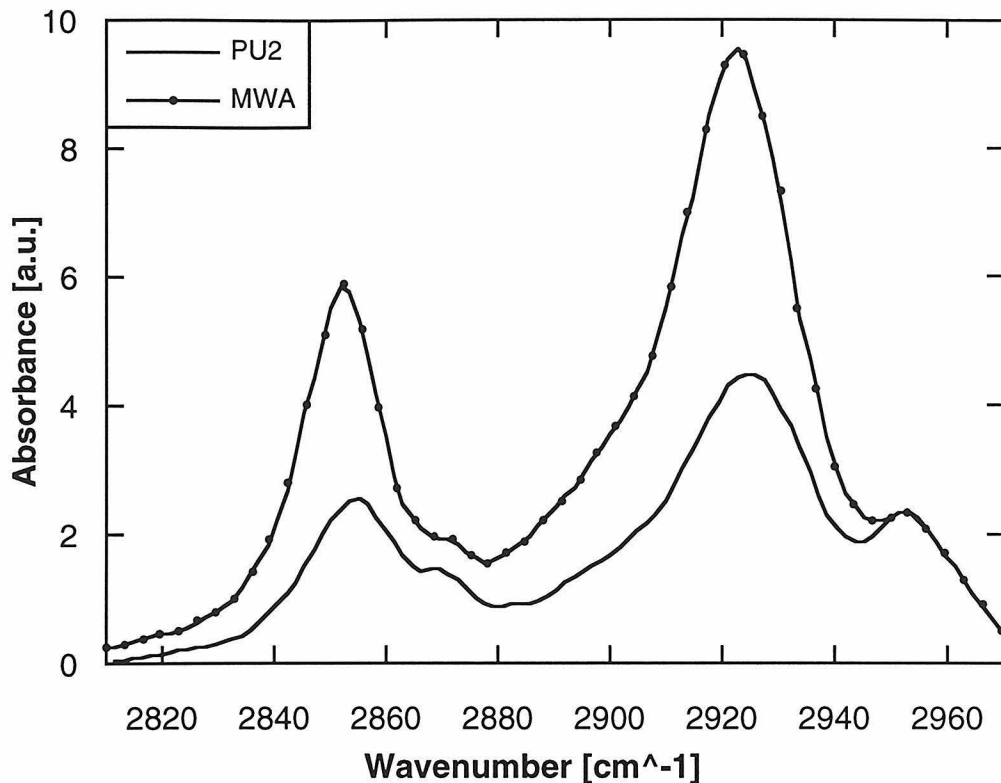
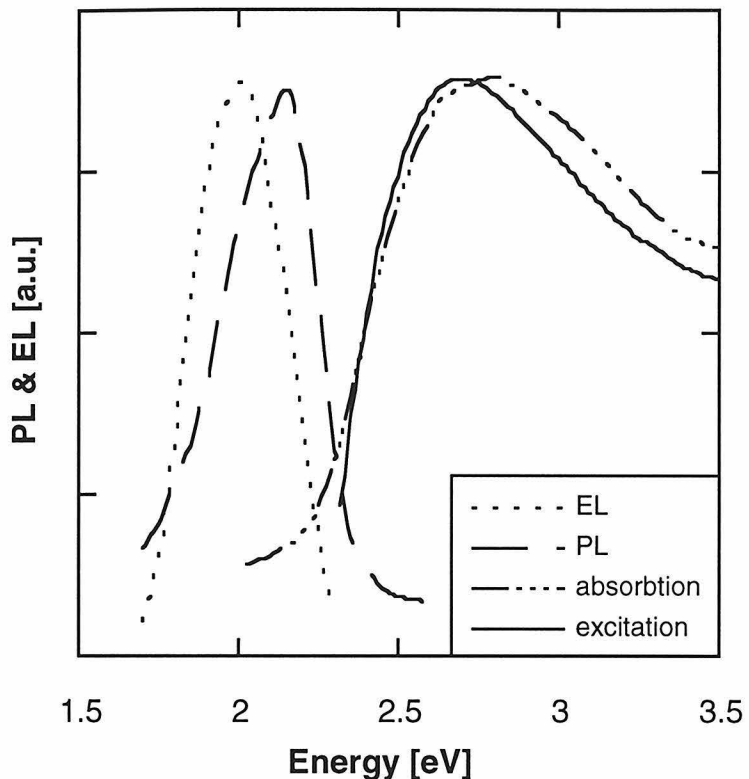


Figure 1. Infrared absorption spectra of MWA and PU2.

PU2 (Scheme 2) was shown by ^1H NMR to be fully oxidized, as revealed by the shift of all of its olefinic protons to the aromatic region of the spectrum. However, MWA (Scheme 2), which was intentionally oxidized to 95% to further improve its solubility, still showed 5% of its protons in the olefinic region after oxidation. The results of gel-permeation chromatography (GPC), performed on solutions of the polymers in dichloromethane (CH_2Cl_2), are summarized in Table 1. The structure and purity of these polymers were further demonstrated by IR spectroscopy. The relative alkyl chain length was confirmed by comparing the intensity (Fig. 1) of the vibrations of the CH_2 -units (at 2851 cm^{-1} and 2922 cm^{-1}) by normalizing on the intensity of the CH_3 stretch (2951 cm^{-1}) of the end groups.

Table 1. Molecular Weights.

	M_n	M_w	M_n/M_w
PU2	2,000	5,000	2.48
MWA	9,900	47,100	4.76

**Figure 2.** EL, PL, excitation and absorption spectra of a PU2 film.

The absorption edge due to the onset of the $\pi - \pi^*$ electronic transition is observed around 2.3 eV (in solution) for both polymers.¹³ The peaks of the absorption spectra in dichlorobenzene solution are found at 2.72 eV and at 2.83 eV for chloroform solutions. The difference in these values is caused by the difference in the dielectric constants of chloroform ($\epsilon_{\text{chloroform}} = 4.806$) and dichlorobenzene ($\epsilon_{\text{dichlorobenzene}} = 2.708$).¹⁴ In the solid state, the absorption peak for both polymers is between 2.7 and 2.8 eV independent of the substrate, film thickness and solvent used for casting the film, while the absorption edge is located at 2.1 eV. Such a reduction of the band gap going from solution to solid

state is usually observed for conjugated polymers and is believed to be due to an increase of intrachain order in the solid state.¹⁵

A few other observations concerning the absorbance spectra should be added: First, the shape of the absorption peak is rather broad and does not show any vibrational splitting similar to that observed for PPP. Second, both the absorption edge and the absorption maxima are slightly red shifted, versus PPV¹⁰ and its alkyl substituted derivatives,¹⁶ due to the electronic modification by the attached phenyl ring on the polymer leading to a reduced dimerization in the main chain.^{13,17} A comparable reduction of the bandgap was also observed for polyisothianaphthene, which is a derivative of polythiophene.^{18,19} Finally, after applying a correction which takes the optical thickness of the sample into account,²⁰ we observe a good overall agreement between the absorption spectrum and the excitation spectrum recorded at an emission wavelength of 580 nm (Fig. 2).

The emission spectra were taken using an excitation of wavelength of 450 nm and match perfectly for MWA and PU2. The peak of the emission spectrum is localized at 2.15 eV (Fig. 2) and its shape does not show vibrational splitting indicating that either photoexcitation does not planarize the neighboring intrachain naphthalenes or electronic disorder is smearing out the vibrational structure. This is in contrast to PPV and PPP where the chain segments carrying the photoexcited state are planarized and therefore the emission is structured. The significant Stokes shift (of about 0.6 eV) is comparable to that of standard PPV.¹⁰

To obtain the EL spectra, the devices were driven with about 6V forward bias. The maximum of the emitted homogeneous visible red-orange light ($\lambda_{\text{peak}} = 620$ nm, luminance ≈ 40 cd/m²) is red shifted compared to the PL spectrum. This shift can be attributed to the overlap between the EL and the absorption spectra causing self-absorption at the high energy side of the PL spectrum (Fig. 2) as observed for PPV.¹⁰

The environmental stability of the PNV is reflected in the shape of the PL and the

absorption spectra, which did not change by exposing the polymer to intense UV light and oxygen. As noted in Chapter 4, however, alkylated PNV does decompose after extended exposure to these conditions. In the EL devices, interface effects between the air-stable polymer and the metal electrodes reduces the lifetime of the devices to a few minutes under cw-operation.

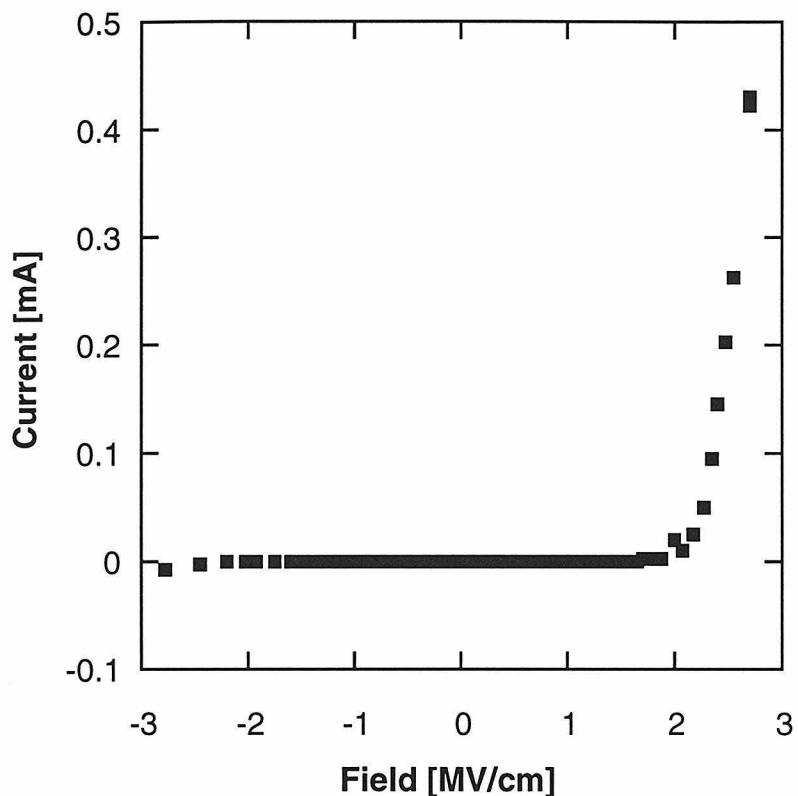


Figure 3. Current - bias (I - V) characteristic of an ITO/PU2/Al device ($d_{PU2} = 40$ nm).

Figure 3 shows a typical current vs. voltage plot characteristic of an ITO/PNV/Al device. The onset field for EL is around 2×10^6 V/cm independent of the film thickness and the rectification ratio at this field is about 500.

The external EL quantum efficiency η_{ext} versus the applied bias voltage for an ITO/PU2/Al device is shown in Figure 4. ($\eta_{ext,max} \approx 0.008\%$, — similar to ITO/MWA/Al devices.) The internal EL quantum efficiency, η_F (the ratio of the emitted photons to the injected charge), can be calculated from the measured η_{ext} .²¹ (n, the

refractive index of PNV ≈ 1.7 , Eq.1).

$$\eta_F = 2n^2 \eta_{ext} \quad (1)$$

Values for η_F up to 0.05% were obtained. Subsequently, the power efficiency, η_E , the ratio of the output light power to the input electric power, can be determined from η_F , using the known values of the applied voltage ($V \approx 6V$) and the average energy of the emitted photons ($E_p \approx 2 \text{ EV}$, Eq. 2).²²

$$\eta_E = \eta_F \frac{E_p}{V} \quad (2)$$

This calculation yielded values around 0.02% for η_E . The physical meaning of η_F can be interpreted using Equation 3,²² where γ is the double charge injection factor, η_R is the efficiency of singlet exciton formation, and Φ_F is the quantum efficiency of fluorescence.

$$\eta_F = \gamma \eta_R \Phi_F \quad (3)$$

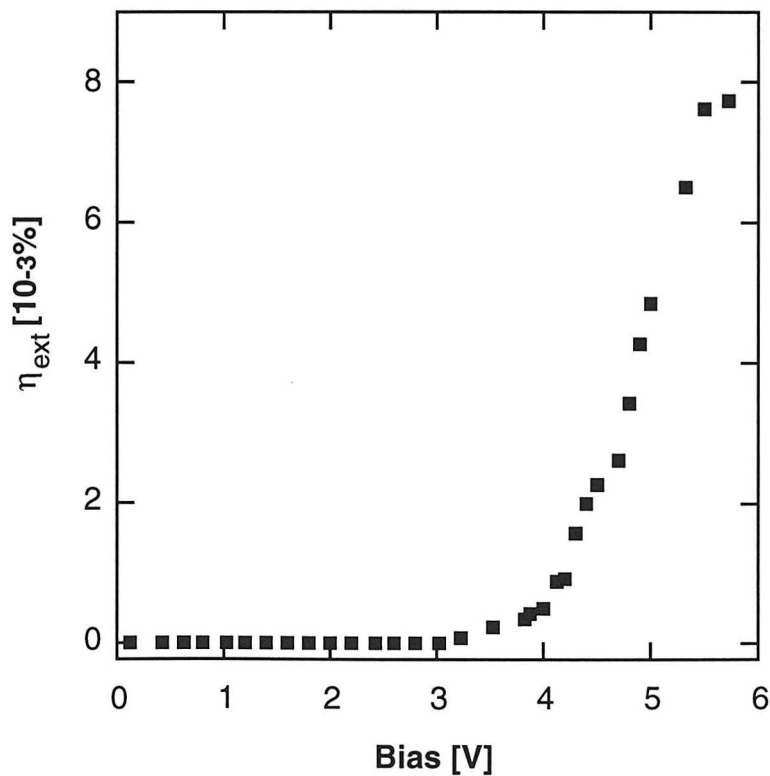


Figure 4. External EL quantum efficiency over the applied bias of an ITO/PU2/Al device.

Φ_F was determined in solution and in the solid state relative to the standard solution Rhodamine 101, which shows an absolute quantum yield of $\Phi_{RHO} \approx 100\%$ ²³ (for details of the measurement and the calculation, see the literature¹²). In solution we obtained values of about 2% for Φ_F .* This comparably low efficiency¹⁵ is attributed to the twisting of the naphthalenes around the polymer chains (resulting in two possible conformational isomers).²⁴ By incorporating the PNV into a rigid matrix, the twisting of the naphthalenes is hindered and we observe that Φ_F increases to more than 10% in PNV/polystyrene blends. In pure homopolymer films Φ_F is about 3%* which we attribute to the role of intermolecular quenching effects.

Although we obtain only moderate values for Φ_F compared to MEH-PPV (Φ_F up to 66% in solution), the value for η_F we obtained for PNV is as high as those reported by Heeger et al.⁹ for ITO/MEH-PPV/Al devices, and higher than those reported by Parker.⁸ Therefore, either balanced charge injection or singlet exciton formation, or both processes, must be more efficient than in MEH-PPV.

By further increasing the bias above 6V, the EL efficiency saturates (Fig. 4). A similar dependence of the efficiency on the current is also observed for EL devices with soluble PPV.²⁵ In order to understand this effect, one must consider how EL occurs. Under an applied bias, opposite charges are injected from the opposing contacts. In conjugated polymers with non-degenerate ground states, transport of these charges is performed by polarons or bipolarons. EL occurs when two polarons of different charge combine to form a singlet exciton, which may then decay radiatively to produce EL. When the applied field begins to pass over a threshold value, the number of polarons and, therefore, the η_F increases rapidly. However, by further increasing the applied field, the efficiency of singlet exciton formation, η_R , which is directly related to η_F , saturates for the following reasons:

- Positively charged polarons have a higher mobility than the negatively charged

polarons and, therefore, the active region is located close to the cathode (e.g., Al).

This high concentration of positive charges near the cathode causes quenching for several reasons.^{26,27,28} First, the probability of quenching near the electrode at defect sites is high. Since only positive polarons are transported efficiently through the emissive layer, as the field is increased, the number of positive polarons transported to the cathode increases, but the number of electrons available for exciton formation does not increase as significantly. Second, the probability of two positively charged polarons generating bipolarons, which do not contribute to EL, is higher when the polaron concentration is higher. Therefore, bipolaron formation leads to saturation at higher applied fields due to the increased concentration of polarons at these higher fields.

- Above a characteristic value of the applied field the current does not increase with the field, but is only controlled by an injection-limited current flow.²⁷
- Because of temperature effects due to the high driving power density (≈ 5000 W/cm³).

In addition to the decrease in η_R , the fluorescence efficiency will decrease under the increasing applied field due to an increasing probability of field-induced fission of singlet excitons.²⁹ Therefore, assuming that the double charge injection factor γ does not change significantly, η_F will not increase by increasing the field much over the threshold field, and saturation will be observed.

Conclusions

We have presented the optical and electronic properties of new soluble types of PNV, which have a well-defined chemical structure and little main-chain stiffness. We obtained photoluminescence quantum yield values of 3% for films of the homopolymers and more than 10% for PNV/polystyrene blends.* In EL devices, the air-stable and processable PNV acted as a red-orange light emitting layer ($\lambda_{\text{peak}} = 620$ nm) showing EL

power efficiencies, η_E , up to 0.02% and external quantum efficiencies, η_{ext} up to 0.008%.

Experimental

All optical measurements, which were done in air at room temperature, were performed on chloroform or dichlorobenzene solutions of the polymers and on films cast from these solutions, on NaCl or sapphire substrates. The experimental setups for UV/vis absorption and steady-state PL have been reported.¹²

The EL-device was fabricated as a sandwich structure ITO/PNV/Al. Indium tin oxide (ITO) layers on glass substrates, patterned by etching ITO from the glass with hydrochloric (HCl), acted as high work function ($\Phi \approx 4.8$ eV) hole injection contacts. After the substrate was thoroughly cleaned with alcohol, acetone and butanone in an ultrasonic bath, it was heat treated in air up to 400 °C to dry the surface and to increase the work function of the ITO. The work function of the ITO samples, which were treated in this way, exhibited stable values up to $\Phi \approx 5.1$ eV over a period of several weeks measured with a Kelvin capacitor. The polymer was cast on the ITO substrates from a dichlorobenzene solution forming homogeneous films. Before Al ($\Phi \approx 3.9$ eV) was evaporated as the top electrode at a pressure below 6×10^6 mbar, the polymer layer was heated to 110 °C to get rid of remaining solvent and to anneal the layer. The EL-quantum efficiency measurements were performed with an SSR 1140 and the EL spectra were taken with the same experimental setup as the PL spectra.

References and Notes

- * Later measurements by us, using a Ru(bipy)₃ standard, and by Sean Shaheen in Nasser Peyghambarian's group at the University of Arizona, using a Rhodamine 6G standard,³⁰ indicate that the quantum yield of the PNV studied here is $\approx 0.5\%$ in solutions and films. The originally reported values have been retained in this section since the numbers are useful for comparison purposes.
- (1) Burroughes, J.H.; Bradley, D. D. C.; Brown, A. R.; Marks, R. N.; Mackay, K.; Friend, R. H.; Burn, P. L.; Kraft, A.; Holmes, A. B. *Nature* **1990**, *347*, 539.
- (2) Bradley, D. D. C. *Adv. Mater.* **1992**, *4*, 756.
- (3) Conwell, E. M.; Stolka, H.; Miller, R. L. (Eds.) *Proc. SPIE* **1993**, 1910.
- (4) Grem, G.; Leditzky, G.; Ullrich, B.; Leising, G. *Adv. Mater.* **1992**, *4*, 36.
- (5) Ohmori, Y.; Uchida, M.; Muro, K.; Yoshino, K. *Jpn. Appl. Phys.* **1991**, *30*, L1941.
- (6) Dyreklev, P.; Berggren, M.; Inganäs, O.; Andersson, M. R.; Wennerström, O.; Hjertberg, T. *Adv. Mater.* **1995**, *1*, 43.
- (7) Braun, D.; Gustaffson, G.; McBranch, D.; Heeger, A. J. *J. Appl. Phys.* **1992**, *72*, 564.
- (8) Parker, I. D. *J. Appl. Phys.* **1994**, *75*, 1656.
- (9) Aratani, S.; Zhang, C.; Höger, S.; Wudl, F.; Heeger, A. J. *J. Electron. Mat.* **1993**, *22*, 745.
- (10) Holmes, A. B.; Bradley, D. D. C.; Brown, A. R.; Burn, P. L.; Burroughes, J. H.; Friend, R. H.; Greenham, N. C.; Gymer, R. W.; Halliday, D. A.; Jackson, R. W.; Kraft, A.; Martens, J. H. F.; Pichler, K.; Samuel, I. D. *Synth. Met.* **1993**, 55-57, 4031.
- (11) Pu, L.; Wagaman, M. W.; Grubbs, R. H. *Macromolecules* **1996**, *29*, 1138.
- (12) Stampfl, J.; Tasch, S.; Leising, G. *Synth. Met.* **1995**, *71*, 2125.
- (13) Onada, M.; Ohmori, Y.; Kawai, T.; Yoshino *Synth. Met.* **1995**, *71*, 2182.

(14) Bruno, T. J.; Svoronos, P. D. N. *CRC Handbook of Basic Tables for Chemical Analysis*; CRC Press: Baca Raton, FL, **1989**, 89.

(15) Gettinger, C. L.; Heeger, A. J.; Drake, J. M.; Pine, D. J. *J. Chem. Phys.* **1994**, *101*, 1673.

(16) Fahlman, M.; Lhost, O.; Meyers, F.; Bredas, J. L.; Graham, S. C.; Friend, R. H.; Burn, P. L. Holmes, A. B.; Kaeriyama, K.; Sonoda, Y.; Loglund, M.; Stafström, S.; Salaneck, W. R. *Synth. Met.* **1993**, *55-57*, 263.

(17) Antoun, S.; Gagnon, D. R.; Karasz, F. E.; Lenz, R. W. *Polym. Bull.* **1986**, *15*, 181.

(18) Wudl, F.; Kobayashi, M.; Heeger, A. J. *J. Org. Chem.* **1984**, *49*, 3382.

(19) Kurti, J.; Surjan, P. R. *Electronic Properties of Conjugated Polymers III*; Springer Series in Solid-State Science, **1991**, 69.

(20) Lakowicz, J. L. *Principles of Fluorescence Spectroscopy*, Plenum Press, New York **1983**.

(21) Greenham, N. C.; Friend, R. H.; Bradley, D. C. *Adv. Mat.* **1994**, *6*, 491.

(22) Tsutsui, T.; Saito, S. *NATO Asi Series* **1993**, 246 .

(23) Karsten, T.; Kobs, K. *J. Phys. Chem.* **1980**, *84* , 1871.

(24) Krasovitskii, B. M.; Bolotin, B. M. *Organic Luminescence Materials*, VCH, Weinheim **1988**, Ch. 3.

(25) Zhang, C.; Höger, S.; Pakbaz, K.; Wudl, F.; Heeger, A. J. *J. Electron. Mater.* **1993**, *22*, 413.

(26) Brown, A. R.; Bradley, D. D.; Burroughes, J. H.; Friend, R. H.; Greenham, N. C.; Burn, P. L.; Holmes, A. B.; Kraft, A. *Appl. Phys. Lett.* **1992**, *61*, 2793.

(27) Vestweber, H.; Sander, R.; Greiner, A.; Heitz, W.; Mahrt, R. F.; Bässler, H. *Synth. Met.* **1992**, *62*, 141.

(28) Swanson, L. S.; Shinar, J.; Brown, A. R.; Bradley, D. D. C; Friend, R. H.; Burn, P. L.; Kraft, A.; Holmes, A. B. *Phys. Rev. B* **1992**, *46*, 15072.

(29) Kersting, R.; Lemmer, U.; Bakker, H. J.; Mahrt, R. F.; Kurz, H.; Arkhipov, V. I.;

Bässler, H.; Göbel, E. O. *Phys. Rev. Lett.* **1994**, *73*, 1440.

(30) deMello, J. C.; Wittmann, H. F.; Friend, R. H. *Adv. Mater.* **1997**, *9*, 230.

Part 2: Electroluminescence of Alkylated PNV and Substituted PPVs

Introduction

In addition to the studies of alkylated PNV, **1**, presented in Part 1, electroluminescence measurements were carried out on this polymer under different conditions and on the two other polymers shown in Figure 1. More extensive studies of **1** were desired since the single layer device originally fabricated had low efficiency. Electroluminescence studies of **2** and **3** were of interest because these are new luminescent conjugated polymers. Therefore, characterization of their ability to exhibit electroluminescence and their compatibility with the LED fabrication process is important for determining whether these materials will be useful for making electroluminescent devices.

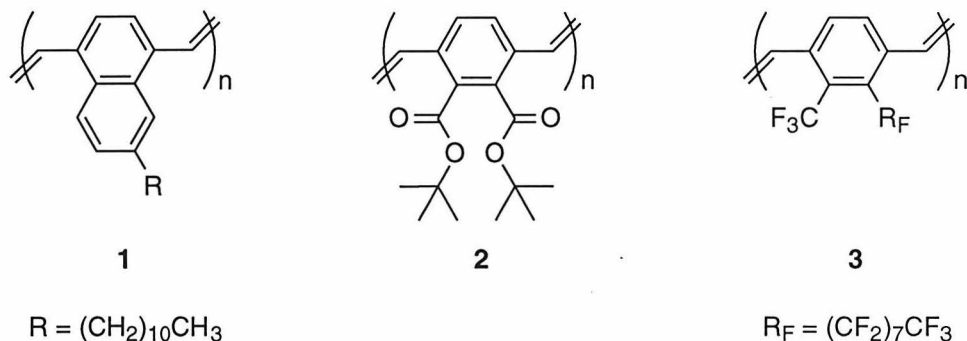


Figure 1. Conjugated polymers studied.

Results and Discussion

Study of Undecyl Substituted PNV, 1. Based on the fact that PPV is a hole conductor but a poor electron conductor,¹ it seemed likely that **1** would also be a hole conductor, but that injection of electrons into this material may have limited the efficiency of the devices studied in Part 1. Therefore, devices were prepared with a layer of aluminum trisquinolate, **4**, between **1** and the LED cathode, which is the electron injection electrode. Complex **4**, shown in Figure 2, is known to allow efficient injection

of electrons, but does not readily transport holes.²⁻⁴ Arranging such electron and hole transporting materials in a two layer structure has been proposed to improve device performance for several reasons.^{2,3,5-9} First, since one material allows injection of holes and the other allows injection of electrons, both charge carriers are readily injected into

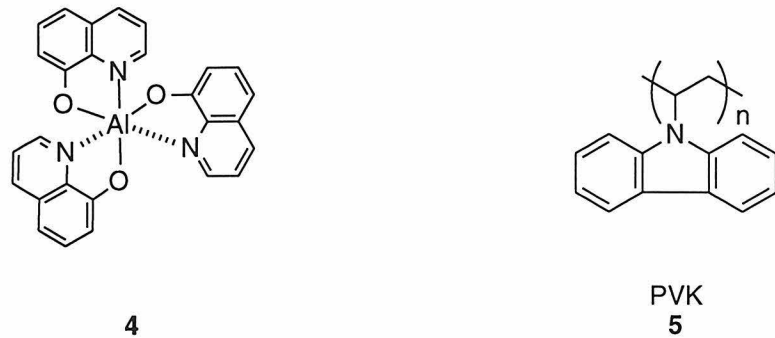


Figure 2. Materials used to improve electron, **4**, and hole, **5**, injection and transport.

the layers between the electrodes. With good injection of both polarons (electrons and holes) a higher number of each is present relative to devices employing emissive layers that only allow facile injection of one type of charge carrier. Consequently, pairing to form singlet excitons, which can then relax and emit light, is more likely in the two layer devices. An advantage of the two layer structure over simply mixing the electron and hole conductors arises from the fact that the layers typically transport only one type of polaron well and prevent migration of the opposite polaron. For example, holes that reach the layer of **4** will not readily migrate through this material and therefore are stopped at the interface of **1** and **4**. Similarly, electrons injected into **4** are stopped when they reach the layer of **1**. As a result, electrons can not readily reach the anode and holes can not readily reach the cathode, where they would be quenched. With both charge carriers essentially trapped at the interface of the two materials, the probability that they will pair with an oppositely charged polaron to form an exciton is increased. Therefore, the efficiency of a device with this structure is expected to increase relative to a single layer device. As shown by the data in Table 1, a rather dramatic increase in efficiency,

relative to the single layer device prepared with only **1**, was observed for the two layer device prepared with **1** and **4**. In addition to providing a more efficient device, this data shows that poor electron injection may have been the cause of the low efficiency of the devices studied in Part 1.

Table 1. Summary of electroluminescence results.^a

Device Structure ^b	Quantum Efficiency ^c	Max. Output (cd/m ²)
1 40 nm Ca 100 nm	0.005	60
1 40 nm 4 18 nm Mg 75 nm	0.12	340
2 50 nm Mg 100 nm	0.1	85
x- 5 ^d 40 nm 2 40 nm 4 15 nm Mg 100 nm	0.2	130
3 60 nm LiF 1.5 nm Mg 200 nm	0.005	5

a) Results are shown graphically as Figures 3 to 7 at the end of this chapter. b) ITO, which was used as the anode for all devices studied, is omitted. c) Reported as percent external quantum efficiency (photons emitted/electrons injected x 100). d) x-**5** is a crosslinked version of PVK, **5**.¹⁰

Study of Di-*t*-butylester Substituted PPV, **2.** In contrast to polymer **1**, polymer **2** was expected to allow better electron injection than hole injection. This expectation was based on the fact that **2** has electron withdrawing substituents and, therefore, the conjugated polymer backbone should be electron deficient. To improve hole injection into this material a hole transporting layer,^{4,11} **5**, was placed between the layer of **2** and the hole injecting electrode, ITO. To prevent washing the layer of **5** away when **2** was spin casted on top of it, **5** was crosslinked to yield an insoluble polymer, x-**5**.¹⁰ As shown in Table 2, the device prepared with this layer had better efficiency and more light output than a similar device without this hole transporting layer. The layer of **4** beside the cathode in this device was used to improve the stability of the device by preventing **2** from reacting with the cathode, but was not necessary for electron injection, as devices without it displayed similar efficiencies.¹²

Study of Trifluoromethylperfluorooctyl Substituted PPV, 3. Preliminary measurements have also been performed using **3** as the emissive layer. The results of this study, shown in Table 1, reveal that **3** does exhibit electroluminescence but the efficiency and light output were low in the device prepared. Light emitted from this device was observed to be blue, as is observed for photoluminescence from polymer **3**. The lithium fluoride layer next to the cathode in the device studied was necessary to obtain good adhesion of the magnesium, which does not adhere well when deposited directly onto **3**. As with polymer **2**, polymer **3**'s electron withdrawing groups are expected to cause **3** to be a better electron transporter and a poorer hole transporter. Therefore, devices made using this material should show better efficiency when a hole injection layer is added between the anode and **3**.

Conclusions

The data presented here shows that all of the materials studied exhibit electroluminescence and, therefore, may be useful for fabricating practical LED devices. In addition, it was found that placing an electron transporting layer between the emissive polymer layer and the cathode improved the efficiency and light output of devices employing polymer **1**. When polymer **2** was the emissive layer, the efficiency was improved when a hole transporting layer was placed between **2** and the anode. This information indicates that holes are more readily injected into and transported by polymer **1** and electrons are more readily injected into and transported by polymer **2**. Because of their complimentary charge injection and transport properties, copolymers of **1** and **2** have been prepared. Study of the photoluminescence spectra of films these copolymers, presented in Chapter 5, showed exciton transport into the smaller bandgap material. Electroluminescence studies of the random and block copolymer are currently in progress. Finally, electroluminescence studies of polymer **3**, which exhibits blue photoluminescence, have shown that this material also exhibits blue electroluminescence.

The efficiency of the device studied was low, but should be improved by adding a hole injection layer since **3**, which is substituted with electron withdrawing groups, is expected to transport electrons better than it transports holes.

Experimental

Device Fabrication. Indium tin oxide (ITO), obtained from the Donnelley Corporation, was cleaned by first ultrasonication in acetone and methanol. The material was then dried in a stream of nitrogen and plasma etched for 60 seconds. Thin films of the polymers were formed by spin casting solutions of the polymers on top of the ITO substrate. Solvents used were xylene (polymer **1**), dichloromethane (polymer **2**), and chloropentafluorobenzene (polymer **3**). To improve solubility of the polymers, the materials used were not completely aromatized. Percent aromatization was as follows: **1** - 95%, **2** - 80%, **3** - 75%. Following spin casting, the polymer layers were dried in a vacuum oven for 1 - 2 hours at 100 °C. Films of crosslinked polyvinylcarbazole (x-**5**) were prepared as previously reported.¹⁰ Aluminum trisquinolate, **4**, was thermally deposited onto the surface of the dried polymers at a rate of 2 - 3 Å/second. Lithium fluoride was thermally deposited onto the surface of the dried polymers at a rate of 0.5 Å/second. Magnesium and calcium cathodes were thermally deposited at a rate of ≈ 8 Å/second. The cathode materials were deposited through a shadow mask so that the resulting cathodes each had dimensions of 3 x 5 mm.

Current-voltage and light output measurements were obtained by driving the devices in forward bias (i.e., using ITO as the hole injection electrode and magnesium or calcium as the electron injection electrode). The absolute value for forward output power was measured by a silicon photodiode that had been calibrated using a NIST traceable integrating sphere (Labsphere).¹³ External quantum efficiencies, which were reported as photons emitted per electrons injected, were calculated by the equation: $\eta = P/(I * E)$ where P is the forward emission power, I is the current and E is the average energy per

photon. All device fabrication and characterization, except cleaning the ITO substrate, was carried out inside a nitrogen filled dry box.

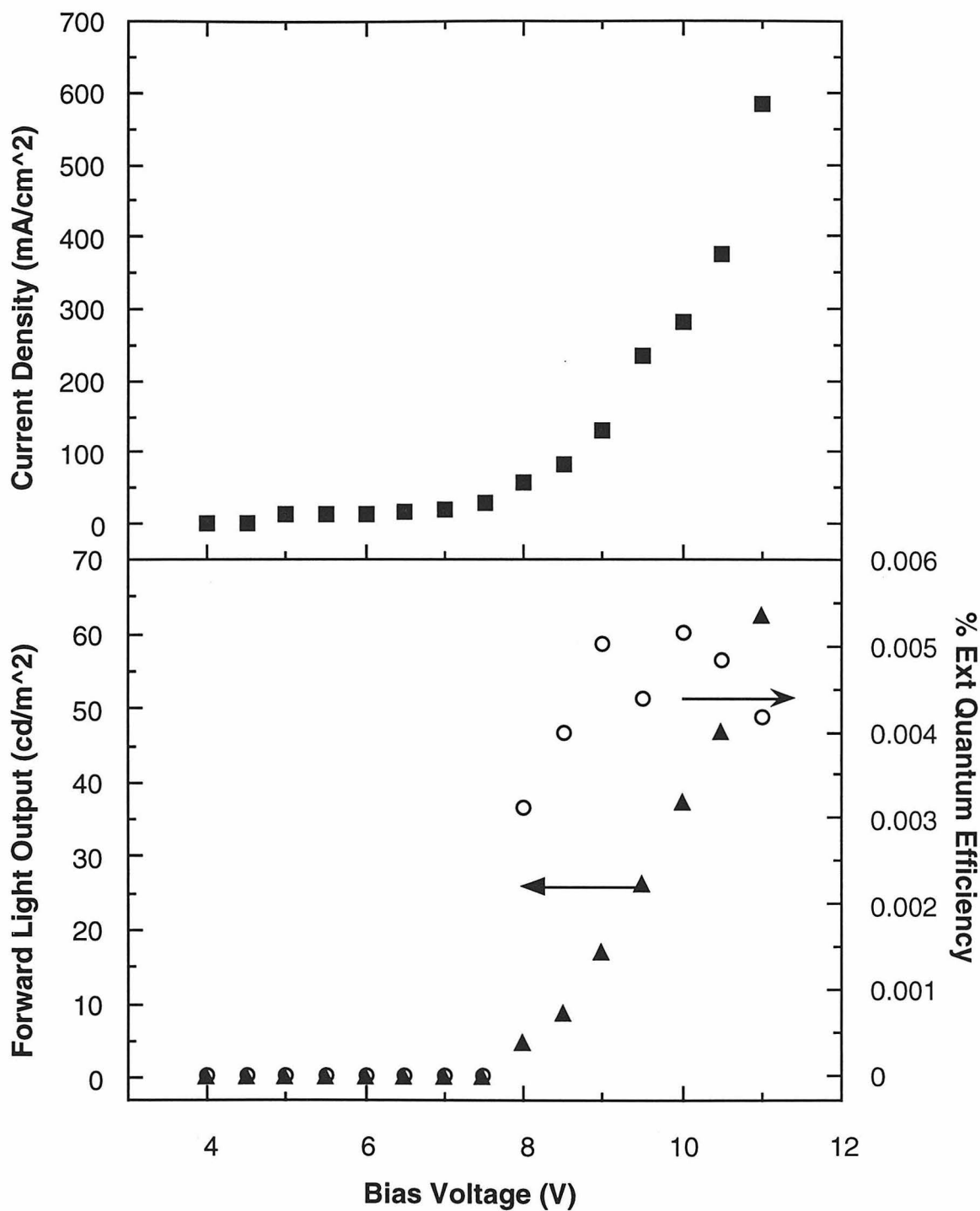


Figure 3. Results for an ITO|1 40 nm|Ca 100 nm device.

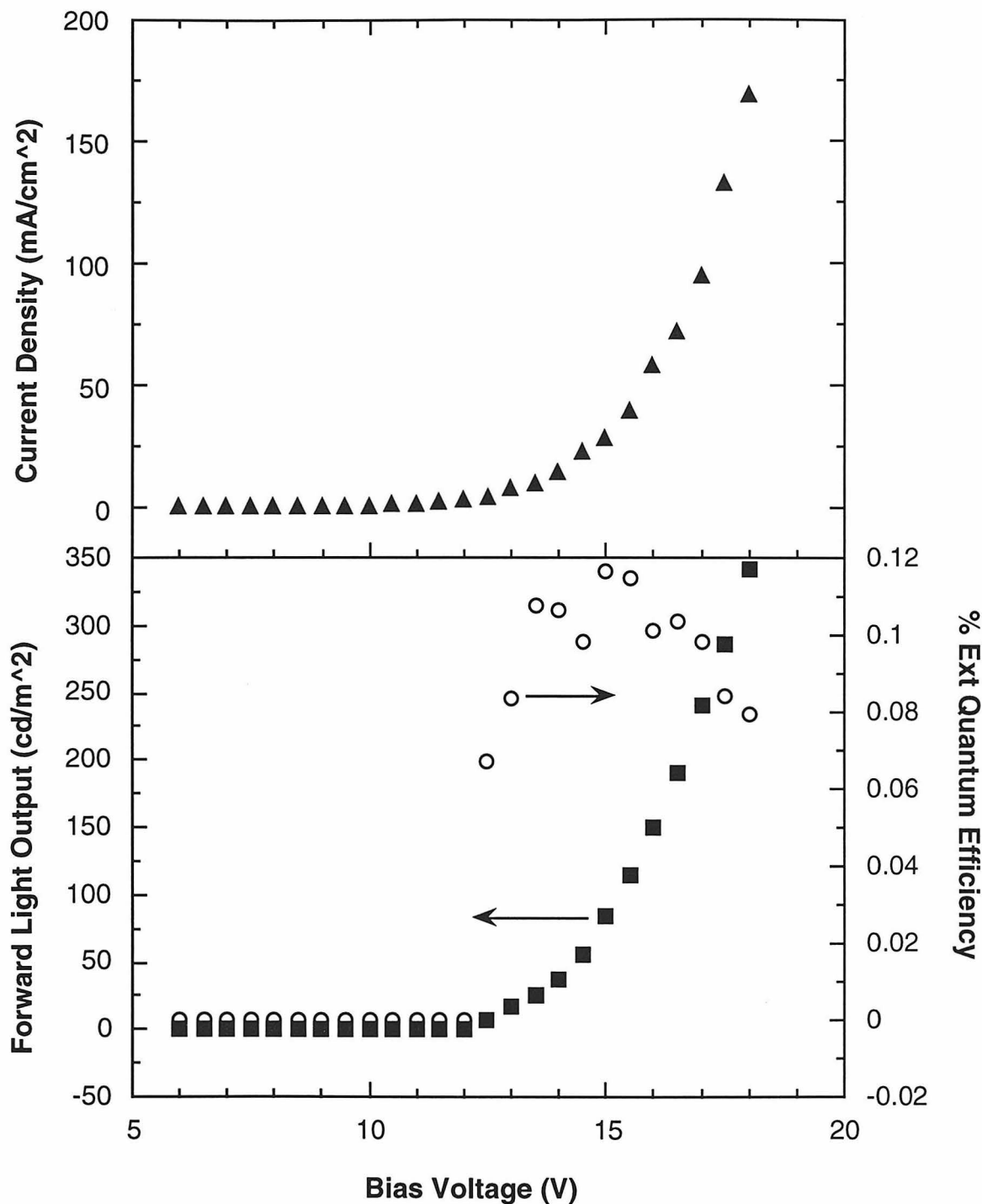


Figure 4. Results for an ITO|1 40 nm|4 18 nm|Mg 75 nm device.

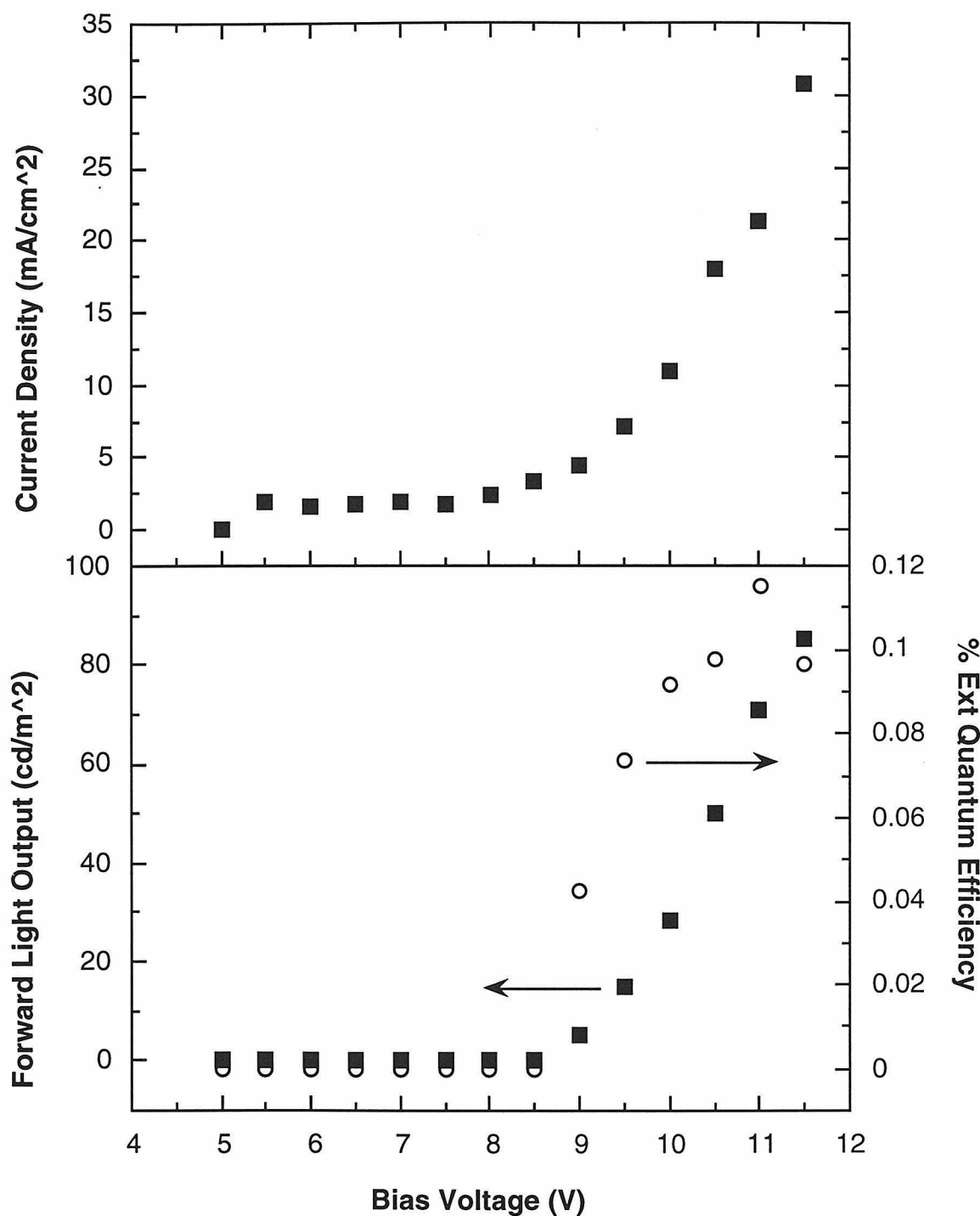


Figure 5. Results for an ITO|2 50 nm|Mg 100 nm device.

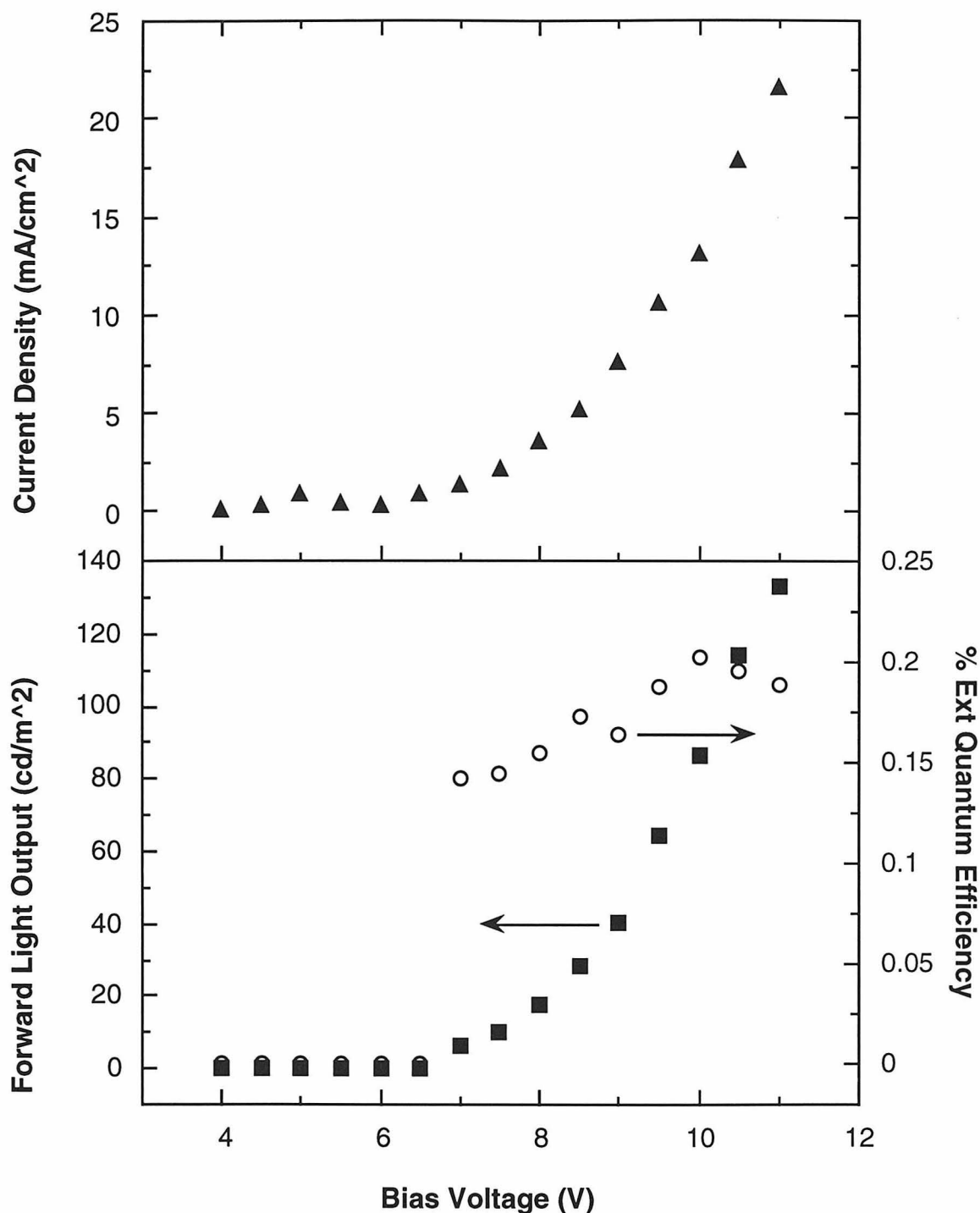


Figure 6. Results for an ITO|x-5 40nm|2 40 nm|4 15 nm|Mg 100 nm device.

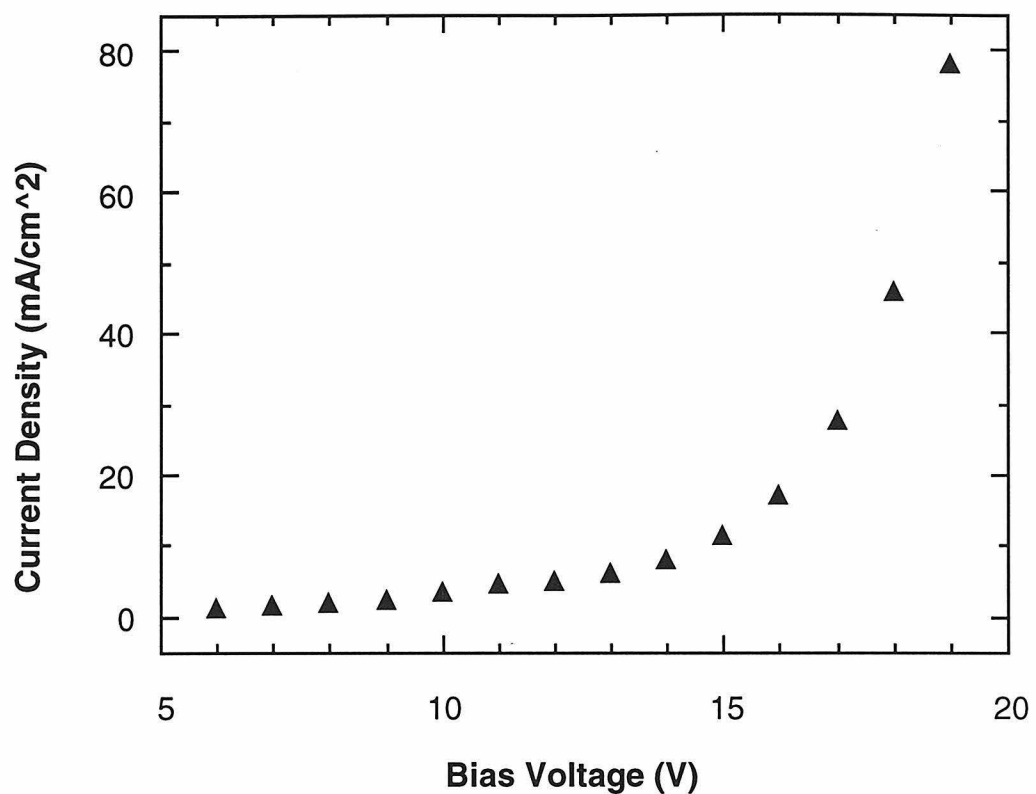


Figure 7. Results for an ITO|3 60 nm|LiF 1.5 nm|Mg 200 nm device.

References and Notes

- (1) Greenham, N. C.; Moratti, S. C.; Bradley, D. D. C.; Friend, R. H.; Holmes, A. B. *Nature* **1993**, *365*, 628.
- (2) Tang, C. W.; VanSlyke, S. A. *Appl. Phys. Lett.* **1987**, *51*, 913.
- (3) Tang, C. W.; VanSlyke, S. A.; Chen, C. H. *J. Appl. Phys.* **1989**, *65*, 3610.
- (4) Hopkins, T. A.; Meerholtz, K.; Shaheen, S.; Anderson, M. L.; Schmidt, A.; Kippelen, B.; Padias, A. B.; Hall, H. K.; Peyghambarian, N.; Armstrong, N. R. *Chem. Mater.* **1996**, *8*, 344.
- (5) Brown, A. R.; Bradley, D. D. C.; Burroughes, J. H.; Friend, R. H.; Greenham, N. C.; Burn, P. L.; Holmes, A. B.; Kraft, A. *Appl. Phys. Lett.* **1992**, *61*, 2793.
- (6) Aratani, S.; Zhang, C.; Pakbaz, K.; Höger, S.; Wudl, F.; Heeger, A. J. *J. Electron. Mater.* **1993**, *22*, 745.
- (7) Garten, F.; Hilberer, A.; Cacialli, F.; Esselink, E.; Dam, Y. v.; Schlatmann, B.; Friend, R. H.; Klapwijk, T. M.; Hadzioannou, G. *Adv. Mater.* **1997**, *9*, 127.
- (8) Granström, M.; Inganäs, O. *Appl. Phys. Lett.* **1996**, *68*, 147.
- (9) Pommerehne, J.; Vestweber, H.; Guss, W.; Mahrt, R. F.; Bässler, H.; Porsch, M.; Daub, J. *Adv. Mater.* **1995**, *7*, 551.
- (10) Partridge, R. H. *Polymer* **1983**, *24*, 733.
- (11) Huang, J.; Zhang, H.; Tian, W.; Hou, J.; Ma, Y.; Shen, J.; Lui, S. *Synth. Met.* **1997**, *87*, 105.
- (12) Shaheen, S.; Peyghambarian, N., personal communication.
- (13) deMello, J. C.; Wittmann, H. F.; Friend, R. H. *Adv. Mater.* **1997**, *9*, 230.

Appendix

Use of Poly(di-*t*-butylester phenylenevinylene) as a Photoresist

The microlithography studies presented here were performed by Shintaro Yamada, a graduate student of C. Grant Willson, at the University of Texas at Austin. I provided the polymer for these studies and performed the original testing of this material to determine at what temperature conversion of the polymer occurs in the presence or absence of acid. Preliminary testing of the polymer was presented in Chapter 4.

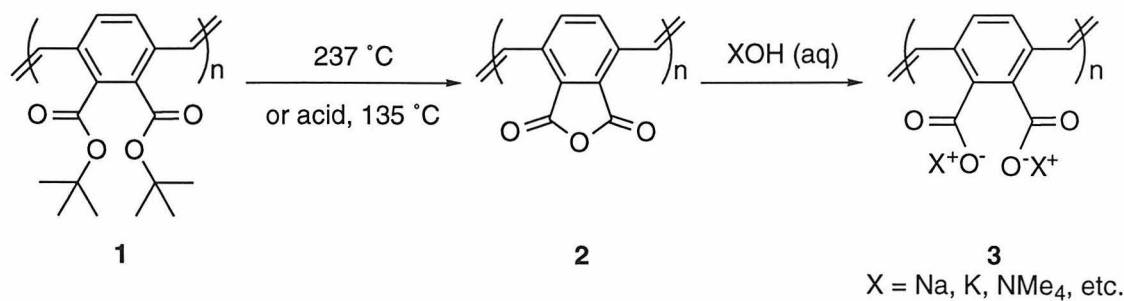
Abstract: This section describes use of poly(di-*t*-butylester phenylenevinylene), **1**, in conjunction with a photo-acid generator (PAG) as a positive photoresist. A mixture of **1** and the PAG triphenylsulfonium hexafluoroantimonate, **4**, was spin casted onto a silicon wafer. The coated wafer was then irradiated through a mask with 248 nm light to create a pattern of exposed areas where **4** decomposed to produce acid and unexposed areas where acid was not generated. Heating the wafer at 150 °C caused **1** to be converted to an anhydride, **2**, in the acid containing regions, but left **1** unconverted in the regions not containing acid. The anhydride was then dissolved in aqueous base, while **1** remained on the silicon surface in the pattern of the mask used during the irradiation step. A picture of the resulting pattern is included.

Introduction

Photoresist materials are used in microlithography to create a pattern on a surface, such as the circuitry of a microprocessor. In general a thin film of photoresist is first formed on the surface of the material to be patterned, which is often a silicon wafer. The desired pattern is then created by irradiating the coated surface through a patterned mask (contact printing). This irradiation causes a transformation of one or more components of the photoresist. After this transformation or following further processing, a solvent is used to dissolve the area that was exposed to light (a positive photoresist) or the area that was not exposed to light (a negative photoresist). The partially coated surface is then exposed to conditions that etch the uncoated areas. For example, when a silicon wafer is being patterned, the uncoated areas of the wafer are etched using a solution of hydrofluoric acid. The remaining photoresist is then usually stripped away to leave behind the patterned substrate.¹

As mentioned in Chapter 4, poly(*di-t*-butylester phenylenevinylene), **1**, can be used in combination with a photo-acid generator (PAG) as a photoresist material. This capability arises from the fact that when this organic-soluble polymer is heated at the appropriate temperature, it is converted into the anhydride **2**, which reacts with aqueous base to form the base-soluble polymer **3**. As shown in Scheme 1, the transformation to form **2** takes place at 237 °C in the presence of an acid catalyst, but in the absence of acid

Scheme 1



this transformation requires heating at 237 °C. Therefore, polymer **1** acts as a photoresist when it is blended with a material that generates acid upon exposure to light. A variety of PAGs are known and have been previously used to make both positive and negative photoresists.¹⁻⁷ Polymers similar to **1** have been used as positive resists^{1,4-6} by dissolving the converted regions in aqueous base and have been used as negative resists¹ by dissolving the unreacted regions in organic solvents. In this case, the exposed regions were not washed away because the transformed polymer was no longer soluble in organic solvents.

Results and Discussion

For these studies, polymer **1** containing 50% unaromatized units, as shown in Figure 1, was used because high solubility was desired and the partially aromatized material is much more soluble than the fully aromatized polymer. To use this polymer as a photoresist, it was blended with the PAG triphenylsulfonium hexafluoroantimonate, **4**, by dissolving both materials in dichloromethane and then spin casting this solution onto a silicon wafer. The wafer was next heated at 60 °C to drive off any remaining solvent and was then irradiated through a mask with deep ultraviolet radiation (DUV) of 248 nm. During the irradiation step, **4** decomposes and generates hexafluoroantimonic acid as shown in Scheme 2.^{2,3} After irradiation, the wafer was heated at 150 °C to cause the

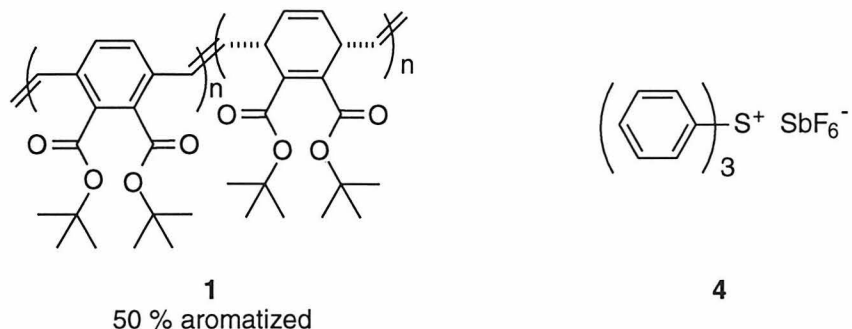
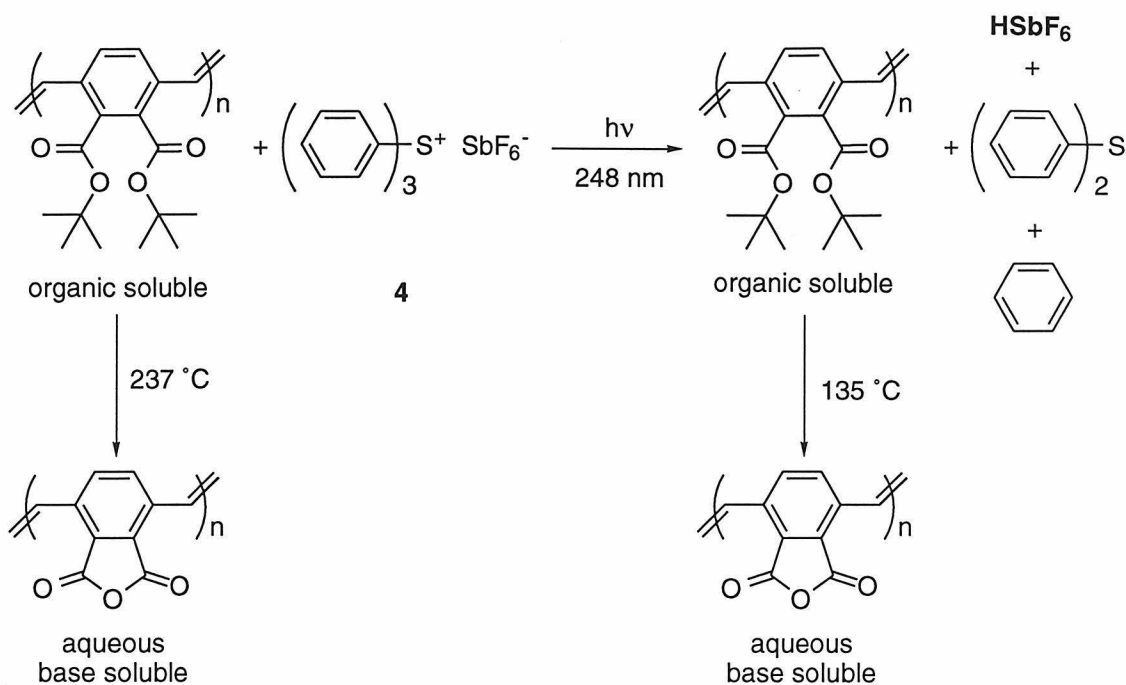


Figure 1. Polymer **1** containing unaromatized units, and photo-acid generator **4**.

Scheme 2



polymer in the exposed, acid-containing areas to be converted to the anhydride form of the polymer **2**, as shown in Scheme 2. Polymer in the unexposed, acid-free areas is not transformed at this temperature.⁸⁻¹⁰ Areas where the polymer was converted to the anhydride were then dissolved by immersing the wafer in an aqueous solution of the base tetramethylammonium hydroxide (TMAH). The unconverted polymer regions, which are not soluble in aqueous base, remained on the silicon substrate. Figure 2 shows a picture of the pattern generated by this process. The rectangular regions, which are the same size and shape as the holes in the mask, show where polymer was washed away to expose the silicon wafer, and the surrounding areas, which were covered by the mask, are where polymer **1** remained on the substrate. Therefore, under these conditions, polymer **1** blended with the PAG, **4**, serves as a positive photoresist.

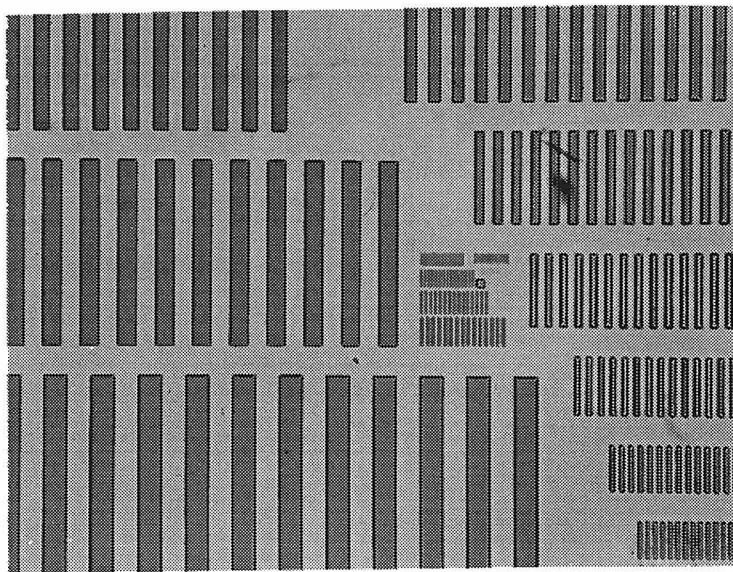


Figure 2. Optical microscope picture of developed positive image magnified 75 times. Left side line widths from top to bottom: 25 μm , 32, μm , 40 μm . Right side line widths from top to bottom: 20 μm , 16 μm , 12 μm , 10 μm , 8 μm , and 6 μm .

Experimental

Partially aromatized polymer **1** was obtained by aromatizing the precursor polymer with 0.5 equivalents of DDQ as previously described for the 80% aromatized version of this polymer.¹⁰ The solution used for spin casting was composed of 0.135 g of **1** and 0.005 g (4 wt % versus **1**) of **4** dissolved in 1.35 g of dichloromethane. The substrate was a 3 inch silicon wafer that had been primed with hexamethyldisilazane (HMDS). HMDS, which provides better adhesion of the photoresist material to the silicon substrate,¹¹ was applied as a liquid to the spinning silicon wafer. Spin casting the photoresist solution onto the wafer yielded a film with a thickness of 1 μm . The coated wafer was heated at 60 °C for 1 minute and then contact printing was performed using DUV (248 nm, 100 mJ/cm²). Irradiation was generated using a xenon arc lamp (Oriel) and was filtered to obtain only 248 nm radiation using a 248 nm filter (Acton Research Corporation). Following exposure, the wafer was heated on a hot plate at 150 °C for 3

minutes. The wafer was then submerged in a solution of tetramethylammonium hydroxide (2.38% in water) to dissolve the converted polymer. The picture of the resulting substrate was taken using an optical microscope at a magnification of 75x.

References and Notes

- (1) Comstock, M. J., Eds. *Introduction to Microlithography*. American Chemical Society, Washington, D. C., 1983.
- (2) Crivello, J. V. *J. Poly. Sci., Poly. Chem. Ed.* **1979**, *17*, 977.
- (3) Crivello, J. V. *Advances in Polymer Science* **1984**, *62*, 1.
- (4) Crivello, J. V.; Shim, S. Y. *J. Poly. Sci., Poly. Chem.* **1995**, *33*, 513.
- (5) Allen, R. D.; Wallraff, G. M.; Hinsberg, W. D.; Simpson, L. L. *J. Vac. Sci. Technol. B* **1991**, *9*, 3357.
- (6) Kim, J. B.; Jung, M. H.; Chang, K. H. *European Poly. J.* **1997**, *33*, 1239.
- (7) Lin, Q.; Steinhäusler, T.; Simpson, L.; Wilder, M.; Medeiros, D. R.; Willson, C. G. *Chem. Mater.* **1997**, *9*, 1725.
- (8) Böhm, I.; Herrmann, H.; Menke, K.; Hopf, H. *Chem. Ber.* **1978**, *111*, 523.
- (9) Weber, G.; Menke, K.; Hopf, H. *Chem. Ber.* **1980**, *113*, 531.
- (10) Wagaman, M. W.; Grubbs, R. H. *Macromolecules* **1997**, *30*, 3978.
- (11) Yamada, S.; Willson, C. G., personal communication.